GA-A14304
UC-77

THORIUM UTILIZATION PROGRAM

QUARTERLY PROGRESS REPORT FOR THE PERIOD ENDING FEBRUARY 28, 1977

Prepared under
Contract EY-76-C-03-0167
Project Agreement No. 53
for the San Francisco Operations Office
U.S. Energy Research and Development Administration

DATE PUBLISHED: MARCH 1977

DISCLAIMER

GENERAL ATOMIC

GA-A14304
UC-77

THORIUM UTILIZATION PROGRAM

QUARTERLY PROGRESS REPORT FOR THE PERIOD ENDING FEBRUARY 28, 1977

Prepared under
Contract EY-76-C-03-0167
Project Agreement No. 53
for the San Francisco Operations Office
U.S. Energy Research and Development Administration

GENERAL ATOMIC PROJECT 3225

DATE PUBLISHED: MARCH 1977

QUARTERLY REPORT SERIES*

GA-A13178 - June 1974 through August 1974
GA-A13255 - September 1974 through November 1974
GA-A13366 - December 1974 through February 1975
GA-A13510 - March 1975 through May 1975
GA-A13593 - June 1975 through August 1975
GA-A13746 - September 1975 through November 1975
GA-A13833 - December 1975 through February 1976
GA-A13949 - March 1976 through May 1976
GA-A14085 - June 1976 through August 1976
GA-A14214 - September 1976 through November 1976

*Prior to GA-A13178, the Thorium Utilization Program was reported in the Base Program Quarterly Progress Report.

ABSTRACT

This publication continues the quarterly series presenting results of work performed under the National HTGR Fuel Recycle Program (also known as the Thorium Utilization Program) at General Atomic Company. Results of work on this program prior to June 1974 were included in a quarterly series on the HTGR Base Program.

The work reported includes the development of unit processes and equipment for reprocessing of High-Temperature Gas-Cooled Reactor (HTGR) fuel, the design and development of an integrated pilot line to demonstrate the head end of HTGR reprocessing using unirradiated fuel materials, and design work in support of Hot Engineering Tests (HET). Work is also described on trade-off studies concerning the required design of facilities and equipment for the large-scale recycle of HTGR fuels in order to guide the development activities for HTGR fuel recycle.

INTRODUCTION

This report covers the work performed by General Atomic Company under U.S. Energy Research and Development Administration Contract EY-76-C-03-0167, Project Agreement No. 53. The work done under this project agreement is part of the program for development of recycle technology for High-Temperature Gas-Cooled Reactor (HTGR) fuels described in the "National Program Plan for HTGR Fuel Recycle Development" (GCR-76/19).

The objective of the program is to provide a demonstration plant for the recycle of HTGR fuels. This plant will demonstrate facility and equipment design and operating procedures which are licensable and commercially feasible for the reprocessing and refabrication of spent fuel from HTGRs. Work at General Atomic Company is concentrating on the following National Program tasks: Program Management and Analysis (Task 100); Reprocessing Technology Development (Task 200); Refabrication Technology Development (Task 300); HTGR Recycle Demonstration Facility (HRDF) design support (Task 600).

Task 100, Program Management and Analysis, includes the functions of overall planning, scheduling, budgeting, reporting, management control of the program, and coordination of activities.

Task 200, Reprocessing Technology Development, includes the definition of flowsheets, the development of components, and the definition of operating techniques, remote maintenance and or disassembly techniques, and coordination of fuel shipping and storage activities. Operations which must be developed include crushing of the fuel elements; burning the graphite in a fluidized bed-burner; separation of the fertile and fissile

particles; crushing the SiC coating on fissile particles; burning the crushed particles; dissolution of thorium and uranium in the burned, crushed particles; separation of the undissolved solids (SiC hulls, etc.) from the leachate; separation of the thorium and uranium from the fission products by solvent extraction; separation and purification of the thorium and uranium by solvent extraction; process and facility off-gas treatments to ensure releases are environmentally acceptable and in compliance with regulations; and the primary treatment of solid, liquid, and gaseous wastes from the process.

Task 300, Refabrication Technology Development, includes the definition of flowsheets, the development of components, and the definition of operating techniques, remote maintenance and/or disassembly techniques, and coordination of fuel shipping and storage activities. The refabrication begins with aqueous uranyl nitrate solution from the reprocessing facility and ends with fuel elements prepared for shipment to the reactor. The principal operations to be developed are loading the ion-exchange resin with uranium, resin carbonization, resin conversion, coating the converted resin with pyrolytic carbon and SiC, fuel rod fabrication, fuel element assembly, fuel and fuel element inspection, scrap recovery, and waste handling.

Task 600, HTGR Recycle Demonstration Facility, includes the design, construction, proof-testing, and operation of a demonstration facility for the recycle of HTGR fuel. The plant is to include all fuel cycle operations from the receiving of spent fuel elements from the reactors to shipping the refabricated fuel elements back to the reactors. The preconceptual design studies and the early conceptual design are to be used to guide the development work for reprocessing and refabrication processes and equipment. The results of the research and development tasks will in turn be used to guide the detailed design of HRDF.

CONTENTS

FIGURES

FIGURES (Continued)

FIGURES (Continued)

FIGURES (Continued)

TABLES

TABLES (Continued)

TABLES (Continued)

1. SUMMARY

General Atomic Thorium Utilization Program activities progressed on schedule during the quarter, with continuation of the head-end reprocessing equipment testing program. Individual testing of the tertiary, oversize crushers and the screener was completed. Preparation of the equipment for testing as a system is under way.

Tests on the tertiary crusher revealed no operating problems. No material holdup areas or bypass of the crushing cavity was detected. In all of the tests the material was crushed at rates equal to or greater than the discharge rates of the secondary crusher. The quantity of oversize product was well within the Design Criteria (DC521001) limits. Design modifications were completed on the secondary crusher stationary jaw and Pitman wear plate to alleviate the previously observed bridging of the larger material entering from the primary crusher. Overheating of the secondary Pitman bearings was attributed to improperly fitted bearing sleeves, and proper tolerancing of these sleeves has been accomplished.

The initial issue of a functional level diagram for the Fuel Element Size Reduction System has been prepared for preliminary review. Investigation into redesign of the Pitman shaft bearings and lubrication system has begun in order to eliminate conventional lubrication methods and materials which are incompatible with a hot cell environment. Repairs to the damaged toggle lift hook drive assembly of the secondary Pitman lift fixture were completed and were tested during reinstallation of the secondary crusher. Screener tests revealed excessive blinding of the perforated plate, which was then replaced with a wire mesh screen. Gradual buildup in blinding occurred, requiring the addition of a screener self-cleaning device.

Heat transfer coefficients were calculated from data obtained in six 0.40-m primary burner heatup runs. The results indicated significantly smaller wall-to-bed heat transfer for deep beds heated with the dual (upper and lower) induction coils compared with shallow beds heated with the single, lower coil.

Six runs were made on the 0.20-m primary burner during the reporting period. The initial four runs were made to test the Diogenes automatic control system; the fifth run was an attempted 48-hr run which was curtailed after ∿12 hr due to mechanical failures in burner subsystems. The sixth run was made to test operating parameters which were revised based upon the need for an extended O_2 ramp period and higher fluidization velocity and to check the burner subsystem repairs.

Other significant 0.20-m burner work included fabrication and initial testing of an electrical resistance probe bed level sensor and preliminary heat transfer design calculations for determining the cooling requirements to maintain the recycling fines cyclone exit temperature at ∿500°C. A parametric study of process variables on the 0.20-m secondary burner has been initiated, with three of seven runs now completed. Extensive automation of the burn cycle has been demonstrated. Shakedown of the 0.10-m secondary burner is now complete, and the burner is ready for burning tests using crushed TRISO, fissile FSV type fuel particles.

Localized side plate wear on the fertile particle roll crusher has necessitated inlaying a very hard sintered tungsten carbide wear pad adjacent to the crushing cavity. The fissile roll crusher has been received and is now undergoing checkout testing.

The conceptual design of the engineering-scale dissolver-centrifuge for incorporation into the head-end line was completed during the quarter with the issuance of the Design Criteria and System Description and the Process Flow and Piping and Instrument Diagrams. A series of bench-scale dissolution runs was made on ThO_2 kernels using the heel operating mode with lower-acidity dissolver acid.

Three solvent extraction feed adjustment runs were completed during the quarter. Two of the runs were representative of the continuous intercycle concentration step. The other run was a continuous operation which utilized leacher product as feed. These runs were used to test the modified equipment and also to familiarize new personnel with the equipment operation. Three solvent extraction runs were completed during the quarter representing the first cycle of the Acid-Thorex flowsheet. The Robatel centrifugal contactor and the five pulsed columns in the solvent extraction pilot plant were used in these experiments. Tracer quantities of radioactive zirconium were added to permit determination of zirconium decontamination throughout this solvent extraction system.

Progress with dry solids handling component and system testing continues. Inlet filter pressure drops have been measured; the storage volume of the bunkers has been established; and the testing of in-bunker filters is complete. The performance of fixed speed blowers has been accurately predicted; experiments with rotary feeder valves have demonstrated their suitability for installation in the system; improvement requirements have been identified for the bunker load cell electronic data processing system. The evaluation of different types of samplers has begun, and results obtained with the primary burner product removal system have been analyzed and particle breakage results have been closely examined. The experience so far with the secondary burner product removal system has been used as the basis for upgrading the design. A substantial measure of agreement between results from shear cells at GA and ORNL has been found using crushed graphite.

The Work Plan for the Maintainability and Reliability Phase I study was prepared and methodology development was initiated. The HET conceptual design has been completed to the 90% level and the Conceptual Design Report is in progress. HET Technical Review meetings were held during the quarter to discuss the facility and equipment arrangement, cost estimating ground rules, sampling plan, waste handling, off-gas treatment, and spent fuel

shipping. System description and design criteria activities were initiated for an integrated HRDF-Reprocessing Head-End and Solvent Extraction remote maintenance system.

During the quarter efforts have been focused on completion of the HET fuel shipping conceptual design report, development of detailed costs, and identification of all system interfaces. This activity has included final selection of the PB-2 cask as the reference design and confirmation of the design and suitability of the welded canister concept. The reference shipping system design has been reviewed with both ORNL and Allied Chemical from an operational and interface standpoint and has been accepted for use on the HETP.

The Reprocessing Flowsheet Review and Material Balance Study of reprocessing head-end and off-gas treatment systems is in technical review. Material balances and summary assumption statements for each process stream were prepared for the Reprocessing Yields and Material Throughput Study. The Spent Fuel Element Decay Heat and Source Term Analysis report was completed and is available for distribution. The SIMSCRIPT program language has been chosen for the reprocessing model to be used in the simulation of the Reprocessing Plant Operating Modes Study.

2. FUEL ELEMENT CRUSHING

2.1. SUMMARY

During this reporting period, testing of the tertiary and oversize crushers and the screener individually (Phase I of the Activity Plan, AP521001) was completed. Preparation of the equipment for testing as a system (Phase II of the Activity Plan, AP521001) is under way.

Tests on the tertiary crusher revealed no operating problems. No material holdup areas or bypass of the crushing cavity were detected. In all of the tests the material was crushed at rates equal to or greater than the discharge rates of the secondary crusher. The quantity of oversize product (+4750-μm mesh size) was well within the <5% specified in the Design Criteria (DC521001).

The oversize crusher was operated with a throughput of ∿10 wt % (i.e., 11.3 kg) of one fuel element composed of equal amounts of plus and minus 4750-μm-mesh crushed graphite. The process time for this quantity was well below the UNIFRAME system's 15-min maximum allowable time. Material holdup was in excess of the required <0.5% in one of the tests, and design modifications are planned to reduce the holdup to the acceptable value. Oversize product (+4750-μm mesh size) still remaining after oversize crushing ranged from 0.01 to 0.46 wt % of an entire fuel element

Screener tests revealed excessive blinding of the perforated plate by lodged graphite particles. The perforated plate was replaced with a 4750-μm wire mesh screen. Blinding of the screen was greatly reduced; however, a gradual buildup in blinding occurred, requiring the addition of a screener self-cleaning device. The screener was tested with both 4750-μm and 6350-μm wire mesh screens in order to observe their screening characteristics. The desired screen efficiency is the removal of all material

greater than 4750-μm mesh with an upper limit of 5% acceptable material in the oversize fraction. With the 4750-μm mesh screen, a maximum of 11% acceptable material was discharged with the oversize material. The 6350-μm screen was effective in reducing the quantity of acceptable (-4750-μm mesh) material discharged to the oversize to a maximum of 0.8%.

However, as expected, the 6350-μm screen did not separate all the oversize (+4750 μm) material from the acceptable material; 1.6% remained. Testing was completed using the 4750-μm screen because calculations of the product size distributions expected from the UNIFRAME when operated as a system revealed that the 4750-μm screen was necessary to meet the primary burner feed size distribution specification.

Design modifications were completed on the secondary crusher stationary jaw and its Pitman wear plate to alleviate the previously observed bridging of the larger material entering from the primary crusher. Overheating of the secondary Pitman bearings was attributed to improperly fitted bearing sleeves, and proper tolerancing of these sleeves has been accomplished.

The initial issue of a functional level diagram for the Fuel Element Size Reduction System has been prepared for preliminary review.

Investigation into redesign of the Pitman shaft bearings and lubrication system has begun in order to eliminate conventional lubrication methods and materials which are incompatible with a hot cell environment.

Repairs to the damaged toggle lift hook drive assembly of the secondary Pitman lift fixture were completed and were tested during reinstallation of the secondary crusher.

2.2. TERTIARY CRUSHER TESTING (J. B. Strand)

2.2.1. Introduction

The tertiary crusher is a double roll crusher consisting of two 100-cm-diameter, 70-cm-wide rolls separated by a 0.276-cm (0.109 in.) gap. Each roll is independently driven at approximately 60 rpm by a constant-speed motor and an in-line, directly coupled speed reducer. The drives are connected through synchronous toothed belts to a drive sprocket on each roll shaft.

2.2.2. Activity

The operational and design capabilities of the tertiary crusher were tested using crushed graphite products from the secondary crusher tests. The feed materials included products from primary and secondary crushing of three half-length, unfueled H-327 graphite fuel elements, one half-length, unfueled H-327 graphite control rod element, and three full-length, unfueled H-327 graphite fuel elements. Each of these materials was separately charged to the tertiary crusher at rates approximately equal to the rate at which they were crushed in the secondary crusher.

Observations of material flows during the crushing operations and inspection of the crusher after the test revealed no material holdup areas or material bypassing the crushing cavity.

In all the tests, the material was crushed as rapidly as it was charged. Therefore, no material surges are expected to occur between the secondary and tertiary crushing stages when the equipment is operated as a system. The maximum feed rate was approximately 33.7 kg/min (67 lb/min), and tertiary crushing rates are at least equivalent. The required throughput of one fuel element in <15 min [$\sim$113 kg/element (250 lb/element) = $\sim$7.53 kg/min (16.7 lb/min)] is easily achieved in the tertiary crushing stage. Table 2-1 summarizes the tertiary crusher tests.

TABLE 2-1
UNIFRAME TERTIARY CRUSHER PHASE I TESTS
Roll Gap: 2770 μm/0.109 in.); Roll Speed: 60 rpm

Test	Feed Material	Results
TC-25	1/2 fuel element after primary (Test PC-1) and secondary (Test SC-13) crushing; 42.6 kg (94 lb)	Complete crushing at charging rate (1 min 29 sec); 28.7 kg/min (63.4 lb/min)
TC-26	1/2 fuel element after primary (Test PC-2) and secondary (Test SC-14) crushing; 43.3 kg (95.5 lb)	Complete crushing at charging rate (1 min 25 sec); 30.6 kg/min (67.4 lb/min)
TC-27	1/2 fuel element after primary (Test PC-3B) and secondary (Test SC-15) crushing; 51.7 kg (114 lb)	Complete crushing at charging rate (1 min 32 sec); 33.7 kg/min (74.3 lb/min)
TC-28	1/2 control rod element after primary (Test PC-4) and secondary (Test SC-16) crushing; 41.5 kg (91.5 lb)	Complete crushing at charging rate (2 min 46 sec); 15.0 kg/min (33.1 lb/min)
TC-31	Full-size fuel element after primary (Test PC-7) and secondary (Test SC-19) crushing; 85.7 kg (189 lb)	Complete crushing at charging rate (3 min 32 sec); 24.3 kg/min (53.5 lb/min)
TC-32	Full-size element after primary (Test PC-8) and secondary (Test SC-20) crushing; 87.1 kg (192 lb)	Complete crushing at charging rate (3 min 19 sec); 26.3 kg/min (57.9 lb/min)
TC-33	Full-size fuel element after primary (Test PC-9) and secondary (Test SC-21) crushing; 87.1 kg (192 lb)	Complete crushing at charging rate (3 min 30 sec); 24.9 kg/min (54.8 lb/min)

Crushed products from each of the tests were hand-screened through a 3/16-in.-mesh screen with actual measured maximum openings of 5512 μm. As shown in Table 2-2, the products indicated no significant differences in the quantities of +5512-μm material produced in tertiary crushing between fuel and control rod elements or between half- and full-size elements. The +5512-μm size fraction averaged 1.0 wt % of the product and ranged from a high of 1.3 to a low of 0.5 wt %.

The -5512-μm size fraction from each test was reduced in a 12-to-1 sample splitter to a suitable size for subsequent screen analysis using 20.32-cm (8 in.) diameter Tyler standard screen sieves. The results of these analyses (shown in Table 2-3) again indicated no significant differences in the products from tertiary crushing fuel or control rod elements or half- or full-size elements. Figure 2-1 shows plots of the three-run average size distribution for the half- and full-size fuel elements and the single control rod element.

2.3. OVERSIZE CRUSHER TESTING (J. B. Strand)

2.3.1. Introduction

The oversize crusher is a standard Centerol crusher consisting of a single roll (20 x 20 cm) mounted on an eccentric shaft between two wear plates, driven by a 5-hp motor through V-belts. For the UNIFRAME system, charging and discharging chutes and cover plates were added to avoid material and dust escape.

2.3.2. Activity

It was estimated that the maximum throughput of the oversize crusher would be 10 wt % of the entire fuel element during the allowable 15-min crushing period, or 0.75 kg/min. It was also estimated that the composition of the feed could be up to 5 wt % of the fuel element as +4760-μm material from oversize passing through the tertiary crushing stage and up

TABLE 2-2
UNIFRAME TERTIARY CRUSHER PHASE I TESTS - PRODUCT SIZE DISTRIBUTION
Roll Gap: 2770 μm (0.109 in.); Roll Speed: 60 rpm

Test	Wt % +5512-μm Material	Wt % -5512-μm Material
1/2 Fuel Element Crushing		
TC-25	1.3	98.7
TC-26	0.5	99.5
TC-27	0.8	99.2
Average	0.9	99.1
1/2 Control Rod Element Crushing		
TC-28	1.0	99.0
Full-Size Fuel Element Crushing		
TC-31	0.8	99.2
TC-32	1.3	98.7
TC-33	1.1	98.9
Average	1.1	98.9
Grand average	1.0	99.0

TABLE 2-3
UNIFRAME TERTIARY CRUSHER 5512-μm PRODUCT
SIZE DISTRIBUTIONS - PHASE I TESTS

Roll Gap: 2770 μm (0.109 in.); Roll Speed: 60 rpm

Crushed Half-Size Fuel Elements

Mesh Size (μm)	TC-25		TC-26[a]		TC-27		Avg.	
	Wt %	Cum. Wt %	Wt %	Cum. Wt %	Wt %	Cum. Wt %	Wt %	Cum. Wt %
-5512 +4000	17.8	100.0	13.9	100.0	14.8	100.0	15.5	100.0
-4000 +2800	43.2	82.2	36.6	86.1	40.5	85.2	40.1	84.5
-2800 +2000	12.0	39.0	12.8	49.5	14.2	44.7	13.0	44.4
-2000 +1000	11.2	27.0	13.5	36.7	13.8	30.5	12.8	31.4
-1000 +850	1.9	15.8	2.6	23.2	2.4	16.7	2.3	18.6
-850 +425	5.8	13.9	8.2	20.6	6.9	14.3	7.0	16.3
-425 +355	1.2	8.1	1.8	12.4	1.3	7.4	1.4	9.3
-355 +250	1.6	6.9	2.6	10.6	1.7	6.1	2.0	7.9
-250	5.3	5.3	8.0	8.0	4.4	4.4	5.9	5.9

Crushed Half-Size Control Rod Element

Mesh Size (μm)	TC-28	
	Wt %	Cum. Wt %
-5512 +4000	16.1	100.0
-4000 +2800	40.0	83.9
-2800 +2000	12.4	43.9
-2000 +1000	11.2	31.5
-1000 +850	2.2	20.3
-850 +425	7.3	18.1
-425 +355	1.6	10.8
-355 +250	2.3	9.2
-250	6.9	6.9

Crushed Full-Size Fuel Elements

Mesh Size (μm)	TC-31		TC-32[a]		TC-33		Avg.	
	Wt %	Cum. Wt %	Wt %	Cum. Wt %	Wt %	Cum. Wt %	Wt %	Cum. Wt %
-5512 +4000	15.7	100.0	18.3	100.0	14.8	100.0	16.3	100.0
-4000 +2800	40.4	84.3	39.8	81.7	38.3	85.2	39.5	83.7
-2800 +2000	12.2	43.9	12.8	41.9	12.7	46.9	12.6	44.2
-2000 +1000	11.8	31.7	11.3	29.1	12.6	34.2	11.9	31.6
-1000 +850	2.2	19.9	2.0	17.8	2.4	21.6	2.2	19.7
-850 +425	7.1	17.7	6.6	15.8	7.8	19.2	7.2	17.5
-425 +355	1.5	10.6	2.0	9.2	2.4	11.4	2.0	10.3
-355 +250	2.1	9.1	1.8	7.2	2.3	9.0	2.0	8.3
-250	7.0	7.0	5.4	5.4	6.7	6.7	6.3	6.3

[a] Average of two screen analyses.

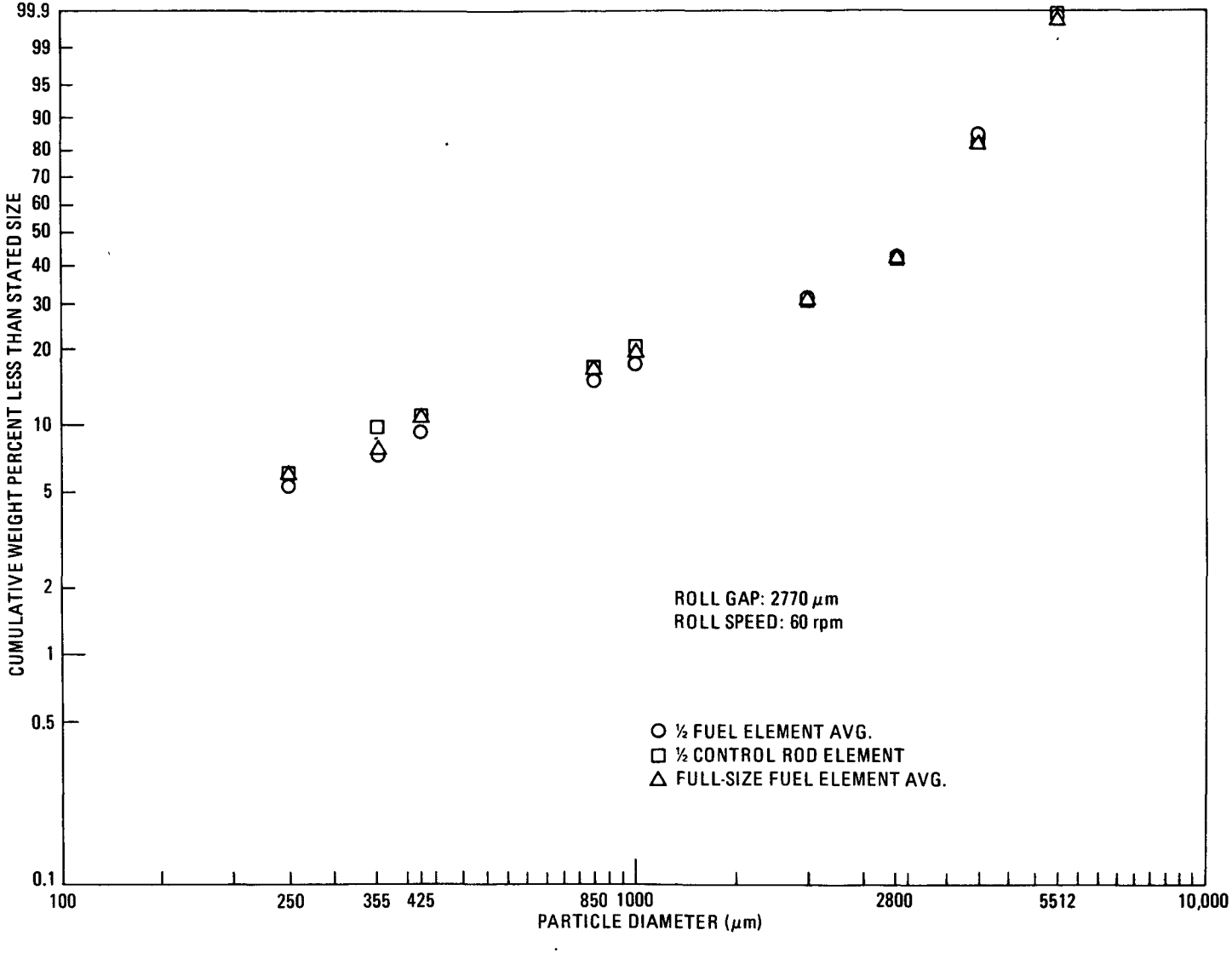

Fig. 2-1. -5512-μm product size distributions from UNIFRAME tertiary crusher Phase I tests

to 5 wt % of the fuel element as -4760-μm material from screener inefficiencies.

To gain insight into the operation of the oversize crusher prior to beginning the parametric studies, two shakedown tests (OP-A and OP-B) were made. The feed materials for both of these tests were made by blending 5.67 kg (equivalent to 5 wt % of one fuel element) of +4760-μm and 5.67 kg of -4760-μm crushed graphite from the secondary crusher. In the initial test (OP-A), the blended feed was charged at a rate of ∿4 kg/min and was crushed as rapidly as it was charged. In the second test (OP-B), the blended feed was choke fed to the crusher to obtain an estimate of the maximum throughput rate. Crushing was completed in ∿50 sec, resulting in a throughput rate of ∿13.6 kg/min. The products from these tests were hand-screened through a 3/16-in. mesh screen with actual measured maximum openings of 5512 μm. The quantity of +5512-μm material in the product was very high for both tests (33.3 wt % in OP-A and 15.2 wt % in OP-B). A summary of the tests is given in Table 2-4. To avoid the excessive oversize material in subsequent tests, the original shaft with a 0.318-cm (1/8 in.) eccentricity was replaced by a shaft with a 0.159-cm (1/16 in.) eccentricity to increase the size reduction. The gaps between the roll and the two wear plates are set, in each case, by adjusting the wear plates inward to the point of contact with the roll at its maximum eccentricity. This results in a gap, at the maximum open position, equal to the shaft eccentricity.

As in the first two tests, the initial test with the 0.159-cm eccentric shaft utilized feed made from secondary crusher product. However, due to a weighing error, the quantity was increased to 7.71 kg for each fraction (see Table 2-4). Nevertheless, the oversize material (+5512 μm) in the product was reduced to 0.1 wt % and the throughput rate of 3.5 kg/min was still in excess of the estimated requirement of 0.75 kg/min.

At this point, the limited supply of +5512-μm crushed graphite from the secondary crusher had been depleted. Additional +5512-μm feed materials were made by recrushing the smallest ring-size fractions from primary

TABLE 2-4
SUMMARY OF UNIFRAME OVERSIZE CRUSHER PHASE I TESTS

Test Number	OP-A	OP-B	OC-43	OC-44A	OC-44B	OC-45	OP-C
Shaft Eccentricity (cm)	0.318	0.318	0.159	0.159	0.159	0.159	0.159
Feed Composition[a]	A	A	A	B	B	B	C
+5512 μm (kg)	5.67	5.67	7.71	5.67	5.67	5.67	0.993
-5512 μm (kg)	5.67	5.67	7.71	5.67	5.67	5.67	0.993
Total feed (kg)	11.34	11.34	15.42	11.34	11.34	11.34	1.986
Charging time (sec)	168	25	150	150	260	216	210
Crushing time (sec)	As charged	50	267	Failed to crush	336	260	As charged
Throughput rate (kg/min)	N/A	13.6	3.5	N/A	2.0	2.6	N/A
Product size distribution							
+5512 μm (wt %)	33.3	15.2	0.1	N/A	4.3	4.6	9.1
-5512 μm (wt %)	67.7	84.8	99.9	N/A	95.7	95.4	90.9

[a] A = Crushed H-327 graphite from secondary crushing tests.

B = Crushed H-327 graphite (+5512 μm) from primary crusher products recrushed in oversize crusher; crushed H-327 graphite (-5512 μm) from secondary crushing tests.

C = Crushed H-327 graphite (+5512 μm) from tertiary crusher test TC-33; crushed H-327 graphite (-5512 μm) from secondary crushing tests.

crusher tests in the oversize crusher. The gaps between the roll and the wear plates were adjusted to allow this operation. The material failed to crush on the succeeding test (OC-44A), apparently owing to improper resetting of the gaps after the feed makeup crushing was completed. The gaps were again reset to the point of contact with the roll at its maximum eccentricity, and the tests continued without further crushing failures.

Throughput rates for all the tests utilizing the 0.159-cm eccentric shaft and feeds equivalent to 10 wt % of an entire fuel element were greater (2.0 kg/min minimum) than the 0.75 kg/min estimated requirement (Table 2-4). At the highest rate obtained (3.5 kg/min in OC-43), approximately 45% of an entire fuel element could be crushed in the oversize crusher in the allotted 15-min period.

Weight percents of +5512-μm material in the products ranged from a high of 4.6 (OC-45) to a low of 0.1 (OC-43). The higher percentages observed in tests OC-44 and OC-45 may have been a result of using the coarser feed made from recrushed primary crusher products. These results correspond to a maximum of 0.46% +5512-μm material which could be expected to end up in the final UNIFRAME product.

A final test (OP-C) was conducted to simulate oversize crushing conditions with actual tertiary crusher product (see Table 2-4). The feed for this test was the entire quantity of +5512-μm material from the product of a tertiary crusher test (TC-33) blended with an equal amount of -5512-μm material. The blended feed was charged to the oversize crusher at a rate equal to the tertiary crushing rate and was crushed as rapidly as it was charged. The weight percent of +5512-μm material in this oversize product was 9.1%. This corresponds to 0.21 wt % of +5512-μm material which could be expected to end up in the final UNIFRAME product.

At the end of test OC-45, the oversize crusher was inspected for material holdup. Approximately 360 g of material was found in back of the two wear plates. This represented material holdup from tests OC-43 through OC-45 in which a total of 49.44 kg of material had been crushed, or 0.7%

holdup. No detectable holdup was found after test OP-C. The difference was attributed to the choke feeding conditions in tests OC-43 through OC-45, which force material through the small spaces between the wear and side plates of the crusher. Although this apparently did not occur under crushing conditions expected in the UNIFRAME (test OP-C), modifications to the oversize crusher are under study to avoid this potential problem.

2.4. SCREENER TESTING

2.4.1. Introduction

The screener consists of two major components: a single, stationary outer housing and an inner vibrating section. The outer housing acts as part of the ventilation enclosure, as a discharge hopper to the material transport system, and as a support for the inner vibrating section. The design of the outer housing avoids the transmission of the necessary screening motions and vibrations to other parts of the UNIFRAME. The inner vibrating section consists of a centrally located motion generator (weights mounted on each end of the shaft of a 1/2-hp electric motor) and a perforated-plate screening table. Material passing through the perforated plate discharges onto the cone-shaped base of the outer housing and into the material transport system. The oversize material discharges through a chute to the oversize crusher for further size reduction.

2.4.2. Activity

Initial screening shakedown tests revealed that many of the holes in the perforated plate were being blinded by lodged graphite particles. This blinding could eventually result in an inefficiency in the separation of acceptable and oversize materials and require maintenance to clear the blinded holes, which would be unacceptable in a hot cell.

The problem was attributed to the length-to-diameter ratio of the holes, which allowed particles with dimensions approaching that of the hole

diameter to easily lodge. To study the effect of reducing the length-to-diameter ratio, the holes in a 15-cm (6 in.) diameter section of the perforated plate were chamfered (1 cm x 45 degrees). Blinding was noticeably reduced in this section compared with the original hole configuration, but was still too severe (>10%) to be acceptable.

A 15-cm (6 in.) square section of the plate was replaced with 4760-μm (3/16 in.) wire mesh screen, and blinding was reduced to <5% in this section. The test array for the two modifications is shown in Fig. 2-2. These results prompted replacement of the entire perforated plate with a wire mesh screen for the screener operational and parametric tests. (See Figs. 2-3 and 2-4.)

The motion generator adjustments greatly influence the flow characteristics of the material on the screen surface and therefore the screening efficiency. The vertical amplitude is increased by increasing the bottom eccentric weight. The lead angle (angle between the top and bottom eccentric weights) affects the material flow pattern across the surface of the screen. To study and optimize the screener efficiency, the motion generator adjustments were varied through a series of tests (Table 2-5) in which batches (145 kg each) of crushed graphite consisting entirely of acceptable material (i.e., -4760-μm mesh size) were charged and screened at the various motion generator settings. The quantity of material which discharged through the oversize chute indicated the screening efficiency at that motion generator setting.

It was found that each 10° increase of the lead angle from 35° to 65° produced an increase in screening efficiency and that the increases were larger as the angles grew larger. At the 65° lead angle, the material showed a tendency to move inward toward the center of the screen and away from the discharge chute, thereby increasing the probability of material remaining on the screen.

Removal of one of the bottom weights produced increases in efficiency which were larger than those produced by any of the tested 10° incremental

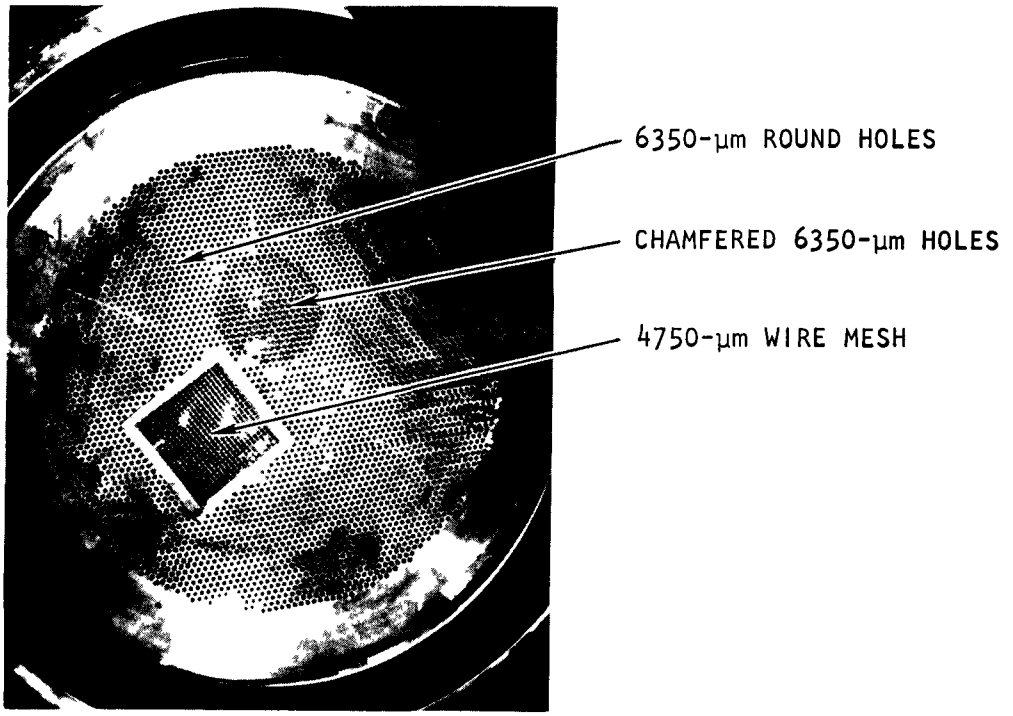

Fig. 2-2. Screener with perforated plate modified for blinding tests

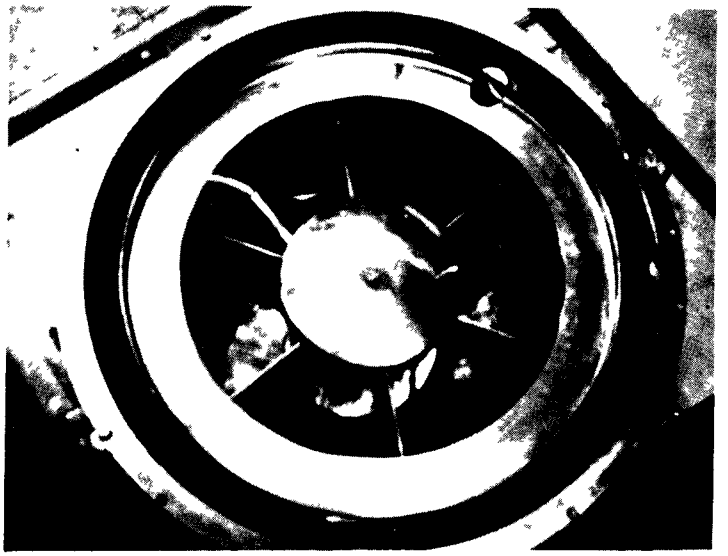

Fig. 2-3. Screener with perforated plate removed

TABLE 2-5
LEAD ANGLE COMPARISONS FROM UNIFRAME SCREENER EFFICIENCY STUDIES

Lead Angle (degrees)	No. of Bottom Weights	Charge[a] (kg)	Material in Oversize Crusher (kg)	Percent in Oversize Crusher	Percent Through Screener (Efficiency)	Δ Efficiency
35	2	145	8.6	5.9	94.1	--
45	2	145	8.1	5.6	94.4	0.4
55	2	145	7.2	5.0	95.0	0.6
65	2	145	4.9	3.4	96.6	1.6
With One Bottom Weight Removed						
55	2	145	7.2	5.0	95.0	--
55	1	145	3.6	2.5	97.5	2.5
65	2	145	4.9	3.4	96.6	--
65	1	145	1.7	1.2	98.8	2.2

[a] 100%; -4760-μm mesh size material.

lead angle changes. To avoid material holdup on the screen while achieving the maximum efficiency, a lead angle of 55° with one bottom weight was selected for further tests.

Although the screener blinding remained lower with the wire mesh screen than it had been with the perforated plate, a gradual increase in the number of blinded holes was observed during the screener efficiency studies. To determine the extent of this buildup, batch screening was continued using the selected motion generator settings, and the number of blinded holes in one quadrant of the screen were periodically counted. The degree of blinding was calculated from an estimate of the total number of holes available (see Table 2-6). Screening efficiencies remained fairly constant throughout the blinding studies (i.e., average of 2.3% ±0.1% from Table 2-6).

The blinding had reached approximately 6% after 1305 kg of material had been screened and was increasing at an average of approximately 0.7% for each 290 kg screened thereafter. This gradual buildup in blinding could be expected to produce the same inefficiency of screening and required maintenance as the perforated plate, only over a longer period of time. To avoid this eventuality, a commercially available screener self-cleaning device was purchased and installed for testing (Fig. 2-5).

The self-cleaning device consists of a perforated plate with holes large enough to prevent blinding [1.9 cm (-3/4 in.) diameter]. This plate is mounted beneath the mesh screen to support nylon cylindrical sliders (6.35-cm diameter, 0.318-cm wall, 1.9 cm long) that bounce and rotate in the space between the plate and the screen to dislodge particles.

The additional weight and dynamics of the self-cleaning device necessitated changing the motion generator settings to those recommended by the manufacturer (i.e., 70° lead angle with two bottom weights). The increase in the lead angle offset the efficiency loss by the addition of a weight, as was shown in later tests, but resulted in some material holdup.

TABLE 2-6
SCREENER BLINDING STUDIES
(4760-μm Wire Mesh Screen, 55° Lead Angle, One Bottom Weight)

Charge[(a)] (kg)	Material in Oversize Crusher (kg)	Percent in Oversize Crusher	Percent Through Screener (Efficiency)	Total Throughput (kg)	Blinded Holes (One Quadrant)	Est. Percent Blinded	Δ Percent Blinded
145	3.5	2.4	97.6	1015			
145	3.5	2.4	97.6	1160			
145	3.3	2.3	97.7	1305	170	6.0	--
145	3.3	2.3	97.7	1450			
145	3.3	2.3	97.7	1595	194	6.8	0.8
145	3.2	2.2	97.8	1740			
145	3.3	2.3	97.7	1885	209	7.4	0.6

(a) 100%; -5513-μm mesh size material.

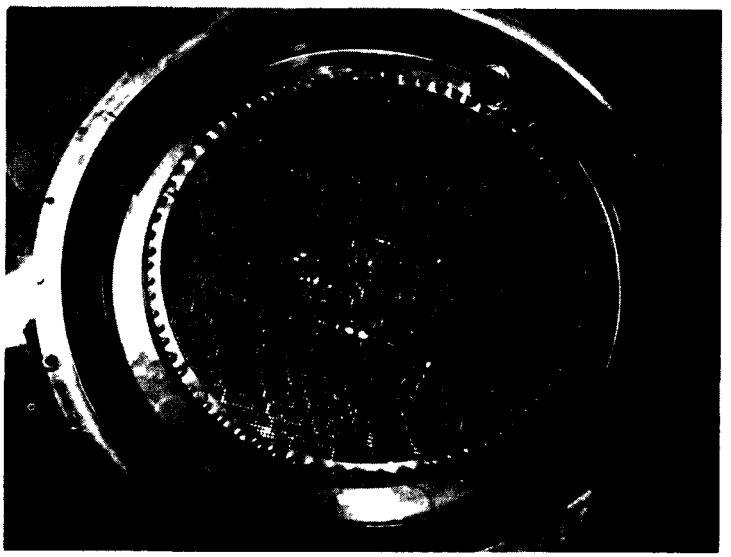

Fig. 2-4. Screener showing 4750-μm wire mesh screen installed

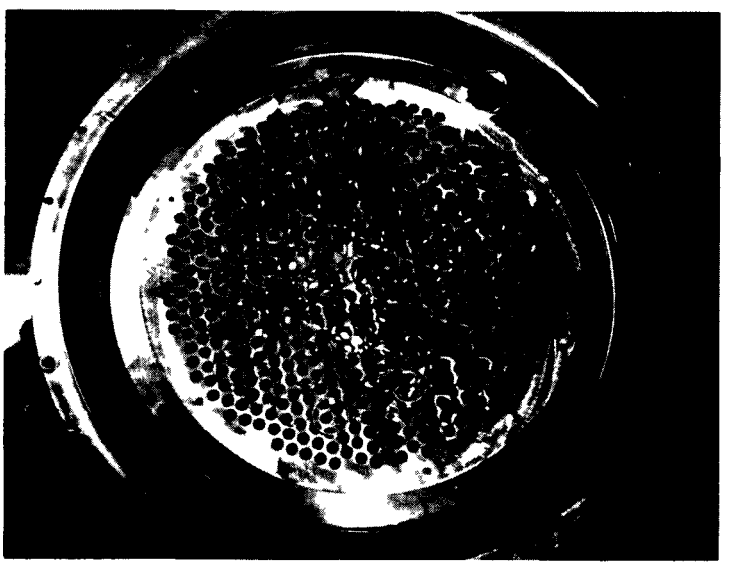

Fig. 2-5. Screener with self-cleaning kit installed (screen removed)

Tests were conducted to establish the ability of the self-cleaning device to minimize blinding and to determine the effect on screening efficiency from the new motion generator settings (Table 2-7). Blinding was reduced to a few particles on the entire screen after 435-kg throughput. The increase in blinding per 290 kg of throughput was reduced to 0.01% with the self-cleaning device from the previously observed average of 0.7% (Table 2-6) without the device.

In all previous tests the material had been charged to the screen through a 5-cm-diameter pipe located 7.6 cm above the screen surface. To simulate the effects of the tertiary crusher discharge chute on screenings, for the remaining tests the material was charged through a chute (30 cm long x 7.6 cm wide) located 60 cm above the screen surface. The effect of the chute on blinding was too insignificant to discern from normal blinding. However, the chute feeding did result in a slightly lower screener efficiency than was observed in either of the two previous identical tests with pipe feeding (97.2% versus 97.7% and 97.5%) (see Table 2-7). This effect was attributed to a reduction in screen surface area exposure by that portion of material which is charged farthest from the center of the screen.

Screener tests were continued using actual product from the UNIFRAME tertiary crusher tests (Table 2-8). The initial use of this material (test ST-A) demonstrated a marked decrease in screening efficiency from the results with 100%, -4760-μm material under the same test conditions (from 97.2% to 94.3% efficiency) and blinding was also increased.

One of the motion generator bottom weights was removed for the second test (ST-B) with tertiary crusher product, and efficiency improved by 1% to 95.3%. Particles show a tendency to migrate toward the center of the screen at these motion generator settings. This contributes to the holdup increase and to the blinding by allowing the marginal-sized particles a longer time period to become lodged in an opening instead of rapidly discharging to the oversize crusher.

TABLE 2-7
SCREENER SELF-CLEANING STUDIES
(4760-μm Wire Mesh Screen, 70° Lead Angle, Two Bottom Weights)

Charge[a] (kg)	Material in Oversize Crusher (kg)	Percent in Oversize Crusher	Percent Through Screener (Efficiency)	Total Throughput (kg)	Blinded Holes (Entire Screen)	Est. Percent Blinded	Δ Percent Blinded
145	3.3	2.3	97.7	145	3	0.03	--
145	3.6	2.5	97.5	290	4	0.04	0.01
With Simulated Tertiary Crusher Discharge Chute							
145	4.1	2.8	97.2	435	6	0.05	0.01

[a] 100%; -5513-μm mesh size material.

TABLE 2-8
SCREENER TESTS WITH TERTIARY CRUSHER PRODUCT
(4760-μm Wire Mesh Screen)

Test No.	ST-A	ST-B	VC-37
Lead angle (degrees)	70	70	70
No. bottom weights	2	1	1
Blinded holes (entire screen)	14	43	73
Estimated percent blinded	0.1	0.4	0.6
Holdup on screen (kg)	0.021	0.138	0.130
Holdup (%)	0.04	0.28	0.32
-4760-μm material in oversize crusher (kg)	2.827	2.402	3.232
-4760-μm material in oversize crusher (%)	5.7	4.7	8.0
Screening efficiency (%)	94.3	95.3	92.0
Feed material (tertiary test No.)	TC-27	TC-27	TC-25

In the third test (VC-37), the efficiency decreased to 92.0%. Because efficiencies were not consistently above the desired 95%, which would assure the limitation of oversize crushing of acceptable material to <5%, it was decided to investigate the screening characteristics of a 6350-μm (1/4 in.) wire mesh screen.

As could be expected, the screening efficiency was increased and blinding and holdup were decreased with the 6350-μm mesh screen because the tertiary crusher product contains fewer particles in this size range (see Table 2-9). Although the effect of using a 6350-μm screen would be to greatly reduce the quantity of acceptable material which was unnecessarily recrushed in the oversize crusher, it would also allow some of the unacceptable product (i.e., >4760 μm) to pass the screen. An estimate of this quantity was obtained from test VC-38 (Table 2-10). In this run, 1.98 wt % of the screened product was greater than 4760 μm and 80.8% of that material (1.60 wt % of the screened product) passed through the screen. Considerable breakup of the particles occurred during screening and transport, as was evidenced by a decrease in the +6350-μm material from 1.44 wt % in the feed to 0.34 wt % in the product (see Table 2-10).

Calculation of the expected UNIFRAME system crushed product size distribution using the average tertiary crusher product size distribution (tests TC-26 through TC-28 and TC-31 through TC-33), assuming it was screened through a 4760-μm screen (average results of tests ST-A, ST-B, and VC-37) and the oversize discharge was recrushed in the oversize crusher (average results of tests OP-C and OC-43 through OC-45), resulted in a product very close to the desired primary burner feed size distribution (Fig. 2-6). The 6350-μm screen test results demonstrated that an insufficient quantity of material would be discharged to the oversize crusher (0.35 wt % in test VC-38, Table 2-10) to achieve the final desired product size distribution. It was decided to complete the screener tests with the 4760-μm screen and accept the inefficiency until the future planned testing of the UNIFRAME as a system demonstrates actual product size distributions.

TABLE 2-9
SCREENER TESTS WITH TERTIARY CRUSHER PRODUCT
(6350-μm Wire Mesh Screen)

Test No.	VC-37B	ST-C	ST-D
Lead angle (degrees)	70	70	70
No. bottom weights	2	1	2
Blinded holes (entire screen)	2	9	1
Estimated percent blinded	0.02	0.08	0.01
Holdup on screen (kg)	0.041	0.031	0.026
Holdup (%)	0.10	0.06	0.05
-4760-μm material in oversize crusher (kg)	0.026	0.038	0.040
-4760-μm material in oversize crusher (%)	0.1	0.1	0.1
Screening efficiency (%)	99.9	99.9	99.9
Feed material (tertiary test No.)	TC-25	TC-27	TC-27

TABLE 2-10
SCREENER TEST VC-38 WITH TERTIARY CRUSHER PRODUCT
(6350-μm Wire Mesh Screen)

	Product From Tertiary Crusher Test TC-28 (wt %)
Feed	
+6350 μm	1.44
-6350 μm +4760 μm	0.88
-4760 μm	97.68
Total	100.00
Screened Product Left on Screen	
+6350 μm	0.07
-6350 μm +4760 μm	0
-4760 μm	0
Total	0.07
Discharged to Oversize Crusher	
+6350 μm	0.27
-6350 μm +4760 μm	0.04
-4760 μm	0.04
Total	0.35
Passed Through Screen	
+6350 μm	0
-6350 μm +4760 μm	1.60
-4760 μm	97.98
Total	99.58
Screened Product Totals	
+6350 μm	0.34
-6350 μm +4760 μm	1.64
-4760 μm	98.02
Total	100.00

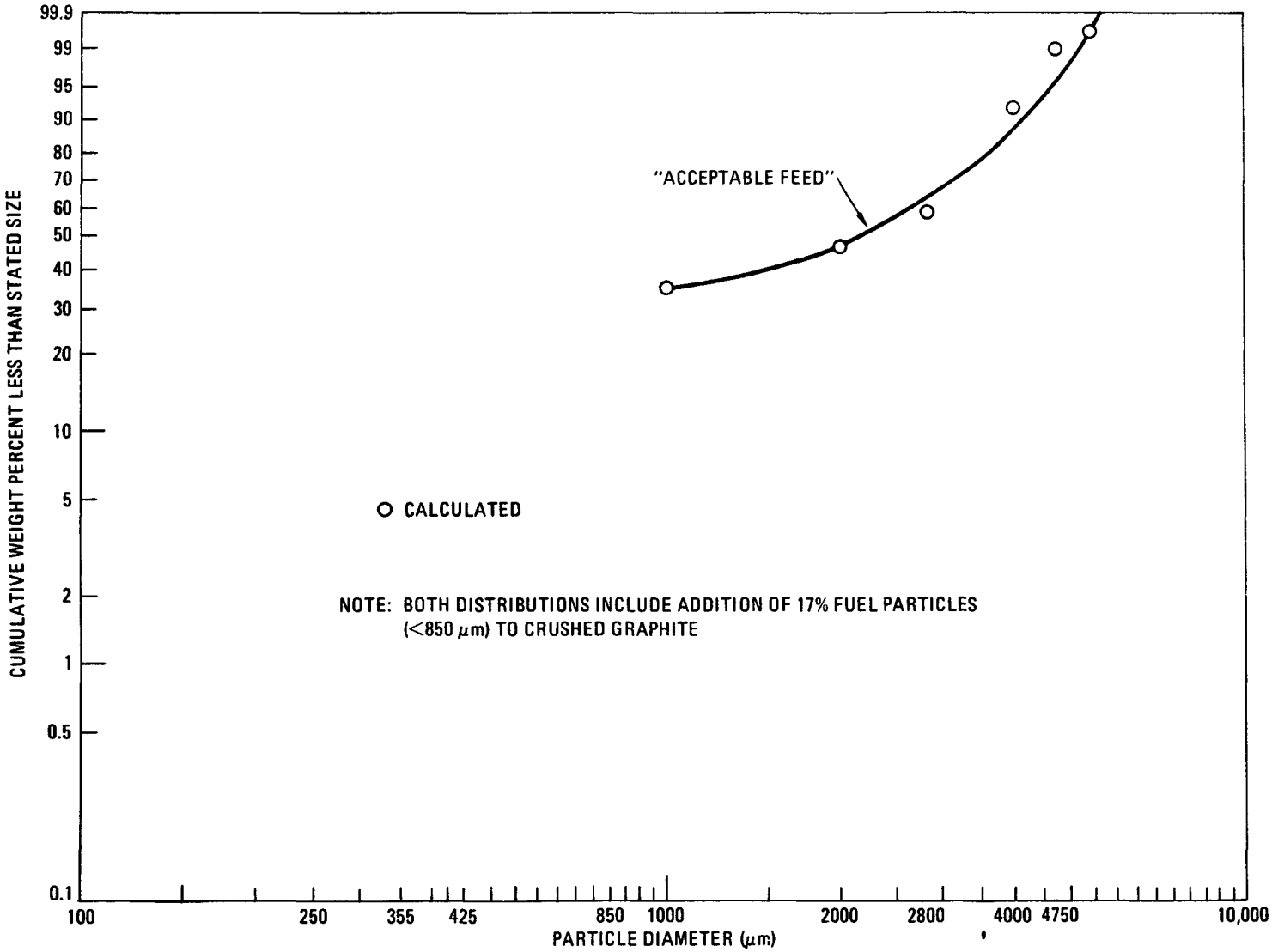

Fig. 2-6. Calculated UNIFRAME system crushed product distribution versus primary burner "acceptable feed" distribution

A comparison of results of screening a half-size fuel element, a full-size fuel element, and a half-size control rod element after crushing in the first three stages of the UNIFRAME system is shown in Table 2-11.

The total screening time in all tests was 15 min. However, the majority of the screening was completed shortly after each charge was complete, and the operation was continued solely to determine the quantity of material holdup left on the screen at the end of the allotted time for processing a fuel element. Holdup varied from a low of 0.3% to a high of 0.6%. Screener blinding varied from 0.6% to 1.0% of the total openings. The efficiency varied from a low of 88.6% with a full-size element to 98.5% with a half-size control rod element. Flooding of the screen due to the rapid charging rate contributed to the lowering of the efficiency in the full-size element tests. In a previous test (ST-B, Table 2-8) which had identical screening conditions to those of VC-37 with material from crushing a half-size fuel element, spreads of 0.2%, 0.04%, and 3.3% were observed in the results from blinding, holdup, and efficiency, respectively. With the data obtained to date, it is difficult to ascertain if the differences between half-size fuel elements, full-size fuel elements, and half-size control rod elements are significant enough to produce variability in the screening of their crushed products.

To demonstrate the ability of the screener to start under loaded conditions and to establish the potential effects on subsequent equipment from this condition, the screener was started after charging a crushed half-size fuel element and again after charging a crushed full-size fuel element. In each case, after charging and prior to starting the screener, the material that discharged "through" the screener, either through the mesh screen or by overflowing the screening table, was weighed and characterized, and the material that discharged through the oversize chute was similarly treated. The screener was then started and operated for 15 min, and the screener and oversize discharges were again weighed and characterized. These results are summarized in Table 2-12.

TABLE 2-11
UNIFRAME SCREENER PHASE I TESTS WITH HALF-SIZE FUEL ELEMENT,
FULL-SIZE FUEL ELEMENT, AND HALF-SIZE CONTROL ROD ELEMENT
(4750-μm Mesh Screen, Motion Generator 70° Lead Angle, One Bottom Weight)

	Test VC-37		Test VC-38B		Test VC-39	
Feed[a]	1/2 std. fuel element		1/2 control rod element		Full size std. fuel element	
Tertiary crushing time	1 min 29 sec		2 min 46 sec		3 min 32 sec	
Screener charging time	1 min 15 sec		1 min 20 sec		2 min 30 sec	
Total screening time	15 min		15 min		15 min	
Material holdup on screen	0.130 kg	0.3%	0.233 kg	0.6%	0.228 kg	0.3%
Blinded holes	73	0.6%	119	1.0%	116	1.0%
Total oversize	5.419 kg	13.4%	1.545 kg	3.7%	13.785 kg	16.3%
-4760-μm matl. in oversize crusher	3.232 kg	8.0%	0.624 kg	1.5%	9.630 kg	11.4%
Efficiency	--	92.0%	--	98.5%	--	88.6%
Material through screen	37.750 kg	86.2%	39.850 kg	95.7%	70.600 kg	83.4%

[a] After primary, secondary, and tertiary crushing.

TABLE 2-12
UNIFRAME SCREENER PHASE I TESTS (START-UNDER-LOAD)
(4750-μm Mesh Screen, Motion Generator 70° Lead Angle, One Bottom Weight)

	Test VC-40		Test VC-42	
Feed	1/2 std. fuel element		Full-size std. fuel element	
Prior to Startup	2.208 kg	5.2%	17.127 kg	20.2%
Material through screener	2.155 kg	5.1%	5.982 kg	7.1%
+4750 μm	0.006 kg	<0.1%	0.675 kg	0.8%
-4750 μm	2.149 kg	5.1%	5.307 kg	6.3%
Material to oversize	0.053 kg	0.1%	11.145 kg	13.1%
+4750 μm	0.007 kg	<0.1%	0.917 kg	1.1%
-4750 μm	0.046 kg	0.1%	10.228 kg	12.0%
During 15-Min Screening	39.945 kg	94.5%	67.542 kg	79.6%
Material through screener	26.397 kg	62.4%	62.487 kg	73.6%
+4750 μm	0.147 kg	0.3%	1.237 kg	1.4%
-4750 μm	26.250 kg	62.1%	61.250 kg	72.2%
Material to oversize	13.548 kg	32.1%	5.055 kg	6.0%
+4750 μm	0.586 kg	1.4%	0.335 kg	0.4%
-4750 μm	12.962 kg	30.7%	4.720 kg	5.6%
Totals	42.274 kg	100%	84.810 kg	100%
Material Hold-up on Screen	0.121 kg	0.3%	0.141 kg	0.2%
Blinded Holes	42	0.4%	71	0.6%
Material Through Screener	28.552 kg	67.5%	68.469 kg	80.7%
+4750	0.153 kg	0.3%	1.912 kg	2.2%
-4750	28.399 kg	67.2%	66.557 kg	78.5%
Material to Oversize	13.601 kg	32.2%	16.200 kg	19.1%
+4750	0.593 kg	1.4%	1.252 kg	1.5%
-4750	13.008 kg	30.8%	14.948 kg	17.6%

The material that passed "through" the screener prior to startup was 5.1% of the total weight of the crushed half-size fuel element and increased to 7.1% with the full-size fuel element. This was the obvious result of additional overflow of the screening table from the increased charge. Although only a small quantity of material (0.1%) discharged through the oversize chute prior to startup with the half-size element, a reasonably large percentage (13.1%) discharged through the oversize chute with the full-size element. The difference is again attributable to the larger charge.

In both tests the screener started up without difficulty and was accompanied by unscreened material discharging both over the screening table and through the oversize discharge chute. Under these conditions, the material which discharged through the oversize chute was a larger percentage in the half-size element test (32.1%) than in the full-size element test (6.0%). The large oversize discharge during charging and the large quantity of material which discharged over the screening table after startup in the full-size element test contributed to equilization of the total quantity of material which discharged through the oversize chute for both sizes of elements (i.e., 13.601 kg for the half-size element and 16.200 kg for the full-size element).

These tests demonstrate that in the event it becomes necessary to start the screener under a loaded condition, (1) the oversize crusher will be required to process additional quantities of material with the potential for excessive fuel particle breakage and (2) the primary burner feed will contain quantities of unacceptable material which has bypassed the screening completely. In addition, the large quantity of material which rapidly enters the pneumatic transport line at startup under load tends to place a burden on the transport system.

2.5. SECONDARY CRUSHER MODIFICATIONS (J. W. Baer)

Design modifications were made to the secondary stationary jaw and the wear plate of the secondary Pitman to alleviate the problem of bridging of

large fragments entering from the primary crusher. These modifications involved deepening of the crushing cavity by approximately 20 cm and continuing for the full depth of the cavity the nominal 14° crushing angle between the stationary jaw and the Pitman wear plate. These changes will permit the secondary crusher to accept and crush, at the 14° angle, fragments up to a 15-cm ring size.

The modification to the stationary jaw (5210034) consisted of extending one of the crushing faces by approximately 9.5 cm. The changes in the wear plate of the Pitman wear plate assembly (5210032) were more extensive, involving not only extending the crushing face but also creating a flat surface on the extension and on the unaltered portion of the wear plate. As a result of these changes, the depth and opening of the crushing cavity were increased and the maximum nominal nip angle was prevented from exceeding 14°. These modifications are shown in Fig. 2-7. Figures 2-8 and 2-9 illustrate the difference in the configuration of the Pitman wear plate before and after modification.

The modifications to the components have been completed and will be evaluated during shakedown testing for Phase II system tests.

The problem with overheating of the secondary Pitman bearings which was encountered in Phase I testing was determined to result from improperly fitted bronze bearing sleeves. New sleeves were installed and bored for proper clearance with the shafts. The units were refitted on the Pitman shaft and installed into the UNIFRAME with the modified secondary Pitman assembly.

2.6. DESIGN EVALUATION

The initial issue of a functional level diagram for the Fuel Element Size Reduction System has been prepared for preliminary internal review and modification.

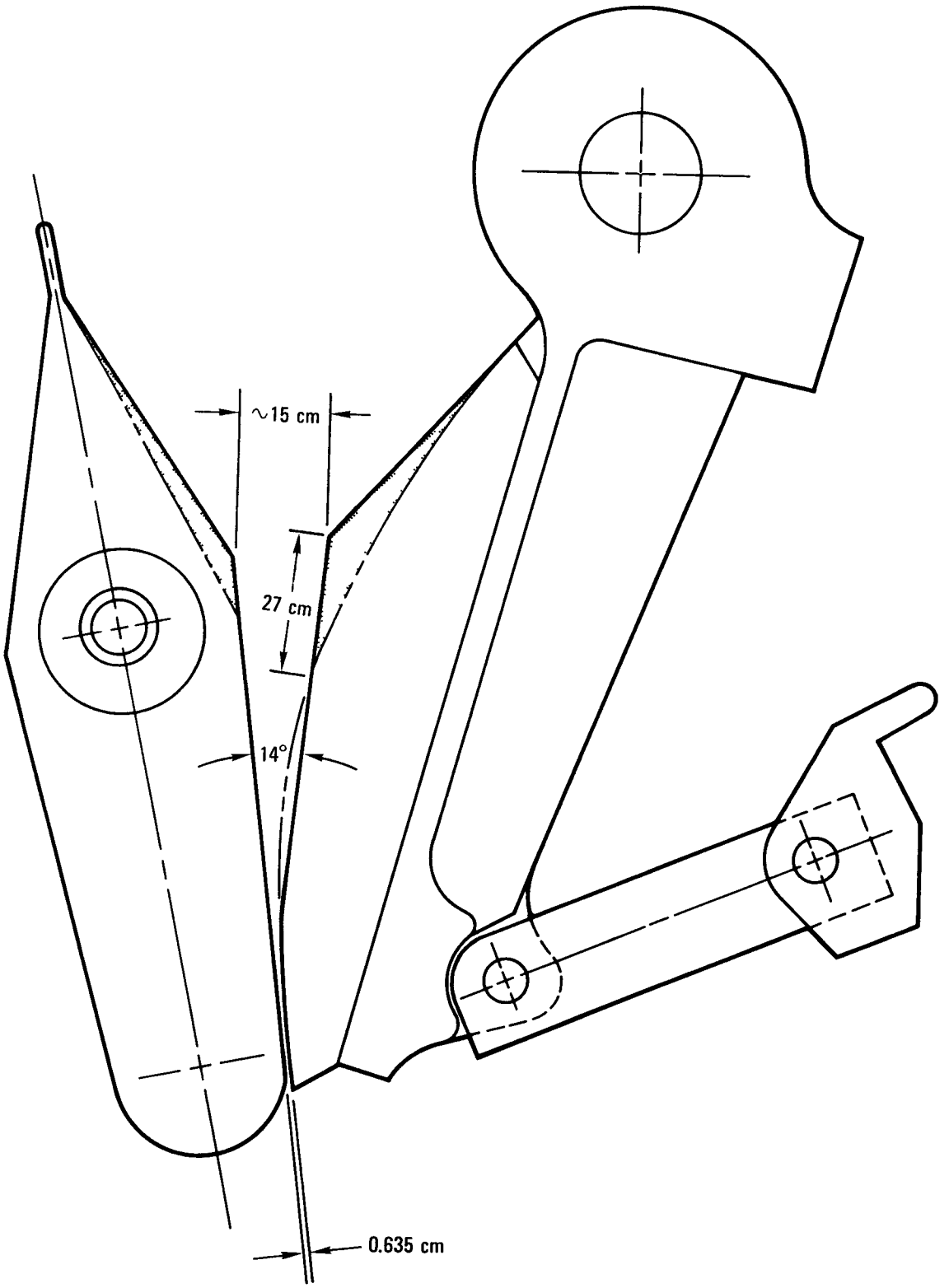

Fig. 2-7. Secondary crusher modification showing deeper crushing cavity and 14° nip angle

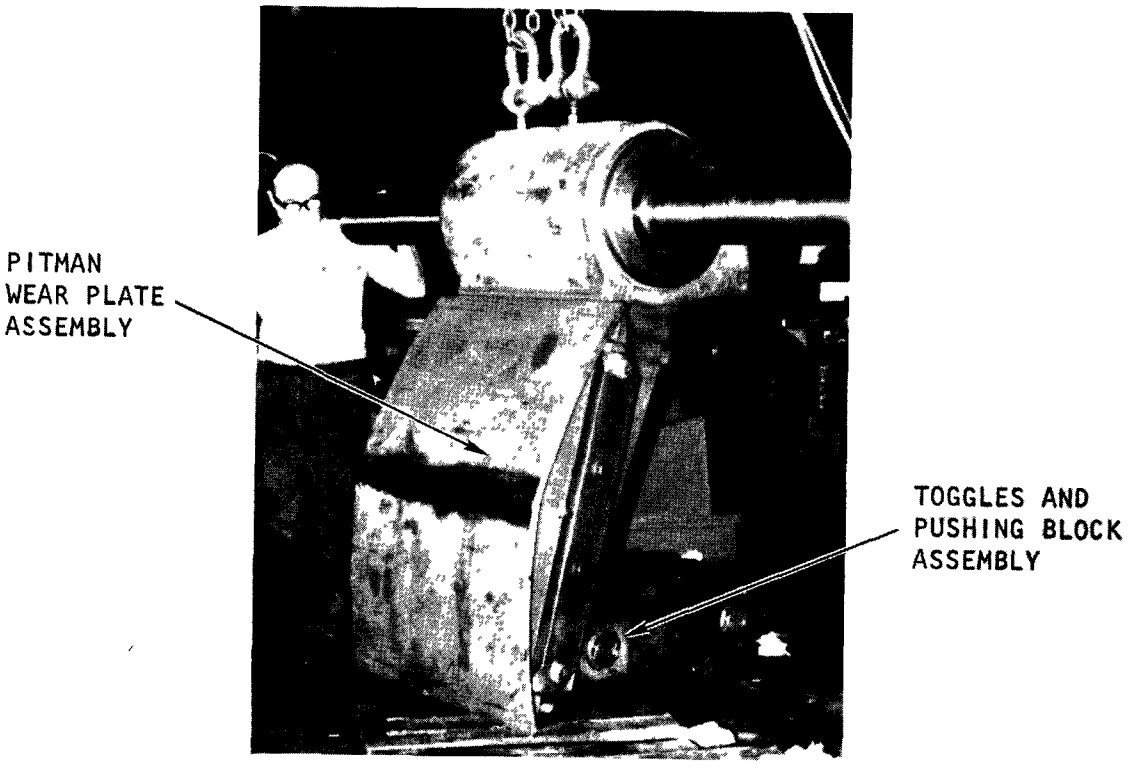

Fig. 2-8. Secondary crusher Pitman assembly with original wear plate

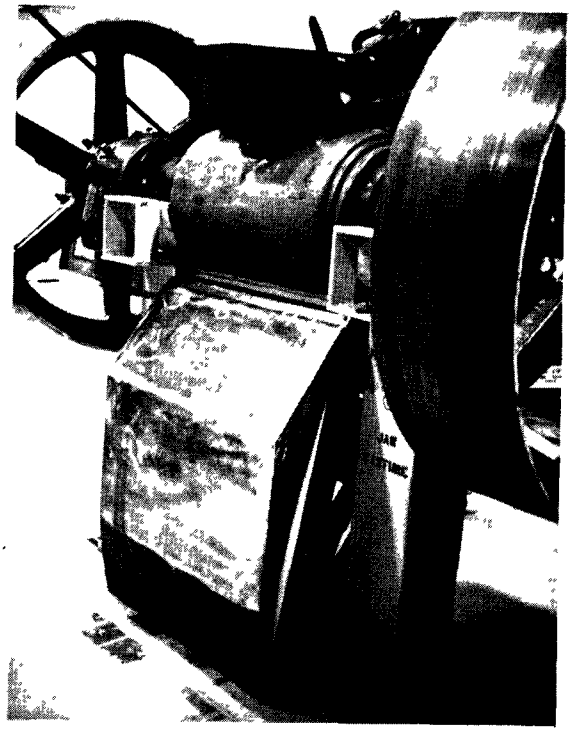

Fig. 2-9. Secondary crusher Pitman assembly with modified wear plate and machined flat

2.7. REDESIGN

Investigation into redesign of the Pitman shaft bearings and lubrication system has begun in order to eliminate conventional lubrication methods and materials. Solid graphite, self-lubricated bearings are being studied in cooperation with a manufacturer of engineered carbon materials.

2.8. REMOTE HANDLING SYSTEM

Repairs to the damaged toggle lift hook drive assembly of the secondary Pitman lift fixture were completed. Proper adjustment of the limit switch which controls the maximum upper travel of the toggle hook proved successful in avoiding damage and assuring the proper positioning of the hook during reinstallation of the secondary crusher.

During reinstallation of the secondary crusher, the lift fixture failed as a result of pull-out of the thrust bearings at the ends of the slide-block drive screw. This failure was unrelated to the previous toggle lift hook drive assembly failure, being instead a result of improper orientation of the thrust bearings. The bearings have been replaced with properly oriented bearings and the fixture is operational.

2.9. CONCLUSIONS

Phase I individual tests of the tertiary crusher revealed no obvious problems, and the tertiary crusher is ready for testing in the UNIFRAME as a system without modification.

Phase I individual tests of the oversize crusher produced throughputs in excess of requirements but revealed potential material holdup areas and the presence of small quantities of oversize material in the product. Design changes are under study for reducing the potential for material holdup. The quantity of oversize material in the product will be monitored in the system tests, and its effect on primary burner feed requirements will be assessed.

Phase I individual tests of the screener revealed the necessity for using a wire mesh screen and a self-cleaning device to reduce blinding. Desired screening efficiencies could not be achieved with a 4750-μm screen but should result in an acceptable product size distribution. The accompanying increase in material discharged to the oversize crusher should be easily accommodated by the crusher's throughput capacity.

Start-under-load is easily achieved with the screener, but this upset condition has potentially negative effects on the operations of subsequent equipment.

The problem of bridging of large fragments and their subsequent failure to crush in the secondary crusher was attributed to an excessive nip angle at the point of contact with the large fragments. Modifications made to reduce the nip angle to 14° will be tested in Phase II of the test program.

Proper adjustment of the limit switch on the toggle lift hook of the semiremote lift fixture was all that was required for proper operation of the hook. Improper orientation of thrust bearings caused failure of the drive screw during a subsequent installation of the secondary crusher. New bearings have been installed properly and should eliminate this problem.

3. CRUSHED FUEL ELEMENT BURNING

3.1. PRIMARY BURNING SUMMARY

Heat transfer coefficients were calculated from data obtained in four of the six 0.40-m primary burner heatup runs. The results indicated significantly smaller wall-to-bed heat transfer coefficients for deep beds heated with the dual (upper and lower) induction coils compared with shallow beds heated with the single, lower coil. This confirmed earlier qualitative observations (Ref. 3-1) that use of the single, lower coil and a minimum bed size is more favorable for both startup of fresh feed and product bed tailburning than use of a deep bed and both induction coils. The data illustrated the response of the heat transfer coefficient to changes in temperature, gas velocity, and particle size.

The Grafoil seal which prevents leakage of cooling air from the 0.40-m cooling jacket was damaged during inspection of the plenum assembly. The Grafoil seal has been replaced with machined sections of graphite, and preparations are being made to reinstall the plenum.

Six runs were made on the 0.20-m primary burner during the reporting period. The initial four runs were made to test the Diogenes automatic control system as called for in Module 7 of the Activity Plan. The runs demonstrated that the proposed automatic control philosophy was applicable in primary burner operation. The fifth run was an attempted 48-hr run which was curtailed after ∿12 hr due to mechanical failures in burner subsystems. The run data indicated that the use of BISO-coated fertile particles and TRISO-coated fissile particles requires higher velocities for adequate fluidization than the BISO fertile and TRISO fertile particles used in prior operations. An extension of the startup O_2 ramp to maximum level was also necessary. The sixth run was made to test operating parameters which were revised based upon the need for the extended O_2 ramp

period and higher fluidization velocity, and also to check the burner subsystem repairs.

Other significant 0.20-m burner work included fabrication and initial testing of an electrical resistance probe bed level sensor and preliminary heat transfer design calculations for determining the cooling requirements to maintain the recycling fines cyclone exit temperature at ∿500°C. The results of the level sensor tests were very promising. The heat transfer design calculations indicate that for a system insulated to ensure surface temperatures of <60°C (HETF criteria), the existing 0.20-m off-gas piping and cyclone surfaces would require finned extension and air cooling to yield an ∿500°C cyclone exit temperature. This temperature is the safe design operating limit of the present fines recycle rotary valve.

3.2. PROTOTYPE 0.40-m PRIMARY BURNER

3.2.1. 0.40-m Burner Bed Depth for Heatup and Tailburning (D. T. Young)

3.2.1.1. Introduction

Preliminary results from the 0.40-m primary burner heatup tests reported in Ref. 3-1 indicated (1) heatup times were similar for single or dual induction heating, but differences in bed material carryover and in-bed temperature profiles made the smaller beds heated with the single coil appear preferable, and (2) a general improvement in bed solids mixing may be expected in the 0.40-m-diameter vessel relative to the 0.20-m-diameter burner. The objectives in the current quarter were to use the heatup test data to better quantify the differences between single coil heating of beds with L/D ∿ 2 to 3 and dual coil heating, which requires beds with L/D ∿ 4 to 5 (L is the height to the top of the static bed measured from the top of the cone distributor; D is the burner internal diameter, or 0.40 m in this case). The heat transfer calculations coupled with material balances and fuel particle breakage calculations provided the information required to quantify the effects of deep bed versus shallow bed startup and tailburning. Four runs were compared for effects of bed depth: run A-2.1, a

heatup using the lower coil to heat a shallow bed of carbon-coated TRISO fertile fuel particles; run A-2.2, which used the lower and upper coils to heat a deep bed of fuel particles; run A-3.1, which used a shallow bed, lower coil operation with a fresh feed mixture consisting of 83 wt % of graphite mixed with 17 wt % fuel particles; and run A-3.2, a dual coil, deep bed test with the fresh feed mixture. Runs A-2.1 and A-2.2 related to tailburning product beds and runs A-3.1 and A-3.2 to startup of fresh feed beds. Two additional runs, the initial graphite bed heatup and an additional particle bed heatup for pneumatic transport study, were not applicable to comparative analysis and are not included in the discussion of experimental results.

3.2.1.2. Experimental Results

Table 3-1 summarizes the results obtained from the four 0.40-m heatup runs described above. The "Material Elutriation" columns refer to material which was carried out of the burner tube due to excessive slugging or gas velocity. The oxides found in this elutriated material were used to calculate "Particle Breakage" as a weight percent of the total particles fed to the burner and fluidized (see Section 7.4.1.2.3 for a discussion of particle breakage in both this case and the case of pneumatic transport of the bed material). The overall and internal heat transfer coefficients given in Table 3-1 are results obtained at comparable temperature, velocity, and gas flow values given in Table 3-2 and are beneficial to the evaluation of heatup or tailburning with shallow versus deep beds. The "Initial Velocity Required for Heatup" of Table 3-1 is the velocity required to initiate sufficient mixing of ambient startup material to transfer wall heat into the bed. This velocity is critical in startup operations, as discussed in Ref. 3-1. Finally, the "Heatup Time" and "Comments" columns present data that were briefly treated in Ref. 3-1.

The material elutriation data for the fuel particle tests show the negative effects of the deep bed used in run A-2.2 compared with the shallow bed of run A-2.1. Carryover of the fuel particles shown in the

TABLE 3-1
0.40-m PRIMARY BURNER HEATUP TEST - GENERAL MATERIAL BALANCE AND HEAT TRANSFER RESULTS

Run	Material Into Burner (kg)	Induction Coil Use	Material Elutriation				Particle Breakage[a] (wt % of feed)	Bed Material Transported (kg)
			≥850μm (kg)	≥425μm (kg)	≤425μm (kg)	Oxides (kg)		
A-2.1	180 (f.p.)[b]	Single	0.055	0.074	1.047	0.277	0.31	≤178
A-2.2	470 (f.p.)[b]	Double	0.002	16.478	3.427	1.849	0.78	≤448
A-3.1	130 (f.f.)[b]	Single	Nil	0.008	9.231	0.105	1.5	≤120
A-3.2	220 (f.f.)[b]	Double	Nil	0.002	5.261	0.25	1.0	≤214

[a] Calculated based on: $\dfrac{\text{(g oxides elutriated with fines)}}{\text{(weight of material fed to burner)}} \dfrac{\left(\dfrac{\text{total particle weight}}{\text{weight of } ThO_2 \text{ in particle}}\right)}{\text{(fraction of particles in feed)}}$

[b] (f.p.) = carbon-coated TRISO "A" fertile particles (bulk density ∿ 2000 kg/m^3; diameter ∿ 600 to 850 μm,
(f.f.) = 83% <3/16-in. ring size graphite + 17% TRISO fertile fuel particles.

TABLE 3-1 (Continued)

Run	$\bar{U}_{Heated}$ (a,b) (W/m^2-K)	$\bar{h}_{i_{Heated}}$ (a,b) (W/m^2-K)	$\bar{U}_{Above\ coil}$ (a,b) (W/m^2-K)	$\bar{h}_{i_{Above\ coil}}$ (a,b) (W/m^2-K)	Initial Velocity Required for Heatup (m/s)	Heatup Time to 708°C (min)	Comments
A-2.1	523	602	47.7	48.5	0.550	120	Heating delayed ~60 min due to feeder problem
A-2.2	381	423	142.2	149.3	0.460	140	Heatup delayed ~50 min to replace a blown fuse
A-3.1	414	456	48.5	49.4	0.305	90	Lower to upper bed $\Delta T < 15°C$ (excellent startup)
A-3.2	322	351	84.1	86.6	0.340	60	Poor mixing as upper bed was 600°C hotter than lower bed in initial 15 min of heating

(a) $\bar{U}_{Heated}$ = overall in-bed heat transfer coefficient,

$\bar{h}_{i_{Heated}}$ = internal in-bed heat transfer coefficient,

$\bar{U}_{Above\ coil}$ = overall above-bed heat transfer coefficient,

$\bar{h}_{i_{Above\ coil}}$ = internal above-bed heat transfer coefficient.

(b) From induction heating of in-bed walls in runs at comparable temperature, velocity, and gas flow rate (Table 3-2).

TABLE 3-2
0.40-m PRIMARY BURNER HEATUP TEST[a] HEAT TRANSFER DATA AND RESULTS

Run	Time	CO_2 Flow Rate (std. m^3/s)	In-bed Gas Velocity (m/s)	Mean Wall Temp. (Heated) (°C)	Bed Temp. (°C)	Mean Wall-Bed ΔT (°C)	Induction Power (kW)	Net Heat Input, Q (kW)	Wall Area Heated, A (m^2)
A-2.1	1313	0.0463	1.23	800	670	130	98.6	68.6	1.151
A-2.1	1510	0.0382	1.03	779	680	99	82.9	59.4	1.151
A-2.1	1642	0.0340	0.92	792	685	107	81.8	56.7	1.151
A-2.1	1837	0.0492	1.27	770	640	130	98.6	71.5	1.151
A-2.1	2003	0.0538	1.22	655	530	125	82.9	57.8	1.151
A-2.2	1449	0.0386	1.05	778	690	88	100.8	77.3	2.302
A-3.1	1342	0.0388	1.06	817	695	122	87.4	58.0	1.151
A-3.2	1310	0.0390	1.05	769	680	89	94.1	66.1	2.302

TABLE 3-2 (Continued)

Run	Time	$\bar{U}_{(Heated)}$ (W/m^2-K)	$\bar{h}_{i\ (Heated)}$ (W/m^2-K)	$T_{CO_2,\ in}$ (°C)	$C_{P_{CO_2},out}$ (J/kg-K)	$T_{CO_2,out}$ (°C)	$C_{P_{CO_2},out}$ (J/kg-K)	$\dot{m}_{CO_2}$ (kg/s)
A-2.1	1313	460	523	20	825	505	1155	0.0909
A-2.1	1510	523	602	20	825	490	1147	0.0749
A-2.1	1642	460	523	20	825	483	1143	0.0668
A-2.1	1837	477	544	20	825	496	1151	0.0966
A-2.1	2003	402	452	20	825	445	1126	0.1056
A-2.1	1449	381	423	20	825	524	1163	0.0759
A-3.1	1342	414	456	20	825	469	1139	0.0763
A-3.2	1310	322	351	20	825	505	1155	0.0767

TABLE 3-2 (Continued)

Run	Time	$Q_{CO_2,out}$ (kW)	Heat Loss Above Coil, Q_{AC} (kW)	Wall Area Above Coil (m^2)	Wall-Bed $\overline{\Delta T}_{AC}$ (°C)	$\bar{U}_{(Above\ Coil)}$ (W/m^2-K)	$\bar{h}_{i\ (Above\ Coil)}$ (W/m^2-K)
A-2.1	1313	51.5	17.1	3.989	100	42.7	43.5
A-2.1	1510	40.9	18.5	3.989	97	47.7	48.5
A-2.1	1642	35.7	21.0	3.989	96	54.8	56.1
A-2.1	1837	53.5	18.0	3.989	99	45.6	46.4
A-2.1	2003	51.1	6.7	3.989	94	17.9	18.0
A-2.2	1449	45.0	32.3	2.838	80	142.2	149.3
A-3.1	1342	39.4	18.6	3.989	96	48.5	49.4
A-3.2	1310	43.4	22.7	2.838	95	84.1	86.6

(a) Underlined data obtained at comparable in-bed operating conditions (temperature, velocity, gas flow rate).

(b) Taken from T/C 18 - T/C 11.

"$\geq$425 μm" column illustrates that the maximum slug height of the deep A-2.2 bed was higher than the burner tube. The particle breakage values indicate a much higher fuel particle attrition rate in the deep, heavily slugging bed.

The values for material elutriation for the fresh feed fluidization tests, A-3.1 and A-3.2, show a trend opposite to that described above. It is assumed that higher breakage occurred with the deeper slugging fresh feed bed, although the data do not clearly show this. The breakage data were based upon a calculated value for the weight of particles in the bed. Prior to these two tests, the feed hopper was filled with sufficient feed for the deeper bed. Part of this material was used for run A-3.1 and was subsequently reused in run A-3.2 along with the additional hopper contents. This obscured the data because (1) the material segregates by density in the hopper and consequently more particles were in the bed in run A-3.1 than were calculated, making the calculated breakage number too high; and (2) reusing the material from run A-3.1 preferentially removed particles with defective coatings.

The values given in Table 3-1 for in-bed heat transfer at comparable process conditions show that deeper beds limit the bed solids capability to pick up and retain heat from the wall. This is an indication of a decrease in bed solids mixing in the radial bed to wall direction and an increase in the axial heat loss due to solids slugging out of the heated zone. This axial heat loss increase is reflected in an increase of the above-bed heat transfer coefficient.

The initial velocity required for heatup data in Table 3-1 do not show significant differences when shallow beds are compared with deep beds. These data were discussed in Ref. 3-1 in terms of an overall mixing improvement when similar materials are fluidized in the 0.40-m-diameter burner versus the 0.20-m-diameter burner.

The time to heat the beds to 700°C and pertinent comments given in Table 3-1 quantify the statements made in Ref. 3-1 regarding heatup time.

The most significant point here is the temporary 600°C segregation of temperature between the upper bed and the lower bed during heatup of the deep fresh feed bed in run A-3.2. This indicated partial mixing of the bed as the upper zone of the deep bed, having an inherently smaller particle size, was mixing but not transferring heat down into the lower zone of larger particles. This same segregation of particle sizes may occur with shallower beds, but the relative effect on the overall bed mixing is apparently much less significant.

3.2.1.3. Conclusions and Recommendations

The single coil, shallow bed heating operation is recommended in preference to dual coil, deep bed startup or tailburning for the following reasons:

1. Elutriation of bed material in slugging is more probable with deep beds.

2. In-bed heat transfer is increased with shallower beds, allowing more efficient startup and tailburning.

3. Heat loss to the upper burner areas is decreased with shallower beds.

4. The tendency for segregated bed particle sizes affecting a segregating bed temperature is reduced with shallower beds.

3.2.2. 0.40-m Primary Burner Heat Transfer Study (R. T. Stula)

3.2.2.1. Introduction

Heat transfer data were obtained during 0.40-m primary burner tests A2 and A3 in accordance with the Activity Plan (AP524401). Mean internal heat transfer coefficients, $\bar{h}_i$, were calculated at various operating conditions

for both fresh feed and particle beds. These tests will verify burner design calculations as well as increase understanding of process phenomena.

3.2.2.2. Experimental Results

The four individual heatup runs described in Section 3.2.1 were utilized to provide heat transfer data. All data were obtained at steady-state conditions; for each point, power input data, temperature readouts, and gas flow rates were recorded. In the case of run A-2.1, five individual data points were recorded at varied power rates, temperatures, and gas flow rates (velocities).

The mean overall heat transfer coefficient, $\bar{U}$, between the burner wall and fluid bed is calculated using the following equation:

$$\bar{U} = \frac{Q}{A\overline{\Delta T}} \quad , \tag{3-1}$$

where Q/A = heat flux through the wall (W/m^2-K),
$\overline{\Delta T}$ = mean difference between the outside wall temperature and fluid bed temperature (°C).

From Eq. 3-1, the mean internal bed to wall heat transfer coefficient, $\bar{h}_i$, may be calculated:

$$\bar{U} = \frac{1}{1/\bar{h}_i + t/\bar{k}} \quad , \tag{3-2}$$

where $\bar{h}_i$ = mean internal bed to wall coefficient (W/m^2-K),
t = wall thickness (m),
$\bar{k}$ = mean wall conductivity (W/m^2-K).

For the 0.40-m burner, t = 6.35×10^{-3} m (1/4 in.) and

k(Hastelloy X) = 27.3 W/m-K at 900°C ,
= 25.1 W/m-K at 800°C ,
= 23.0 W/m-K at 700°C .

The total induction heat input into the fluid bed, Q, is determined by actual power measurement during steady-state operation and then subsequently corrected for conduction and electrical losses. Conduction losses were calculated based on temperature data, while electrical losses were calculated as insignificant. Mean bed-to-wall temperature differences were determined using a step-wise integration procedure utilizing thermocouples located at various elevations both in the burner and on the outer wall.

Table 3-2 presents the experimental heat transfer data and results. Once $\bar{U}$ and $\bar{h}_i$ are determined for the heated section of the vessel, an overall heat balance (Fig. 3-1) may be performed to determine the U and h_i for the section of the vessel above the active heating coil(s). The results of these calculations are also presented in Table 3-1.

Figures 3-2 and 3-3 present data taken during run A-2.1 at two different steady-state points. The gas velocity through the bed opposite the lower coil (Fig. 3-2) was essentially constant for these two points. Results show an increase in $\bar{h}_i$ as temperature increases over the range 540° to 670°C. Similarly, Fig. 3-3 shows an increase in h_i as temperature increases at constant velocity for the section of wall above the lower induction coil. With relatively few bed particles in the space above the lower coil, a significant decrease in h_i would be expected in this region. Calculations show h_i to be approximately 10 times greater for the heated wall than for the non-heated wall, as expected for a dilute solids phase heat transfer.

Figures 3-4 and 3-5 show the effect of fluidization velocity (i.e., mixing, slugging, bed porosity, etc.) on h_i at three different steady-state points. In the case of the heated section of wall and bed solids (Fig. 3-4), a maximum in the curve is observed. As velocity is increased from a low value, the bed goes from a static condition to one of minimum fluidization and expansion and then to a bubbling condition. As these changes occur, the primary result is a continually increasing degree of solids mixing and particle-to-wall contact. The internal heat transfer coefficient, h_i, increases until a certain velocity is reached, whereupon it

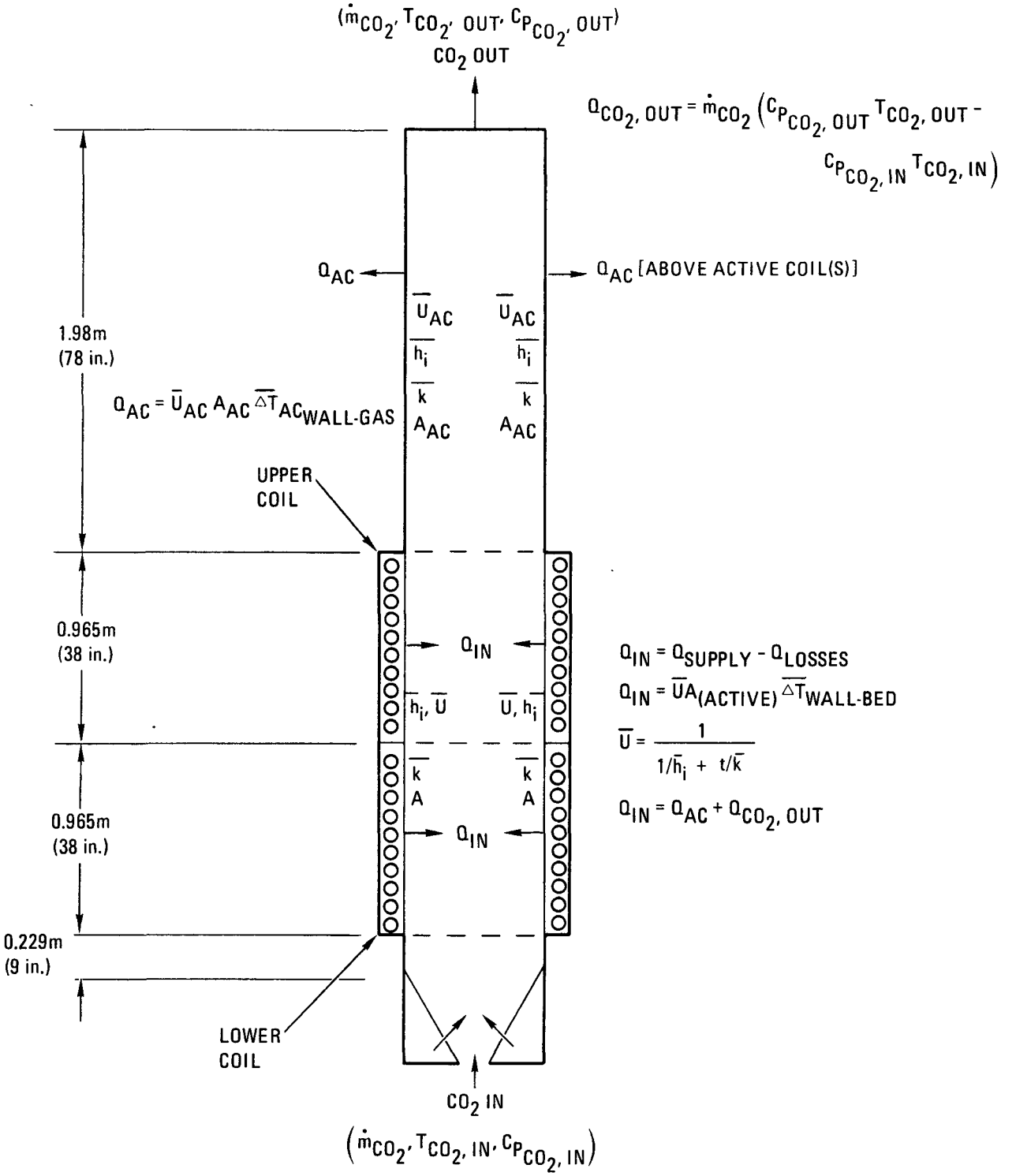

Fig. 3-1. 0.40-m primary burner heat balance

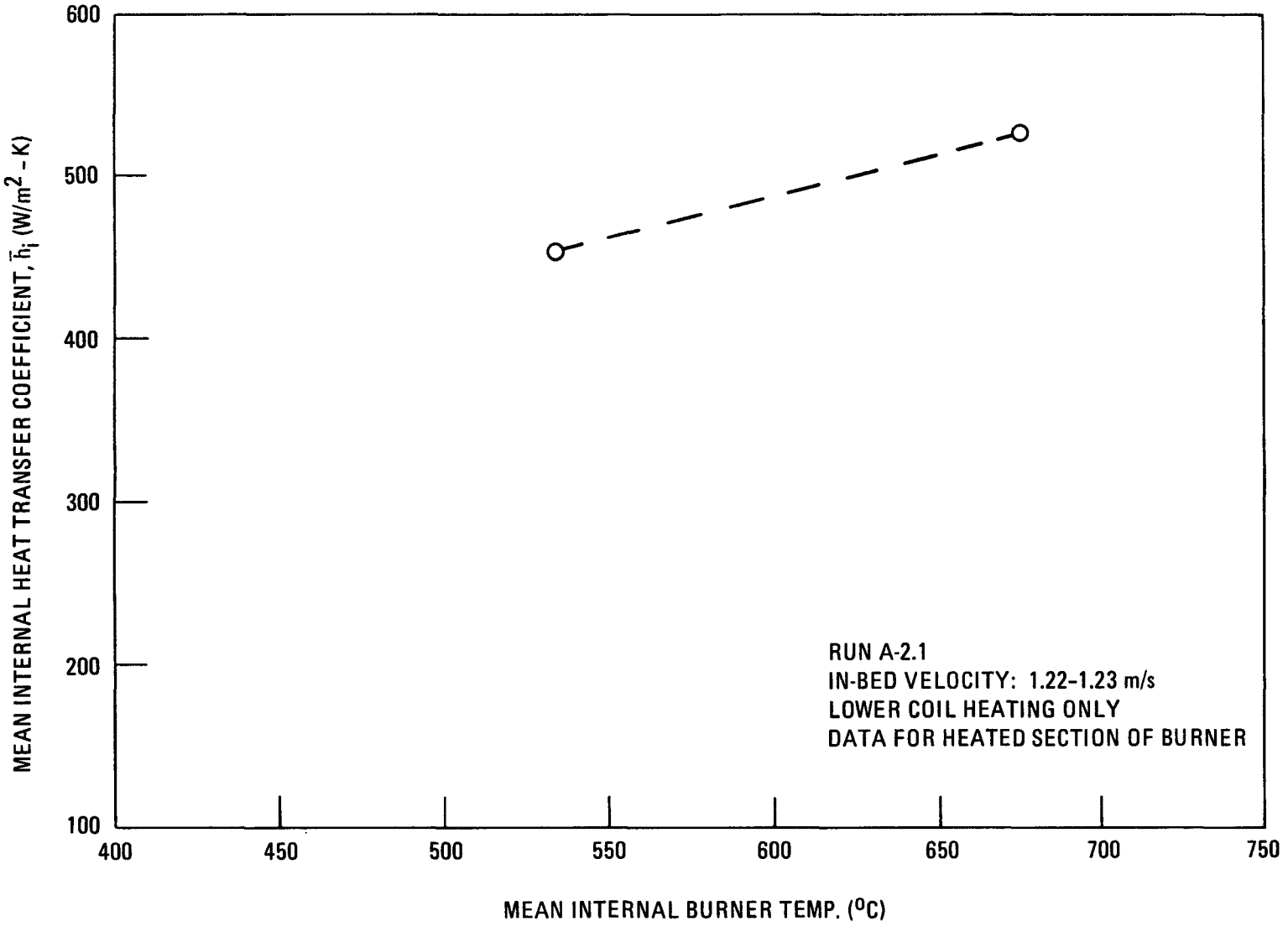

Fig. 3-2. Effect of temperature on in-bed heat transfer - 0.40-m primary burner

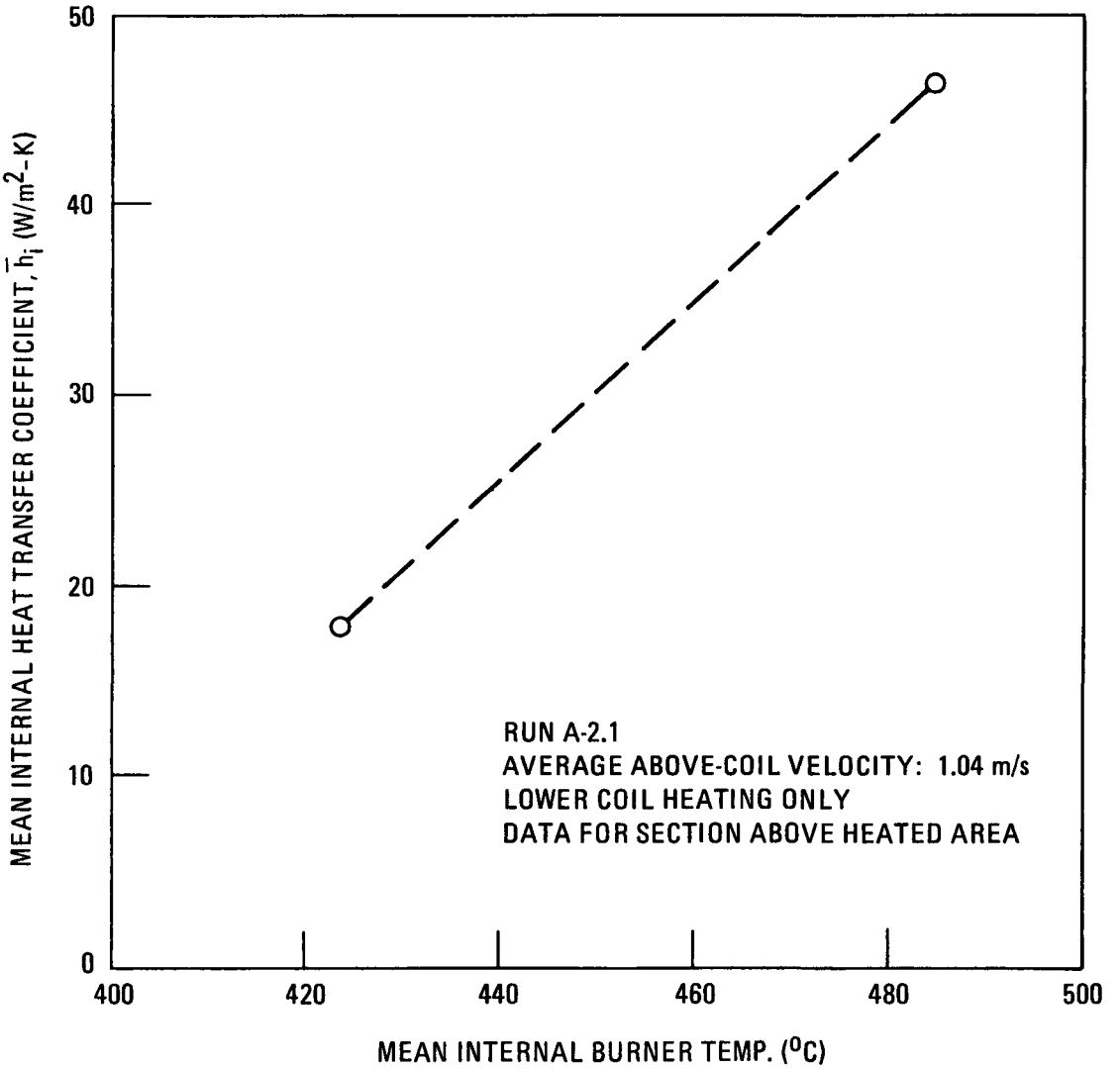

Fig. 3-3. Effect of temperature on above-bed heat transfer - 0.40-m primary burner

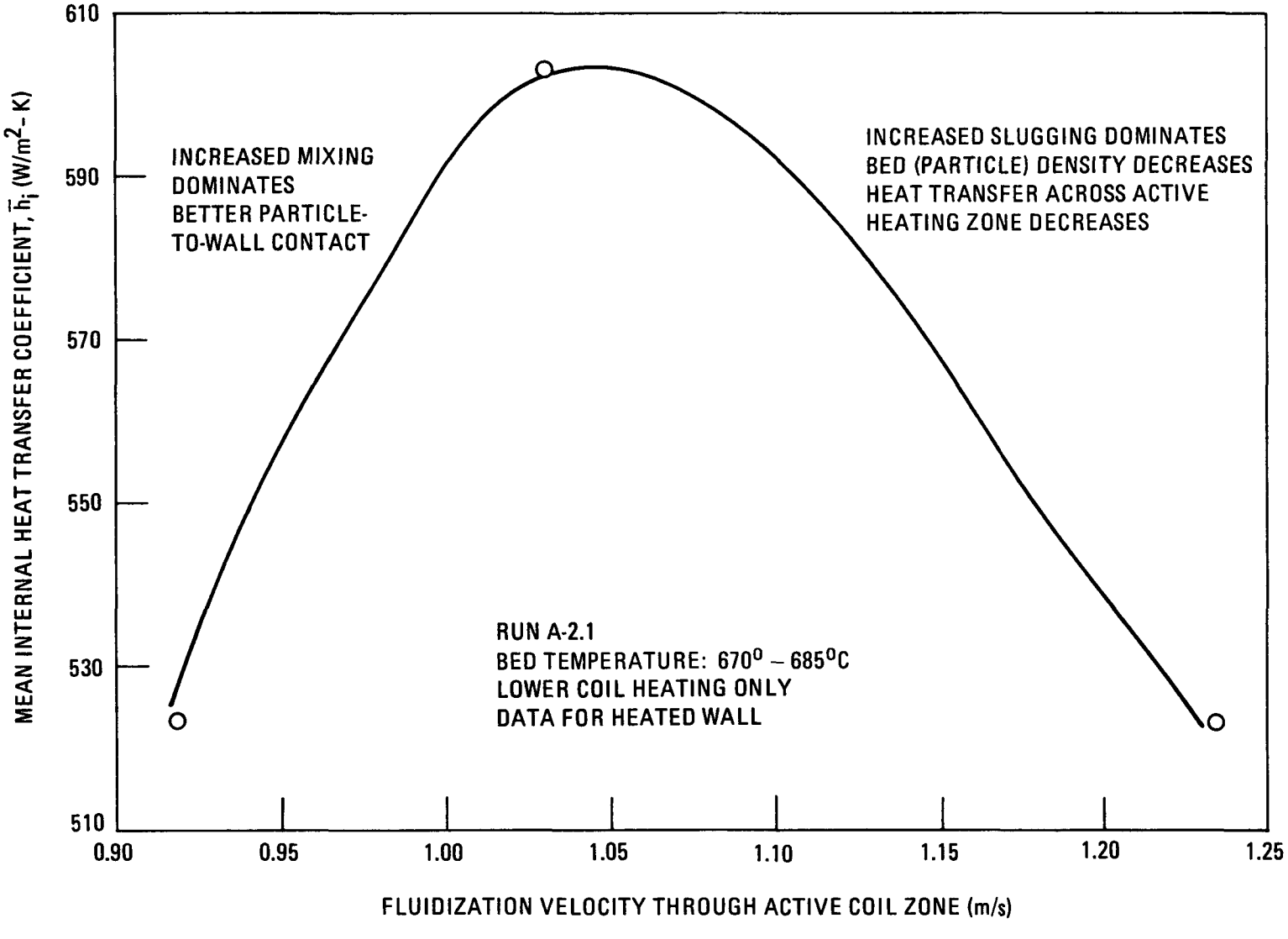

Fig. 3-4. Effect of fluidization velocity on in-bed heat transfer - 0.40-m primary burner

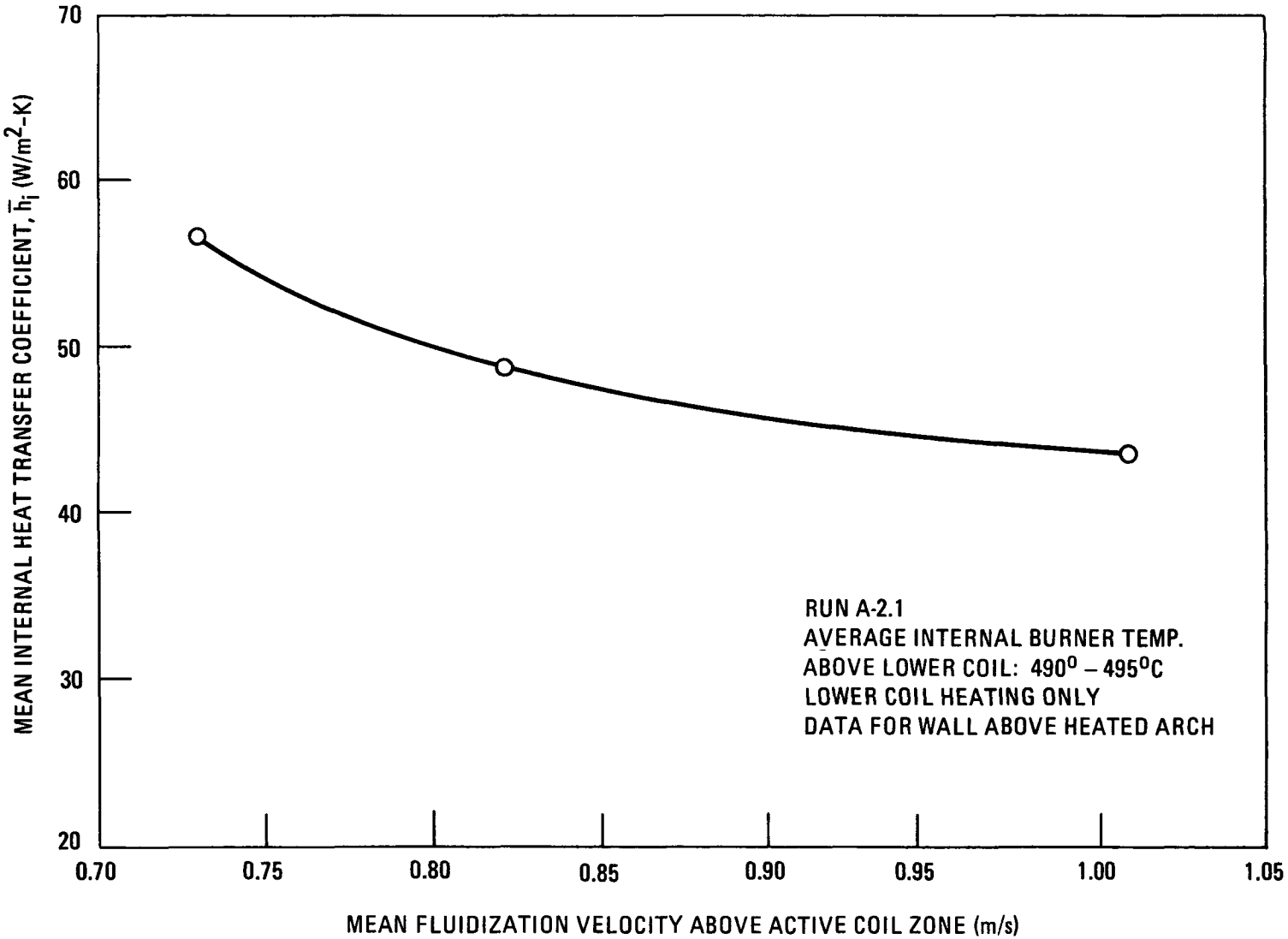

Fig. 3-5. Effect of fluidization velocity on above-bed heat transfer - 0.40-m primary burner

starts to decrease. This occurs as bubble size and the degree of solids slugging increase. Slug height increases with velocity; hence, increased bubble size and slugging result in a decreased particle density in the lower heated section of the burner. Particle-to-wall contact in this region occurs less frequently and heat transfer is adversely affected.

The effect of gas velocity on h_i above the heated wall is shown in Fig. 3-5 for three different steady-state points in run A-2.1. As mean gas velocity increases, h_i decreases. This is explained by the fact that as velocity is increased, slugging characteristics change from axisymmetric formation to asymmetric (Ref. 3-2). Horizontal gas voids as well as wall slugging become more prevalent, which results in decreased particle-to-wall contact in the upper section of the vessel.

Figure 3-6 shows the effect of bed material on $\bar{h}_i$. All four runs were performed at comparable bed temperature and gas velocity. Power input to the bed was varied as required to maintain the desired bed temperature. The results show that for runs utilizing a greater heat transfer area and bed size (double coil runs), $\bar{h}_i$ was significantly smaller. In addition, $\bar{h}_i$ decreased as average bed particle size increased independent of bed weight or heat transfer area.

3.2.2.3. Conclusions and Recommendations

1. As the steady-state bed temperature increases ($T \leq 700°C$) at constant gas velocity, h_i increases.

2. As gas velocity through the heated bed increases at constant bed temperature, h_i increases initially to a maximum at an optimum gas velocity and then decreases. The optimum gas velocity is dependent primarily on bed weight and particle size.

3. As the temperature above the heated bed increases at constant velocity, h_i increases.

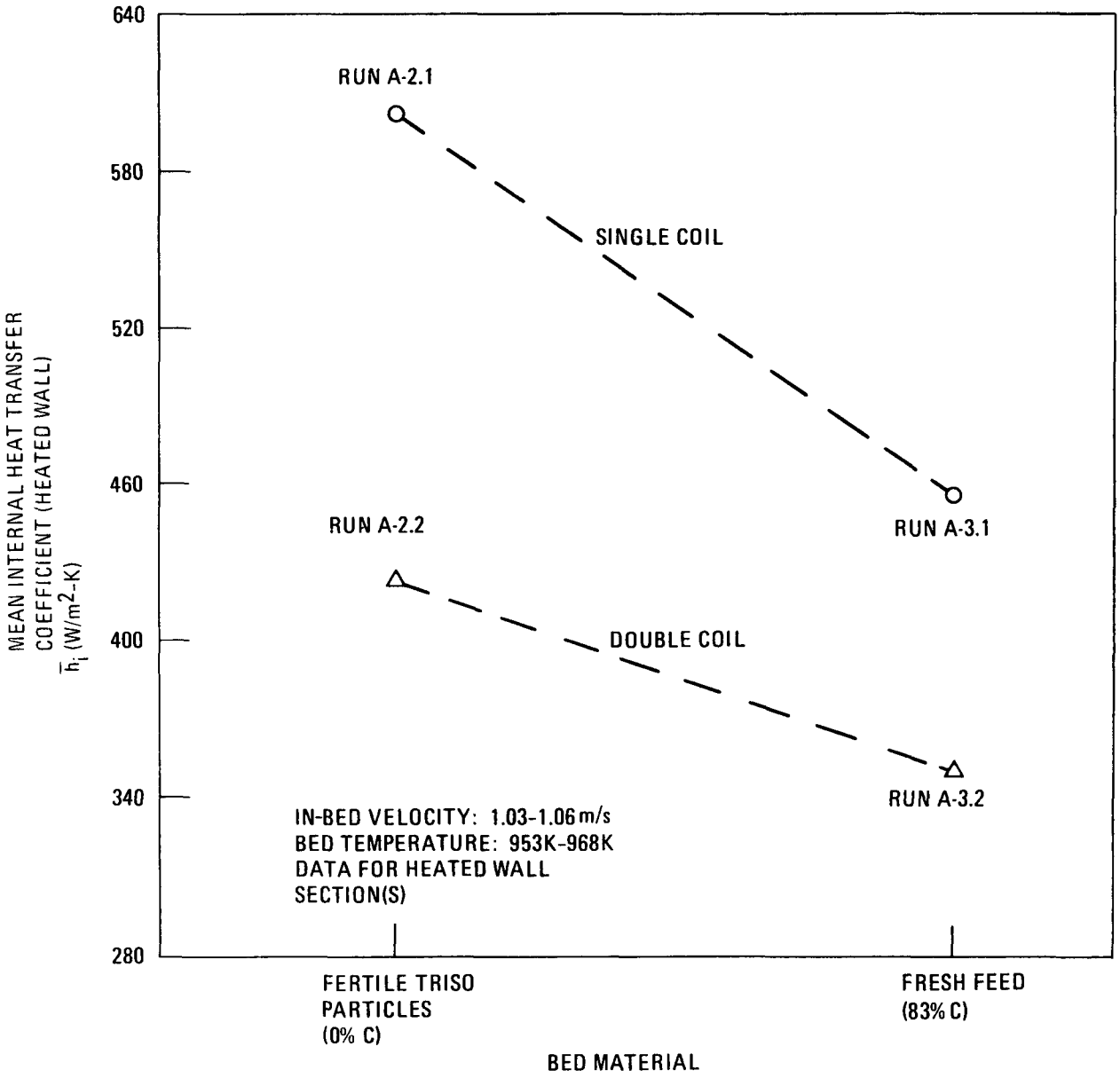

Fig. 3-6. Effect of bed material on in-bed heat transfer - 0.40-m primary burner

4. As gas velocity above the heated bed increases at constant temperature, h_i above the heated wall decreases.

5. As bed particle size increases, h_i in the heated section decreases at constant bed temperature and gas velocity.

6. All experimental results and conclusions are in agreement with the expected behavior of the fluidized bed system.

7. The desired heatup procedure involves operation with only the lower induction coil and a minimum bed size and gas velocity.

3.2.3. 0.40-m Primary Burner Inspection and Reassembly (D. T. Young, J. W. Baer)

3.2.3.1. Introduction

The 0.40-m burner clamp/plenum section was to be removed, inspected, and reinstalled prior to further burner test activities.

3.2.3.2. Discussion

The plenum assembly was disassembled for inspection as specified in the Maintenance Manual (MM524401B).

Difficulty was encountered in separating the plenum assembly from the burner tube despite the fact that the plenum assembly weighed approximately ∿50 kg. Apparently, the seal ring undergoes sufficient plastic deformation when the clamp is made up to hold the plenum and the burner tube together after removal of the clamp. A jackhammer was required to vibrate the plenum assembly loose from the seal ring.

On removing the inspection port (see Ref. 3-3, Fig. 4-1) of the plenum chamber below the distributor, approximately 10 kg of fuel particles, carbide hulls, and oxides was discovered. Particle drainage through the

distributor perforations had been high, apparently due to the severe slugging with the bed sizes tested.

Visual and dye penetrant inspections were performed on critical plenum areas as specified in the Maintenance Manual. All dye penetrant test results were satisfactory and were approved by Quality Assurance. The remote clamp seal ring was checked for satisfactory stand-off and was recoated with Everlube (a baked-on lubricant manufactured by E/M Lubricants, Inc.) before reassembly. Burned-out thermocouples required for the clamp heater control were also replaced.

The Grafoil seal (P/N 5244041) which prevents cooling air from leaking out of the cooling jacket was found damaged. An Inspection Report (IR29876) was issued to document the damage. One layer of the seal was completely "peeled off," leaving a 1/8-in. gap between the sealing surfaces. This condition may result in excessive air leakage to the clamp heater. A repair method was evaluated by the Design Group.

A metal seal was made to replace the outer Grafoil ring seal. This seal was inadequate since it did not conform to the Grafoil seal segments, which were out of round. A graphite seal was then fabricated to replace the Grafoil seal after design review indicated this would have a minimum schedule impact relative to redesign of the seal.

The modified seal arrangement shown in Fig. 3-7 is mounted in an identical fashion as the Grafoil seals and was installed without removal or repositioning of the burner or burner shrouds. The inner and outer seal elements are segmented solid graphite machined to contour and retained by pinning or containment. The horizontal parting line of the inner seal is to facilitate assembly and to eliminate direct leak paths for the cooling air. The outer seal incorporates annular grooves to minimize conductive heat transfer and to reduce leakage through an increased resistance to gas flow.

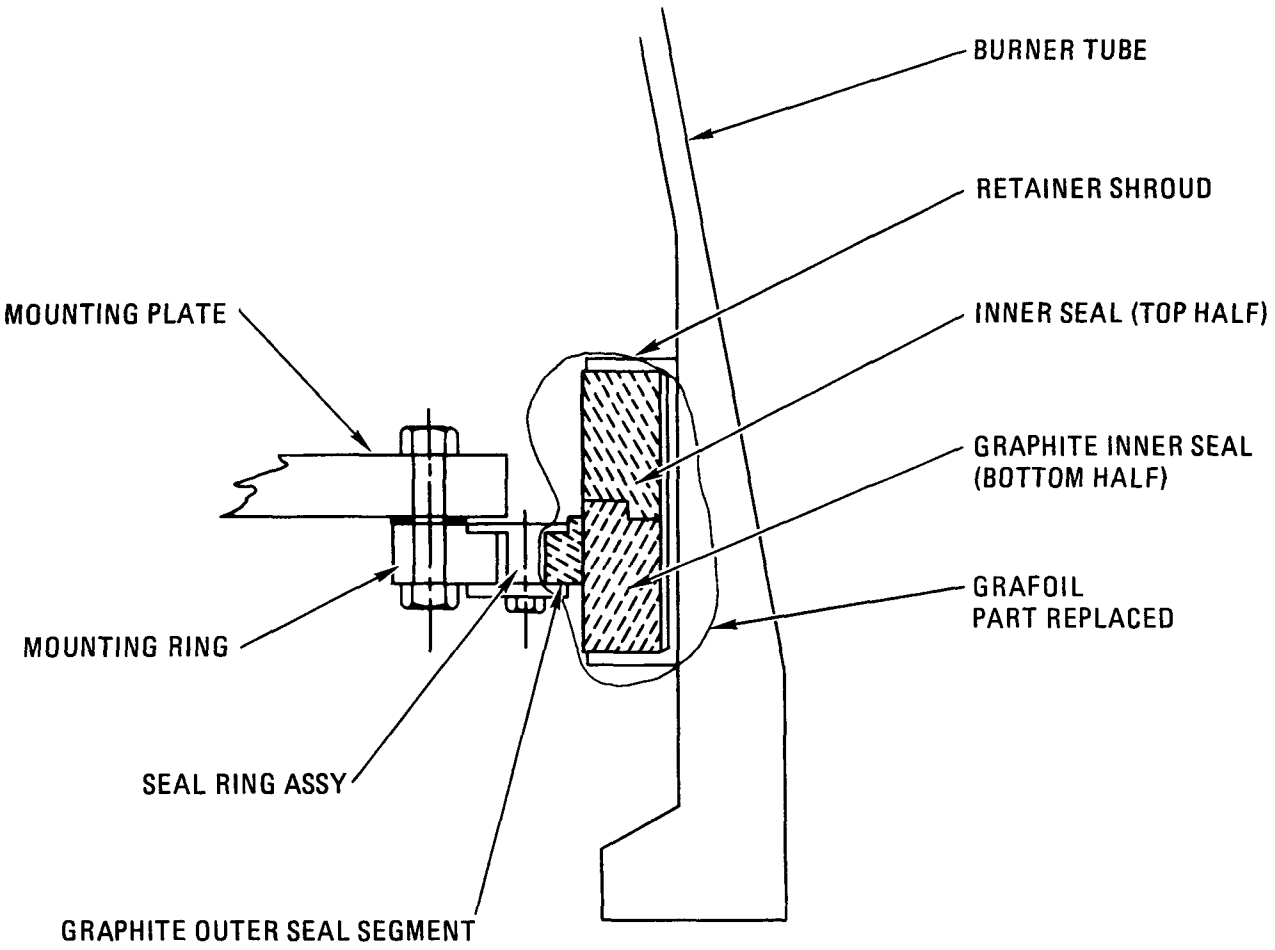

Fig. 3-7. 0.40-m primary burner modified lower seal assembly with inner and outer seals of solid graphite

The graphite seal has recently been installed on the burner, and preparations are under way for plenum installation and reactivation of the burner.

3.2.3.3. Conclusions and Recommendations

The plenum binding condition indicates that a special impact tool may be required to facilitate clamp removal should Grayloc connectors be used in hot cell operation.

Drainage of fuel particle product into the plenum chamber requires further design and development work. A plenum drain line will be incorporated in future distributor designs. Future investigations on the 0.20-m primary burner will determine whether alternate distributor designs can eliminate this requirement.

The graphite sliding seal will be monitored for performance for input into future seal design considerations.

3.2.4. 0.40-m Primary Burner System Design Evaluation (J. S. Rode)

3.2.4.1. Introduction

Possible modification of the present cold engineering-scale equipment to reliable, maintainable equipment that is prototypical of the HRDF design requires an evaluation of the present equipment. This evaluation considers the performance, maintainability, and cost of the present system and of feasible alternative designs.

Such an evaluation was initiated for the 0.40-m primary burner system during the quarter and is nearly complete. At this point, 13 particularly significant features of the present burner system have been evaluated, and alternative designs for these features have been considered. Five of these 13 features are concerned with remote maintenance requirements, and the other eight features involve aspects of process equipment design or manufacturing.

3.2.4.2. Discussion

The following activities were completed during the quarter and comprise over 60% of the design evaluation effort planned for the 0.40-m primary burner system:

1. Preparation of a Functional Level Diagram which depicts the hierarchy of functional relationships between the system and its constituent parts.

2. Preparation of Functional Analysis System Technique (FAST) Diagrams which graphically isolate the basic and secondary functions of a design and show the functional interactions between them.

3. Definition of the scope of the evaluation to include only those features which significantly affect the performance, maintainability, quality, reliability, or cost of the system and, additionally, which are mandated either by basic process requirements or by HRDF facility requirements.

4. Evaluation of the present system design within the defined scope with respect to how it satisfies current technical specifications and requirements such as ease of installation, operability, and maintainability.

5. Analysis of the costs of these selected features of the present design, including labor and materials to manufacture, assemble, and install them in the burner system.

6. Selection and evaluation of alternative design features, using the technique of value engineering.

Table 3-3 lists the 13 design features under evaluation, their basic functions, and the alternative designs being considered for each of these

TABLE 3-3
0.40-m PRIMARY BURNER SYSTEM
PRESENT DESIGN FEATURES AND ALTERNATIVES

Design Feature	Basic Function	Alternative Designs
1. Separability of upper and lower cooling shrouds	1. Allows removal of vessel, coil, and shroud.	1(a) Use single shroud. Remove heating coil out bottom. (b) Eliminate upper shroud. (c) Use single shroud. Eliminate induction heating coil (alternate heating method required).
2. Hinged doors on upper shroud and lower plenum	2. Allows removal of vessel.	2(a) Upper shroud (1) Provide integral upper shroud. (2) Eliminate upper shroud. (b) Lower plenum (1) Eliminate plenum. Provide integral insulated clamp with bolt extended through insulation. (2) Revise method of burner removal.
3. Seal between cooling shroud and vessel	3. Permits separation of tube from shroud for maintenance.	3(a) Use welded shroud (integral with vessel). (b) Use bellows-loaded face seal. (c) Change location of seal to low-pressure zone. (d) Use different seal material.
4. Remote disconnects on burner and auxiliary piping	4. Allows remote disassembly/assembly, esp. distributor.	4(a) Main vessel flanges (1) Relocate lower 14-in. remote flange to cooler zone below distributor. Simplify distributor assembly disconnects, eliminating 14-in. swing-bolt connection. (2) Eliminate core distributor. Use multiple gas entry ports or nozzles. (b) Small flanges (aux. piping). (1) Use modified tri-clover clamps. (2) Cut pipe and re-weld.

TABLE 3-3 (Continued)

Design Feature	Basic Function	Alternative Designs
5. External vessel cooling shroud	5. Transfers heat.	5(a) Use internal heat exchanger. (b) Use cooling tubes imbedded in vessel wall.
6. (Absence of) recycle fines cooling capability.	6. Transfers heat.	6(a) Cool and/or redesign rotary valve. Design other components for high temperature.
7. Waste heat rejection to environment (hot cell)	7. Transfers heat.	7(a) Cool the equipment rejecting heat to the environment. (b) Design the hot cell liner to withstand higher temperatures by material selection or cooling.
8. Method of heating burner	8. Transfers heat.	8(a) Induction heating (b) CO_2 gas preheat
9. Method of thermocouple attachment to vessel	9. Senses temperature.	9(a) Use spring-loaded thermocouples. (b) Weld pad to outside of vessel. Weld metal thermocouple sheath to pad for at least 1 in.
10. Method of fabrication of susceptor	10. Transfers heat.	10(a) Use non-magnetic stainless steel. (b) Use centrifugal casting. (c) Use forging.
11. Type of burner insulation	11. Reduces heat transfer.	11(a) Ceramic (b) Fiber
12. Cap insulator assembly	12. Allows separation for maintenance.	12(a) Unitized design (present 0.40-m primary burner) (b) "Split-dome" design (present 0.20-m secondary burner)
13. Vessel tube length	13. Reduces particle elutriation.	13(a) Enlarge upper section of burner. (b) Lengthen burner to L/D $\approx$ 15. (c) Add baffles to top section of existing burner (L/D $\approx$ 10).

features. In general, at least two alternatives have been selected for cost analysis with each design feature.

3.2.4.3. Conclusions

The cost differentials of the alternatives are being developed prior to comparison with the present design and selection of the preferred design. The merits of each alternative are being evaluated not only individually but in conjunction with the other alternatives in order to achieve compatibility of the 13 features in an integrated prototype design concept. The key features that will influence the selection of the prototype design concept are the methods of heating and cooling the burner vessel and its contents.

3.3. 0.20-m PRIMARY BURNER

3.3.1. Primary Burner Automation Studies (D. T. Young)

3.3.1.1. Introduction

Automation of the burner system using the Diogenes process control computer was specified for Module 7 of the Activity Plan (AP524301B). Four runs were made to test the postulated control philosophy.

3.3.1.2. Discussion

Preliminary results of the automation study indicate that the postulated automation philosophy can control the primary burner in the initial heatup, in the O_2 ramp used for startup, and in the major steady-state portion of the run. It has been necessary to use manual override during the unstable phase of operation both following fresh feed startup and during the final tailburning phases. This override consists of manually controlling the O_2 flow and/or the cooling air flow, with all other functions remaining on automatic control.

The control philosophy is shown in Fig. 3-8. This figure illustrates that the "0. Induction Heater Controller" only supplies power when the bed temperature is <860°C. As the induction heater brings the startup bed temperature to its 700°C auto-ignition temperature, an "1. O_2 Ramp Controller" is activated which increases O_2 flow to the plenum gas inlet (the gas then enters the bed through the distributor perforations). The rate of O_2 increase and the maximum level to which the O_2 increases are automatically controlled and can be varied through the "1. O_2 Ramp Controller." While the O_2 flow is being increased, the "2. Plenum O_2/CO_2 Total Gas Controller" adjusts the plenum CO_2 gas flow to keep the combined total plenum O_2 and CO_2 gas flows constant. This controller functions automatically throughout the run to hold the total gas, hence the superficial velocity, constant even if the O_2 flow controller requires manual operation. At 860°C bed temperature the induction heater is automatically deactivated, and at 880°C (±10°) the cooling air flow is activated by the "3. Cooling Air Controller." The cooling air flow control valve opening is varied to hold the bed temperature at ∿900°C. If the wall cooling is incapable of preventing bed temperature excursions above 930°C, the "4. High Temperature Plenum O_2 Controller" reduces the plenum O_2 until the bed temperature returns below ∿930°C. The plenum is returned to its preset maximum below ∿930°C. This prevents damage to the vessel wall. During tailburning the decreased bed carbon allows the O_2 concentration in the off-gas to increase. The "5. Off-gas O_2 Controller" reduces the plenum O_2 to maintain a preset maximum off-gas O_2 concentration.

This control philosophy has been very beneficial in simplifying the burner operator's duties and in providing safer, more constant operating conditions. Fine tuning of the "3. Cooling Air Controller" and the "4. High Temperature Plenum O_2 Controller" is required to further improve the automatic control. Tuning of the "3. Cooling Air Controller" appears to be the most difficult. The slow response of bed temperature to wall cooling and the dependence of this response upon bed-to-wall heat transfer, which can fluctuate with fluidization conditions, complicate the control of the cooling air flow.

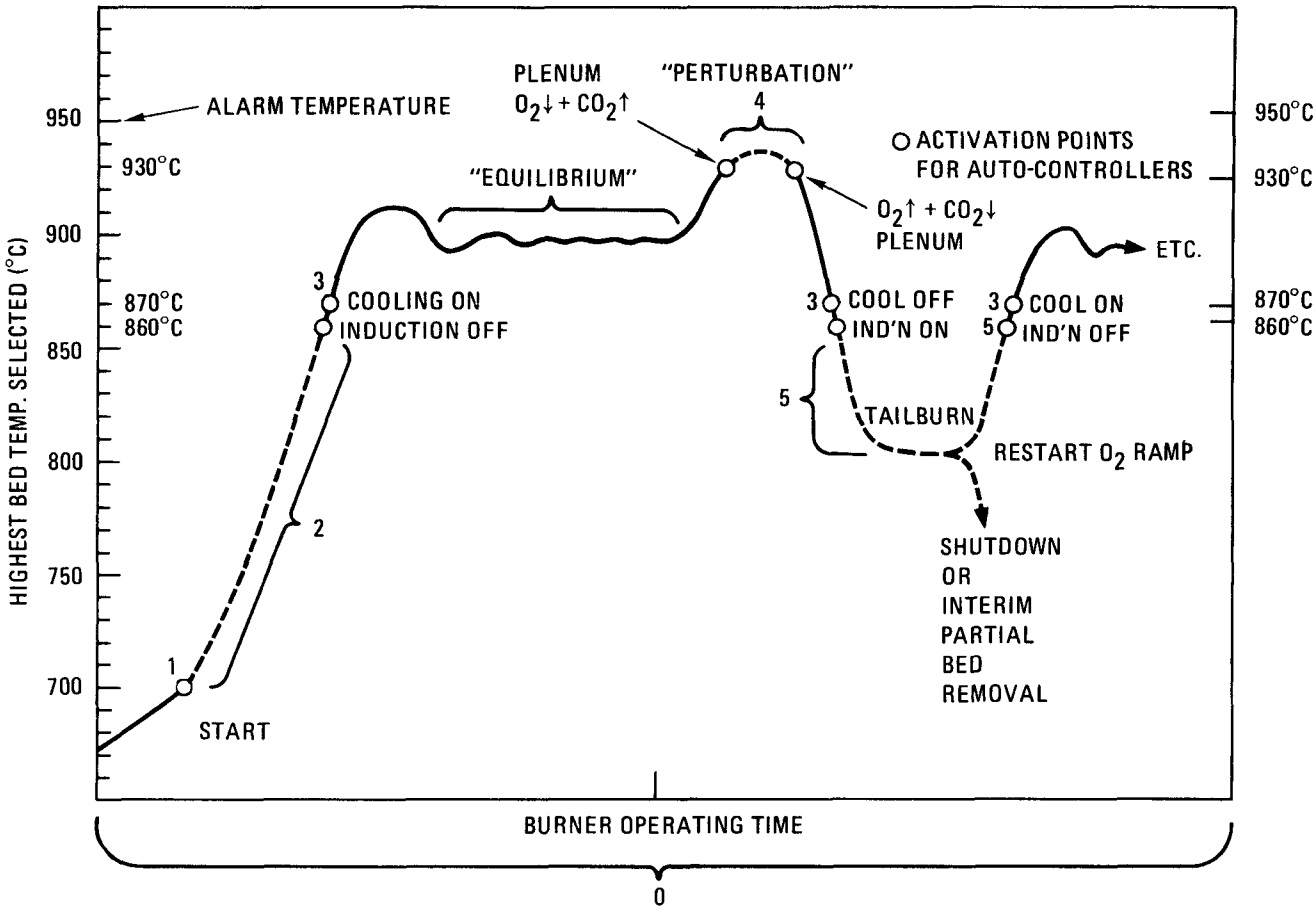

0. INDUCTION HEATER CONTROLLER – ADJUSTS INDUCTION POWER AND RESULTANT HEAT INPUT INTO BURNER IF BED TEMPERATURE IS <860°C, LIMITS WALL TEMPERATURE ≤900°C AND (OR) SUSCEPTOR TEMPERATURE ≤1080°C
1. O_2 RAMP CONTROLLER – INCREASES PLENUM O_2 AT A PRESET RATE, STOPS O_2 AT A PRESET MAXIMUM FLOW
2. PLENUM O_2/CO_2 TOTAL GAS CONTROLLER – ADJUSTS TO MAINTAIN CONSTANT TOTAL PLENUM GAS FLOW – $O_2\uparrow$, $CO_2\downarrow$
3. COOLING AIR CONTROLLER – ADJUSTS COOLING AIR FLOW TO MAINTAIN 900°C BED TEMPERATURE; TURNS COOLING AIR ON AND OFF AT PRESET TEMPERATURE
4. HIGH-TEMPERATURE PLENUM O_2 CONTROLLER – REDUCES PLENUM O_2 IF BED TEMPERATURE EXCEEDS 930°C
5. OFF-GAS O_2 CONTROLLER – ADJUSTS PLENUM $O_2\downarrow + CO_2\uparrow$ SO THAT OFF-GAS O_2 <7%

Fig. 3-8. Proposed primary burner automatic control

The Diogenes system (manufactured by Rosemount Inc. of Minneapolis) has been satisfactory except for intermittent problems with an erroneous low bed temperature signal from the "4. High Bed Temperature Selector." The problem has been traced to a computer malfunction. This signal is <1 sec in duration and briefly activates the induction heater and deactivates the cooling air. This has complicated the tuning of controllers.

3.3.1.3. Conclusions and Recommendations

Fine tuning of the postulated automatic control philosophy will continue in an effort to reduce the requirement for periods of partial manual control. The Diogenes high bed temperature selector problem will be investigated further, both with the vendor and in-house.

3.3.2. 0.20-m Primary Burner Operating Cycle Test Runs with BISO Fertile/TRISO Fissile Particles (D. T. Young)

3.3.2.1. Introduction

A 48-hr run was called for in the Activity Plan (AP524301B) as the completion of Module 7 automation studies. This run was not only planned to study the automation system in long-duration operation, but was also an intended study of the proposed primary burner operating cycle. This cycle involves starting up a fresh feed bed containing crushed graphite (∿83 wt %) and carbon-coated BISO fertile and TRISO fissile fuel particles (∿17 wt %). The burning bed is then continuously fed the fresh feed mixture at a carbon mass flow rate equivalent to the carbon burn rate. Consequently, the bed level slowly increases as the burned-back fuel particles accumulate. When the bed level reaches the maximum bed level, which occurs when the bed slug height approaches the burner tube height, feed is stopped. Subsequently, the bed carbon is burned out and a 15 to 20 wt % portion of the product bed is removed. The burner is then restarted and feeding is resumed until the bed level is rebuilt to the maximum level. Another partial bed removal (or total removal) is then required. One such complete cycle requires ∿48 hr.

3.3.2.2. Discussion

The attempted 48-hr run was shut down after ∿12 hr. The shutdown was necessary due to three mechanical failures: (1) the erroneous cycling controller signal caused the cooling air blower switch contactor to overheat and fail, (2) a break occurred in a joint of the off-gas line, and (3) the product removal valve jammed in a partially opened position. Operations during the 12-hr run indicated that the fluidization of the very dense, large-diameter BISO fertile particles mixed with the small-diameter, less dense TRISO fissile particles required adjustments to previously established process control levels. These levels had been established during prior operation with more homogeneous mixtures of fuel particles. The BISO fertile particles segregated to the inlet cone distributor region and required a higher total gas velocity and a longer O_2 ramp period to safely burn the carbon coatings. Approximately 4 hr was required to ramp the O_2 to its maximum flow (full burn rate). As the burned-back inert BISO particles accumulated in the lower burner zone, the operation became more typically smooth.

Following the 12-hr run, a 6-hr run was made to test repairs to the burner system. This run confirmed the integrity of the mechanical repairs and the revised control levels, but revisions to the Diogenes controller were not successful in eliminating problems with cycling of the cooling air control signal. These could be avoided by eliminating the problem control circuit, a signal selector, and relying on a single bed temperature for cooling air control. Although this philosophy apparently is successful for control of the secondary burner, the bed temperature profile expected in the primary burner operating cycle is more varied, therefore requiring the selection capability.

3.3.2.3. Conclusions and Recommendations

The Diogenes problem is apparently within the computer and will require repair by the supplier.

The cooling air blower has been provided with a manual override.

Operating techniques using vertex gas to limit the solids flow through the product valve when it must be closed during partial bed product removal should be analyzed. Alternate valve and product removal system designs should also be reviewed.

These process revisions should be tested in one or two more short-duration runs prior to another attempt at a full-cycle 48-hr burner run.

3.3.3. 0.20-m Primary Burner Fines Recycle (R. T. Stula)

3.3.3.1. Introduction

Upon completion of the 0.20-m primary burner Module 5 and 6 test phase, it was determined that above-bed fines recycle using the gravity fines transport system (see Fig. 3-9) was the best of the fines recycle alternatives tested (Ref. 3-4). One of the design considerations associated with this system is the maximum design operating temperature of the fines rotary valve. It is desirable to maintain recycle fines temperature as hot as practicable, but within recycle equipment thermal design limits. Removal of significant heat from the recycle loop may be required to meet rotary valve temperature limitations.

3.3.3.2. Discussion

Contacts with the rotary valve manufacturer have been made to further define valve thermal operating limitations. The limiting factor on the maximum operating temperature of the valve is the outboard bearing (seal) design. This consideration limits the valve to a maximum operating temperature of 500°C. The valve body is designed to a maximum operating temperature of 540°C. However, this includes an unknown safety factor; the valve could be operated at a somewhat higher temperature. Since no previous data for high-temperature valve application are available, maximum operating temperature, as well as valve design life, is uncertain.

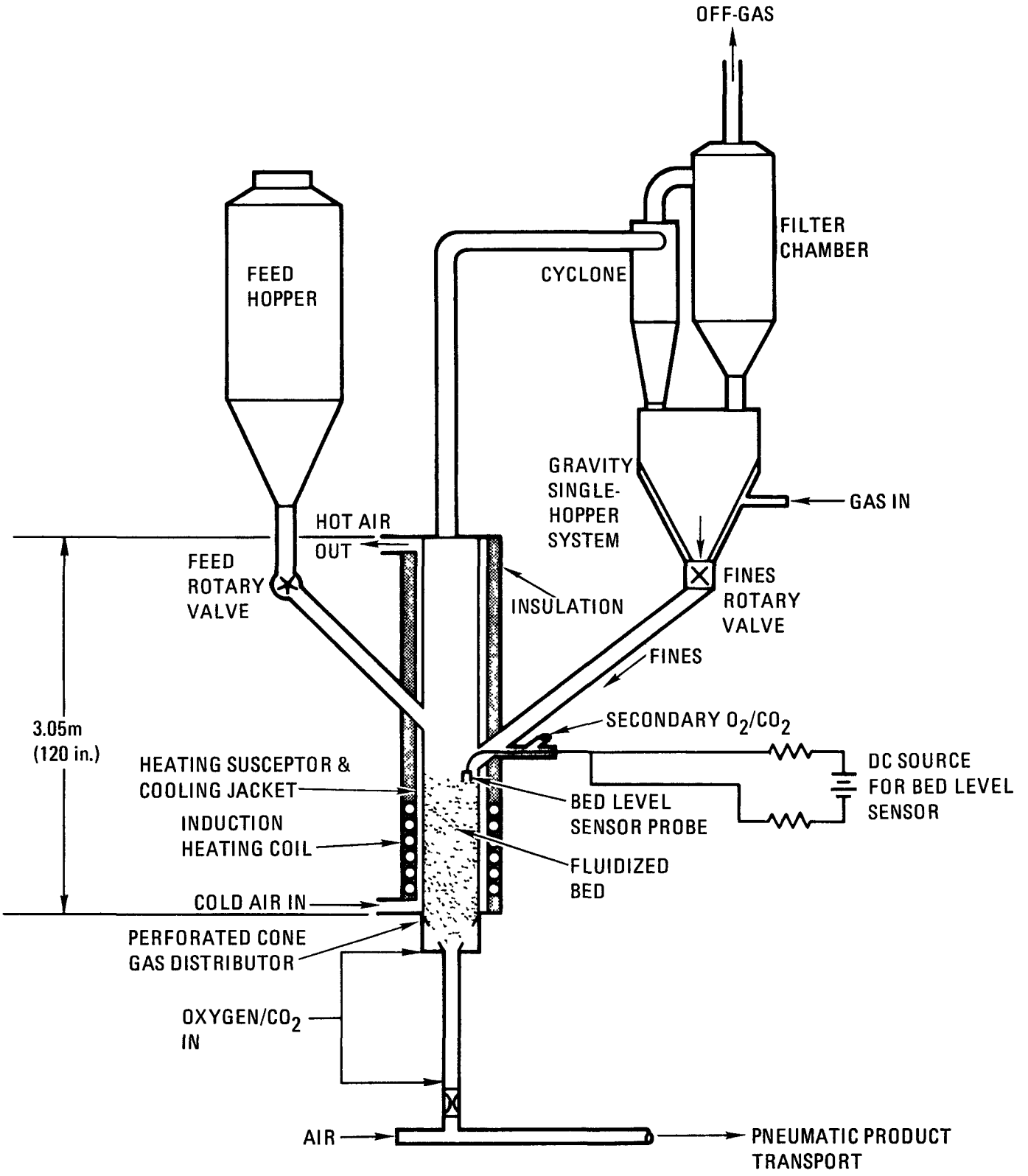

Fig. 3-9. 0.20-m primary burner configuration

Preliminary calculations have been initiated to determine the feasibility of removing process heat from the off-gas to obtain cyclone exit temperatures compatible with current fines recycle equipment.

3.3.3.3. Conclusions and Recommendations

Preliminary calculations indicate that external air cooling of the present recycle piping and cyclone may be sufficient to lower the cyclone exit temperature to the present rotary valve maximum design operating temperature. It is recommended that this possibility be considered further.

It is recommended that alternative recycle loop geometry and cooling systems as well as rotary valve designs be investigated in detail.

A detailed process heat transfer study should be conducted to determine the feasibility of cooling the fines recycle stream to temperatures compatible with the recycle equipment.

3.3.4. 0.20-m Primary Burner Bed Level Sensor (R. D. Crabtree)

3.3.4.1. Introduction

A need to determine a discrete bed level in the primary burner to back up the bed ΔP reading initiated a program to develop such a sensor.

3.3.4.2. Activity

A dual element probe was constructed, as shown in Fig. 3-10, and installed through the above-bed fines recycle side penetration of the 0.20-m primary burner. It extended down into the burner tube to the point to which the highest desired bed level would reach (see Fig. 3-9).

This probe was tied into a simple DC resistive circuit as shown in Fig. 3-9. As the bed level reaches the probe, the DC circuit is completed

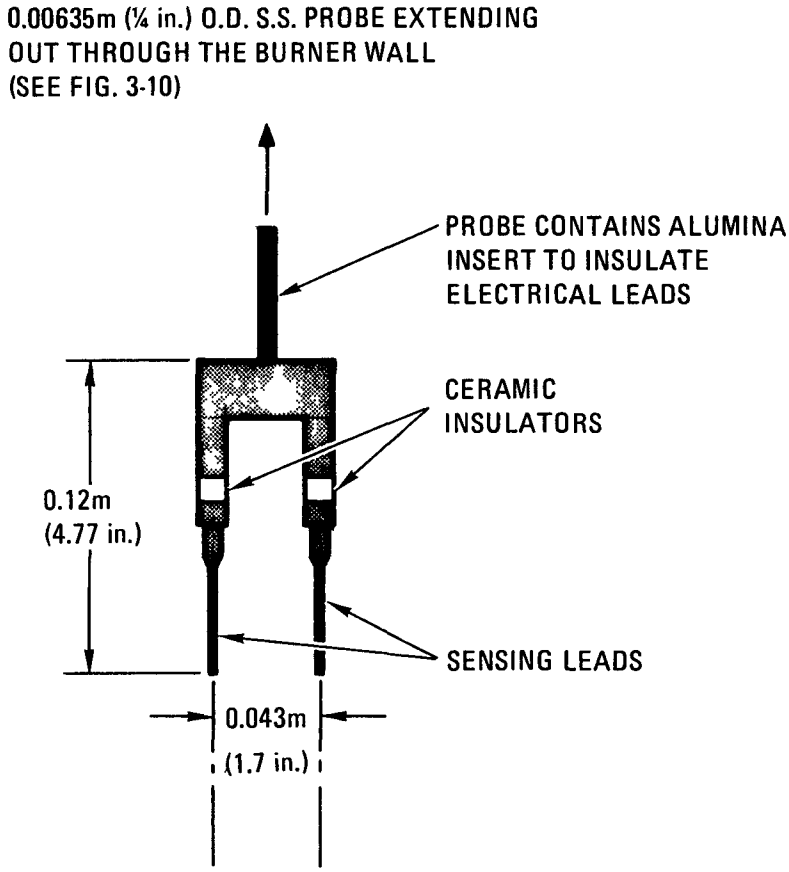

Fig. 3-10. 0.20-m primary burner bed level sensing probe

through the low resistance of the carbon in the bed. A current flow proportional to the resistance of the carbon bed (or suspended above-bed carbon) is induced between the two elements of the probe and the current is then measured on a strip chart recorder.

3.3.4.3. Conclusions and Recommendations

The technique described above has proven quite successful. Some side effects observed are resistance changes due to slugging, gas velocity changes, fines recycle, increasing bed level below the probe, and carbon depletion in the bed at the end of a run. It is recommended that these effects continue to be studied to determine if they can be characterized and the technique made useful for monitoring burner operation.

REFERENCES

3-1. "Thorium Utilization Program Quarterly Progress Report for the Period Ending November 30, 1976," ERDA Report GA-A14214, General Atomic Company, December 1976, pp. 3-2 to 3-4.

3-2. Baeyens, J., and D. Geldart, "An Investigation into Slugging Fluidized Beds," Chem. Eng. Sci. 29, 255 (1974).

3-3. "Thorium Utilization Program Quarterly Progress Report for the Period Ending August 31, 1975," ERDA Report GA-A13593, General Atomic Company, September 30, 1975.

3-4. "Thorium Utilization Program Quarterly Progress Report for the Period Ending November 30, 1976," ERDA Report GA-A14214, General Atomic Company, December 1976, pp. 3-4 to 3-14.

4. PARTICLE CLASSIFICATION, CRUSHING, AND BURNING

4.1. SUMMARY

A parametric study of process variables on the 0.20-m secondary burner has been initiated, with three of seven runs now completed. Extensive automation of the burn cycle has been demonstrated. Crushed TRISO fertile FSV type fuel particles are used as feed for these runs. Shakedown of the 0.10-m secondary burner is now complete, and the burner is ready for burning tests using crushed TRISO fissile FSV type fuel particles.

Localized side plate wear on the fertile particle roll crusher has necessitated inlaying a very hard sintered tungsten carbide wear pad adjacent to the crushing cavity. The fissile roll crusher has been received and is now undergoing checkout testing.

4.2. 20-m SECONDARY BURNER (W. S. Rickman)

4.2.1. Introduction

After completion of construction, the 0.20-m secondary burner was checked out and calibrated prior to making two burner runs for system shakedown and heat transfer coefficient measurement. Several areas were upgraded at that time, including the distributor plate design and the filter blowback tube welds. During the quarter, three runs were completed out of seven runs planned as a parametric study of the following burner process variables:

1. Bed ignition temperature.
2. Bed operating temperature.
3. Bed superficial velocity.
4. Filter blowback rate.

The Operating Procedure (OP524701) and Activity Plan (AP524701) were followed throughout these three burner runs except where noted. Some conclusions are drawn concerning the results, but since fewer than half of the runs in the series have been completed, it is premature to make specific recommendations at this time. Graphs depicting feed and product size distributions, fluidized bed and off-gas filter temperatures, off-gas composition, and inlet gas flows and pressure drops are shown in Figs. 4-1 through 4-12.

4.2.2. 0.20-m Secondary Burner Experimental Runs

4.2.2.1. Run 3 (Figs. 4-1 Through 4-4)

In this run, all variables were set at a baseline determined from previous 0.10-m secondary burner tests. They represent the best estimate of proper variable selection, and are as follows:

700°C bed ignition temperature.
900°C bed operating temperature.
0.90 m/s bed superficial velocity.
2 full blowback cycles per minute.

Feed material for Run 3 was 60,000 g of crushed TRISO fertile FSV type fuel particles. It was acceptable feed for the burner and contained ∿0.1% unbroken fuel particles. The crusher roll gap was 0.495 mm (0.0195 in.) during Run 3 feed preparation. Forty-five minutes were required for feed preparation with a 44-rpm roll speed.

Feed addition to the burner required 4 min using the gravity pneumatic feeder. Bed heatup was initiated after feeding was completed and required 80 min to reach 700°C ignition temperature. At that time, a manual O_2 ramp was begun by jumping to 0.080 std. m^3/min O_2 and then increasing to pure O_2 over a 20-min period. Total flow was maintained at 0.402 std. m^3/min at all times to yield 0.90 m/s superficial velocity at 900°C.

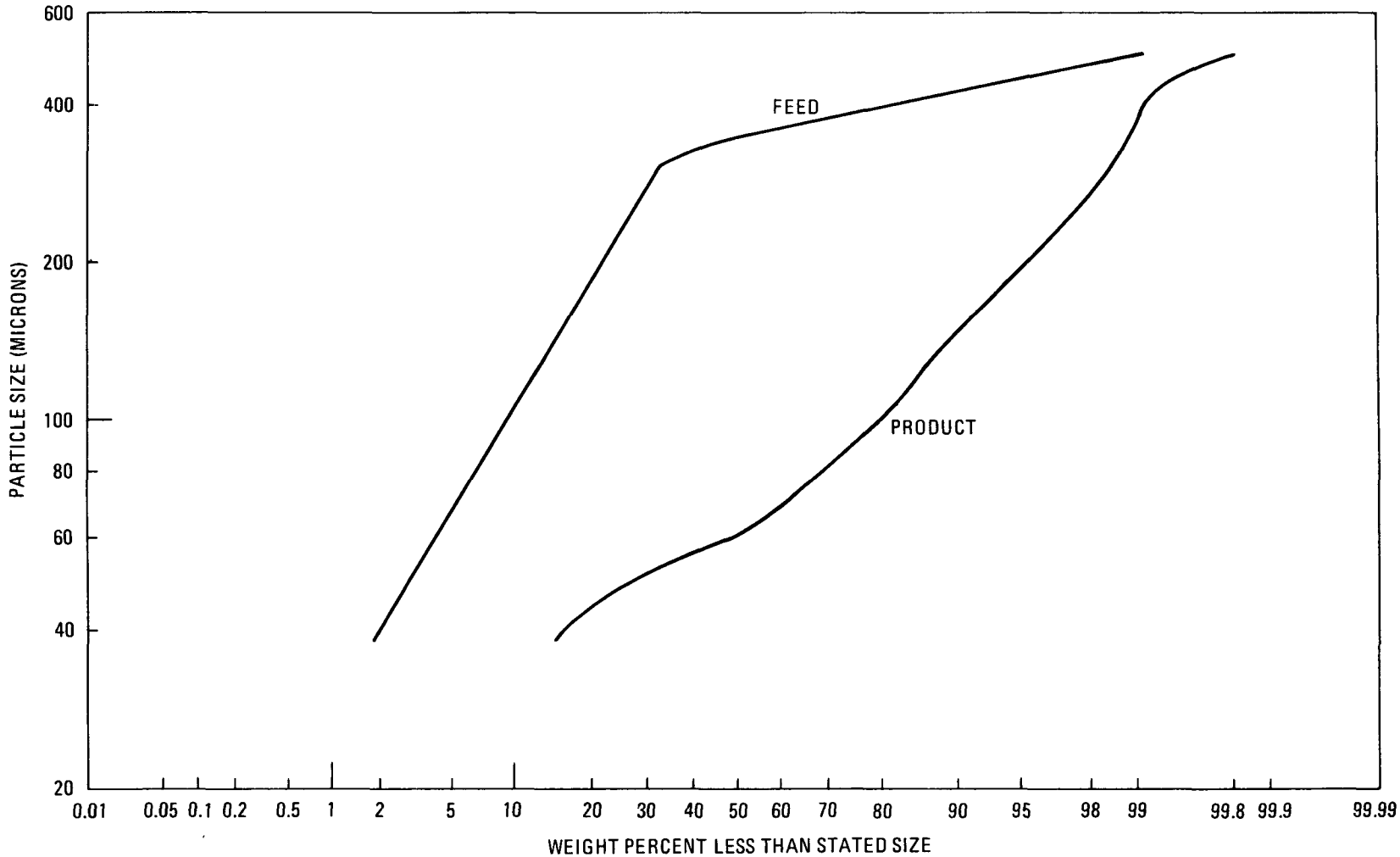

Fig. 4-1. Feed and product size distribution, 0.20-m secondary burner Run 3

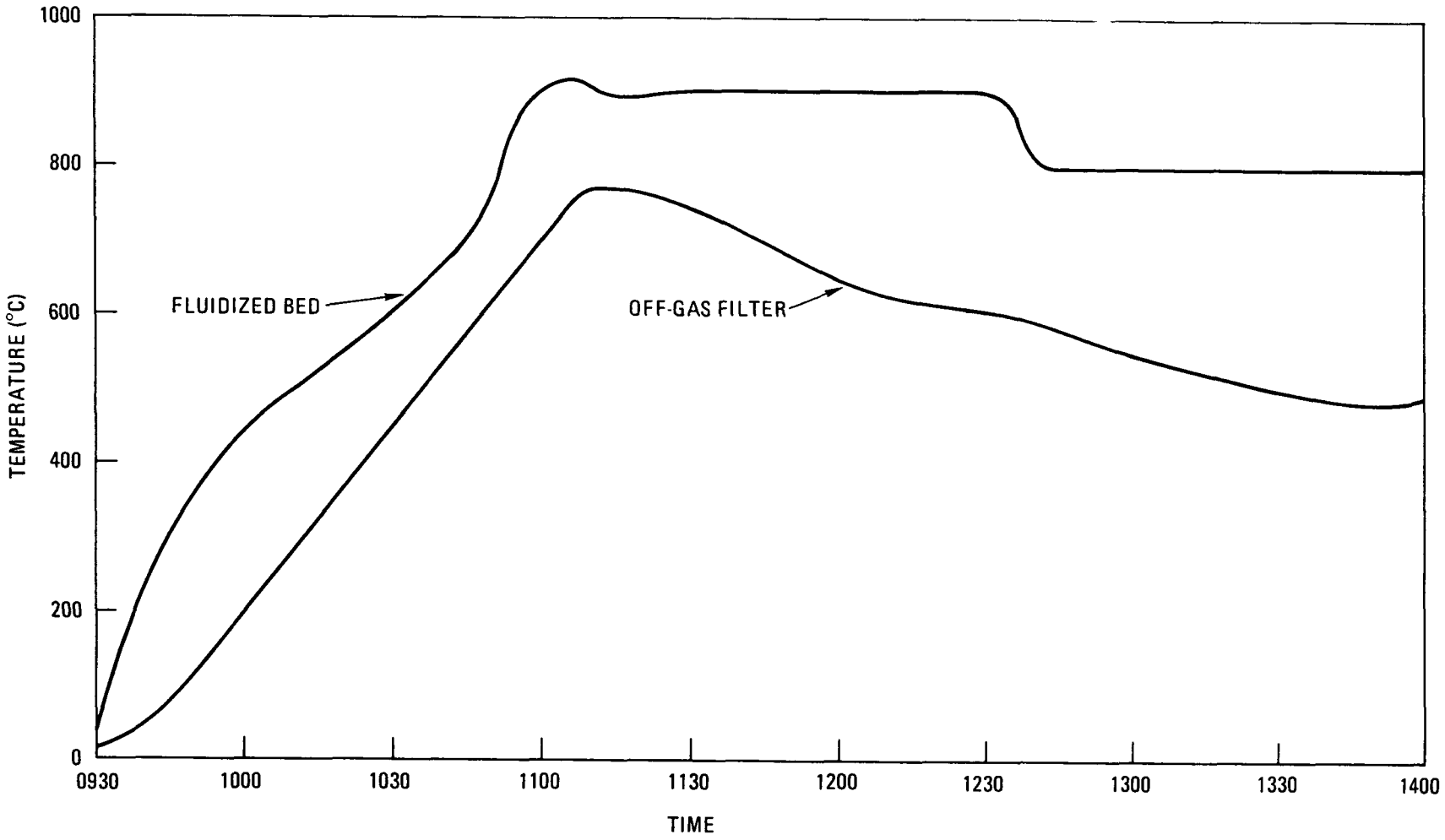

Fig. 4-2. Fluidized bed and off-gas filter temperatures versus time, 0.20-m secondary burner Run 3

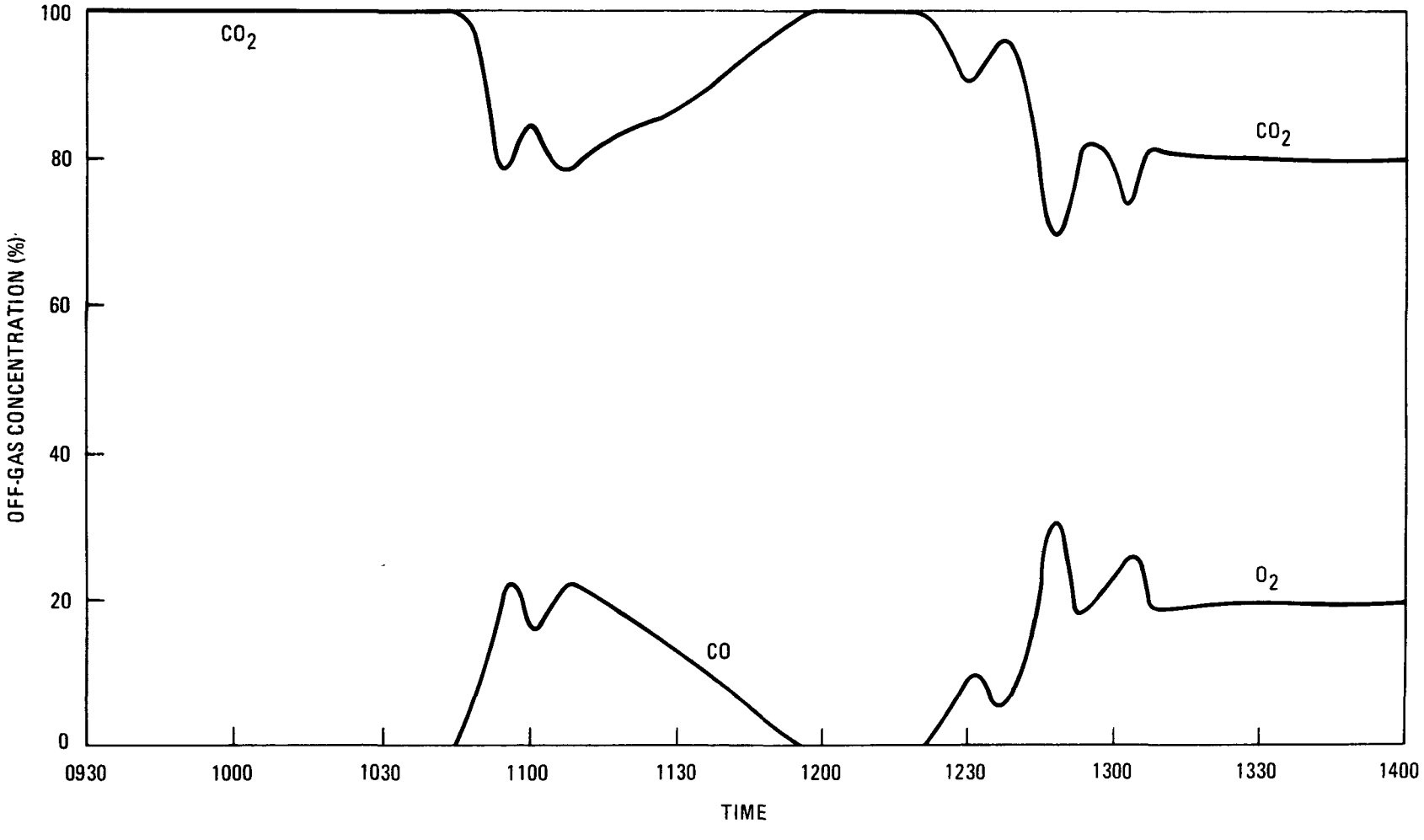

Fig. 4-3. Off-gas composition versus time, 0.20-m secondary burner Run 3

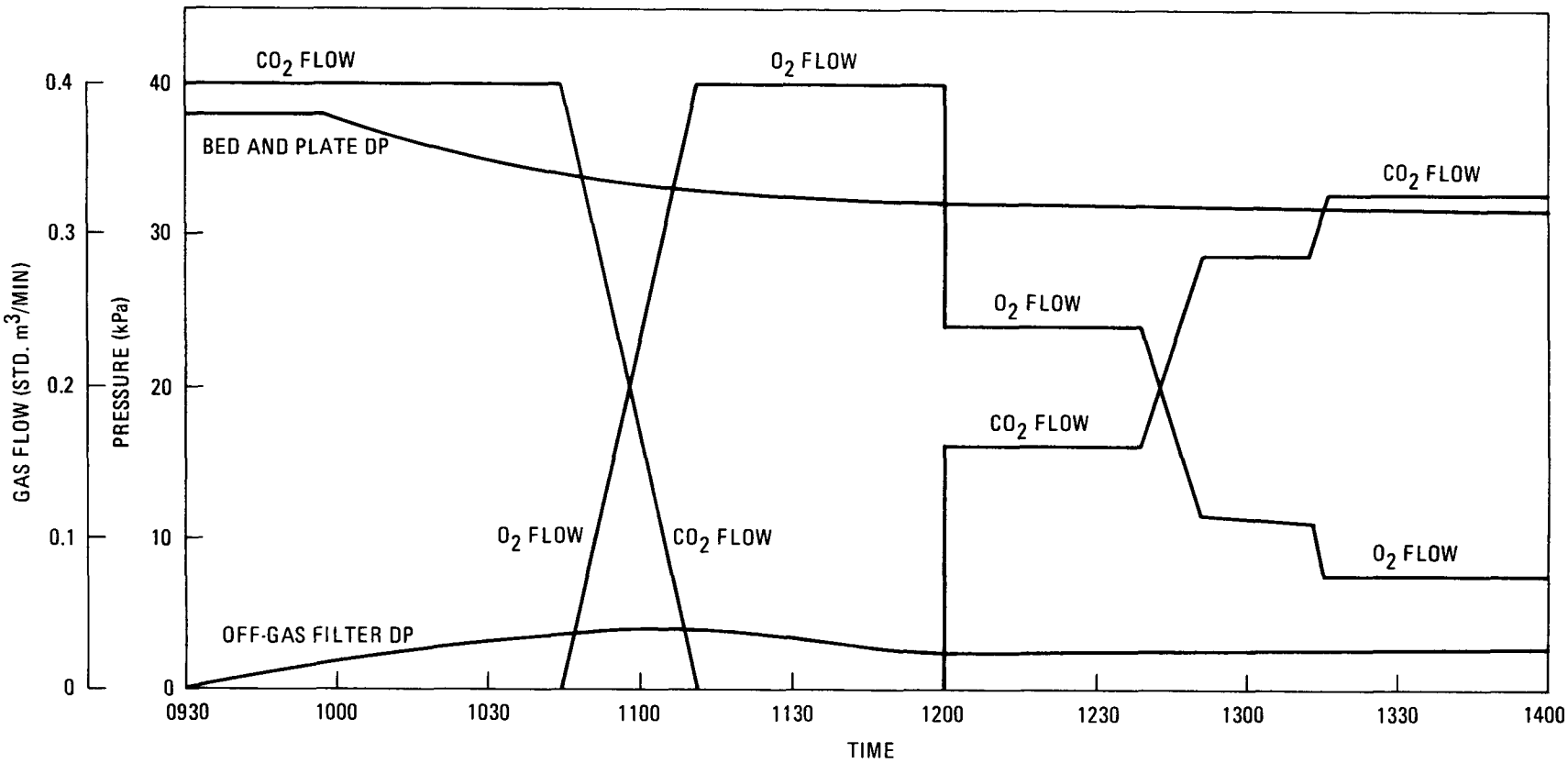

Fig. 4-4. Inlet gas flows and pressure drops versus time, 0.20-m secondary burner Run 3

Cooling air flow was manually adjusted to keep the fluid bed at 900°C. Following an initial 25°C overshoot, the bed stayed within 10°C of setpoint throughout the main burning period. This is well within the ±50°C called out in the Design Criteria (DC52701). Filter chamber annular cooling air was on during the entire main burning period, with a peak filter temperature of 775°C and a filter pressure drop of 3.5 kPa maximum.

When the off-gas CO concentration declined to zero, the inlet gas composition was changed from 100% to 60% to preclude a pure O_2 front from contacting the hot filter surface. Thirty minutes later, O_2 did penetrate the bed, but the filter had cooled from 720° to 600°C and no filter area hot spots were detected by the thermowell.

The fluid bed then cooled to 800°C due to a lack of carbon to burn. Induction heating was on automatic to keep the bed hot without overheating the wall (900°C setpoint on wall temperature). Off-gas O_2 content was kept at 20% by modulating inlet O_2 content. A filter vibrator was used to help dislodge carbon from the filter area so that it could descend to the bed for combustion. The vibrator was of definite use as demonstrated by increased oxygen utilization following vibrator actuation.

Total run time when O_2 was present in the off-gas was 90 min. This was followed by cooling the bed to ambient in preparation for product removal. Using a 7.08 act. m^3/min blower, the product was pneumatically transported as it exited the burner product valve located just above the distributor plate. The distributor sweep tube was actuated after the bulk of the product had left the burner, and the transport gas was intermittently drawn back through the burner off-gas filters to effect a cleanout of dust from the burner.

Disassembly of the burner revealed a heel of material resting on the distributor plate. The burner was then reassembled and fitted with an air-driven vibrator adjacent to the gas distributor to help move material off the plate. After a cleanout using the vibrator, the burner was again disassembled and had only a light coating of dust on the distributor and some

material in the outer edges. Total product weight left on the plate was 50 g, which amounts to 0.1% of total product weight. The product weighed 47,836 g and had a 1.5 wt % carbon content.

4.2.2.2. Run 4 (Figs. 4-5 Through 4-8)

The ignition temperature and the superficial velocity were changed in this run to 650°C and 0.80 m/s, respectively, as part of the parametric study.

Feed preparation required 45 min at a 44-rpm roll crusher speed to process 60,000 g of TRISO fertile FSV type fuel particles. Feed addition took 3.8 min to complete, and bed heatup required 55 min to reach 650°C. Gas flow was 0.475 std. m^3/min of CO_2 until the bed reached 300°C, at which time the flow was reduced to 0.362 std. m^3/min (which yields 0.80 m/s superficial velocity at 900°C).

An automatic inlet O_2 flow ramp was used with an 0.080 std. m^3/min initial jump and a 15-min ramp time to pure inlet O_2. CO_2 flow was automatically adjusted to keep the total at 0.362 std. m^3/min.

Cooling air flow was on automatic with an initial 50°C overshoot followed by ±15°C control. Controller settings were manipulated to help determine optimal values. Maximum filter pressure drop was 2.3 kPa with a peak filter temperature of 720°C. After 65 min of combustion, the off-gas CO concentration declined to zero, with inlet O_2 concentration lowered at that time to 60%.

For 60 min, the bed was burning sufficiently to maintain temperature at 850° to 900°C. After that time, the carbon content of the bed was such that 810°C was the maximum temperature attainable with the induction heater limited by a 900°C burner wall constraint. Off-gas O_2 content was again limited to 20% by adjusting the inlet O_2 flow rate. Total flow was gradually reduced over a 100-min span to 0.226 std. m^3/min, yielding 0.46 m/s

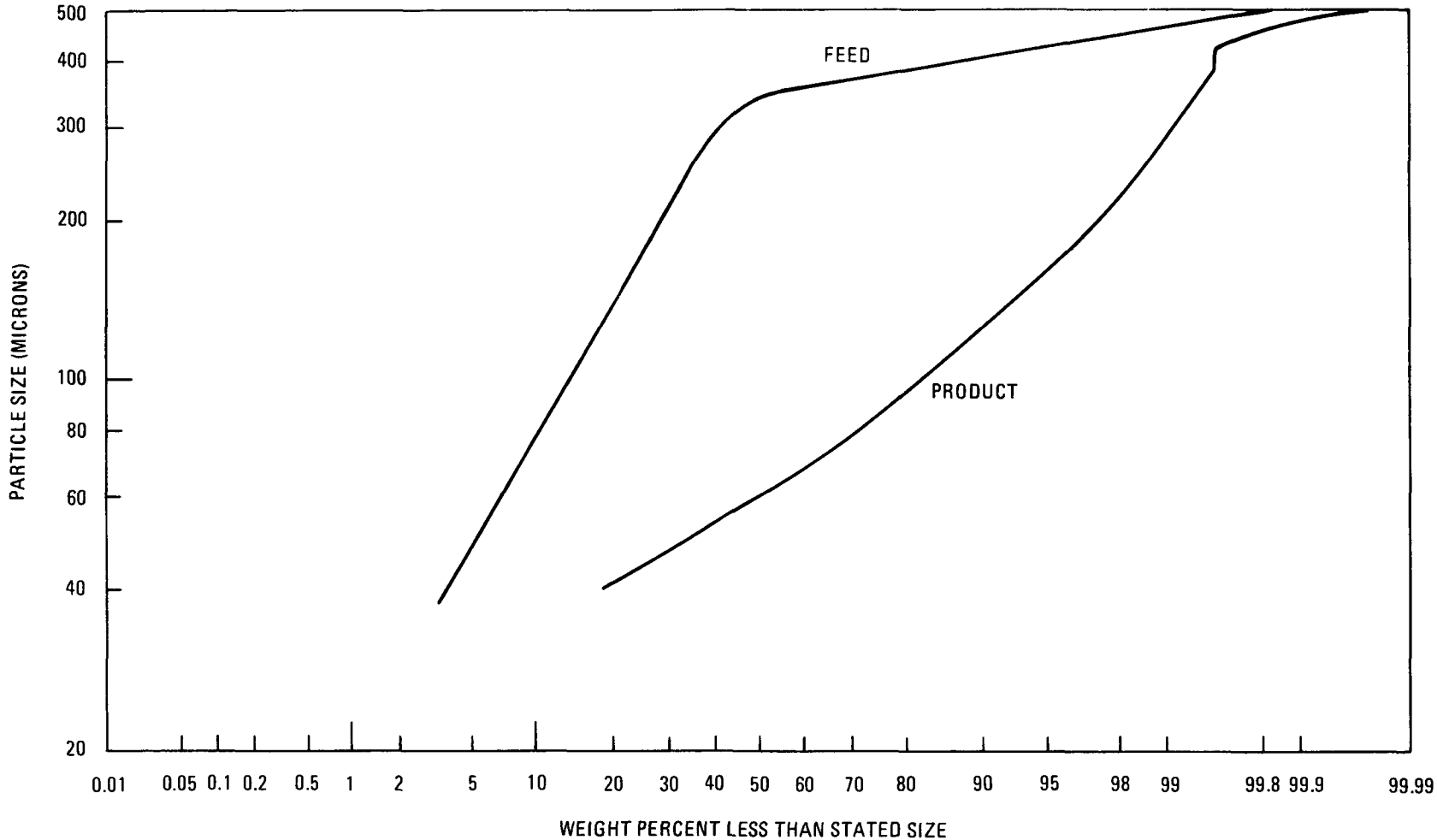

Fig. 4-5. Feed and product size distributions versus time, 0.20-m secondary burner Run 4

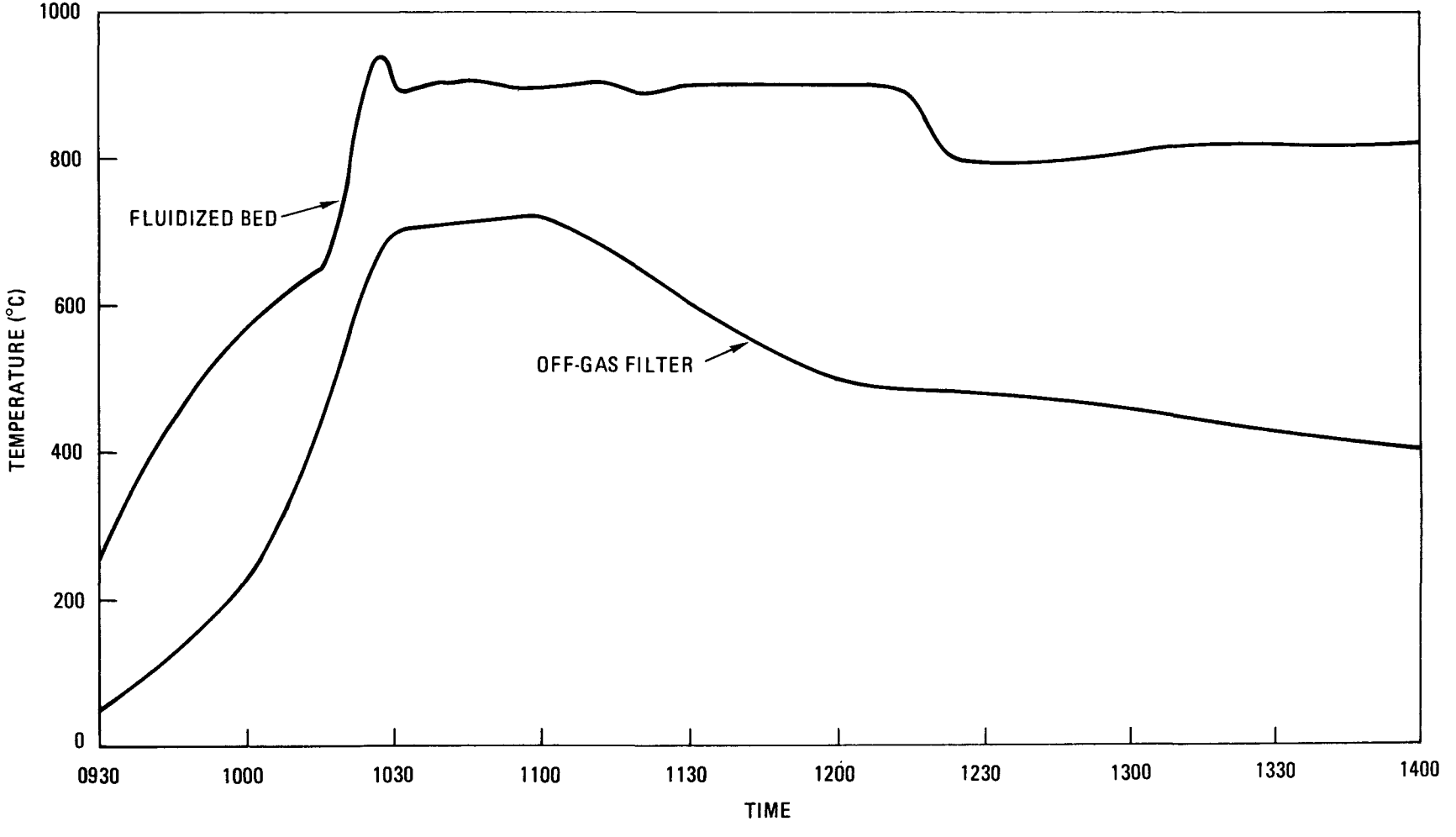

Fig. 4-6. Fluidized bed and off-gas filter temperatures versus time, 0.20-m secondary burner Run 4

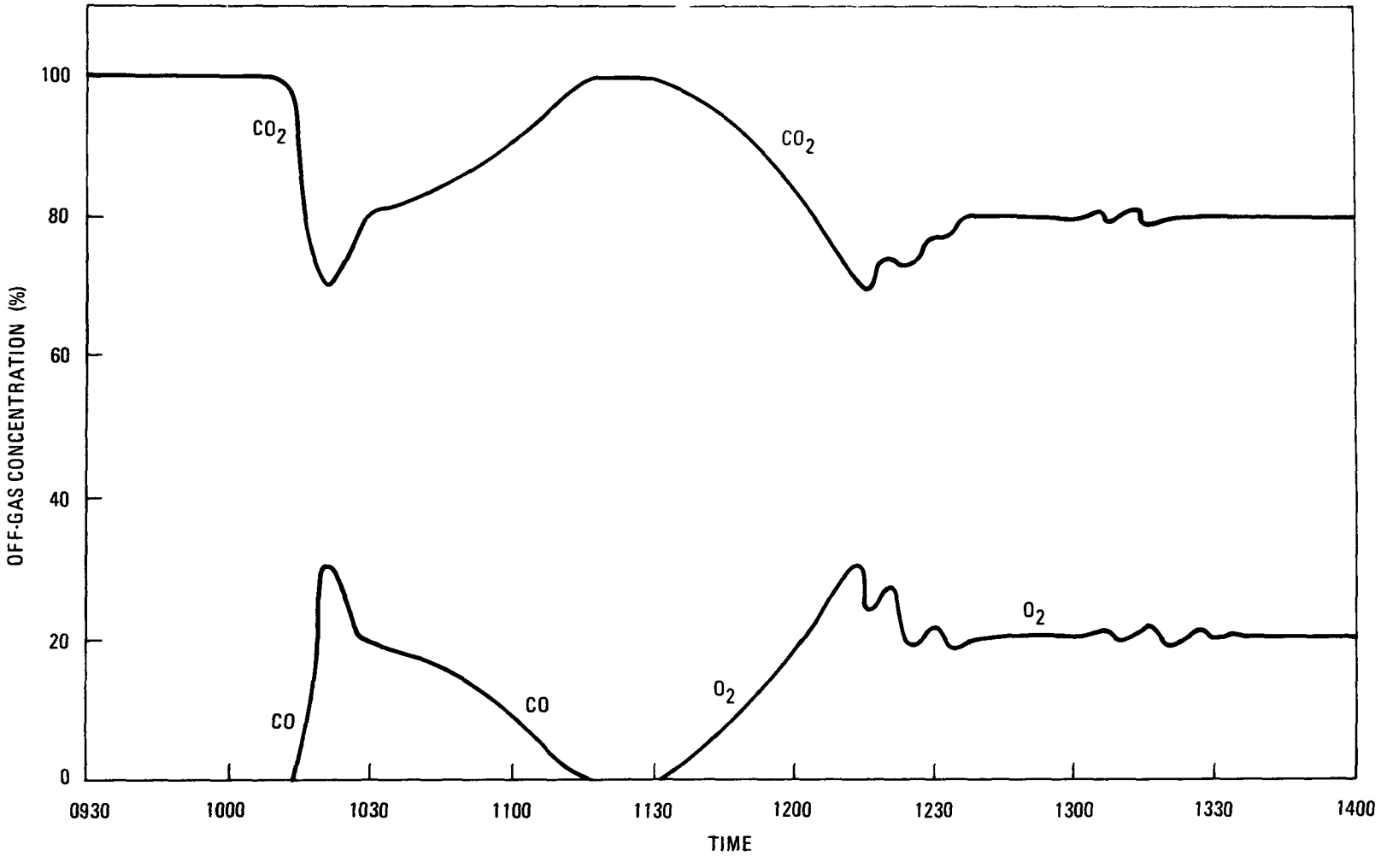

Fig. 4-7. Off-gas composition versus time, 0.20-m secondary burner Run 4

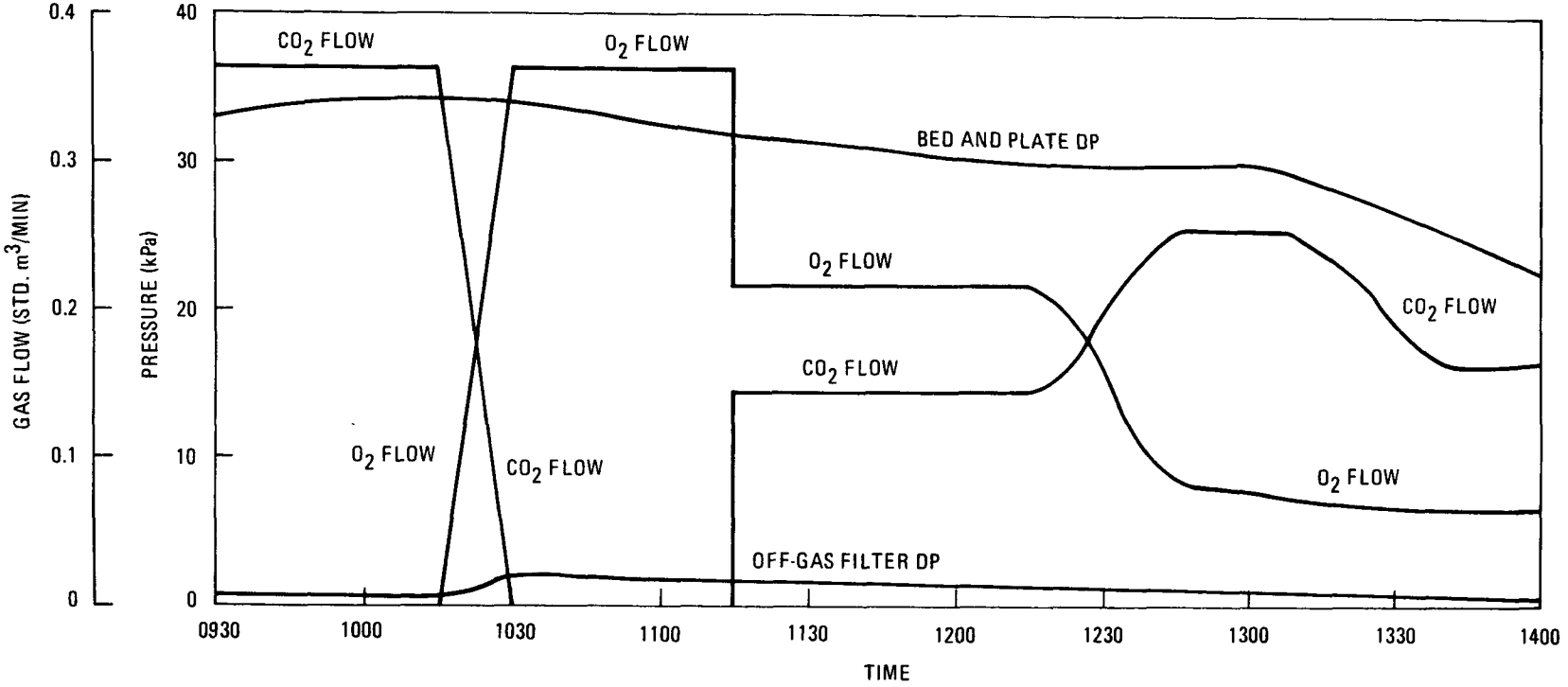

Fig. 4-8. Inlet gas flows and pressure drops versus time, 0.20-m secondary burner Run 4

(1.5 ft/sec) at 810°C. This allowed fines a better opportunity to reenter the bed than at the higher normal operating velocity of 0.80 m/s.

Product transport was initiated after cooling the bed to 140°C. Initial transport was unsuccessful due to bursting of a rupture disc attached to the transport blower suction line. This disc was installed to preclude overpressure of the product bunker but had not been designed to withstand the vacuum associated with pneumatic transport. It was then capped off, the lines were cleared manually, and the balance of the product was transported pneumatically to the product bunker. A 300-g heel (0.6% of the total product) remained on the distributor after the run, even after the distributor plate vibrator was used. Product carbon content was 1.2 wt %, which is an improvement over the last run and can be attributed, in part, to the reduced-velocity operation during final tailburn. Some product was lost due to the transport line cleanout, so a total product weight cannot be determined.

4.2.2.3. Run 5 (Figs. 4-9 Through 4-12)

In this run, ignition temperature was further lowered to 600°C while the main burn period superficial velocity was raised to 1.0 m/s as part of the parametric study.

Feed was 60,000 g of crushed TRISO fertile FSV type fuel particles.

Bed heatup required 45 min to reach 600°C. An O_2 ramp was used for ignition, as in Run 2, but with a 0.452 std. m^3/min O_2 flow at the end of the ramp period. Cooling air was completely on automatic, yielding a 15°C initial overshoot and ±10°C control thereafter. This is very satisfactory and will be used in the future.

Filter pressure drop peaked at 5 kPa with a high filter temperature of 800°C. The main burning period lasted for 60 min until the off-gas CO concentration declined to zero. Inlet flow was then altered to 60% O_2, lowering the filter temperature to 600°C by the time that O_2 appeared in

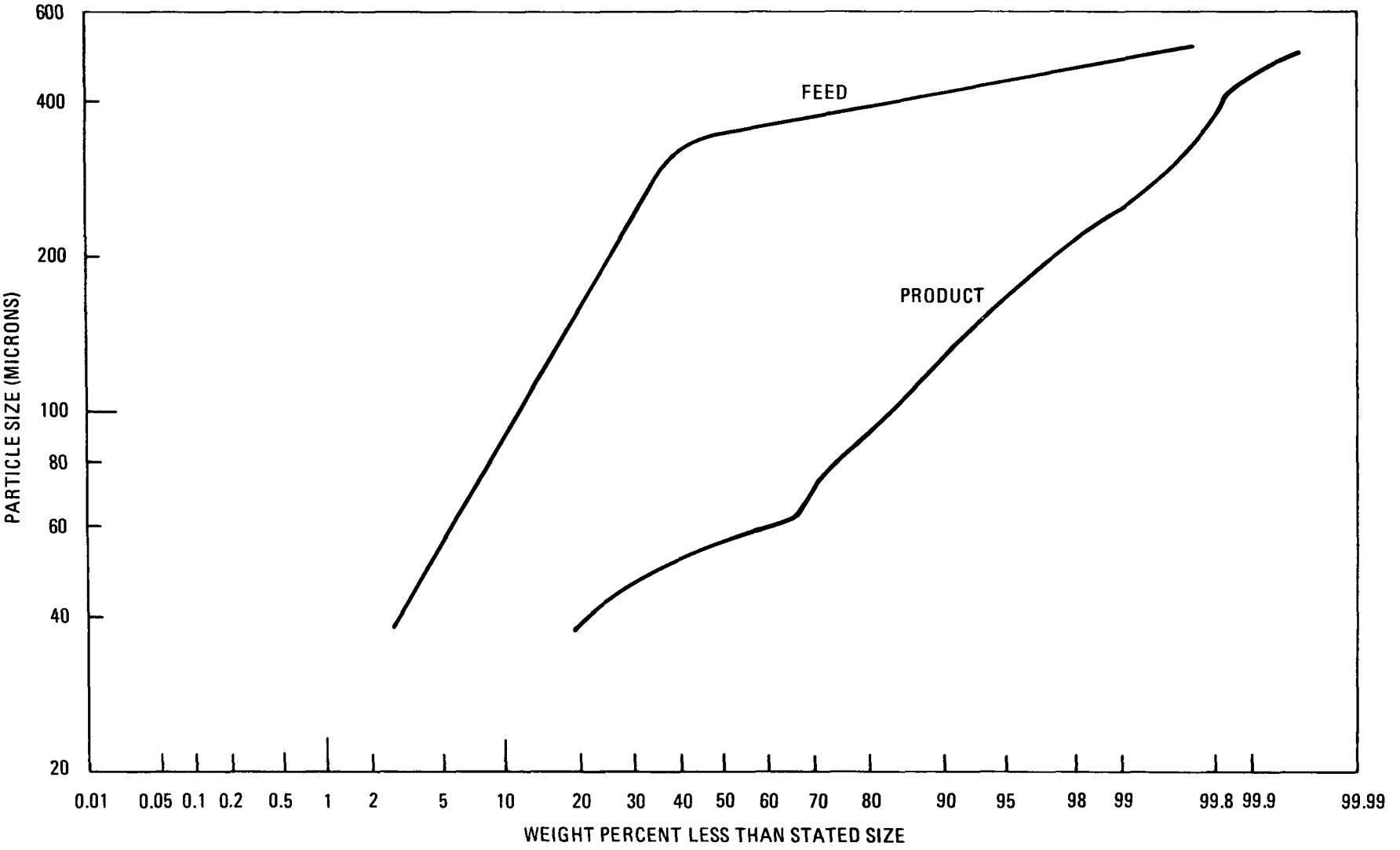

Fig. 4-9. Feed and product size distributions, 0.20-m secondary burner Run 5

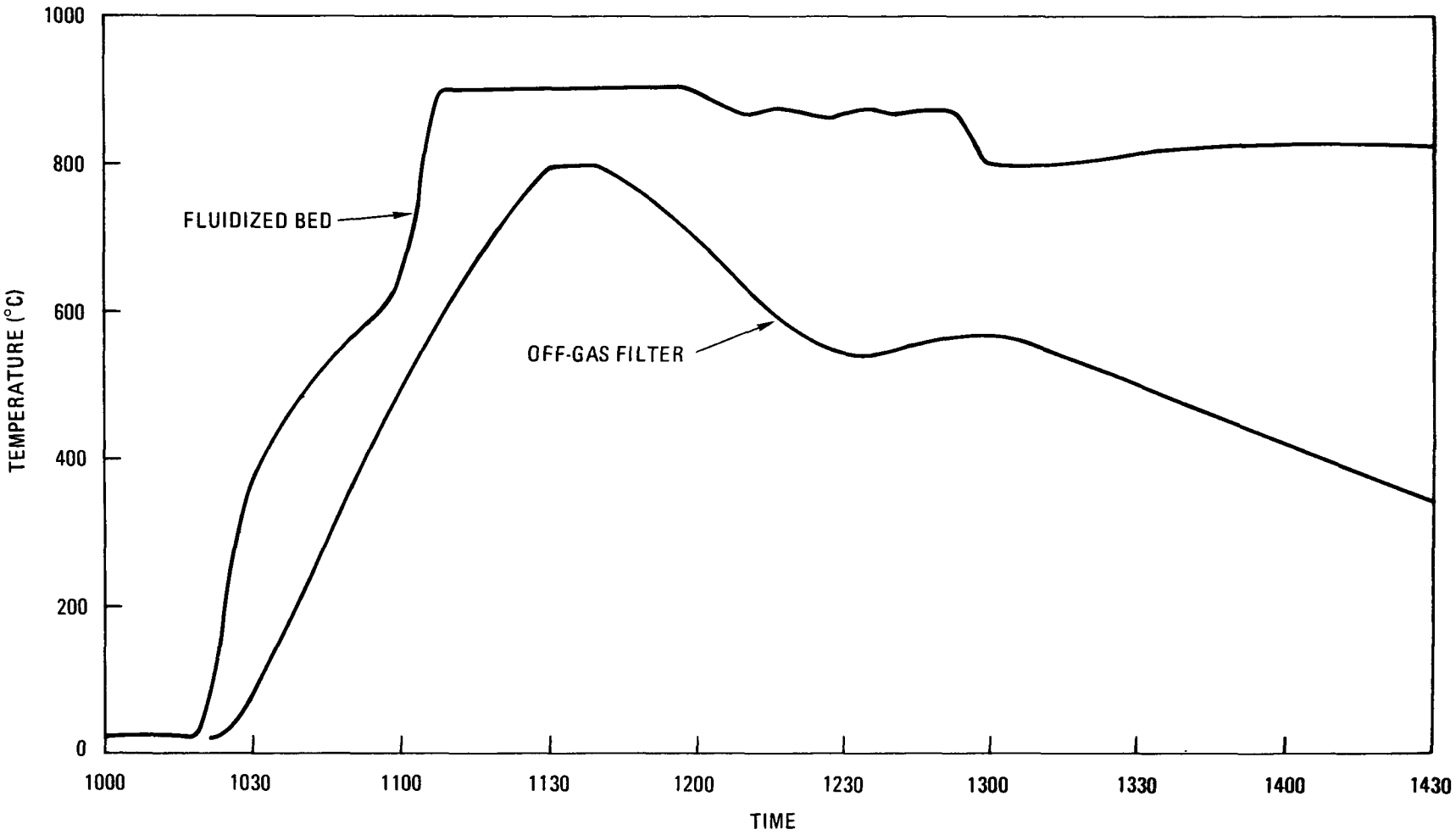

Fig. 4-10. Fluidized bed and off-gas filter temperatures versus time, 0.20-m secondary burner Run 5

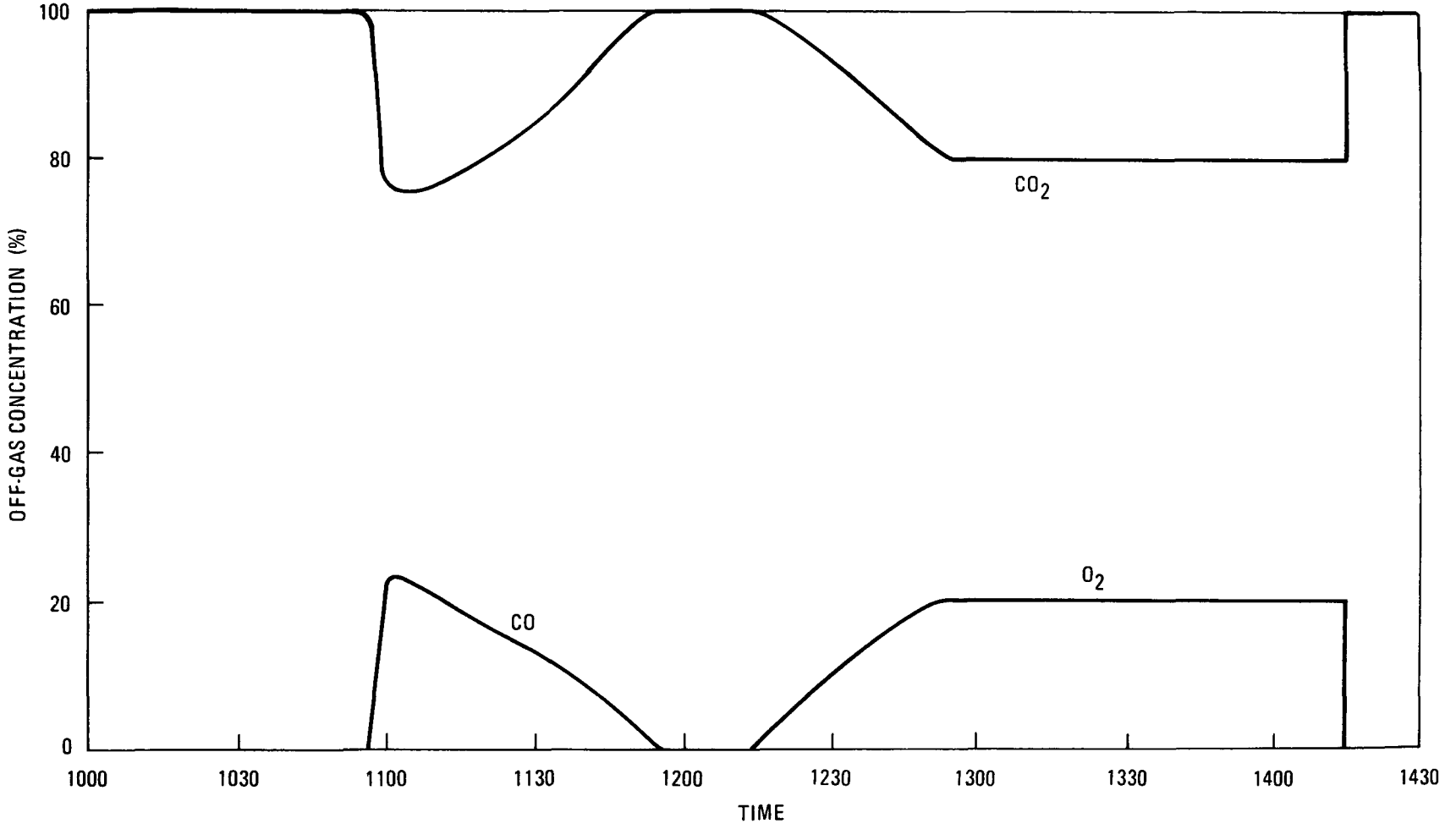

Fig. 4-11. Off-gas composition versus time, 0.20-m secondary burner Run 5

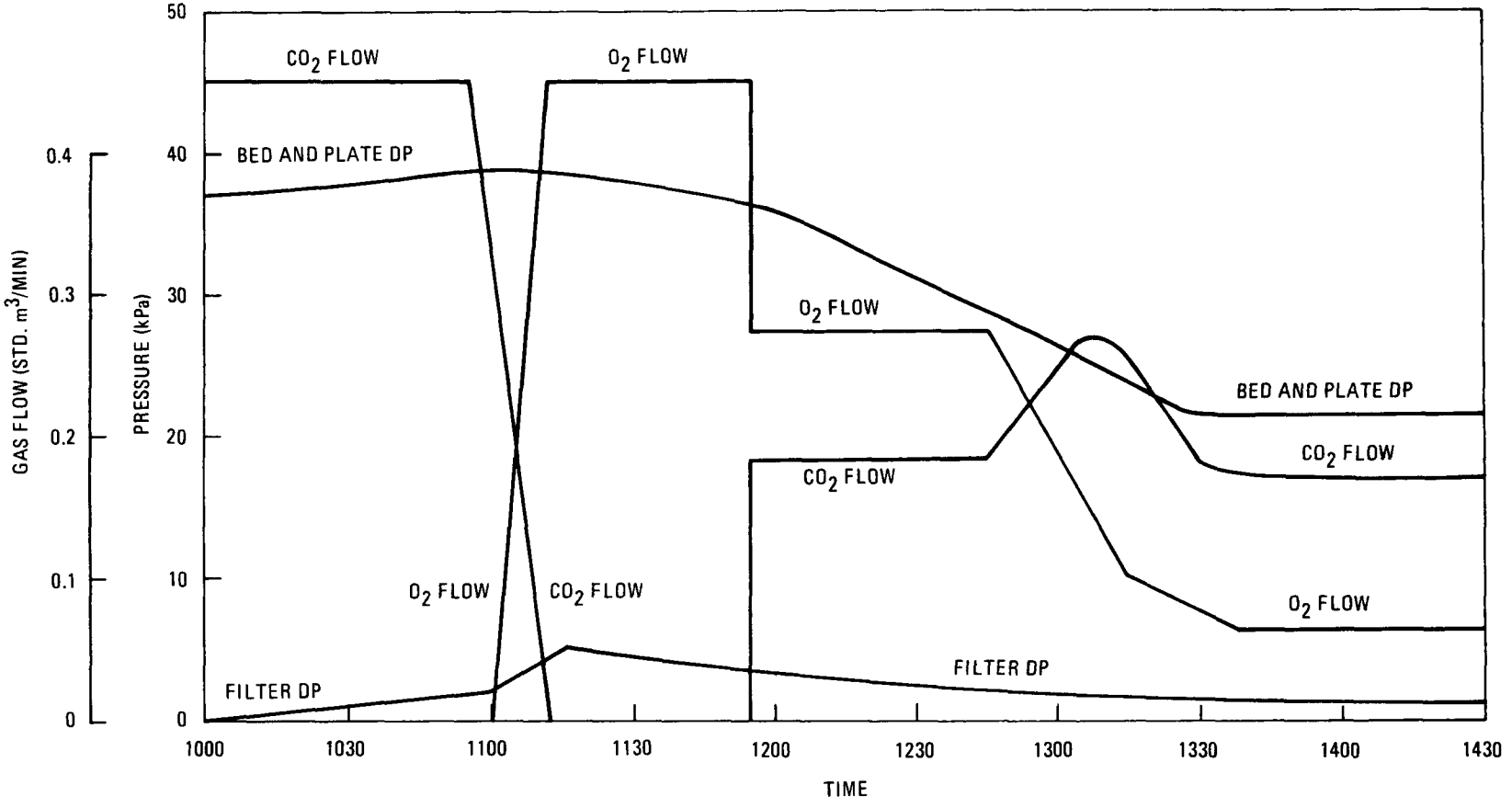

Fig. 4-12. Inlet gas flows and pressure drops versus time, 0.20-m secondary burner Run 5

the off-gas 35 min later. Off-gas O_2 content was not allowed to increase above 20% during the final tailburning period. Superficial velocity was again reduced to 0.46 m/sec (1.5 ft/sec) over the span of the 100-min tailburning period.

Product removal proceeded after the bed was cooled to 100°C. Twenty seconds after the product valve was opened, the system pressure drop became great enough to open a safety relief valve. The product valve was then closed to allow the transport line a chance to clear itself. This was followed by reopening and cleanout procedures.

A heel again remained on the distributor plate after the run. The function of the sweep tube was questioned at that time, so pressure gauges were installed. This revealed that the 6-mm (1/4 in.) CO_2 supply line was undersized so that only 276-kPa (40 psi) CO_2 was delivered to the sweep tube rather than the intended 689 kPa (100 psi). A 13-mm (1/2 in.) supply line was then plumbed in and the burner was reassembled. Following another cleanout procedure using the high-pressure distributor plate sweep tube, a 40-g heel of dusty material was left in the burner. This is an 0.08% heel and is quite acceptable.

Burner product weighed 47,229 g and contained 0.9 wt % carbon, which is the lowest amount yet attained in this burner. Use of low-velocity final tailburning will be continued.

4.2.3. Conclusions

Activity Plan AP524701 details ten acceptance criteria for the parametric study. These are discussed below:

1. No feed or product line blockage: The product line was blocked in Run 4 due to a rupture disc bursting under vacuum.

2. Feed time less than 15 min: yes.

3. Product removal time less than 30 min: See criterion 1.

4. Bed heatup in 1 hr, ability to idle at 800°C: Required 80 min to heat to 700°C in Run 3; can idle at 800°C (see Fig. 4-10).

5. Cooling system keeps bed at 900° ± 25°C: yes; in two runs overshot initially, in Run 4 by 50°C.

6. Control systems function properly: yes.

7. Distributor plate functions properly: yes.

8. Filter pressure drop <7.5 kPa: yes.

9. No appreciable leaks or cracks: acceptable.

10. No shroud frame deformation: aceptable.

4.3. 0.10-m SECONDARY BURNER (W. S. Rickman)

4.3.1. Introduction

The 0.10-m secondary burner Activity Plan (AP524701) includes a burner run using crushed FSV fertile fuel particles for the purpose of equipment shakedown. The remainder of the Activity Plan is concerned with crushed fissile particle burning.

Two burner runs were required due to operational problems encountered in the first burner run. The equipment is now ready for crushed fissile particle burning tests.

4.3.2. 0.10-m Secondary Burner Experimental Runs

4.3.2.1. Run 1-A

Fourteen kilograms of FSV TRISO fertile particles without outer PyC coatings were crushed through the prototype double roll particle crusher [0.1-m (4 in.) diameter rolls x 0.1 m (4 in.) wide] operating at 36 rpm roll speed. Samples taken before and after crushing this material yielded differing percentages of unbroken particles. This was traced back to improperly preloaded tapered roller bearings on the crusher. As material was being crushed, the rolls were being spread apart progressively so that the crushing action was altered. The distance between the rolls (the gap setting) had gone from 0.495 mm to 0.559 mm, allowing 2.8% of the fuel particles to go through uncrushed. Approximately 5% of the particles were only cracked in their outer coating of silicon carbide, but the fuel kernel had not broken free of the silicon carbide shell. An overall size distribution of feed material is shown in Fig. 4-13.

Crushed feed was added to the burner using the gravity pneumatic feeder. There was an upflow of 0.100 std. m^3/min CO_2 during feed addition and subsequent fluid bed heatup. The lowest bed thermocouple [located 0.08 m (3 in.) above the distributor plate] did not change from ambient during the entire heatup period. At the time, this was attributed to a short in the wiring.

Ignition came after the bed had been heated to 700°C. The inlet gas was changed from 0.1 std. m^3/min CO_2 to 0.1 std. m^3/min O_2 over a 10-min period. Cooling air was actuated to the filter chamber jacket but was not required for lower burner tube cooling.

The lowest bed thermocouple responded soon after combustion began. This suggests that the bed below the induction heated zone was stagnant during heatup and initial combustion due to insufficient gas velocity. Bed temperature throughout the run never reached the 900°C setpoint, being limited to 870°C due to heat removal in the filter chamber. Decreasing

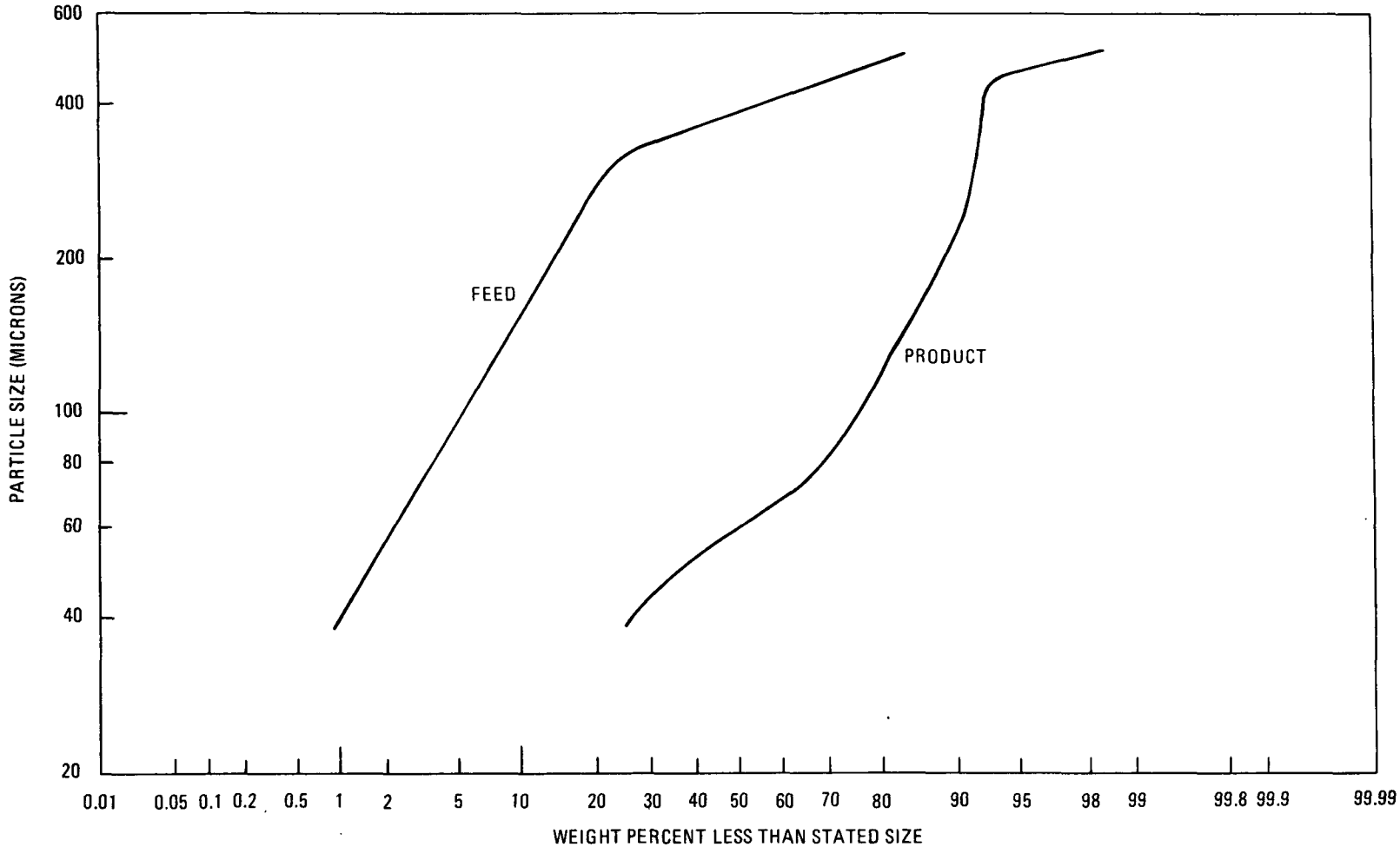

Fig. 4-13. Crushed feed and product size distributions, 0.10-m secondary burner Run 1-A

filter chamber cooling would allow the bed temperature to reach 900°C. However, the filters would then be hotter than desired (over 800°C), so the filters were cooled throughout the main burning period.

After the off-gas CO concentration dropped to zero, inlet gas was changed to 60% O_2 and 40% CO_2 to preclude any combustion in the filter chamber. As the bed burned out, O_2 flow was adjusted to keep the off-gas less than 20% O_2.

Product removal followed with the bed at 450°C. With the product valve open 6.4 mm (1/4 in.), ∿50 sec was required to empty the burner. An additional 5 min was utilized for heel cleanout.

Product material had a size distribution as shown in Fig. 4-13 and contained 1.8% burnable carbon. Burner disassembly revealed an agglomerate on the top of the distributor plate. It weighed 196 g and was roughly pyramidal in shape. Many cracked particles were observed in the agglomerate, with their kernels having melted and flowed through the cracks. Evidently, the stagnation during early combustion allowed particles to burn without a means to transport heat away. They melted and stuck together to form the agglomerate.

4.3.2.2. Run 1-B

A second burner run was made to try to eliminate the agglomeration problem. The roll crusher bearings were correctly preloaded to reduce the number of partially cracked and unbroken fuel particles. Also, lower bed temperatures were carefully watched. If they began to deviate from the rest of the bed, fluidizing velocity was increased to improve bed mixing.

Feed and product size distributions are shown in Fig. 4-14. The run proceeded much the same as Run 1-A, but bed temperatures were kept uniform by increasing gas flow; a flow of over 0.1 std. m^3/min was required only until the bed reached 350°C.

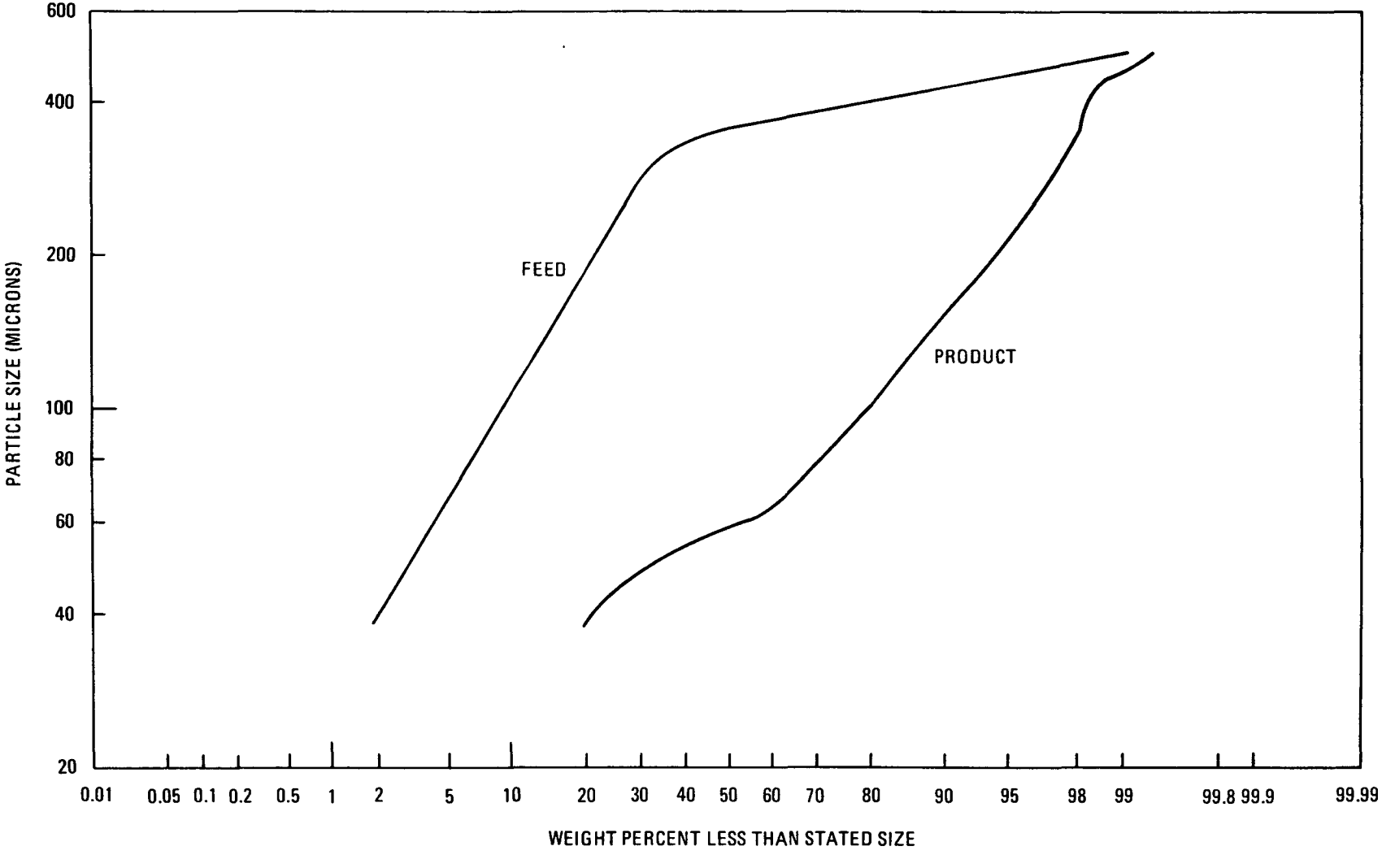

Fig. 4-14. Crushed feed and product size distributions, 0.10-m secondary burner Run 1-B

No burner tube cooling air was required throughout the run. Tail-burning and product removal were again trouble-free.

Product carbon content was 0.9% burnable carbon. Burner disassembly revealed a 2-g agglomerate resting on the distributor plate. This is a dramatic reduction from the first run, but could still be a source of problems if not eliminated completely.

Workers at Allied Chemical had reported small agglomerates forming whenever the inlet O_2 content was above 70 vol %. Their studies were at <0.3 m/s (<1 ft/sec) superficial velocity, while the present studies are at >1 m/s (>3 ft/sec). However, the implications are that reducing the inlet O_2 concentration from the present 100% will be required to eliminate the formation of these small agglomerates. The GA 0.20-m secondary burner has a reduced-diameter lower section which increases velocity to over 1.5 m/s (5 ft/sec). No agglomeration has been found after three runs on that burner. There is evidently a certain envelope of fluidizing velocity and inlet O_2 concentration that allows agglomeration. The current course of action is to proceed on the 0.20-m burner with pure O_2 at 1.5 m/s (5 ft/sec) in the lower burner portion and reduce to 70% O_2 on the 0.10-m burner at 1 m/s (3 ft/sec).

4.3.3. Conclusions

After the two runs, all the acceptance criteria listed in AP524701 had been met, as follows:

1. Induction heating - heat bed to 600°C in 1-1/2 hr: bed heated to 650°C in 1 hr.

2. Fluidization - keep axial bed $\Delta T < 100°C$: axial bed ΔT of <30°C.

3. Feeder - add bed in 10 min: bed added in 5 min.

4. Off-gas - no explosive mixture: filter DP < 7.5 kPa.

5. Cooling - burn at 50 g/min without exceeding 900°C: yes.

6. Product - <0.5% heel: <0.05% heel; carbon content < 2%: 0.9% carbon content.

7. Auto control - keep variables within specified limits: yes.

Shakedown operations have been concluded. The burner is ready for crushed fissile particle operations to begin.

4.4. PARTICLE CRUSHING (J. W. Baer, W. S. Rickman)

4.4.1. Introduction

The crusher was used for making crushed feed for six runs on the 0.20-m secondary burner. A localized wear problem has been identified in the crusher body side plate, with several fixes being evaluated and tested.

The fissile particle roll crusher has been received from manufacturing.

4.4.2. Fertile Crusher

Following completion of checkout procedures, as described in Ref. 4-1, six 60-kg batches of fertile FSV TRISO fuel particles were crushed through the roll crusher. Wear was noted in the crusher body side plates adjacent to the actual crushing area. This was in a local area between the rolls, about 1 to 2 cm long, consisting essentially of a groove. Silicon carbide fuel particle coatings were evidently abrading the hardened steel surface, thus causing the groove.

There was concern that sufficient wear would allow fuel particles to bypass the crushing action intact, so corrective action was taken. First, a chromium oxide flame spray was used to fill the groove; this wore excessively after crushing one 60-kg batch. Second, a tungsten carbide flame

spray was tried, and it too was unsuccessful following crushing of a 60-kg batch. The side bodies were next slotted by electrical discharge machining (EDM), and inserts of high-density, cemented tungsten carbide were embedded in the slots. Each side plate contains a different candidate insert material for comparative evaluation purposes. These materials have hardnesses typically equivalent to R_c 80 to 83, as compared with the plasma-sprayed chromium oxide at R_c 74 and the tungsten carbide composites at R_c 60 to 70. The crusher with inserts has processed 60 kg of material without disassembly and there is no evidence of wear. The unit will be disassembled and inspected after the next 60-kg throughput. One side plate with the tungsten carbide insert is shown in Fig. 4-15.

4.4.3. Fissile Crusher

The fissile crusher has been received and is undergoing preparation for crushing of FSV type, depleted uranium TRISO fissile particles for secondary burner feed. Problems encountered during construction required imposing 100% inspection on all parts of the assembly. Substantial reworking of components was necessary to obtain hardware built to engineering specifications.

Inspection of the finished rolls by HDE dye penetrant revealed the presence of fine, intermittent, small circumferential cracks at a common location at the identical end of two of the four rolls purchased. The rolls were accepted for installation after consideration of the crack severity and location and the anticipated roll service. The cause of the cracking is under investigation. The crushing surfaces of the four rolls were scanned using a surface analyzer, and the surface profiles and surface finishes were documented for future comparative wear determinations.

REFERENCE

4-1. "Thorium Utilization Program Quarterly Progress Report for the Period Ending August 31, 1976," ERDA Report GA-A14085, General Atomic Company, September 30, 1976.

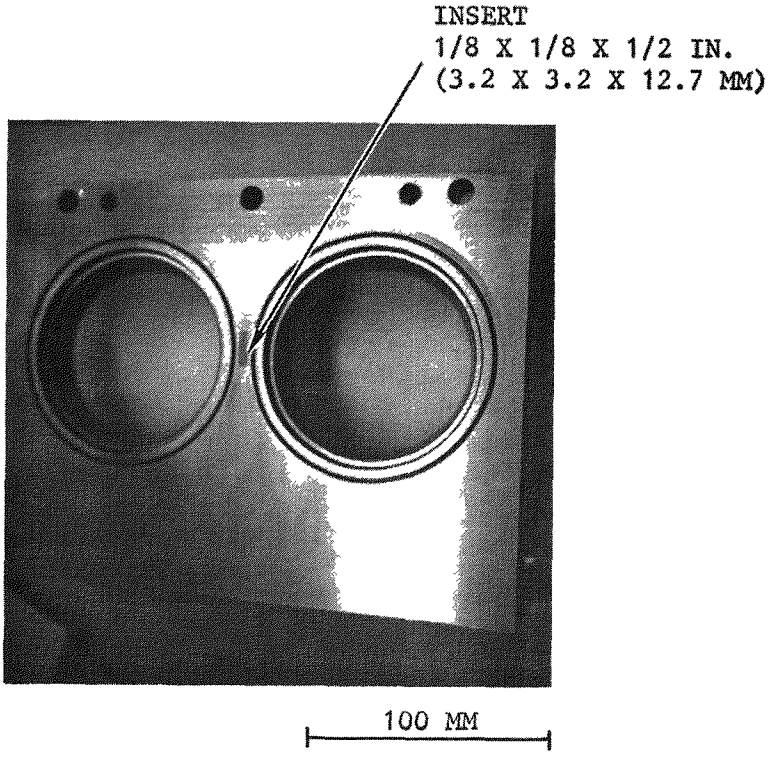

Fig. 4-15. Fertile crusher side body with tungsten carbide insert

5. AQUEOUS SEPARATIONS

5.1. SUMMARY

The conceptual design of the engineering-scale dissolver-centrifuge for incorporation into the head-end line was completed during the quarter with the issuance of the Design Criteria and System Description and the Process Flow and Piping and Instrument Diagrams.

A series of bench-scale dissolution runs was made on ThO_2 kernels using the heel operating mode with lower-acidity dissolver acid. Preliminary results indicate the dissolver nitric acid concentration can be lowered from 13M to 11M while using a 60% heel without decreasing dissolution rates.

5.2. ENGINEERING-SCALE DISSOLUTION (H. H. Yip)

5.2.1. Large Engineering-Scale Dissolver-Centrifuge System

5.2.1.1. Introduction

During previous quarters, commercially available centrifuges were reviewed and a vertical continuous unit was ordered.

The conceptual design of the engineering-scale dissolver-centrifuge for incorporation into the engineering-scale head-end line was completed during the quarter with the issuance of the System Description (SD526101), Design Criteria (DC526101), and Process Flow (PF) and Piping and Instrumentation (PI) Diagrams.

5.2.1.2 System Definition

Dissolution of the HTGR fertile fuel occurs after classification of the fissile and fertile particles. The fissile particles must be crushed and burned in the 0.20-m prototype fluidized-bed crushed fuel particle burner (the secondary burner). The burner ash is then added to a dissolver containing a boiling nitric acid solution (fissile particles) or a boiling Thorex solution (fertile particles). After the uranium oxides have been dissolved, the slurry consisting of the insolubles and the mother liquor is transported to a centrifuge which separates the liquid from the solids. The mother liquor is then fed directly to the solvent extraction system. The solids fall into the repulp tank, where they are mixed with water and recentrifuged. The mother liquor from thorium-containing particles, however, is processed through the feed adjustment equipment prior to entering the solvent extraction process.

The large engineering-scale dissolver-centrifuge system consists of the following subsystems:

1. Dissolver.
2. Condenser.
3. Centrifuge.
4. Repulp tank.
5. Feed and product tanks.
6. Insols dryer (a future addition).

The dissolver size controls the interface and size requirements of other equipment in the system. The dissolver is sized to accommodate a maximum charge of 200 liters of dissolvent and the equivalent amount of BISO or TRISO fuel to yield:

1. A throughput of approximately 200 moles of $Th(NO_3)_4$ solution ($\sim$1M) in <24 hr (BISO operation), or

2. A predetermined concentration (TBD) of $UO_2(NO_3)_2$ solution in ≤6 hr. (The amount of uranium to be dissolved will depend on (a) the allowable concentration of silicon carbide in the slurry and (b) the allowable fission product concentration in the 200 liters of dissolvent. A maximum ∿0.1M UO_2^{++} solution will be used as a design basis for the purpose of sizing the dissolver.)

The capacity of the dissolver will be twice the volume of its maximum charge while boiling to accommodate foaming and splashing. The liquid portion of the dissolver will be ∿0.45 m (∿18 in.) in inside diameter and will have an L/D ∿ 2.7. The vapor phase of the dissolver will not be under the aforementioned L/D or inside diameter constraints.

With the dissolver as a basis, the following equipment capacities (TBV) are required:

KF tank	38 liters	10 gal
$Al(NO_3)_3$ tank	57 liters	15 gal
Thorex tank	377 liters	100 gal
Dissolver	400 liters	106 gal
Product tank	1130 liters	300 gal
Condenser	(TBD) lpm	(TBD) gpm
Repulp tank	377 liters	100 gal
Centrifuge	4 to 15 lpm	1 to 3 gpm (TBV)

5.2.1.3. Functional Requirements

The engineering-scale dissolver-centrifuge system will be used to gather data to be used in the design of the aqueous portion of the head-end in the HTGR Recycle Demonstration Facility (HRDF). Specifically, this system is to accomplish the following system functions:

1. Receive solid feed material from:

   a. The secondary burner product bunker.

b. The classifier product bunker.

c. Stored material.

2. Dissolve the contained heavy metals of FSV and reference TRISO/BISO fuels.

3. Separate the nitrate solution from insols (after completion of dissolution).

4. Provide adequate product clarity suitable for feed adjustment and solvent extraction.

5. Wash and rinse the insols, with the rinse solution joining the mother liquor from dissolution.

6. Demonstrate the aqueous portion of HRDF head-end sequential operation by an integrated head-end test.

5.2.2. Engineering-Scale Experimental Investigation

Dissolution runs have been made in previous quarters to determine the potential advantage of using a heel operating mode for sol gel ThO_2 kernel dissolution. The results have indicated that a 40% heel can reduce dissolution time by a factor of three.

Due to equipment repair and a change in lead engineer, no reportable dissolution runs were obtained. Segment 3 in Section 3.1 of the Activity Plan (AP526001) will be initiated in the coming quarter to establish operating parameters for dissolution with heel operation in the 0.13- and 0.20-m leachers.

5.3. BENCH-SCALE DISSOLUTION (R. G. Wilbourn)

5.3.1. Introduction

Dissolution rate data for ThO_2 in Thorex have been previously reported for bench-scale heel operations (Ref. 5-1). Heel operation takes advantage of the rapid dissolution rate during the first portion of leaching of ThO_2 kernels.

Dissolution rate data were obtained during the present reporting period for bench-scale heel operations using diluted Thorex. These experiments were performed in order to provide operating parameters for use in the event of inadvertent Thorex dilution in plant operations.

5.3.2. Discussion

As in earlier bench-scale experiments, the diluted Thorex dissolution experiments were performed in a conical-bottom glass dissolver (Fig. 5-1). A ThO_2 heel sufficient to yield a 2.5M thorium-Thorex mother liquor on complete dissolution was used in all experiments. Figure 5-2 compares the results obtained with two diluted Thorex solutions [11M HNO_3, 0.1M $Al(NO_3)_3$, 0.05M F^- and 9M HNO_3, 0.1M $Al(NO_3)_3$, 0.05M F^-, respectively] and similar data from a test using Thorex of normal process specification [13M HNO_3, 0.1M $Al(NO_3)_3$, 0.05M F^-].

Examination of Fig. 5-2 indicates the rate of ThO_2 dissolution to a 1M thorium-Thorex mother liquor is essentially identical for 13M and 11M Thorex with a 60% heel. However, a substantial reduction in dissolution rate is observed for an initial Thorex nitric acid concentration of 9M.

5.3.3. Conclusion

The positive results obtained from bench-scale experiments with diluted Thorex are encouraging and may permit a reduction of the required

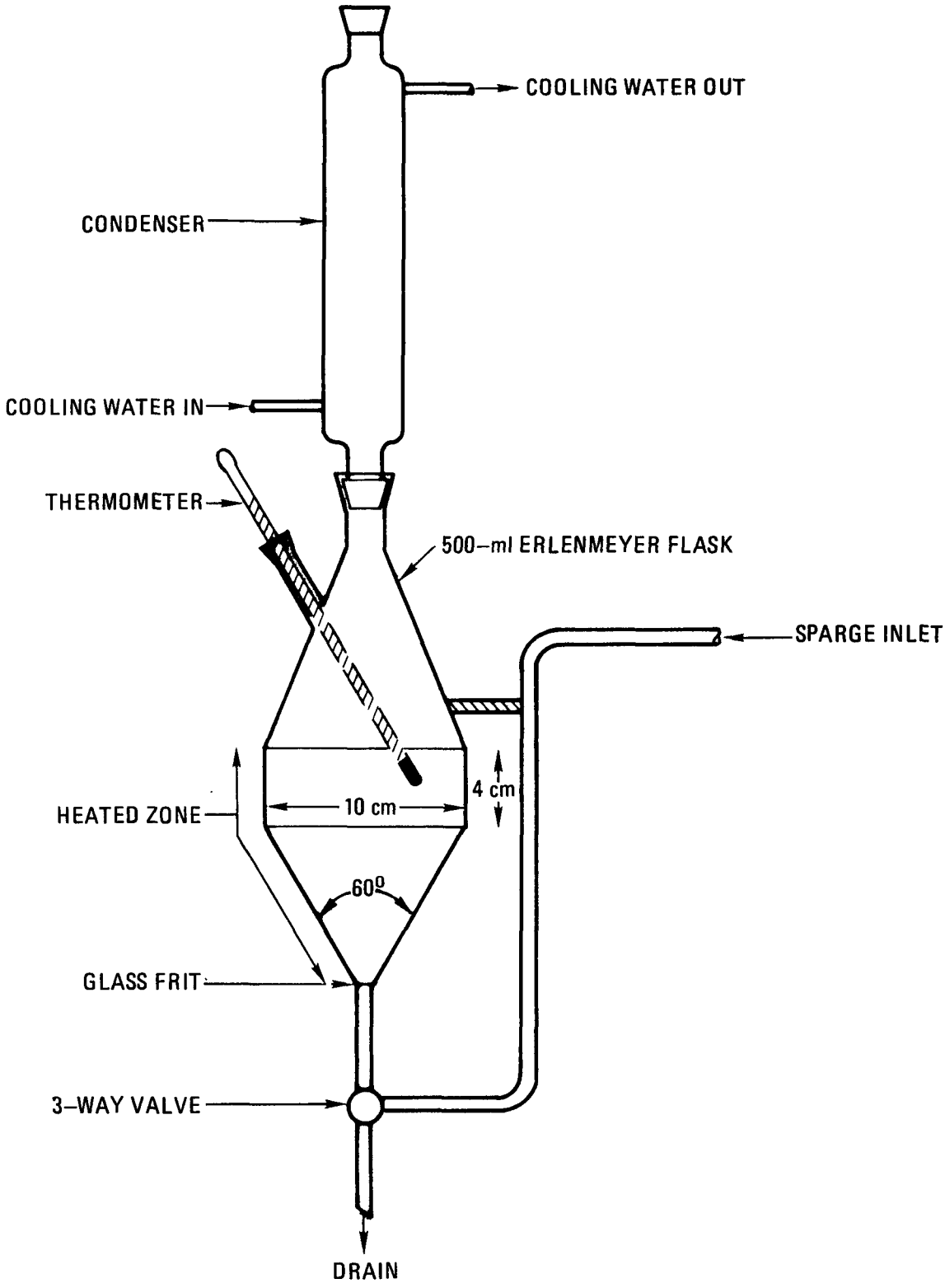

Fig. 5-1. Bench-scale conical dissolver

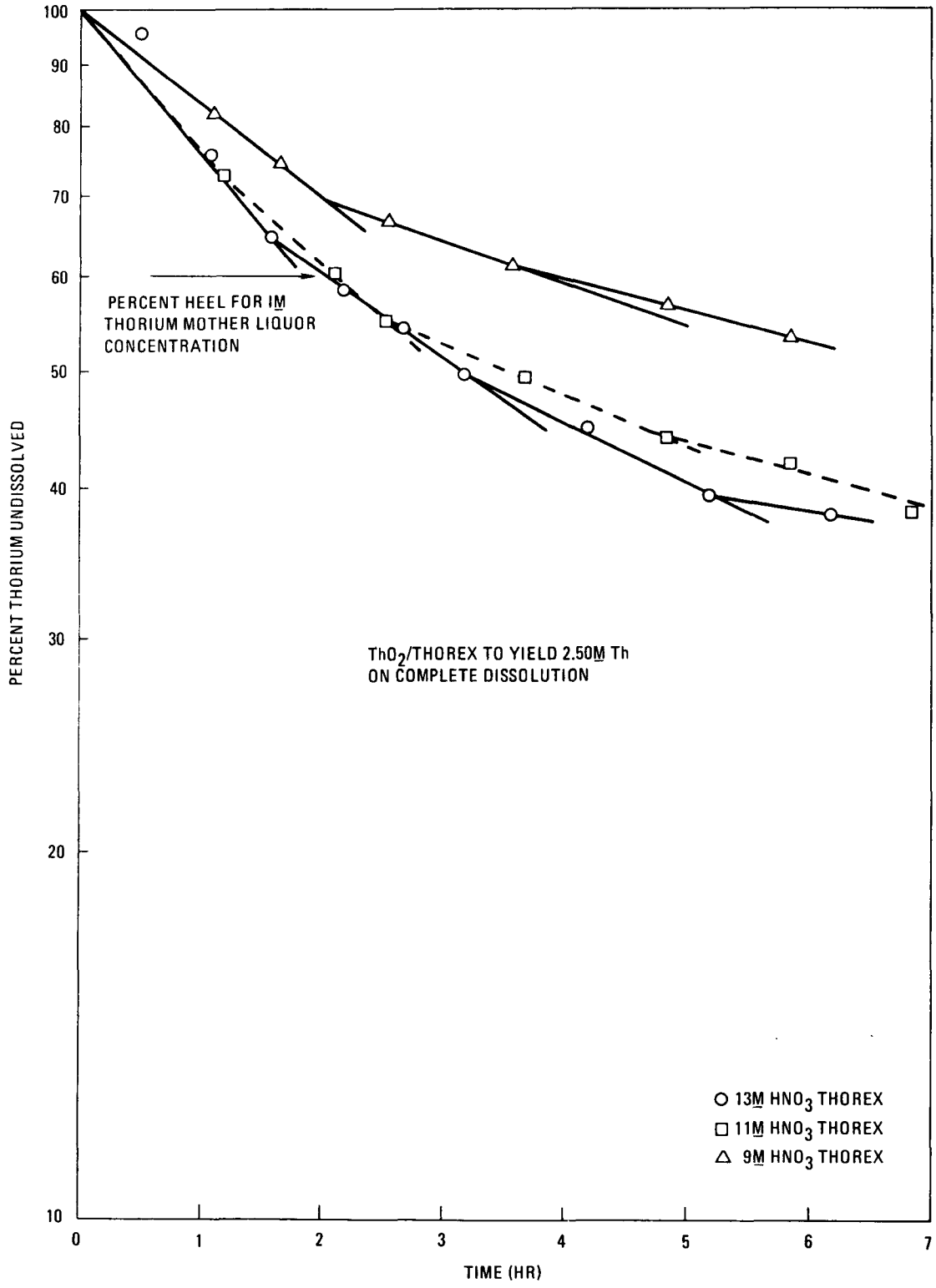

Fig. 5-2. Comparison of dissolution rates from bench-scale conical dissolver tests with 60% heel

concentration of acid in the HRDF recycle, thereby simplifying the recycle acid system design and easing its operating requirements.

REFERENCE

5-1. "Thorium Utilization Program Quarterly Progress Report for the Period Ending November 30, 1976," ERDA Report GA-A14214, General Atomic Company, December 1976.

6. SOLVENT EXTRACTION

6.1. SUMMARY

Three solvent extraction feed adjustment runs were completed during the quarter. Two of the runs were representative of the continuous intercycle concentration step. The other run was a continuous operation which utilized leacher product as feed. These runs were used to test the modified equipment and also to familiarize new personnel with the equipment operation. The runs were generally successful, although some operating problems did arise. Additional runs will be used to test modifications and further define the flowsheet.

Three solvent extraction runs were completed during the quarter. These runs represented the first cycle of the Acid-Thorex flowsheet (shown in Fig. 6-1). The Robatel centrifugal contactor and the five pulsed columns in the solvent extraction pilot plant were used in these experiments. Tracer quantities of radioactive zirconium were added to permit determination of zirconium decontamination throughout this solvent extraction system.

In each of the solvent extraction runs, higher than anticipated losses occurred from the 1A centrifugal contactor via the 1AW stream. Poor partitioning efficiencies, as indicated by the analyses of the 1CU and 1BT streams, are discounted and attributed to analytical error. The analytical values shown in earlier publications (e.g., Ref. 6-1) are accepted as more reliable data. Subsequent to the analyses for these runs, analytical techniques were modified to yield more accurate values for the low-level constituents (see Section 6.3.1).

The zirconium decontamination factors (DFs) were as much as 50% higher with the centrifugal contactor than with the all-pulse-column system. This

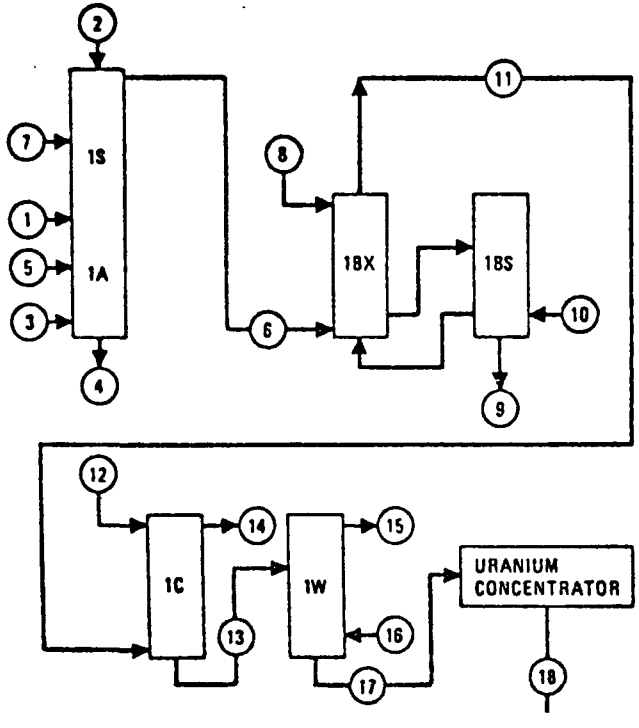

STREAM	STREAM NO.	RELATIVE FLOW	COMPOSITION U (G/L)	COMPOSITION Th (G/L)	COMPOSITION HNO_3 (M)
1AF	1	100	35	348	1.0
1AS	2	104			0.01
1AX	3	1000		(30% TBP)	
1AW	4	262		(FISSION PRODUCTS)	
1AA	5	32			13.0
1SP	6	1000	3.5	35	
1AIS	7	26			5.0
1BX	8	600			0.2
1BT	9	600	Trace	102	
1BS	10	179		(30% TBP)	
1BU	11	1180	2.98		
1CX	12	593			0.01
1CU	13	593	5.93		
1CW	14	1180		(30% TBP)	
1WW	15	59		(NPH)	
1WS	16	59		(NPH)	
1WU	17	593	5.93		
2AF	18	6	233		

Fig. 6-1. Thorex solvent extraction partition flowsheet

DF improvement could be due to reduced extraction of zirconium in the high-acid end of the extraction section resulting from the lower residence time of the centrifugal contactor.

6.2. SOLVENT EXTRACTION FEED ADJUSTMENT* (G. W. Reddick)

6.2.1. Introduction

The continuous solvent extraction feed preparation process consists of continuously feeding an acidic thorium nitrate stream to a boiler pot of boiling concentrated, acid-deficient thorium nitrate solution. Excess acid from the feed stream is boiled off (steam stripped), leaving more acid-deficient thorium nitrate in the boiler pot. The acid-deficient thorium nitrate product is continuously or semicontinuously removed from the boiler pot and is then diluted with water to prevent solidification upon cooling. There is potential for using formic acid to provide some denitration of the feed in addition to steam stripping.

A continuous feed preparation system has the advantage of providing a uniform condensate flow and composition, thereby facilitating operation of the downstream waste processing system. Also, since the solvent extraction process is inherently continuous, there is an additional incentive to have a continuous feed preparation step for the dilute, intercycle thorium stream.

Bench-scale demonstration of the feasibility of the process for continuous feed preparation has been completed. Pilot plant testing is being done (1) to determine necessary equipment items for commercial-scale operation, in particular, for the difficult task of concentrated product removal, and (2) to determine scale-up effects from the bench-scale work. In the runs discussed below, the tower on the pilot plant unit was void of packing.

*Previously in Section 5.

6.2.2. Results and Discussion - Run 25

Run 25 in the feed adjustment system was a representation of the startup operation of the continuous intercycle concentration and denitration step. The feed to the evaporator/stripper was representative of 1BT stream expected from the first cycle of the Thorex flowsheet.

The system operated well after some initial operating problems which resulted from a pressurization of the evaporator/stripper. The product was made acid deficient without adding any stripping medium other than the water contained in the simulated 1BT stream. The average feed rate to the evaporator/stripper during the run was about 1/2 liter/min. This was a significantly improved rate over those attained in previously reported runs (Ref. 6-2). Modifications to increase the coil area were responsible for the improved boil-off rate, which allowed higher feed rates.

This run successfully demonstrated startup with acid-deficient solution in the evaporator/stripper. The desired product concentration in the pot was achieved. Future runs will be required to demonstrate startup and equilibrium operation with nominal 1BT stream as feed. Run 25 achieved the desired thorium concentration in the product. The stream analyses are given in Table 6-1.

The evaporator/stripper contained 32 liters of acid-deficient solution for startup. However, at startup the full steam flow was used. The high boil-up rate pressurized the evaporator/stripper, and about half of the solution was pushed into the collection tank for the condensed overheads. The evaporator was then refilled with the nominal 1BT feed and restarted. No other operational problems developed during the run. Based on this startup experience, the recommended startup procedure for future runs will be to control the volume of the solution to a minimum operating level and slowly bring the temperature of the solution to boiling.

The concentration of the nominal 1BT feed which was fed to the evaporator/stripper was 0.16$\underline{M}$ $Th(NO_3)_4$, 0.40$\underline{M}$ HNO_3, 0.015$\underline{M}$ $Al(NO_3)_3$, and

TABLE 6-1
FEED ADJUSTMENT RUN 25 STREAM SAMPLE ANALYSES

	g-moles H^+/ g-mole Th	H^+ (M)	Th (M)	Al (M)	F^- (M)	Density (g/cm^3 at 22°C)
Initial Pot Solution	-0.33	-0.034	1.02	0.074	0.054	~1.30
Feed	2.5	0.4	0.16	0.015	1.2×10^{-2}	1.05
Product (after dilution)	-0.086	-0.231	2.70	0.218	0.017	1.84
Overheads[a]	2.8×10^{3}	0.441	1.58×10^{-4}	1 ppm	2.21×10^{-4}	1.015

[a] These analyses do not reflect the loss of about half of the initial pot solution. These analyses are an average of the distillate samples, excluding the first sample, which has a high thorium analysis due to pressurization in the pot. The analysis of the overheads composite sample yielded the following results: HNO_3 = 0.33M, Th = 0.056M, Al^{+++} = 0.006M, F^- = 3.9×10^{-3}M, density = 1.03 g/cm^3.

0.012 g KF. The total volume of this feed was about 276 liters and was fed at the rate of 0.5 liter/min. This feed stream was added directly to the pot and was not steam stripped for TBP removal. The volume of solution in the evaporator/stripper was controlled near 20 liters. As the concentration of thorium increased in the evaporator/stripper, the temperature and specific gravity also increased. The maximum solution temperature was 135°C at a specific gravity of 2.2.

The product transfer jet system was tested under the conditions of peak concentration. The transfer of product proceeded without difficulty. The liquid level dip leg plugged near the peak concentration but was unplugged by using water. The final product volume in the evaporator/stripper before dilution was about 16 liters. This solution was diluted with water to about 27 liters before cooling.

Some difficulty in sampling the evaporator contents occurred before and after the operation. The contents of the evaporator/stripper were apparently not thoroughly mixed after the dilution water was added prior to sampling. In each case the analyses were representative of the solution present in the evaporator/stripper prior to dilution. The analysis of the product in the evaporator/stripper was 2.7M thorium and -0.23M nitric acid after dilution.

The overheads nitric acid composition is plotted versus time in Fig. 6-2. The analyses of two samples of the evaporator are also shown. The nitric acid concentration in the overheads is a function of boiling temperature (thorium concentration) of the evaporator/stripper solution, the acidity of the solution, and the feed acidity.

Based on the analyses of the overheads, about 1% of the fluoride in the feed was volatilized.

6.2.3. Results and Discussion - Run 26

Run 26 in the feed adjustment system was made to test continuous operation with feed which was representative of the leacher product. This run

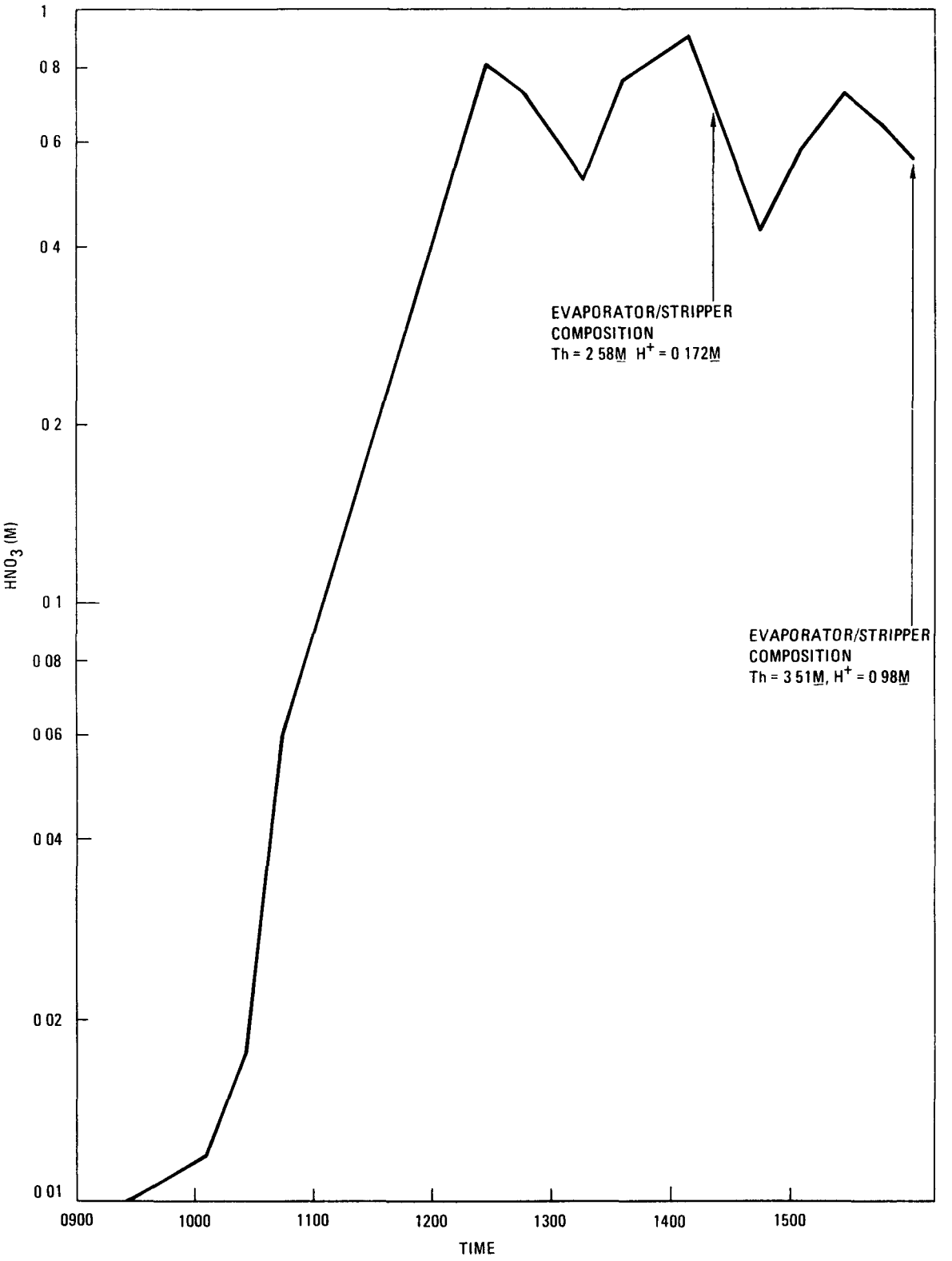

Fig. 6-2. Feed adjustment Run 25 - HNO_3 concentration of overheads versus time

was used to test both the flowsheet requirements and the operability of the equipment. The purpose of this flowsheet step is to produce feed for the first cycle of the solvent extraction. The concentration requirement for this feed stream is 1.5M $Th(NO_3)_4$ and 1.0M HNO_3.

This run demonstrated that a continuous operation can be used to produce feed which is acceptable for the first cycle of solvent extraction. The concentrated feed adjustment product had a hydrogen to thorium mole ratio of 0.34. A ratio of less than 0.67 is required for the solvent extraction feed. The addition of water to the pot was required to strip the nitric acid from the thorium.

Very little thorium or fluoride was carried into the overheads stream. Product was successfully removed from the pot throughout the run. No significant operational or equipment problems occurred during the run.

The evaporator/stripper was started up with acid-deficient solution in the pot. This solution was brought to boiling temperature, and the feed addition was begun. The feed was typical of the expected leacher product solution.

Some perturbations in the startup operation resulted in fluctuations of the solution density and temperature. During this period of operation the density of the pot solution increased enough that the dip leg on the liquid level instrumentation plugged. The dip leg was flushed to remove the plug.

After the desired liquid level and temperature for steady-state operation were achieved, water addition was begun as the stripping medium. The operating solution volume for the pot was about 21 liters. The temperature was controlled near 135°C. The feed and stripping water were continuously added at these conditions. Product was also continuously removed.

The distillate acidity during the run is plotted versus time in Fig. 6-3. The steady-state operation began about 10:15 a.m. During the period

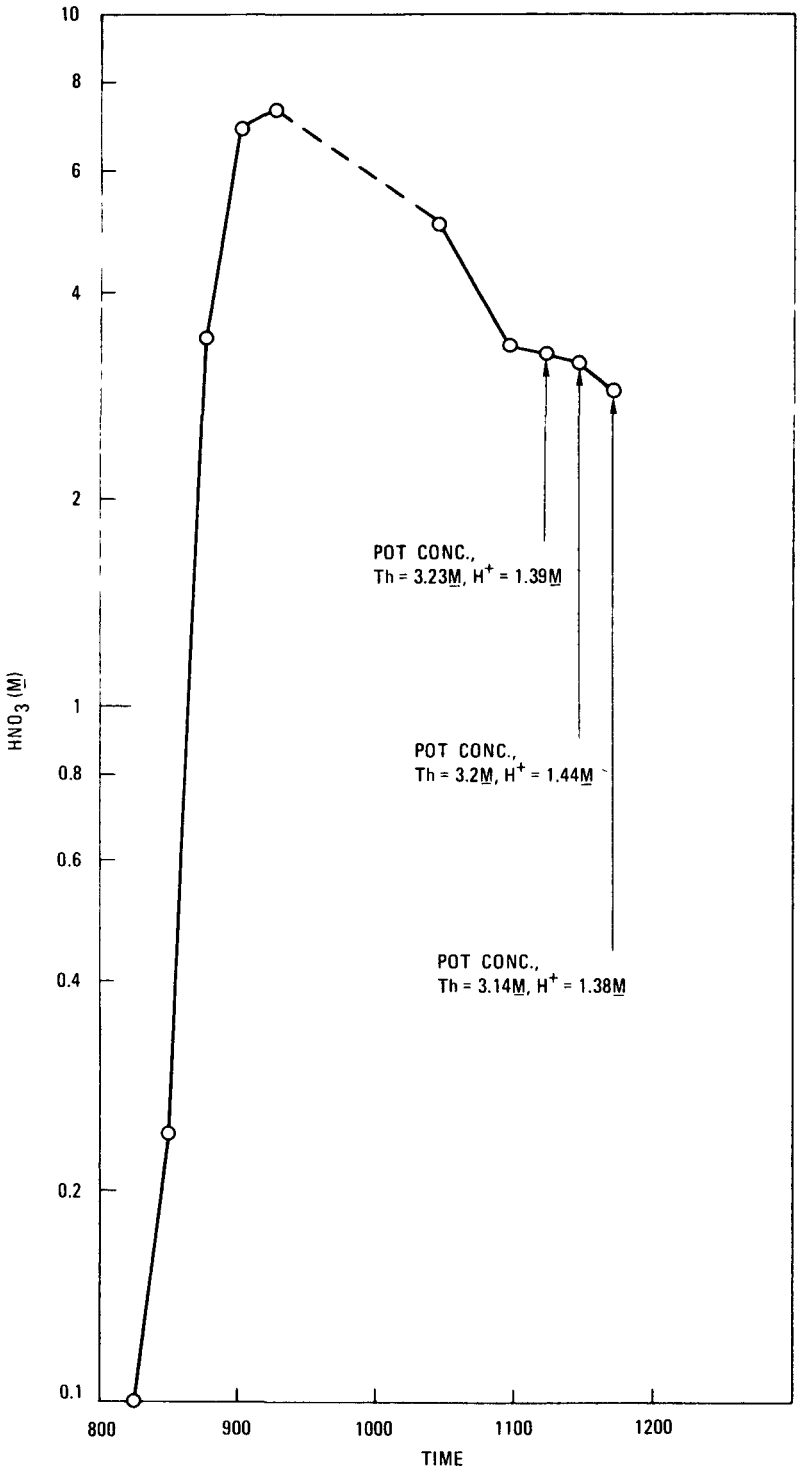

Fig. 6-3. Feed adjustment Run 26 - HNO_3 concentration of overheads versus time

of constant volume in the pot, the distillate acidity ranged between 3M and 5M. The only slight decrease in acidity in the distillate which occurred from 10:00 a.m. until the end of the run was accompanied by essentially no change in the nitric acid to thorium ratio in the pot. The average volume ratio of the addition rates for the stripping water and feed during this operating period was about 1.15. The average addition rate (stripping water plus feed) was about 0.37 liter/min.

The mole ratio of nitric acid to thorium in the pot during the steady-state operation was about 0.45. The requirement for feed to solvent extraction is a ratio of nitric acid to thorium of 0.67. Based on the data from Run 26, meeting this requirement appears feasible with the continuous system.

Table 6-2 contains the sample analyses for the various input and output streams of Run 26. Approximately 1% of the fluoride present in the feed was volatilized into the overheads. The amount of thorium entrainment was very low (approximately 0.01%).

6.2.4. Results and Discussion - Run 27

Run 27 in the feed adjustment system was a representation of the continuous intercycle concentration and denitration step. The evaporator/stripper in the leaching room was used for this operation. The feed was representative of the 1BT stream expected from the first cycle of the Acid-Thorex flowsheet. The purpose of this run was to demonstrate both startup and continuous operation of the intercycle step.

The evaporation/stripper system operated well throughout the run. Pressurization of the evaporator/stripper at startup caused the loss of some solution from the evaporator/stripper via the overheads. Acid-deficient product was not obtained from this operation. The average feed rate to the evaporator/stripper during the run was about 0.61 liter/min.

TABLE 6-2
COMPOSITION OF FEED ADJUSTMENT RUN 26 STREAM SAMPLE ANALYSES

	g-moles H^+/ g-mole Th	H^+ (M)	Th (M)	Al (M)	F^- (M)	Density (g/cm^3 at 25°C)
Initial Boiler Pot	-0.086	-0.23	2.70	0.22	0.017	1.82
Feed	9.74	7.69	0.79	0.104	0.075	1.53
Product (after dilution)	0.34	0.47	1.38	0.15	0.10	1.60
Distillate	1.43×10^4	2.77	2×10^{-4}	0.48 ppm	5.1×10^{-4}	1.11

The run lasted about 17 hr over a 3-day period. The evaporator/stripper was started up and shut down each day, with no startup or shutdown difficulties being experienced except on the first day of startup. About 12 hr of operation were required before the steady-state thorium concentration was achieved in the evaporator/stripper. After this steady-state concentration was achieved, product was semicontinuously removed from the evaporator/stripper. Sample analyses are given in Table 6-3. Some modifications in the future operation of the evaporator/stripper will be required to yield a product which is acid deficient.

The evaporator/stripper was pressurized at startup with resultant loss of solution from the boiler pot similar to that which occurred in Run 25. Since these problems with startup control were encountered, the off-gas train has been significantly modified to reduce the potential of accidental liquid loss from the boiler pot.

The feed for Run 27 was essentially the same as that used for Run 25. In Run 27 this feed was also used for the startup material in the evaporator/stripper, whereas in Run 25 acid-deficient material was used in the evaporator/stripper for startup. The feed which is equivalent to the 1BT stream is dilute in thorium concentration. About 12 hr of boiling operation were required to achieve the desired thorium concentration in the evaporator/stripper. After this concentration (specific gravity of 2.0 at 130°C) was achieved, product was semicontinuously removed for the remainder of the run.

The product removal system worked well. Steam was used as the motive fluid for this operation. The steam was on about half of the time after the desired steady-state concentration had been achieved in the evaporator/stripper.

An acid-deficient product was not achieved in this operation. The acid/thorium ratio in the boiler pot is shown as a function of time in Fig. 6-4. Run 25 demonstrated that an acid-deficient condition in the boiler pot can be maintained without the addition of a stripping medium other than

TABLE 6-3
FEED ADJUSTMENT RUN 27 STREAM SAMPLE ANALYSES

	g-moles H^+/ g-mole Th	H^+ (M)	Th (M)	Al (M)	F^- (M)	Density (g/cm^3 at 25°C)
Initial Pot Solution	2.5	0.50	0.20	0.02	0.015	1.09
Feed	2.7	0.54	0.20	0.025	0.015	1.10
Product (after dilution)	0.08	0.12	1.47	0.151	0.075	1.55
Overheads[(a)]	3×10^{4}	0.60	2.0×10^{-5}	<0.25 ppm	1×10^{-4}	1.016

[(a)] Typical steady-state values. These are not average values for the run and do not reflect the loss of about half of the initial pot solution via the overheads at startup.

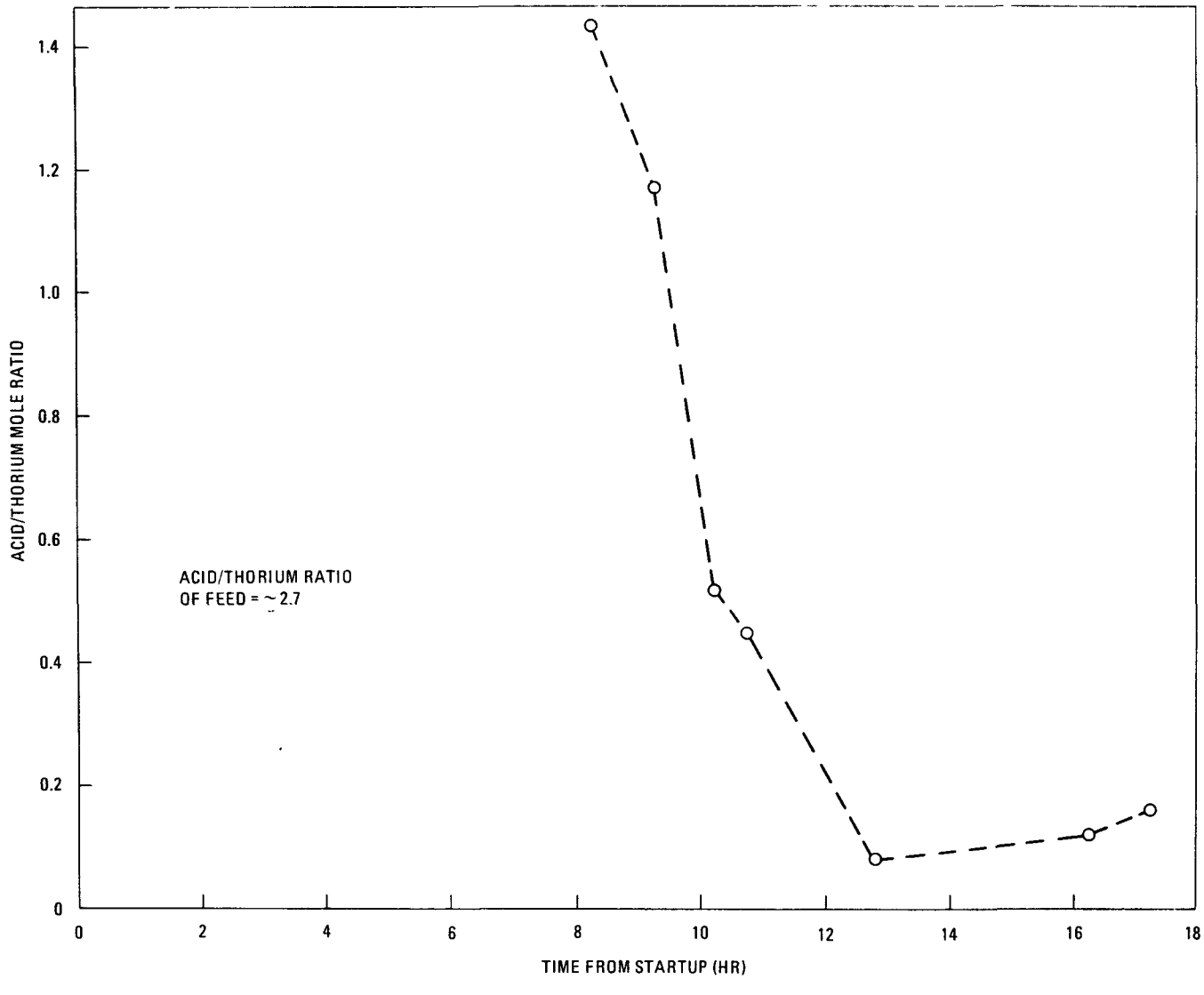

Fig. 6-4. Feed adjustment Run 27 - boiler pot acid/thorium ratio versus time

the water present in the 1BT stream. The steady-state conditions in Run 25 were a specific gravity of about 2.2 at a temperature near 135°C. As mentioned above, the steady-state conditions in Run 27 were near a 2.0 specific gravity at 130°C. To attain and maintain an acid-deficient condition in the boiler pot at a temperature lower than 135°C, stripping steam or water can be added. Another method which can be used is chemical denitration with an agent such as formic acid. This method has been tested on the bench scale, but not yet in the evaporator/stripper.

6.3. SOLVENT EXTRACTION (G. W. Reddick)

6.3.1. Introduction

The first cycle of the Thorex solvent extraction process was tested in the solvent extraction pilot plant. The Thorex process is used to separate thorium and uranium from the fission products. Thorium and uranium are partitioned in the first cycle. This flowsheet (see Fig. 6-1) has been tested in the solvent extraction pilot plant using pulsed columns. In Runs 58, 59, and 60, a Robatel centrifugal contactor was used for the 1A extraction section. Pulsed columns were used for the remainder of the process operations.

The advantage of the centrifugal contactor over other types of contactors is the reduction of solvent degradation through reduced residence time. Creation of solvent degradation products is detrimental to the operation of the Thorex process. However, a centrifugal contactor has only a limited capacity to handle solids which may be present in the feed.

6.3.2. Results and Discussion - Run 58

Table 6-4 contains the stream analyses and flow rates for Run 58. Table 6-5 contains the loss data and the operating conditions. Table 6-6 contains the descriptions of the contactor, columns, and column cartridges.

TABLE 6-4
STREAM AND ANALYTICAL DATA FOR SOLVENT EXTRACTION RUN 58

Stream	Stream No.	U (g/l)	Th (g/l)	HNO_3 (M)	ZrNb (cpm)	Flow (ml/min)	Relative Flow
1AF	1	26.69	354	0.956	677,000	93 (98.9) (107.5)	100 (100) (100)
1AS	2			0.956		180.5 (178.5) (178.1)	194 (180) (166)
1AA	5			∿ 13		28.7 (31.2) (31.7)	30.9 (31.5) (29.5)
1AX	3			[30%TBP]		947.5 (950) (956.5)	1019 (961) (890)
1BX	8			0.188		726 (719) (720)	781 (727) (670)
1CX	12			0.012		582 (582) (577)	626 (588) (537)
1BS	10			[30%TBP]		215 (213) (208.5)	231 (215) (194)
1AW	4	2.5×10^{-2} (2.65×10^{-2}) (2.55×10^{-2})	0.181 (0.488) (0.494)	2.206 (2.258) (1.998)	77,622 - (95,645)		
1AP		2.58 - (3.94)	40.2 - (67.5)	0.226 - (0.222)	8374 - (14,807)		

TABLE 6-4 (Continued)

Stream	Stream No.	U (g/l)	Th (g/l)	HNO_3 (M)	ZrNb (cpm)	Flow (ml/min)	Relative Flow
1SR		0.54 ·	74.9	1.824	26,815		
		–	–	–	–		
		(0.61)	(121.3)	(1.859)	(27,297)		
1SP		2.3	24.3	0.075	54.3		
		–	–	–	–		
		(2.44)	(31.1)	(0.085)	(443)		
1BXT		0.52	42.8	0.394	81.8		
		–	–	–	–		
		(0.53)	(59.3)	(0.390)	(571.9)		
1BU	11	1.59	5.8×10^{-3}	0.017	2.31		
		–	–	–	–		
		(3.06)	(1.3×10^{-3})	(0.034)	(2.14)		
1BT	9	2×10^{-2}[a]	39.4	0.394	64.5		
		(8×10^{-3})	(27.9)	(0.388)	–		
		(3×10^{-2})	(46.5)	(0.353)	(366.8)		
1BSU		1.35	16.87	0.034	3.01		
		–	–	–	–		
		(1.89)	(20.2)	(0.024)	(8.91)		
1CU	13	3.22	1.5×10^{-3}	0.104	7.18		
		(6.44)	(1.5×10^{-3})	(0.104)	–		
		(3.28)	(0.4×10^{-3})	(0.111)	(3.09)		
1CW	14	1.05×10^{-2}	1.12×10^{-2}	0.0068	1.30		
		–	–	–	–		
		(2.0×10^{-3})	(1.3×10^{-3})	(0.010)	(2.55)		
1OS						130	140
						(120)	(121)
						(127)	(118)
1OW		–	–	–	12.45		
		–	–	–	–		
		(1.82×10^{-2})	(1.9×10^{-3})	–	(2.12)		
1OO		1×10^{-3}	0.5×10^{-3}		1.28		
		–	–		–		
		(0.7×10^{-3})	(1.3×10^{-3})		(0.65)		

[a] Analytical results are uncertain.

TABLE 6-5
PERCENT LOSS, Zr DECONTAMINATION FACTOR, AND FLOODING DATA FOR SOLVENT EXTRACTION RUN 58[a]

Column	Purpose	Vol Velocity ($gal/hr/ft^2$)	$\overline{V}_a$ (cm/sec)	$\overline{V}_o$ (cm/sec)	Flooding Freq (cycles/min)	Continuous Phase
1A Centrifugal Contactor	Extraction	908.4			< 500 RPM	
1S Pulse Column	Scrub	820.1 (820.4) (824.9)	0.149 (0.147) (0.146)	0.778 (0.780) (0.786)	101 (101) (101)	Organic
1BX Pulse Column	Partition	610.2 (608.1) (609.1)	0.265 (0.262) (0.263)	0.425 (0.425) (0.425)	82 (82) (82)	Aqueous
1BS Pulse Column	Partition-Scrub	684.1 (677.6) (675.0)	0.596 (0.591) (0.591)	0.177 (0.175) (0.172)	83 (83) (83)	Aqueous
1C Pulse Column	U-Strip	563.7 (563.8) (562.9)	0.212 (0.212) (0.211)	0.425 (0.425) (0.425)	86 (86) (86)	Aqueous
1O Pulse Column	Solvent Wash	939.6 (932.7) (939.3)	0.107 (0.098) (0.104)	0.955 (0.956) (0.956)	119 (119) (119)	Organic

Column	Aqueous to Organic Ratio	Percent Loss		Zr-Nb DF		% Flooding Frequency	Temp.
		U	Th	U Basis	Th Basis		
1A	0.319 (0.325) (0.332)	0.30[c] (0.31) (0.28)	0.17 (0.43) (0.41)	7.8 - (6.8)	9.2 - (8.7)		26°C[b] - (28°C)
1S	0.191 (0.188) (0.186)	- - -	- - -	138 - (21)	93 - (15)	79 (79) (72)	Ambient
1BX	0.625 (0.618) (0.618)	- - -	0.02 - (4×10^{-3})	16.3 - (260)	- - -	72 (72) (72)	Ambient
1BS	3.377 (3.376) (3.453)	0.58 (0.22) (0.75)	- - -	- - -	1.2 - (1.2)	63 (63) (63)	Ambient
1C	0.5006 (0.5004) (0.4953)	0.49 - (0.08)	- - -	0.7 - (0.7)	- - -	81 (81) (81)	53°C
1O	0.112 (0.103) (0.109)	- - -	- - -	- - -	- - -	67 (67) (67)	

[a] The data in parentheses correspond to a second and third set of operating conditions.

[b] Average of 1AW and 1AP temperatures.

[c] Analytical results are uncertain.

TABLE 6-6
CENTRIFUGAL CONTACTOR AND COLUMN CARTRIDGE DESCRIPTION FOR SOLVENT EXTRACTION RUNS 58, 59, AND 60

Unit	Purpose	Diameter (mm)	Total Height of Mixing Area (m)	Other			
1A Contactor	Extraction	180	0.32	8 stages with 0.4-liter total holdup per stage			
				Plates			Plate Spacing (mm)
				Nozzle Direction	Hole Size (mm)	% Free Area	
1S Column	Scrub	51	6.7	Down	3.2	23	51
1BX Column	Partition	76	5.8	Up	4.8	23	Graded[a]
1BS Column	Partition, Scrub	51	5.2	Up	4.8	23	51
1C Column	U Strip	76	4.6	Up	4.8	23	Graded[a]

[a] Graded cartridge is, from the bottom, 2.6 m with 100-mm spacing, 0.5 m with 76-mm spacing, and the remainder with 51-mm spacing.

No significant operating difficulties were encountered during Run 58. Some local flooding occurred in the top of the 1S column. The flooding was caused by the presence of the third phase (second organic phase) in the top disengaging section. The third phase results from a high thorium concentration in the organic phase. High thorium concentration in the top disengaging section reduces the density differentials between the organic phase and the 1AS stream. The 1AS stream is added at the top of the 1S column. Holdup of the aqueous phase can occur under these conditions.

The flooding in the top of the 1S column is characterized by an aqueous continuous region which extends into the top disengaging section. This type of flooding does not always occur when the saturation is raised high enough to discharge two organic phases into the disengaging section and may be due, in part, to column plate wetting variations from run to run.

Higher than expected uranium and thorium losses (approximately 0.3%) occurred from the centrifugal contactor via the 1AW stream. High solvent loading and/or the inability of the centrifugal contactor to separate the third phase from the aqueous phase may be an explanation for the measurable losses.

A significant amount of uranium was analyzed in the 1BT stream. Analytical difficulties are discussed in Section 6.4. Of the 1BT analyses in Table 6-7, the worst run for separation of uranium from thorium is Run 58. No operational reason is available to explain this lack of separation.

Run 58 was the first run in the centrifugal contactor which contained zirconium in the feed. Most of the zirconium-niobium decontamination in Run 58 occurred in the 1A-1S system. However, significant zirconium-niobium decontamination from uranium occurred in the 1BX column.

6.3.3. Results and Discussion - Run 59

Table 6-8 contains the stream analyses and flow rates for Run 59. Table 6-9 contains the loss data and the operating conditions.

TABLE 6-7
COMPARISON OF 1BT AND 1CU ANALYSIS FOR SOLVENT EXTRACTION RUNS 57-60[a]

Run Number	1BT, Uranium Concentration in Parts per Million Parts of Thorium	1CU, Thorium Concentration in Parts per Million Parts of Uranium
57[b]	350.5 (450.6) (204.4)	2147.8 (1507.4) (790.6)
58	507.6 (286.7) (645.2)	465.8 (232.9) (122.0)
59	197.0 (48.1) (73.2)	1107.9 (1269.8) (762.1)
60	79.6 (24.8) (19.6)	1435.5 (613.8) (418.3)

[a] The uranium analysis of the IBT samples and the thorium analysis of the ICU samples are all questionable in these runs. All values are considered to be less than those tabulated, as discussed in Section 6.4.

[b] From Ref. 6-3.

TABLE 6-8
STREAM AND ANALYTICAL DATA FOR SOLVENT EXTRACTION RUN 59

Stream	Stream No.	U (g/l)	Th (g/l)	HNO_3 (M)	ZrNb (cpm)	Flow (ml/min)	Relative Flow
1AF	1	34.6	365	0.860	957,400	81 (99) (83)	100 (100) (100)
1AS	2			1.077		167 (179) (175)	206 (181) (211)
1AA	5			∿ 13		21 (24) (28)	26 (24) (34)
1AX	3			[30%TBP]		∿ 940 (1058) (940)	1160 (1069) (1133)
1BX	8			0.212		684 (698) (717)	844 (705) (864)
1CX	12			0.0092		554 (579) (521)	684 (585) (628)
1BS	10			[30%TBP]		152 (192) (264)	188 (194) (318)
1AW	4	9.5×10^{-4} (1.0×10^{-3}) (1.8×10^{-3})	1.5×10^{-2} (0.56) (0.15)	1.789 (1.734) (1.754)	291,346 (365,134) (317,240)		
1AP		2.78 (3.88) (2.22)	42.8 (61.8) (26.4)	0.42 (0.30) (0.44)	21,085 (12,264) (21,447)		
1SR		0.30 (0.41) (0.54)	54.5 (77.3) (104.6)	1.634 (1.651) (1.720)	72,749 (68,844) (90,294)		

TABLE 6-8 (Continued)

Stream	Stream No.	U (g/l)	Th (g/l)	HNO_3 (M)	ZrNb (cpm)	Flow (ml/min)	Relative Flow
1SP		2.80 (2.37) (2.80)	25.8 (24.0) (27.0)		216 (4488) (5475)		
1BXT		0.80 (0.63) (0.71)	36.0 (43.9) (46.6)	0.393 (0.388) (0.393)	193 (4480) (3032)		
1BU	11	2.02 (2.54) (2.70)	5×10^{-4} (2.5×10^{-2}) (3.2×10^{-2})	0.052 (0.052) (0.045)	< 4.1 (1500) (897)		
1BT	9	5.2×10^{-3}[a] (1.9×10^{-3}) (2.7×10^{-3})	26.4 (39.5) (36.9)	0.391 (0.388) (0.382)	35 (4255) (5387)		
1BSU		3.19 (2.08) (1.99)	10.5 (17.4) (18.9)	0.121 (0.104) (0.069)	< 5.2 (58) (58)		
1CU	13	3.43 (4.41) (5.38)	3.8×10^{-3} (5.6×10^{-3}) (4.1×10^{-3})	 (0.086) (0.052)	< 5.7 (253) (284)		
1CW	14	$< 5\times10^{-4}$ (1.1×10^{-3}) ($< 5\times10^{-4}$)	$< 5\times10^{-4}$ ($< 5\times10^{-4}$) ($< 5\times10^{-4}$)	0.010 (0.010) (0.012)	< 3.2 (2471) (75)		
1OS				pH=10.7		109 (139) (114)	135 (140) (137)
1OW		$< 5\times10^{-4}$ (0.99) (0.94)	$< 5\times10^{-3}$ (1.7×10^{-2}) (1.1×10^{-2})		< 19.1 (7675) (5772)		
1OO		$< 5\times10^{-4}$ ($< 5\times10^{-4}$) ($< 5\times10^{-4}$)	$< 5\times10^{-4}$ (6×10^{-4}) ($< 5\times10^{-4}$)		< 1.0 (23) (24)		

[a] Analytical results are uncertain.

TABLE 6-9
PERCENT LOSS, Zr DECONTAMINATION FACTOR, AND FLOODING DATA FOR SOLVENT EXTRACTION RUN 59[a]

Column	Purpose	Vol Velocity (gal/hr/ft^2)	$\overline{V}_a$ (cm/sec)	$\overline{V}_o$ (cm/sec)	Flooding Freq (cycles/min)	Continuous Phase
1A Centrifugal Contactor	Extraction				< 500 RPM	
1S Pulse Column	Scrub	805 (899) (811)	0.137 (0.147) (0.144)	0.763 (0.869) (0.773)	102 (94) (102)	Organic
1BX Pulse Column	Partition	612 (629) (621)	0.266 (0.255) (0.262)	0.425 (0.456) (0.440)	82 (81) (82)	Aqueous
1BS Pulse Column	Partition, Scrub	608 (647) (713)	0.562 (0.574) (0.589)	0.125 (0.158) (0.217)	86 (84) (81)	Aqueous
1C Pulse Column	U-Strip	532 (591) (557)	0.202 (0.211) (0.190)	0.399 (0.456) (0.439)	98 (94) (96)	Aqueous
1O Pulse Column	Solvent Wash	873 (1010) (958)	0.090 (0.114) (0.094)	0.897 (1.027) (0.989)	124 (116) (118)	Organic

Column	Aqueous to Organic Ratio	Percent Loss		Zr-Nb DF		% Flooding Frequency	Temp.
		U	Th	U Basis	Th Basis		
1A	0.286 (0.285) (0.304)	0.01 (0.01) (0.02)	0.01 (0.56) (0.14)	3.65 (8.75) (2.86)	5.32 (13.22) (3.23)	(2200 RPM)	28°C[b] (31°C) -
1S	0.178 (0.169) (0.186)	- - -	- - -	98.3 (1.67) (4.94)	58.8 (1.06) (4.01)	81 (88) (81)	Ambient
1BX	0.626 (0.558) (0.596)	- - -	2×10^{-3} (0.09) (0.13)	> 38.0 (3.21) (5.89)	- - -	73 (74) (73)	Ambient
1BS	4.50 (3.64) (2.72)	0.13[c] (0.11) (0.10)	- - -	- - -	4.04 (0.95) (4.47)	63 (64) (67)	Ambient
1C	0.507 (0.463) (0.433)	< 0.02 (0.04) (<0.02)	- - -	1.22 (10.29) (6.29)	- - -	72 (76) (74)	49°C
1O	0.100 (0.111) (0.095)	- - -	- - -			68 (72) (71)	

[a] The data in parentheses correspond to a second and third set of operating conditions.

[b] Average of 1AP and 1AW temperatures.

[c] Analytical results are uncertain.

Run 59 utilized the same equipment and flowsheet as Run 58. Dibutyl phosphate (DBP) was added to the 1AP pump tank during the second half of the run. During the startup oepration, the 1A contactor became plugged and no liquid left the contactor via the aqueous 1AW route. Both aqueous and organic streams were leaving the contactor via the normal organic stream outlet. To remove the plug, the contactor was flushed by increasing both the 1AA acid flow rate and the rotating speed of the contactor. The plug had apparently been formed by the settling of residual solids into an interstage aqueous port following completion of Run 58.

Run 58 was the first centrifugal contactor run which included zirconium in the feed. Some of the solids which are present in this feed apparently were left in the contactor following the run. Although the feed stream is filtered prior to the addition to the contactor, some finely divided particles pass through the filter and probably centrifuged out in the contactor.

In Run 59, the DBP was added to the 1AP pump tank to simulate solvent degradation effects. The addition of the DBP had the predictable effect of lowering the zirconium-niobium decontamination in the 1S column and perturbing the dispersion characteristics in the 1C column. The addition of the DBP was not at a constant flow rate because a siphon was set up in the addition system which added the DBP in large increments.

The total amount of DBP added was about 88 g. Much of the DBP was added in the initial increment. However, some DBP was added over a 3-hr period. Based on the total organic input to the solvent extraction system during that period, the average DBP concentration in the organic phase was about 0.43 g of DBP per liter. This is five times the concentration of DBP expected to be formed in the HRDF due to radiolysis.

After the decrease of zirconium-niobium decontamination with the initial increment of DBP, the decontamination in the 1S column began to increase. The decontamination did not improve enough to return to values obtained before the addition of the DBP.

The presence of DBP in the 1C column effectively increased the zirconium decontamination of uranium in that column. Uranium losses from the 1C column also increased, as indicated by the uranium concentration in the 10W stream; however, these losses were not indicated by the 1CW stream analyses.

Some thorium losses occurred via the 1AW stream in Run 59. These were similar to the losses reported in Run 58. However, the uranium losses were in the anticipated range.

6.3.4. Results and Discussion - Run 60

Table 6-10 contains the stream analyses and flow rates for Run 60. Table 6-11 contains the loss data and the operating conditions.

Run 60 was operationally similar to Runs 58 and 59. Prior to Run 60 the solvent was cleaned using macroreticular ion exchange resin (Ref. 6-3). This cleanup removes the heavy metals, fission products, and degradation products. No DBP addition was made to the system during Run 60.

The 1AS stream was run at two selected flow rates to determine the effects on zirconium-niobium decontamination in the 1A-1S system.

During Run 60 the 1S column developed an aqueous continuous region near the top of the column which was similar to the local flood in Run 58. This flooded condition occurred at the normal 1AS flow rate of 175 ml/min. The flood dissipated after the planned reduction in 1AS flow rate to 110 ml/min.

The reduction in the 1AS flow rate caused a significant reduction of the zirconium-niobium separation from thorium. Zirconium-niobium decontamination of uranium was reduced in the 1A-1S system, but the overall decontamination was relatively unchanged. The good decontamination of uranium was due to the scrubbing of zirconium-niobium in the 1BX column. Most of the zirconium-niobium in the 1SP stream was stripped from the organic phase

TABLE 6-10
STREAM AND ANALYTICAL DATA FOR SOLVENT EXTRACTION RUN 60

Stream	Stream No.	U (g/l)	Th (g/l)	HNO_3 (M)	ZrNb (cpm)	Flow (ml/min)	Relative Flow	Other
1AF	1	30.7	370	0.53	944,700	115 (97) (107)		Al^{+++}=0.16M, F^-= 0.07M
1AS	2			1.072		176 (178) (110)		
1AA	5			∿ 13		16.5 (24) (30)		
1AX	3			[30%TBP]		963 (979) (974)		DBP=13.0ppm
1BX	8			0.193		708 (716) (734)		
1CX	12			0.012		592 (589) (609)		
1BS	10			[30%TBP]		211 (212) (238)		
1AW	4	1.9×10^{-3} (1.8×10^{-3}) (1.2×10^{-3})	1.05 (0.33) (0.16)	1.58 (1.43) (1.43)	341,319 (302,324) (328,042)			Zr=475ppm
1AP		3.15 (2.54) (2.86)	57.0 (61.5) (51.0)	0.212 (0.28) (0.27)	5567 (28,766) (19,865)			
1SR		0.47 (0.56) (0.49)	88.8 (127.7) (108.4)	1.58 (1.76) (2.04)	79,107 (245,784) (284,592)			

TABLE 6-10 (Continued)

Stream	Stream No.	U (g/l)	Th (g/l)	HNO_3 (M)	ZrNb (cpm)	Flow (ml/min)	Relative Flow	Other
1SP		2.59 (2.48) (2.33)	29.1 (30.3) (35.1)	0.20 (0.18) (0.15)	201 (329) (1373)			
1BXT		0.58 (0.60) (0.60)	43.0 (59.4) (65.0)	0.39 (0.39) (0.38)	457 (593) (2223)			
1BU	11	1.87 (1.98) (2.13)	3×10^{-4} (4×10^{-3}) (4.5×10^{-3})	0.04 (0.02) (0.04)	23.9 (29.5) (29.2)			
1BT	9	3.2×10^{-3}[a] (1.2×10^{-3}) (1.1×10^{-3})	40.2 (48.3) (56.0)	0.39 (0.39) (0.37)	593 (635) (1608)			Zr=6ppm Zr=12ppm
1BSU		1.96 (1.90) (1.61)	16.0 (22.0) (27.2)	0.09 (0.08) (0.07)	13.4 (14) (32)			
1CU	13	4.11 (7.82) (5.26)	5.9×10^{-3} (4.8×10^{-3}) (2.2×10^{-3})	0.07 (0.07) (0.05)	43 (58) (52)			
1CW	14	3×10^{-4} (3×10^{-4}) (4×10^{-4})	4×10^{-4} (9×10^{-4}) (7.7×10^{-3})	0.006 (0.012) (0.016)	4.0 (2.0) (< 1.2)			DBP=10ppm
1OS				pH=10.7		120 (120) (118)		
1OW		1.2×10^{-3} (5×10^{-4}) (7×10^{-4})	1.9×10^{-3} (1.3×10^{-3}) (2.0×10^{-3})		37 (23.5) (19.4)			
1OO		$< 3\times10^{-4}$ $(< 3\times10^{-4})$ $(< 3\times10^{-4})$	$< 3\times10^{-4}$ (4×10^{-4}) (4×10^{-4})		< 1.0 (< 1.0) (< 1.0)			DBP=6ppm

[a] Analytical results are uncertain.

TABLE 6-11
PERCENT LOSS, Zr DECONTAMINATION FACTOR, AND FLOODING DATA FOR SOLVENT EXTRACTION RUN 60[a]

Column	Purpose	Vol Velocity ($gal/hr/ft^2$)	$\overline{V}_a$ (cm/sec)	$\overline{V}_o$ (cm/sec)	Flooding Freq (cycles/min)	Continuous Phase
1A Centrifugal Contactor	Extraction				(<500 RPM)	
1S Pulse Column	Scrub	828 (841) (788)	0.145 (0.146) (0.090)	0.791 (0.804) (0.800)	101 (99) (105)	Organic
1BX Pulse Column	Partition	608 (616) (629)	0.258 (0.261) (0.268)	0.429 (0.435) (0.443)	82 (82) (81)	Aqueous
1BS Pulse Column	Partition-Scrub	668 (675) (707)	0.581 (0.588) (0.603)	0.173 (0.174) (0.196)	84 (83) (82)	Aqueous
1C Pulse Column	U-Strip	571 (575) (588)	0.216 (0.215) (0.222)	0.429 (0.435) (0.442)	95 (95) (94)	Aqueous
1O Pulse Column	Solvent Wash	941 (953) (967)	0.098 (0.099) (0.097)	0.965 (0.978) (0.996)	118 (118) (118)	Organic

Column	Aqueous to Organic Ratio	Percent Loss		Zr-Nb DF		% Flooding Frequency	Temp.
		U	Th	U Basis	Th Basis		
1A	0.319 (0.305) (0.254)	0.02 (0.02) (0.01)	0.76 (0.27) (0.10)	17.41 (2.72) (4.43)	26.1 (5.46) (6.56)	(1200 RPM)	27°C[b] (32°C) -
1S	0.183 (0.182) (0.113)	- - -	- - -	22.8 (85.4) (11.8)	14.1 (43.1) (9.96)	83 (72) (68)	Ambient
1BX	0.603 (0.601) (0.606)	- - -	$<10^{-3}$ (0.01) (0.01)	6.07 (8.90) (43.0)	- - -	72 (72) (73)	Ambient
1BS	3.355 (3.377) (3.084)	0.06[c] (0.03) (0.02)	- - -	- - -	0.72 (0.76) (1.19)	63 (64) (65)	Ambient
1C	0.504 (0.495) (0.502)	0.01 (0.01) (0.01)	- - -	1.22 (2.01) (1.39)	- - -	69 (69) (70)	52°C
1O	0.102 (0.101) (0.097)	- - -	- - -	- - -	- - -	68 (69) (69)	

[a] The data in parentheses correspond to a second and third set of operating conditions.

[b] Average of 1AP and 1AW temperatures.

[c] Analytical results are uncertain.

along with the thorium. The additional zirconium-niobium, which reached the 1BX column after the 1AS stream flow rate was reduced, left the partition system in the 1BT stream and accounted for the reduction of the thorium decontamination.

Significant thorium losses occurred via the 1AW stream before the 1AS stream flow rate was reduced. Reducing the 1AS flow rate had the expected effect on the losses. Uranium losses via the 1AW stream were not significantly affected, remaining low.

The uranium concentration in the 1BT stream was lower than that observed in Runs 57 (Ref. 6-3), 58, and 59. This reduction can be partially attributed to the improved quality of the solvent following cleanup with the macroreticular resin.

6.3.5. Zirconium-Niobium Decontamination Using Robatel Contactor

The zirconium decontamination factors (DFs) were as much as 50% higher with the centrifugal contactor than those measured with the all-pulse-column system (Fig. 6-5). This DF improvement could be due to reduced extraction of zirconium in the high-acid end of the extraction section caused by the lower residence time in the centrifugal contactor.

6.4. LOW-LEVEL HEAVY METAL ANALYSES - SOLVENT EXTRACTION STREAMS (R. G. Wilbourn)

6.4.1. Introduction

Particularly difficult analytical challenges are encountered in the 1BT and 1CU Thorex solvent extraction stream samples. The 1BT and 1CU samples are generated during solvent extraction partitioning and have the following composition: (1) 1BT = 40 g/liter thorium, 0-10 mg/liter uranium; (2) 1CU = 8 g/liter uranium, 0-10 mg/liter thorium.

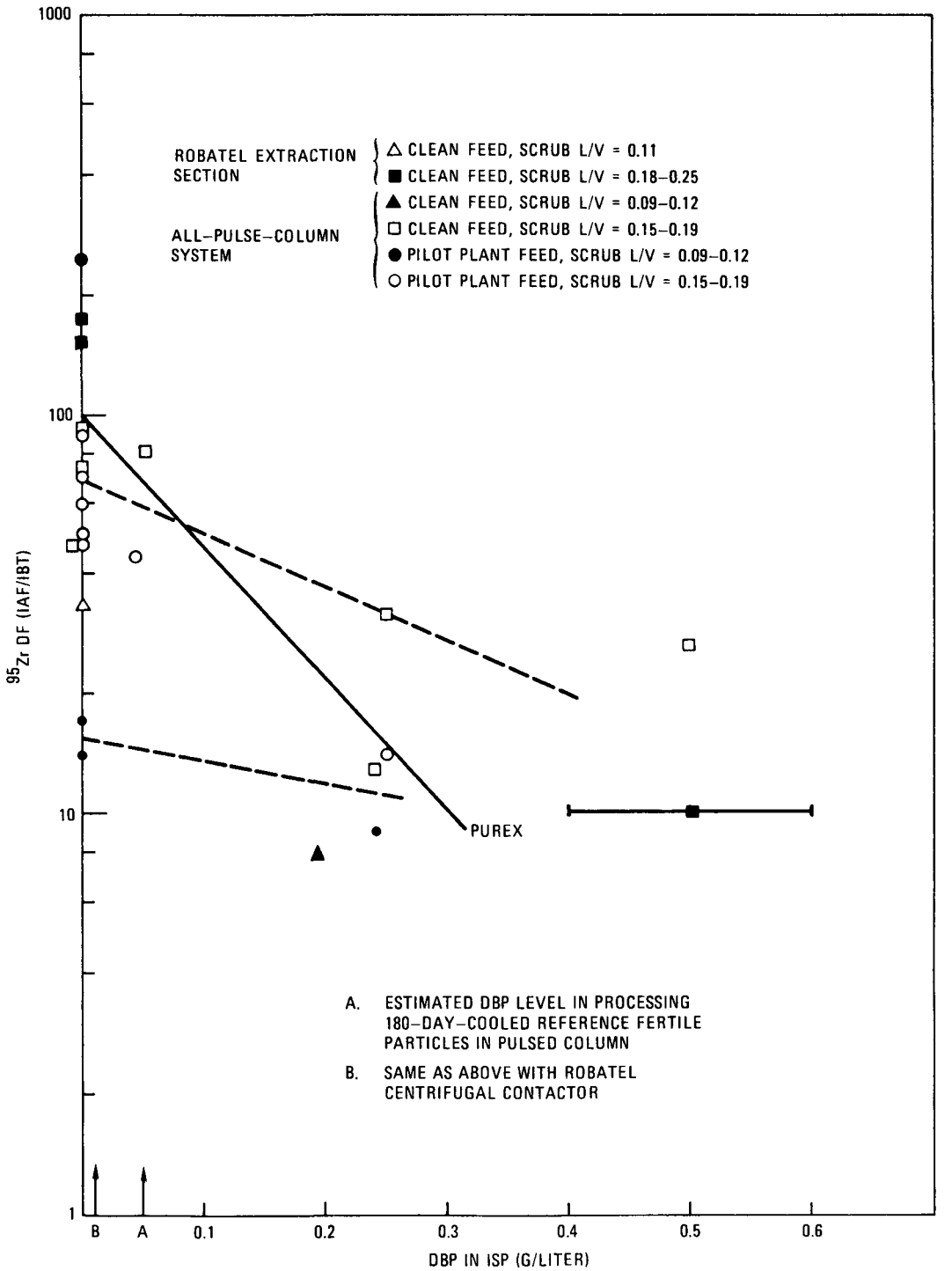

Fig. 6-5. Measured Zr-95 decontamination factors

Procedures were developed during the reporting period to permit rapid analyses of 1BT and 1CU stream samples and to resolve apparent discrepancies between expected trace metal levels (based on solvent extraction run parameters) and results obtained from the GA Analytical Chemistry Department. Details of the analytical procedures are given in Section 6.4.3.1.

6.4.2. Titrimetric 1BT Uranium Stream and Thorium Nitrate Salt Analyses

A titrimetric procedure has been evaluated for 1BT stream samples. Earlier work at ERDA's New Brunswick Laboratory (Ref. 6-4) has shown the feasibility of a titrimetric determination for low levels of uranium in the absence of thorium. Results from the present study indicate a titrimetric approach is also suitable for the determination of 0.5 to 10.0 mg/liter uranium in 1BT solutions containing <40 g/liter thorium. Data for recovery of uranium "spikes" indicate an error of <5% absolute is attainable in this compositional range. In addition, the titrimetric procedure is specific for uranium (thorium and zirconium do not interfere), and therefore separation is not needed. Samples (1BT) may be prepared for analysis directly from nitric acid solution by volume reduction of a 200-ml aliquot. Sample preparation and analysis may be done in the same container, virtually eliminating contamination potential. The only apparent constraint for the titrimetric procedure is the need for a 200-ml sample.

A comparison of titrimetric recovery data for low-level uranium standards with and without the presence of 40 g/liter thorium is given in Fig. 6-6. This figure indicates no deleterious effect of the presence of 40 g/liter thorium in the 0.5 to 10 mg/liter uranium range.

As a further check of the method, the GA Quality Assurance Department was requested to prepare standards containing 40 g/liter thorium and 0 to 10 mg/liter uranium for analysis by Aqueous Separations personnel. The results obtained for the QA standards are given in Table 6-12.

Figures 6-7 and 6-8 contain data for the uranium analysis of 1BT stream samples from solvent extraction runs S72 and S73. The relatively

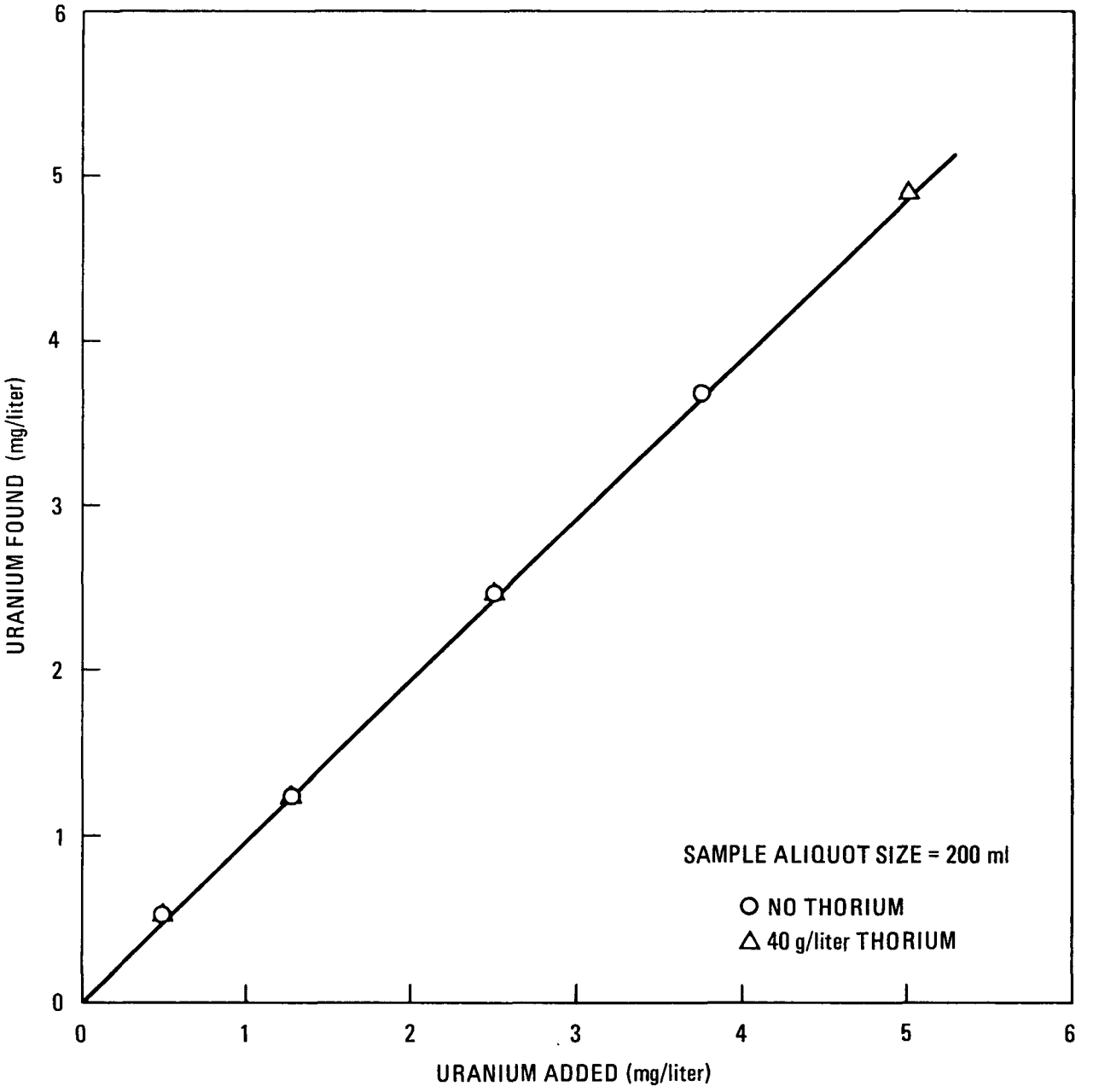

Fig. 6-6. 1BT stream analyses - effect of 40 g/liter thorium content on uranium recovery

TABLE 6-12
URANIUM ANALYSIS OF QA STANDARDS[a] - DATA SUMMARY

Standard Solution No.	U Makeup (mg/liter)	U Analysis (mg/liter)	Accuracy (%)
1	0	<0.07	--
2	4.0	3.88	97.0
3	1.0	0.97	97.0
4	7.0	6.78	96.9
5	9.0	8.85	98.3

[a]All standards contained 40 g/liter thorium.

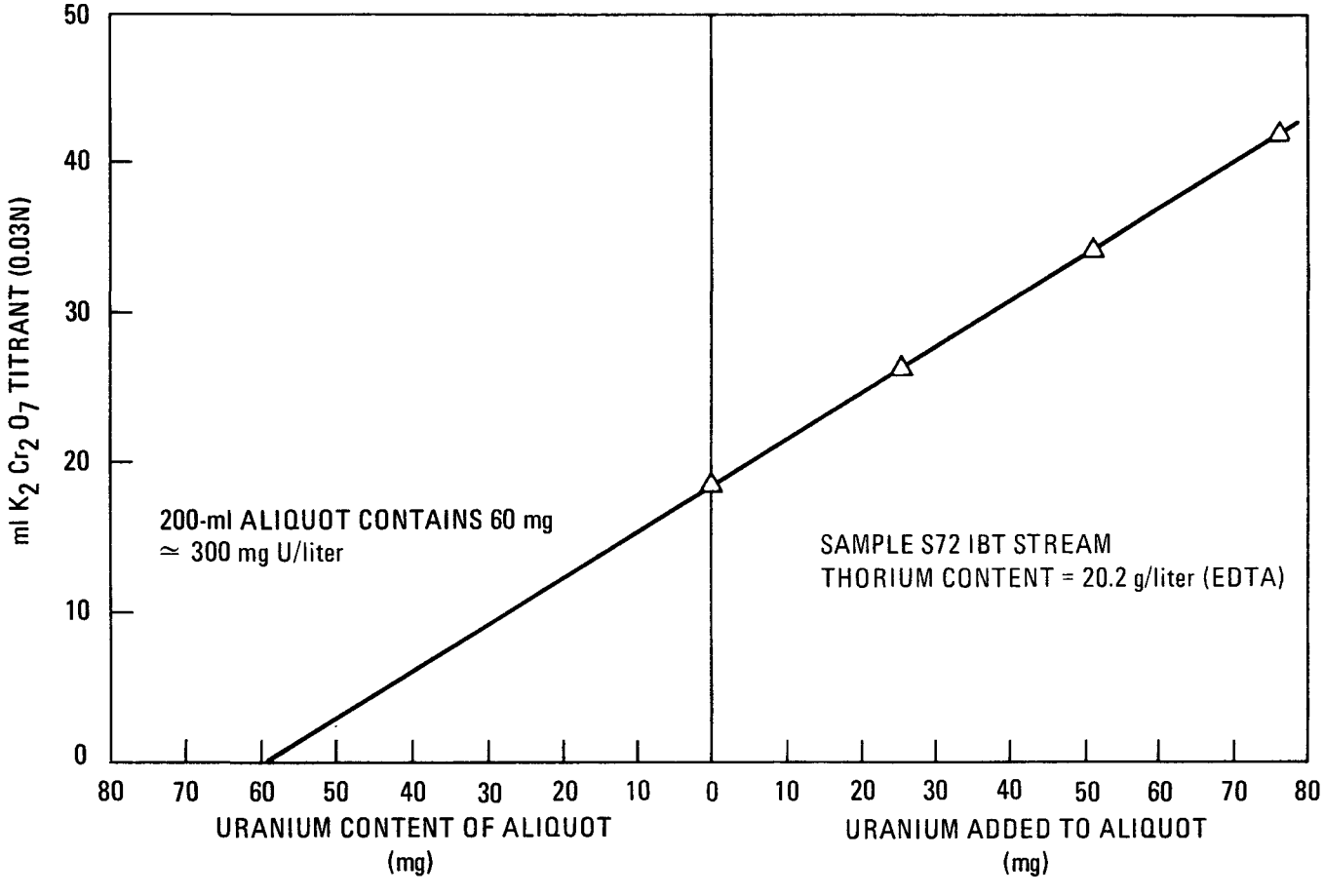

Fig. 6-7. 1BT stream uranium analysis - method of addition, Run 72

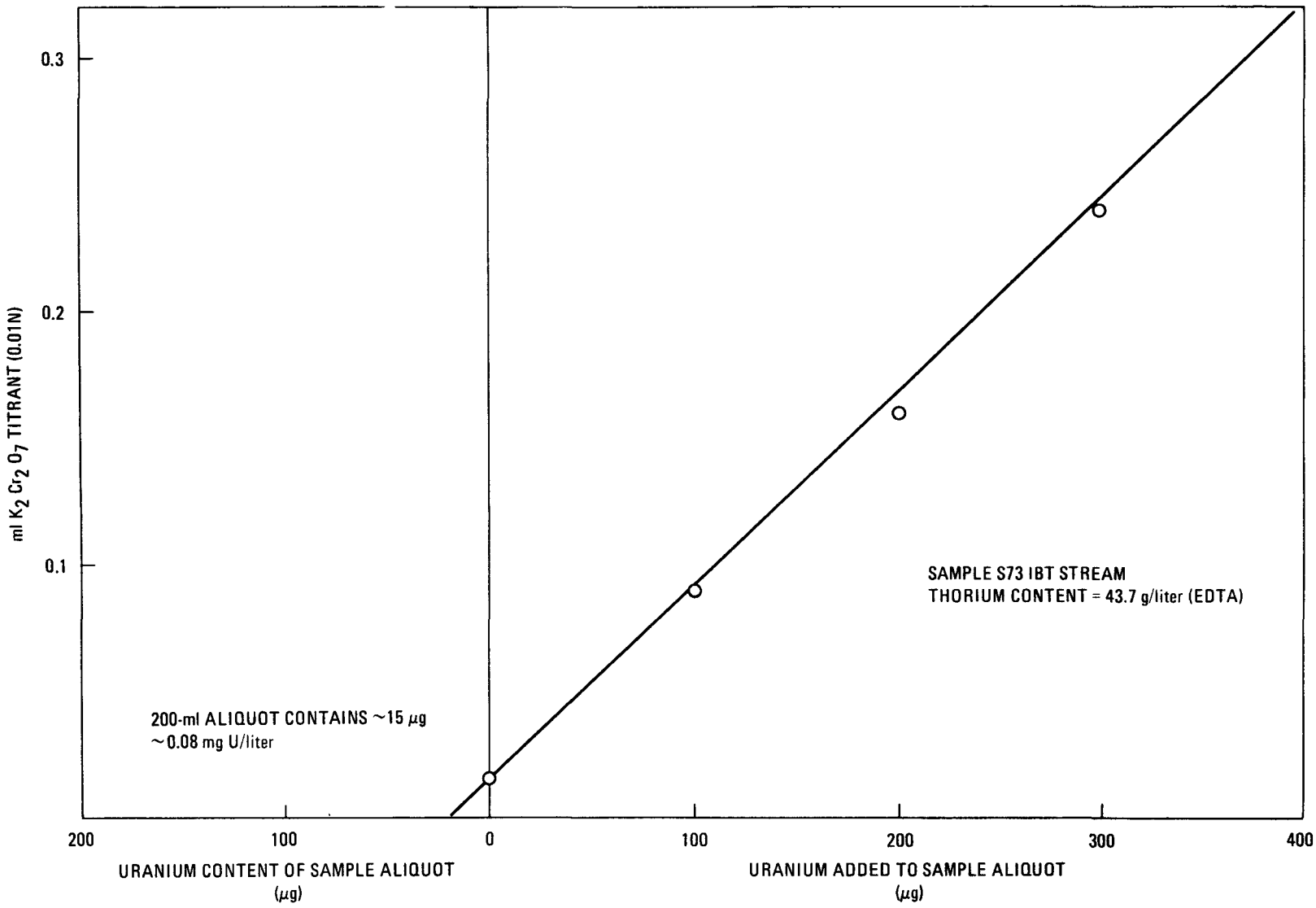

Fig. 6-8. 1BT stream uranium analysis - method of addition, Run 73

large uranium concentration measured for the S72 1BT sample (∿300 mg U/liter) reflects flooding difficulties reported for this run. The composition of the S73 1BT sample (43.7 g Th/liter, ∿0.08 mg U/liter) is considered to be representative of thorium partition product from a normal first cycle Thorex solvent extraction run.

The titrimetric procedure was also utilized during the reporting period to establish the uranium impurity level in reagent grade $Th(NO_3)_4 \cdot 4H_2O$ used in preparation of above standard solutions and $Th(NO_3)_4 \cdot xH_2O$ (Tennessee Nuclear) purchased for use in future solvent extraction runs. Results are presented graphically in Fig. 6-9.

The titrimetric procedure for low-level uranium analysis of 1BT samples has been verified and accepted by the GA Analytical Chemistry Department and will be used for the analysis of future 1BT stream samples.

6.4.3. Colorimetric 1CU Stream Thorium Analysis

A colorimetric procedure for thorium analysis based on a reaction with Thorin Dye (Ref. 6-5) was modified to increase the sensitivity for thorium. The tolerance level for uranium in the modified procedure is quite high (absorbance for 1 mg uranium in the final solution being equivalent to the absorbance obtained for 3 mg thorium), as shown in Fig. 6-10. Because of the high uranium-to-thorium ratio generally present in 1CU stream samples ($\sim 20 \times 10^3/1.0$), a heavy metal separation is required prior to application of the colorimetric procedure. However, the degree of separation required is not high, as it is only necessary to bring the uranium content of the sample aliquot within the above-noted tolerance level.

In the present work, two methods of 1CU heavy metal separation were evaluated: solvent extraction and ion exchange chromatography. Ion exchange is the more rapid method and gave reproducible results with standard solutions. Ion exchange is therefore recommended as the separative method prior to colorimetry. The ion exchange separation of uranium from thorium is well documented (Ref. 6-6) and is based on the formation of

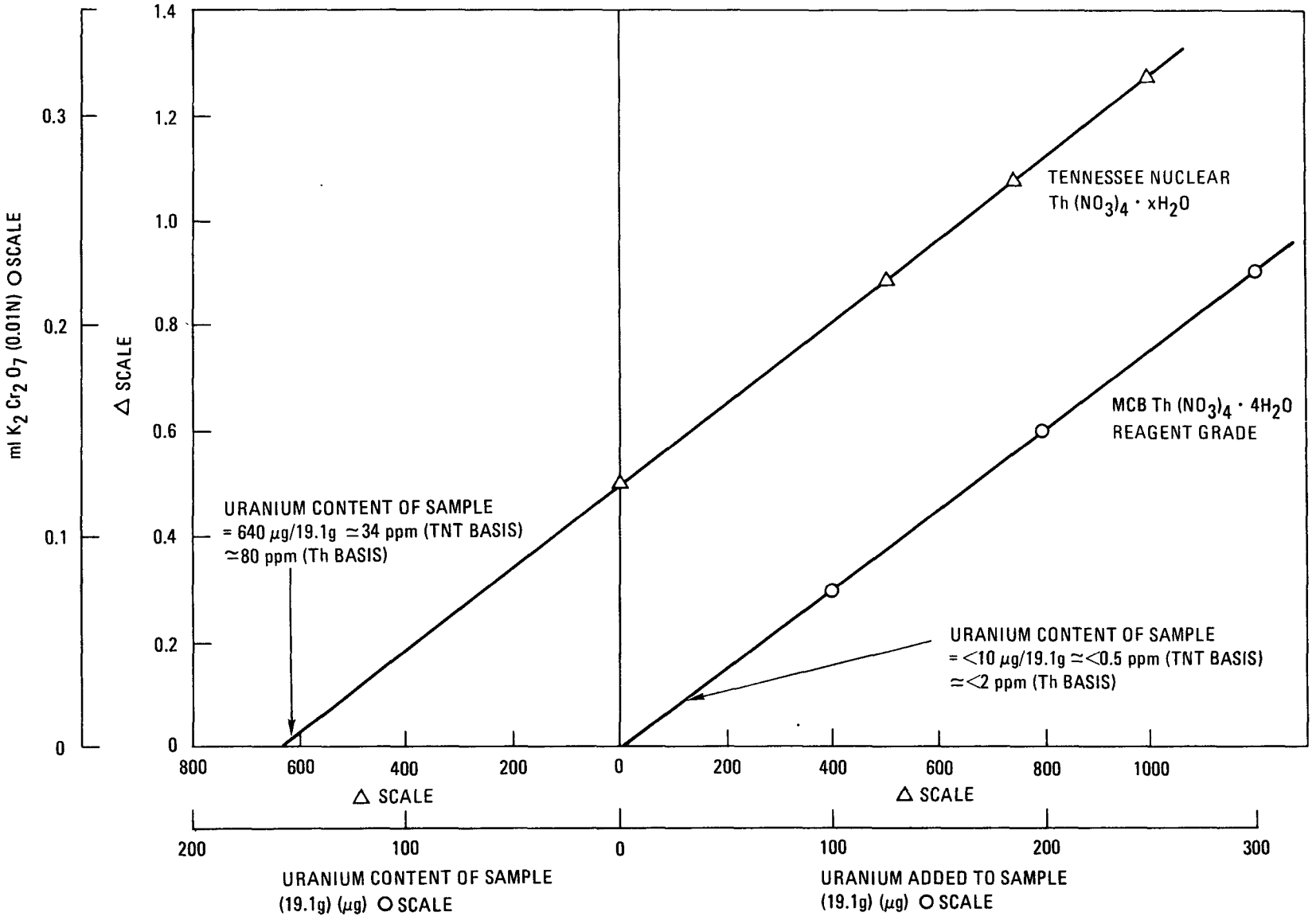

Fig. 6-9. Uranium determination of additions, thorium nitrate salts

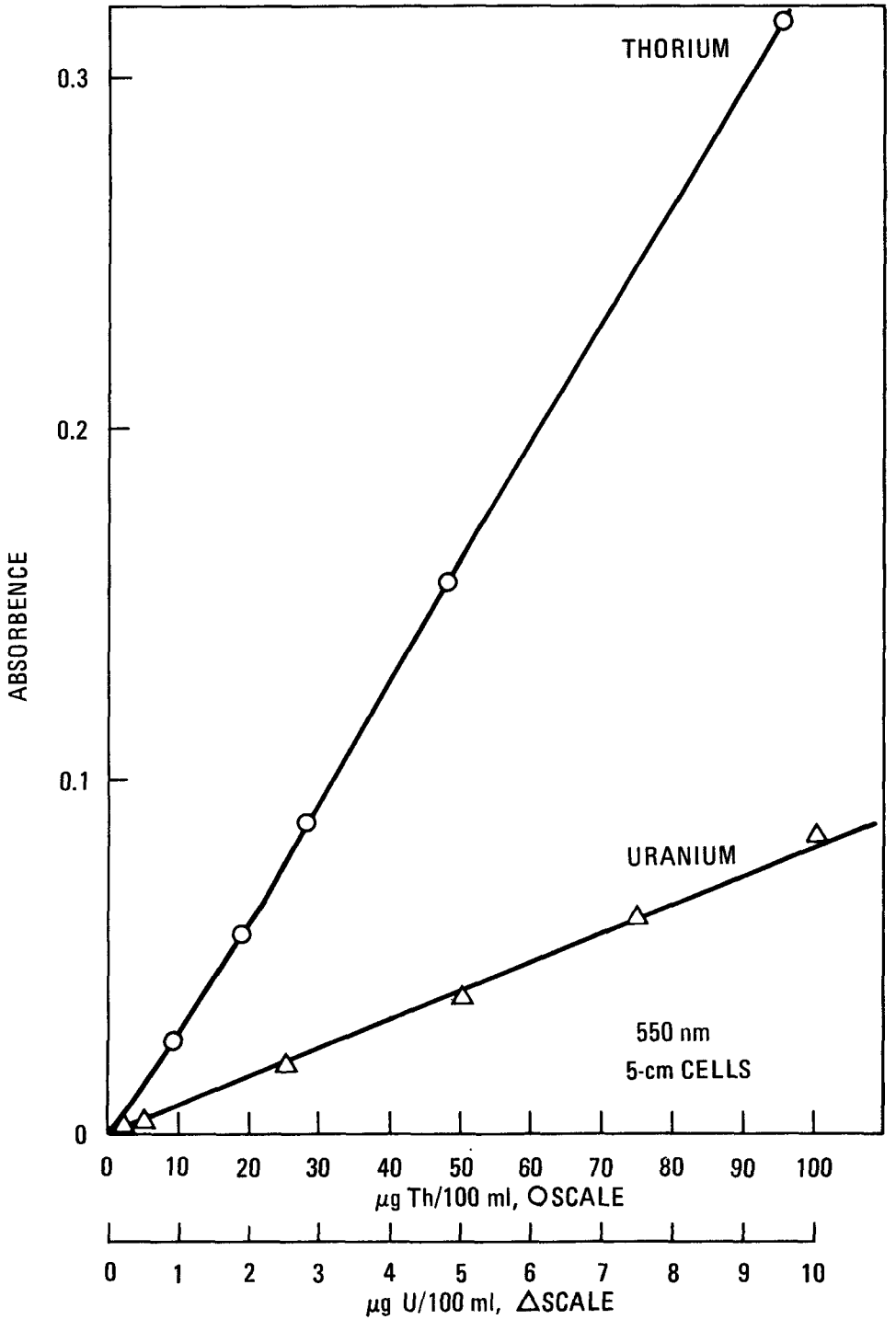

Fig. 6-10. Results of colorimetric thorium analysis

uranium-chloride complexes (assumed to be $UO_2Cl_3^-$ and $UO_2Cl_4^=$) in a strong HCl medium. Thorium forms no anion complex and therefore can be eluted from an anion exchange resin.

Results obtained with the colorimetric procedure for NBS 960 uranium metal and Run S73 1CU samples are given in Table 6-13. The low thorium values obtained for the S73 1CU samples demonstrate a high degree of uranium-thorium separation is achievable in the Thorex solvent extraction studies.

6.4.3.1. Detailed Procedure for 1BT Uranium Analysis

A stepwise procedure for the preparation and titrimetric uranium analysis of 1BT solvent extraction stream samples is given below:

1. In a thoroughly cleaned 400-ml beaker, evaporate 200 ml of 1BT sample (aliquot may contain $\leq$8 g of thorium) to $\sim$50 ml on a hot plate.

2. Add 45 ml of 85% H_3PO_4 and swirl to dissolve any thorium phosphate formed. Continue heating until the total volume is $\sim$60 ml. Add 2 drops of 1% $K_2Cr_2O_7$ solution.

3. Cool to ambient temperature. Insert a Teflon stir bar and initiate slow stirring. Add 2 ml of concentrated HNO_3.

4. Add 5 ml of 15M sulfanic acid solution down the sides of the beaker.

5. Add 5 ml of 1M $FeSO_4$ solution to the body of the sample solution. Wait 30 sec.

TABLE 6-13
1CU THORIUM ANALYSES - DATA SUMMARY

Sample	Aliquot Volume (ml)	Calc. Uranium Content in Aliquot (mg)	Thorium Spike Added (µg)	Absorbance	Spike-corrected[(a)] Thorium Content (µg)	Thorium Concentration of Sample (mg/l)
NBS 960	5.0	125	None	0.001	∿0.5	∿0.1
NBS 960	5.0	125	10	0.032	1.0	0.2
S73 1CU 1	15.0	123	None	0.010	3.5	0.23
S73 1CU 1	15.0	123	20	0.067	2.5	0.17
S73 1CU 2	15.0	114	None	0.015	5.5	0.37
S73 1CU 3	15.0	134	None	0.006	2.0	0.13

(a) See Fig. 6-10.

6. Add ∿10 ml of molybdate solution* to the sample solution down the sides of the beaker. Wait 3 min after disappearance of the brown color.

7. Slowly add 100 ml of distilled water down the sides of the beaker.

8. Add ∿125 mg solid $VOSO_4$. Wait 30 sec.

9. Titrate to an end point potential of 590 mV with 0.01N $K_2Cr_2O_7$ solution using a microburet.

10. Calculation: sample uranium content, mg/liter = (ml $K_2Cr_2O_7$ titrant) (N of $K_2Cr_2O_7$) (meq. wt. U) (5).

6.4.3.2. Detailed Procedure for 1CU Thorium Analysis

A stepwise procedure for the preparation and colorimetric thorium analysis of 1CU solvent extraction stream samples is given below:

1. Transfer a sample aliquot containing ≤125 mg uranium (∿15 ml for a typical 1CU sample) to a 100-ml beaker. Add 5 ml of concentrated HNO_3 and evaporate to dryness on a hot plate.

2. Dissolve the residue in 5 ml of 9M HCl and transfer the solution to a 5-ml AG 1x8, 100-200 mesh resin bed previously conditioned with 10 bed volumes of 9M HCl in a 1 cm x 15 cm glass column.

3. Pass the sample solution through the resin bed and elute the thorium with 5 bed volumes of 9M HCl.

4. Evaporate the effluent containing thorium to ∿5 ml on a hot plate and add 5 ml of concentrated nitric and 3.0 ml of concentrated

*Molybdate solution is prepared as follows: Dissolve 4.0 g $[(NH_4)_6Mo_7O_{24}\cdot 4H_2O]$ in 400 ml of distilled H_2O. Add 100 ml of 1.5M sulfanic acid and mix. Add 500 ml of concentrated HNO_3 and mix.

perchloric acid. Heat until incipient $HClO_4$ fumes are observed. Cool to ambient temperature.

5. Transfer the sample solution to a 100-ml volumetric flask, dilute to ∿80 ml, and add 10.0 ml of 0.1% w/v Thorin solution. Dilute to mark and mix.

6. Prepare a set of thorium calibration standards by transferring 0, 10, 20, 50, and 100 µg thorium to 100-ml volumetric flasks. Add 3.0 ml of concentrated $HClO_4$ and proceed as in step 5.

7. Measure the absorbance of the standard and sample solutions at 550 nm in 5-cm cells and determine the sample thorium content by comparison with standards (see Fig. 6-10).

6.5. PHOSPHORUS DISTRIBUTION DURING CONCENTRATION OF URANYL NITRATE

6.5.1. Introduction

Work was performed during the reporting period to determine the distribution of phosphorus during concentration of 1CU (uranium partition stream) with steam stripping in recent LWR solvent extraction operations. The data are reported here for cross reference into the Thorium Utilization Program. Steam stripping is currently being used in pilot plant equipment for the removal of organic phosphorus containing compounds, e.g., tributyl and dibutyl phosphate, present in the 1CU stream as a result of solvent contact. This operation is done to clean up the uranium stream prior to recycle as feed for subsequent runs.

6.5.2. Discussion

Samples generated during concentration of 1CU feed were analyzed for phosphorus by colorimetry following reduction of a phospho-molybdate complex to "molybdenum blue." The method is commonly used for phosphorus

analysis in nuclear materials (Ref. 6-7). A plot of absorbance versus phosphorus concentration obtained with this procedure is given in Fig. 6-11.

Sample aliquots were prepared for phosphorus analysis by hydrolyzing organic phosphorus compounds to PO_4^{-3} ion by treatment with 5 ml of concentrated nitric acid and 3 ml of concentrated perchloric acid. The resultant solutions were diluted as necessary to bring the phosphorus content within the range of the analytical method.

Data summaries for samples from three concentrator runs are presented in Table 6-14. Duplicate results for the phosphorus content of a TBP-water solution (phosphorus make-up value = 34 μg/ml) of 28 μg/ml and 34 μg/ml were obtained for representative aliquots processed through the sample preparation step.

Results for sample phosphorus distribution indicate the bulk of phosphorus was transferred to the overhead in three concentration runs and the phosphorus to uranium recycle fuel specification of 200 ppm was achieved in all product samples. However, material balances are not greater than 50%.

REFERENCES

6-1. Reddick, G. W., "Solvent Extraction in HTGR Reprocessing - Interim Development Report," ERDA Report GA-A13835, General Atomic Company, February 1976.

6-2. "Thorium Utilization Program Quarterly Progress Report for the Period Ending May 31, 1976," ERDA Report GA-A13949, General Atomic Company, June 30, 1976.

6-3. "Thorium Utilization Program Quarterly Progress Report for the Period Ending November 30, 1976," ERDA Report GA-A14214, General Atomic Company, December 1976.

6-4. "Annual Progress Report for the Period July 1969 to June 1970," ERDA New Brunswick Laboratory Report NBL-258, 1970.

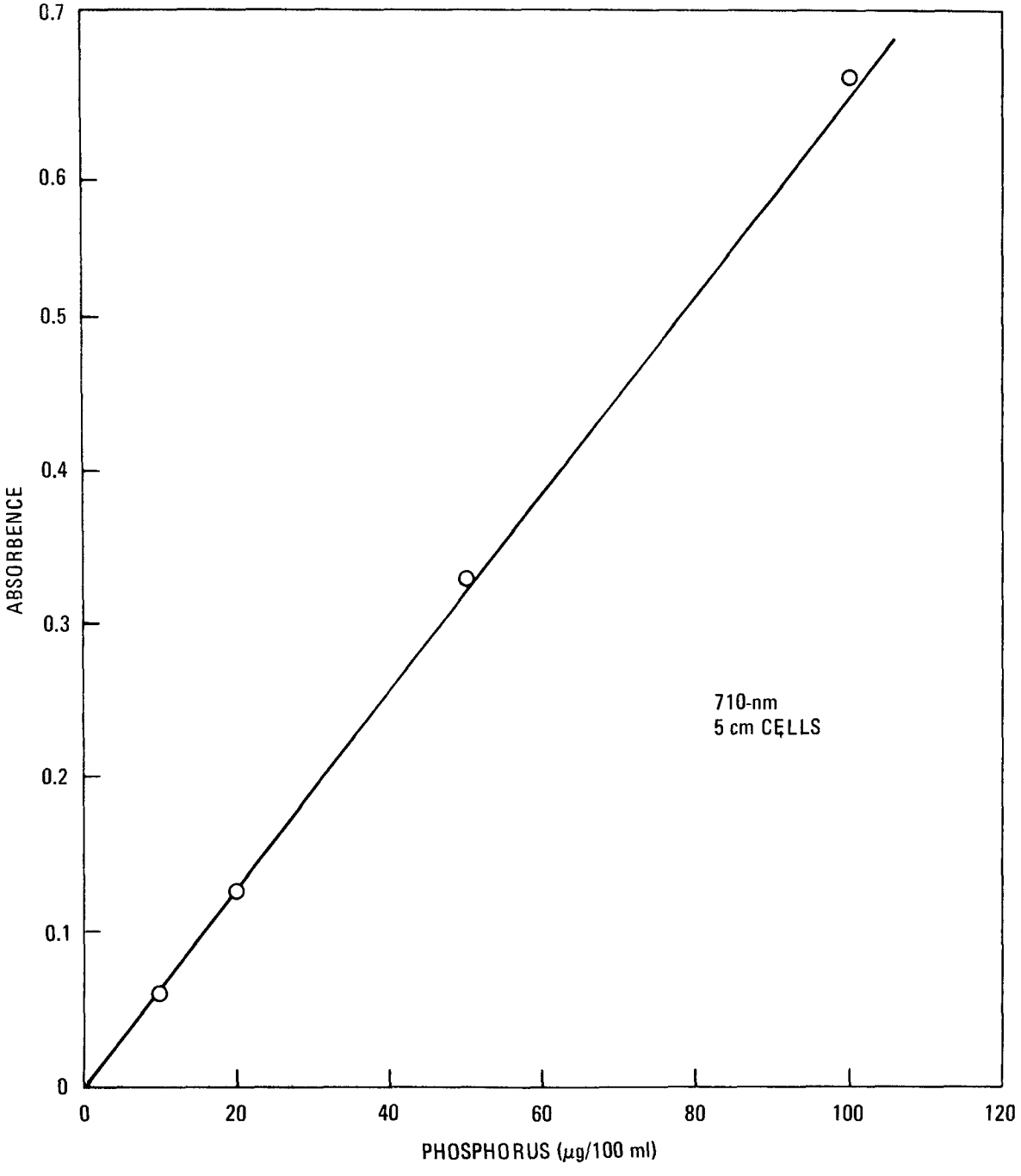

Fig. 6-11. Phosphorus calorimetric data plot

TABLE 6-14
PHOSPHORUS DATA SUMMARY

Sample	Phosphorus Content (µg/ml)	Uranium Content (M)	P/U Product (rpm)
	Run L-1		
1CU feed	20		
1CU product	9	1.65	23
Overhead 1	4		
Overhead 2	3		
Overhead 3	2		
Overhead 4	3		
Overhead 5	3		
Overhead 6	2		
Overhead 7	5		
	Run L-2		
1CU feed	--		
1CU product	6	1.20	32
Overhead 1	13		
Overhead 2	14		
Overhead 3	13		
Overhead 4	17		
Overhead 5	18		
Overhead 6	19		
	Run L-3		
1CU feed	20		
1CU product	8	1.35	25
Overhead 1	16		
Overhead 2	14		
Overhead 3	10		
Overhead 4	6		
Overhead 5	8		
Overhead 6	8		
Overhead 7	6		
Overhead 8	9		
Overhead composite	9		

6-5. Shank, R. C., "Analytical Methods Used by Remote and Services Laboratory," ERDA Report ICP-1029, Allied Chemical Company, October 1973.

6-6. Palei, P. N., Analytical Chemistry of Uranium, Ann Arbor-Humphrey Science Publishers, Ann Arbor, Michigan, 1970, pp. 299-307.

6-7. "Determination of Trace Elements in Uranium Compounds," Goodyear Atomic Company, GAT 507-Chem, TID 4500, 1967.

7. DRY SOLIDS HANDLING

7.1. SUMMARY

Progress with component and system testing continues. Inlet filter pressure drops have been measured. The experimental determination of the volume of three bunkers has established a general pattern, which enables calculation of the storage volume of the remaining bunkers. The testing of in-bunker filters is complete. The performance of fixed speed blowers can be accurately predicted. Experiments with rotary feeder valves have demonstrated their suitability for installation in the system. An evaluation of the electronic data processing system of the bunker load cells together with repeatability trials has indicated the direction in which improvements could most profitably be sought. The evaluation of different types of samplers has begun. Tests with two samplers thus far are encouraging.

Results obtained with the primary burner product removal system have been analyzed. There is a measure of agreement between observation and prediction. Particle breakage results have been closely examined. The experience so far with the secondary burner product removal system has been used as the basis for upgrading the design.

A substantial measure of agreement between results from shear cells at GA and ORNL has been found using crushed graphite.

7.2. INTRODUCTION

The development work, as described in the Experimental Plan, is divided into several stages:

1. Cold laboratory development.

2. Hot laboratory development.
3. Cold engineering development.
4. Hot engineering development.
5. Cold prototype development.
6. Procedure development.

During the quarter, progress was made in development stages 1 and 3.

7.3. COLD LABORATORY DEVELOPMENT (DEVELOPMENT STAGE 1) (P. C. Richards)

The behavior of particulate solids in gravity flow equipment depends on material properties such as internal friction, cohesive strength, wall friction, and density. In order to establish the effect of irradiation on cohesive strength and internal friction, ORNL and GA are conducting a joint investigation using crushed graphite. The flow properties of particulate solids are measured on a laboratory scale in a shear cell. For this investigation Jenike shear cells are used. A cylindrical top, filled with material, is loaded with weights and pushed across a filled cylindrical base at a constant speed. The force required to overcome friction in the shear plane between the top and the base is recorded. The strength required by a particulate solid depends on the stresses it has undergone during consolidation. The testing of a sample comprises:

1. Consolidation of the material in the cell under a normal load V and a shear load S.

2. Shearing of the same material under a smaller vertical load $\bar{V}$ and a smaller shear load $\bar{S}$.

The determination of a yield locus, which is required to determine angles of internal friction and cohesion, requires testing at least three samples, each with different values of $\bar{V}$, but all with the same value of V. V and $\bar{V}$ are applied in the form of weights, and S and $\bar{S}$ are recorded by the shear tester as the top of the shear cell is pushed across the base. The

values of S tend to vary from sample to sample, and they are normalized, or pro-rated, to one value, and the corresponding values of $\bar{S}$ are similarly adjusted. The yield locus is then drawn as shown in Fig. 7-1.

Before proceeding with the determination of the effect of irradiation on flow properties, agreement between shear cell results in the two locations is required. After some differences between the shear cells at the two locations had been eliminated, duplicate experiments were done with graphite crushed at ORNL. Before testing, the material was put through a 0.001-m screen. Since the shear cell is only 0.1 m in diameter, and since packing arrays of particles where there are fewer than 100 on a container diameter are not very reproducible, 0.001 m is a practical maximum allowable particle size for accurate measurements. The results are given in Table 7-1. Each measurement, at a given V and $\bar{V}$, was repeated at least once. As can be seen, the shear forces recorded by ORNL were lower than those at GA. A further difference is the weight of graphite in the top half of the cell, as measured after each sample is tested:

ORNL: range = 101-109 g, average = 104.4 g

GA: range = 111-112 g, average = 111.5 g

This indicates a less severe preconsolidation of the samples at ORNL. It would also explain the trend toward lower shear forces under equal normal loads. Rather than subject the two sets of results to the vagaries of geometrical constructions, as shown in Fig. 7-1, a statistical analysis of the values of $\bar{S}/S$ from the two locations, which would indicate precisely the measure of agreement, was performed. The results of the analysis are shown in Table 7-2.

The agreement between the two sets of results is most encouraging, with the exception of those at V = 2.27 kg, $\bar{V}$ = 0.769 kg. It is to be hoped that resolution of the differences between densities in the shear cells will make the agreement even better. Even in the absence of

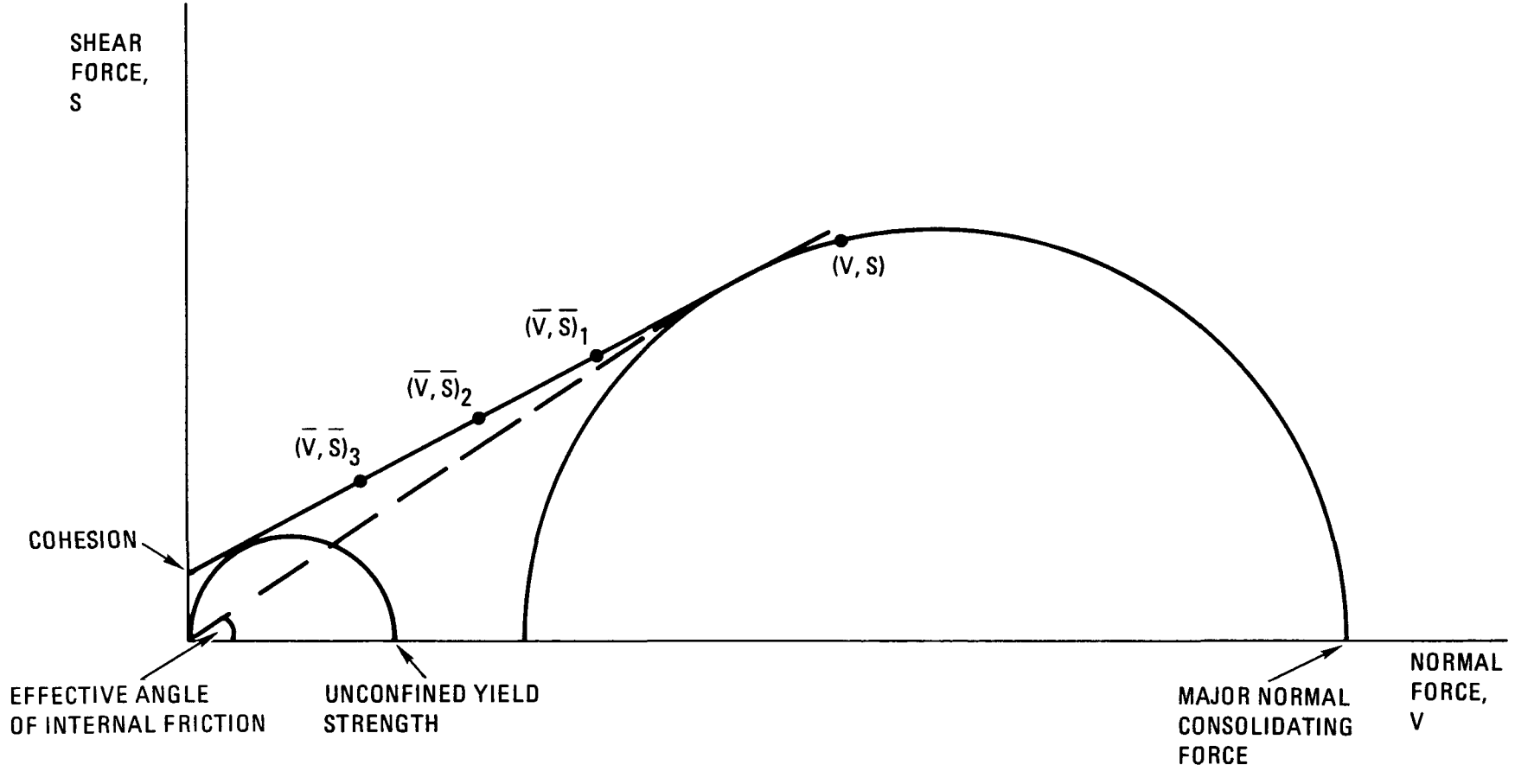

Fig. 7-1. Construction of a yield locus

TABLE 7-1
SHEAR CELL RESULTS WITH CRUSHED GRAPHITE (MINUS 1 mm)
AT GA AND ORNL

V, Normal Force During Consolidation (kg)	S, Shear Force During Consolidation (kg)	$\overline{V}$, Normal Force During Shear (kg)	$\overline{S}$, Shear Force During Shear (kg)	Location
2.72	2.81,2.63	1.81	1.90,1.82	
2.72	2.72,2.93	1.35	1.42,1.06	GA
2.72	2.72,2.88	0.900	1.00,1.60	
2.72	2.51,2.59,2.51	1.81	1.76,1.80,1.68	
2.72	2.43,2.47,2.43	1.35	1.28,1.32,1.32	ORNL
2.72	2.43,2.59,2.40	0.900	0.844,0.922,0.803	
2.27	2.20,2.31,1.98	1.52	1.54,1.56,1.45	
2.27	2.39,2.36,2.15	1.13	1.24,1.06,1.22	GA
2.27	2.31,2.36,2.19	0.769	1.00,0.970,0.890	
2.27	1.96,1.96,1.96	1.52	1.36,1.41,1.36	
2.27	1.96,2.03,2.08	1.13	1.08,1.04,1.13	ORNL
2.27	1.96,1.96,1.96	0.769	0.604,0.681,0.681	

TABLE 7-2
COMPARISON OF THE SHEAR CELL RESULTS WITH CRUSHED GRAPHITE AT GA AND ORNL

V, Normal Force During Consolidation (kg)	$\bar{V}$, Normal Force During Shear (kg)	$\bar{S}/S$, Ratio of Shear Forces in Shear and Consolidation		Chance That the Values of $\bar{S}/S$ Come From the Same Distribution (%)
		At GA	At ORNL	
2.72	1.81	0.674,0.690	0.703,0.697,0.671	>25
2.72	1.35	0.520,0.554	0.532,0.540,0.548	>25
2.72	0.900	0.368,0.362	0.355,0.364,0.344	25
2.27	1.52	0.700,0.677,0.734	0.700,0.720,0.700	>25
2.27	1.13	0.520,0.450,0.567	0.560,0.519,0.547	>25
2.27	0.769	0.433,0.412,0.405	0.320,0.300,0.360	1

improvement, however, the measure of agreement is probably sufficient for proceeding with hot cell testing.

7.4. COLD ENGINEERING DEVELOPMENT (DEVELOPMENT STAGE 3) (E. J. Cook, P. C. Richards)

7.4.1. Qualification Testing

The activities in the coming months will be concerned with qualification testing, which can be defined as partial verification of the design under simulated conditions, followed by complete verification during sequential operation. The testing is divided into two phases. Phase I is concerned with component testing and Phase II with system testing.

The solids handling system is divided into six subsystems (see Fig. 7-2):

Subsystem No. 1. Crusher product removal system.
Subsystem No. 2. Primary burner feed system.
Subsystem No. 3. Primary burner product removal system.
Subsystem No. 4. Particle classifier feed system.
Subsystem No. 5. Particle crusher feed system.
Subsystem No. 6. Secondary burner product removal system.

7.4.1.1. Component Qualification and Improvement

In the last quarterly report (Ref. 7-1), a detailed description of various components of the solids handling systems was given. Progress in component testing has been made with the following:

Inlet filters
Bunkers
In-bunker filters
Blowers
Feeders

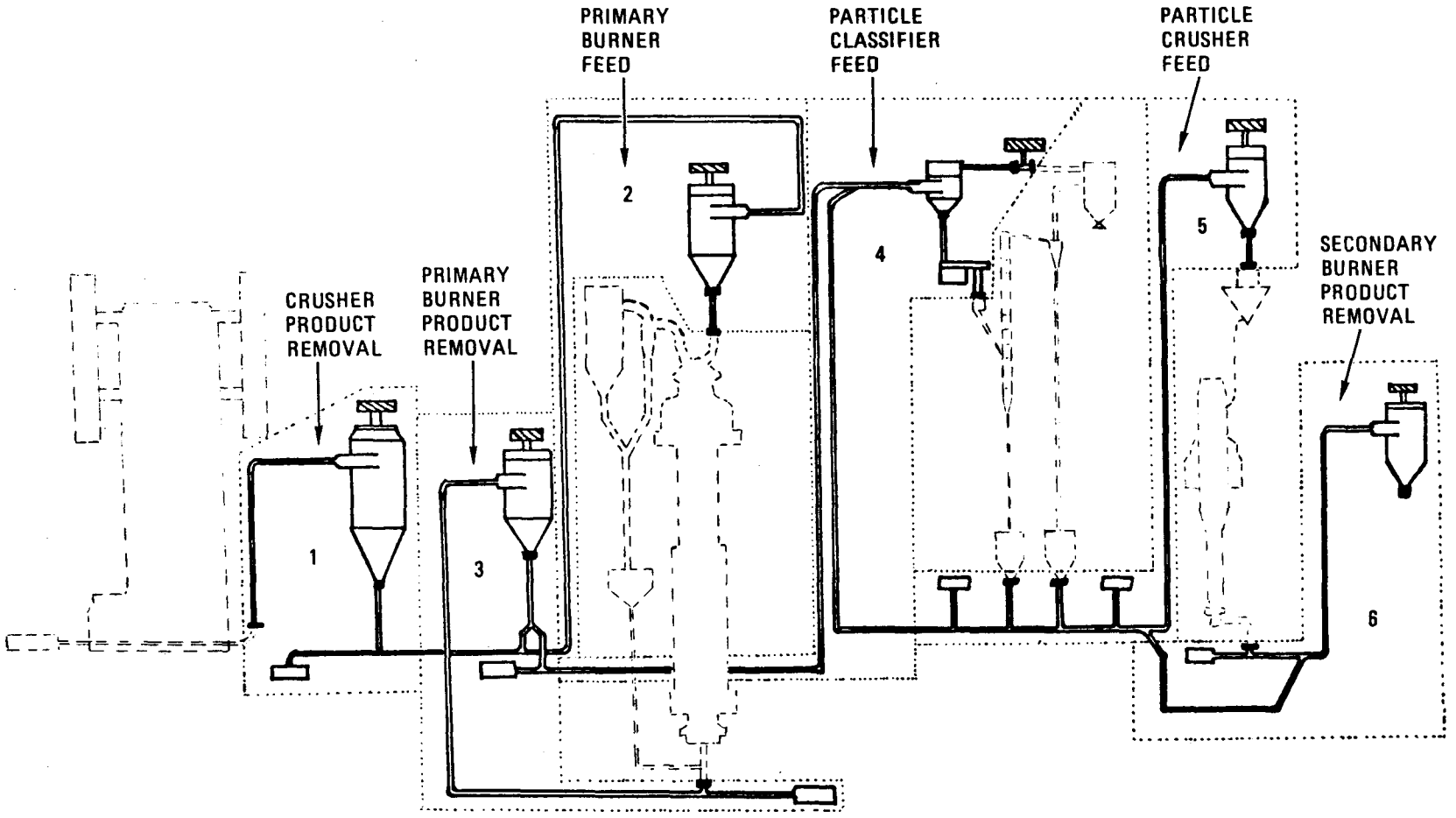

Fig. 7-2. Solids handling subsystems

Weigh cells

Samplers

7.4.1.1.1. Inlet Filters. The pressure drop across the inlet filters of the various transport systems was measured so that future degradation of filter performance may be monitored. The filters were all tested individually on the same transport system so that results could be compared directly. The results were disappointing since the measured pressure drops exceeded the manufacturer's rated pressure drop numbers in all cases.* The pressure drop data are given in Table 7-3. Although the inlet filters presently do not pose a significant hindrance to transport system operation, they do reduce the total system capacities somewhat. The filters will be studied closely during operation of each individual system to determine the specific impact on the performance of each system.

7.4.1.1.2. Bunkers. The solids handling system bunker volumes were determined by a combination of experimental and analysis methods. The original design volume, as calculated, was found to be conservative. Since feed material enters a bunker tangentially, the material was assumed to fill from the bunker walls inward, declining in height as a function of the material's angle of repose. Calculations of bunker volumes under these assumptions were conservative, assuring that actual bunker volumes would be greater than the minimum required by the design criteria.

The actual volumes of three bunkers were determined experimentally by filling the bunkers with known volumes of crushed graphite until the high-level sensors signalled. Upon inspection, the material was found to be deposited in a uniform, nearly flat configuration as shown in Fig. 7-3. This material configuration closely approximates the actual internal bunker volume as calculated up to the top of the high-level sensors. From these

*This is presumably caused by the contraction in flow area (from a diameter of 0.30 m to 0.048 m or 0.035 m).

TABLE 7-3
MEASURED PRESSURE DROP ACROSS INLET FILTERS

Inlet Filter Location	ΔP Measured (Pa at 212.3 m^3/s)	ΔP Rated (Pa at 424.7 m^3/s)
Fuel element size reduction system	1145	234
Crusher product bunker	1071	229
Primary burner	1170	229
Secondary burner	1071	234
Primary burner product bunker[(a)]	1942	239
Fissile classifier product burner[(a)]	1868	239
Fertile classifier product bunker[(a)]	2141	234
Spare filter	1195	239

[(a)] 0.035-m filter outlet; all others are 0.048 m.

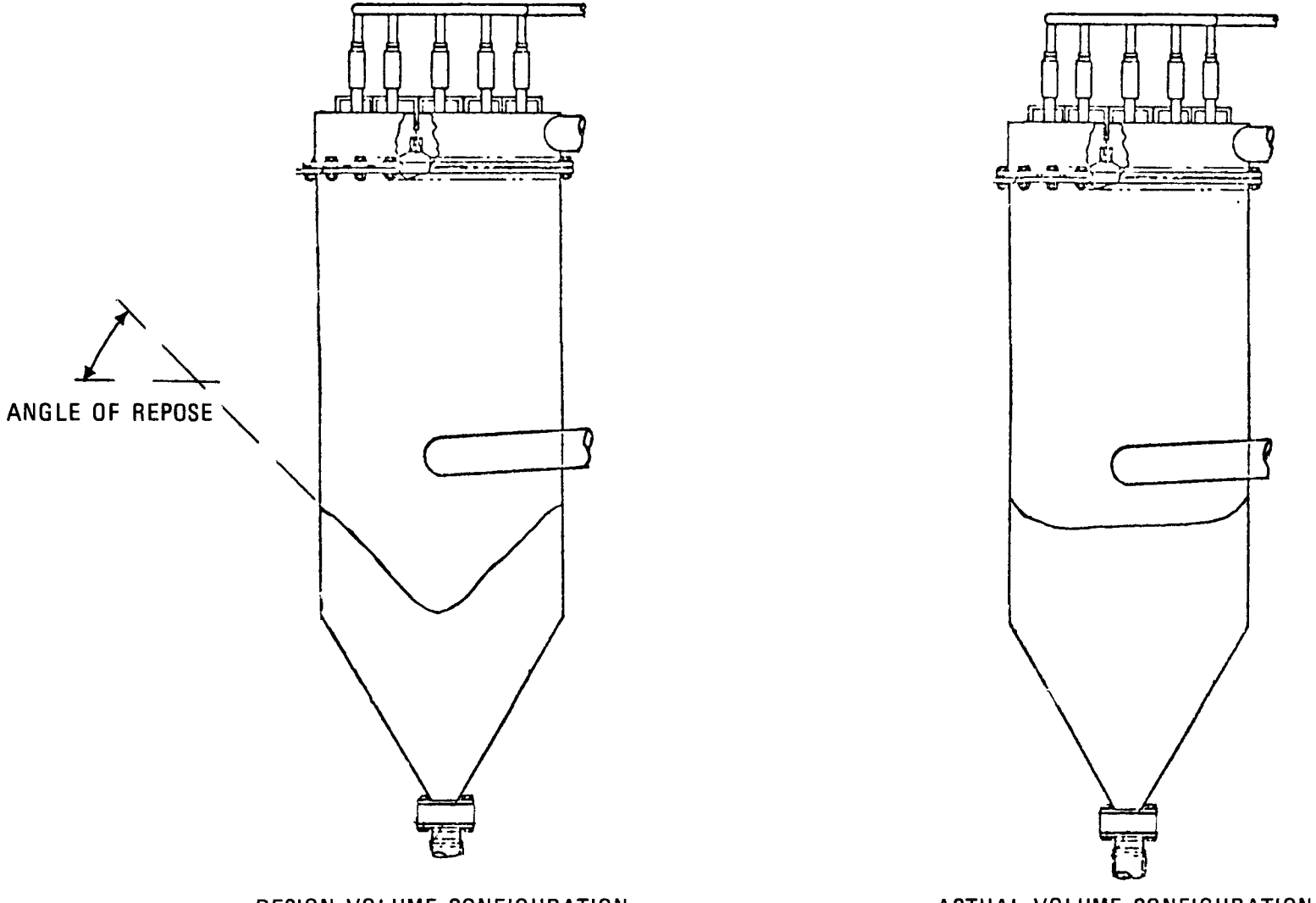

Fig. 7-3. Design and actual solids handling system bunker volumes

results, the volumes of the remaining bunkers were determined by calculation.* The volumes of these remaining bunkers are probably still conservative to some degree, because fuel particles have a low angle of repose and will tend to deposit within a bunker in a level configuration, even more so than crushed graphite, allowing a slightly larger portion of the bunker to be filled. Results of the bunker volume experiments and volume calculations are compared in Table 7-4.

7.4.1.1.3. In-Bunker Filters. The procedure for pre-loading and testing the efficiency of the in-bunker filters was described in detail in the last quarterly report (Ref. 7-1), together with efficiency results from four of the bunkers. The filter testing is now complete, and, for completeness, all the results are given in Table 7-5. The difference in the mean values is substantially smaller than the joint estimate of the standard deviation. In other words, there is no significant change in the size of particles deposited on filter exhaust lines. This verifies the efficiency of the filters.

During operation of the secondary burner product removal system (see Section 7.4.1.2.4, Fig. 7-15), a rupture disc downstream of the bunker burst and the blower inlet filter was subsequently dismantled, with no trace of radioactivity revealed. Secondary burner product is one of the finest powders present in the head-end process (average size of 60 μm) and is radioactive. This finding further verifies the effectiveness of the in-bunker filters.

7.4.1.1.4. Blowers. Although no specific tests are required to verify the performance of the blowers, knowledge of their behavior is required for the time when the speed must be set for permanent operation.

---

*The original equipment qualification plans included filling the classifier and particle crusher feed bunkers with design basis materials until the high-level alarms were activated. Since the volume of material required can be estimated with a fair degree of certainty, such experiments are not required. Furthermore, a severe strain on the available fuel particle inventory would have resulted.

TABLE 7-4
EFFECTIVE BUNKER VOLUMES

Bunker	Design Volume (m^3)	Experimentally Determined Volume (m^3)	Volume Below Top of Sensor (m^3)
Crusher product	0.550	0.736	0.790
Primary burner product	0.136	0.283	0.252
Primary burner feed	0.110	0.150	0.158
Classifier feed	0.082		0.130
Particle crusher feed	0.034		0.086
Secondary burner product	0.028	Has no level sensors	0.110 (to top of cone)

TABLE 7-5
SIZE DISTRIBUTIONS OF SAMPLE WIPES TAKEN FROM
IN-BUNKER FILTER EXHAUST LINES

Subsystem No.	No. Particles in Sample		Percent Particles >4.2 μm	
	Before Loading	After Loading	Before Loading	After Loading
1	1764	3496	55.8	43.1
2	1465	389	20.8	45.2
3	344	709	58.2	58.0
4	1204	648	60.2	32.3
5	1563	1687	48.6	50.1
6	962	247	59.1	43.1
Mean Value[a]			50.5	45.3

[a] Difference in the mean values = 5.2. Joint estimate of the standard deviation = 12.3.

The solids handling system has six blowers, one of which has a variable speed motor to serve the classifier, while the other five have fixed speed motors. The speed at which the blower rotates is controlled by the relative sizes of the sheaves, or pulleys, on the motor and blower shafts. The Gardner-Denver Company, which supplied the blowers, gives performance specifications for the relevant model (3PDR9) (see Fig. 7-4). The data can be accurately described by the following formula:

$$\frac{\text{rpm}}{1000} = \frac{2118\ V + 30 + 0.833\ P}{151 - 1.57\ P} \quad ,$$

where rpm = blower speed (revolutions/min),
V = gas volume flow rate (m^3/s) (standard),
P = underpressure at blower inlet (kPa).

Opportunities to verify this formula occurred during experiments with the secondary burner product removal system (see Section 7.4.1.2.4).

7.4.1.1.5. Feeders. Rotary feeder valves with variable speed drives were tested for possible use in the pilot plant under the following bunkers:

1. Crusher product bunker.
2. Primary burner product bunker.
3. Fertile classifier product bunker.
4. Fissile classifier product bunker.

The valves could be utilized in place of the fixed size orifices now used to control the feed rate from these bunkers into their respective transport systems. A substantial variation in flow rates through a fixed size orifice can be expected with the range of materials likely to be deposited in the bunkers. Rather than replace fixed orifices each time that a different material or mixture of materials is deposited into a bunker, a rotary feeder could be used, by varying its speed, to control feed rates into transport systems. Another, similar problem is imposed by the tendency of

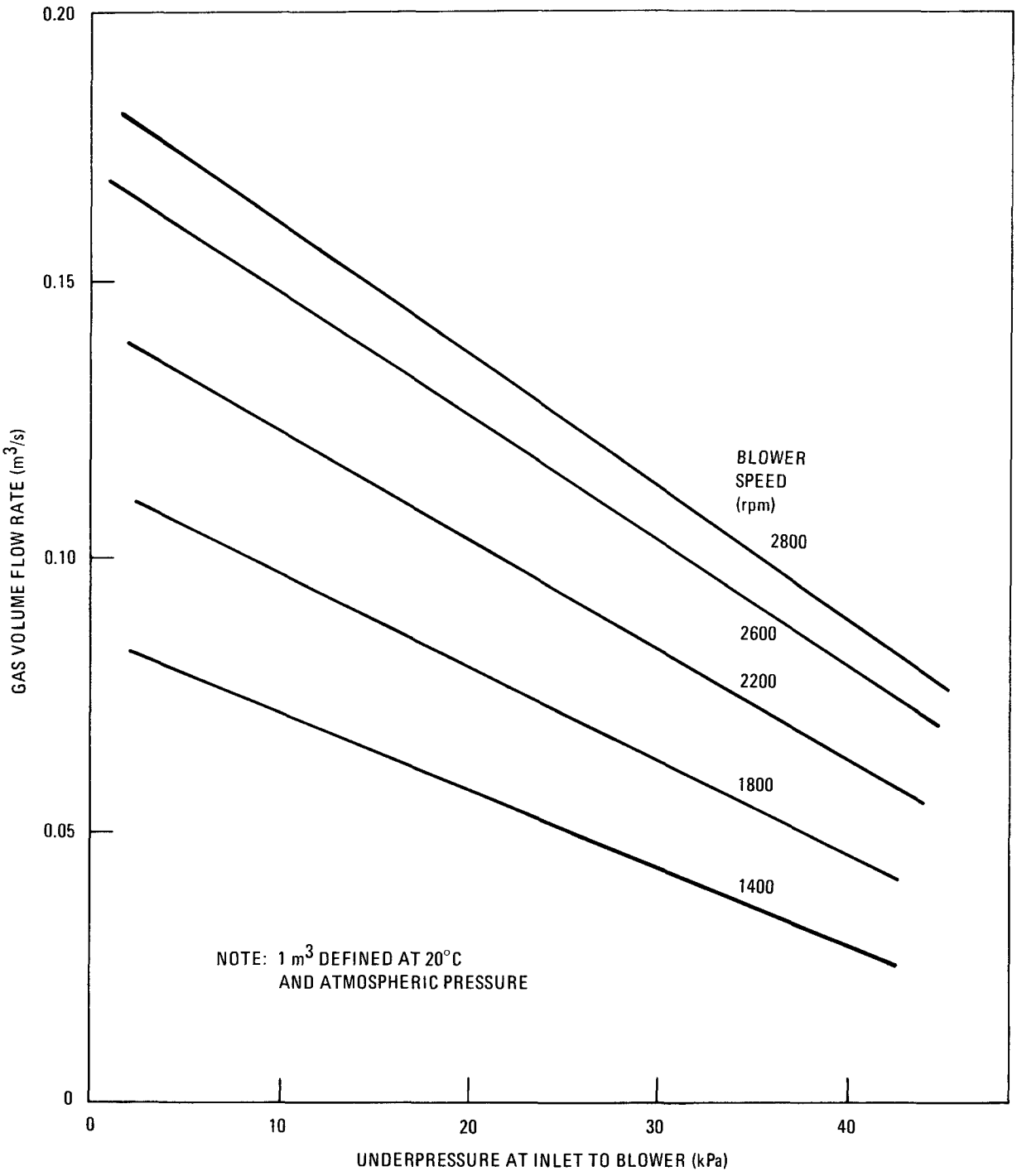

Fig. 7-4. Blower performance specifications (Gardner-Denver 3PDR9)

fuel particles to segregate in the bottom of bunkers containing fuel particle and graphite mixtures, causing an initial surge of fuel particles upon emptying a bunker, and thus overwhelming the conveying system. A rotary feeder valve would dampen any such surges by providing steady and controllable feed rates.

The tests were preliminary in nature and were performed to establish vane clearances and throughput capacities of the rotary valves. Steel shot, glass beads, and crushed graphite were used as feed materials for the tests to simulate actual feed materials encountered in pilot plant operations without the radiological safety constraints that would have been required if actual feed materials had been used. By comparing the particle size and density of the steel and glass with that of fuel particles, rotary valve performance may be extrapolated to predict valve performance with fuel particles. By varying valve clearances and valve speeds during the tests, the proper valve settings were determined for subsequent system testing to verify the valve performance under actual operating conditions in future sequential pilot plant tests. Results of these tests are shown in Fig. 7-5.

7.4.1.1.6. Weigh Cells. Preliminary weigh system calibration was performed to determine an accuracy level which may be feasible to attain with the present equipment. Under optimum or static conditions (no pilot plant operation or nearby work activity), the individual systems functioned within ±1/2% accuracy for the maximum design load only. The design load is much smaller than the possible bunker loads in most cases, since the bunker design volumes were conservatively estimated as explained in Section 7.4.1.1.2.

One-half percent accuracy is considered adequate for the pilot plant operations, so further work on the weigh system has been to improve the accuracy under more dynamic conditions, such as pilot plant operation. Preliminary evaluation of the weigh system dealt with the Orbitran electronics, including the load cells. Discussions were held with Orbitran,

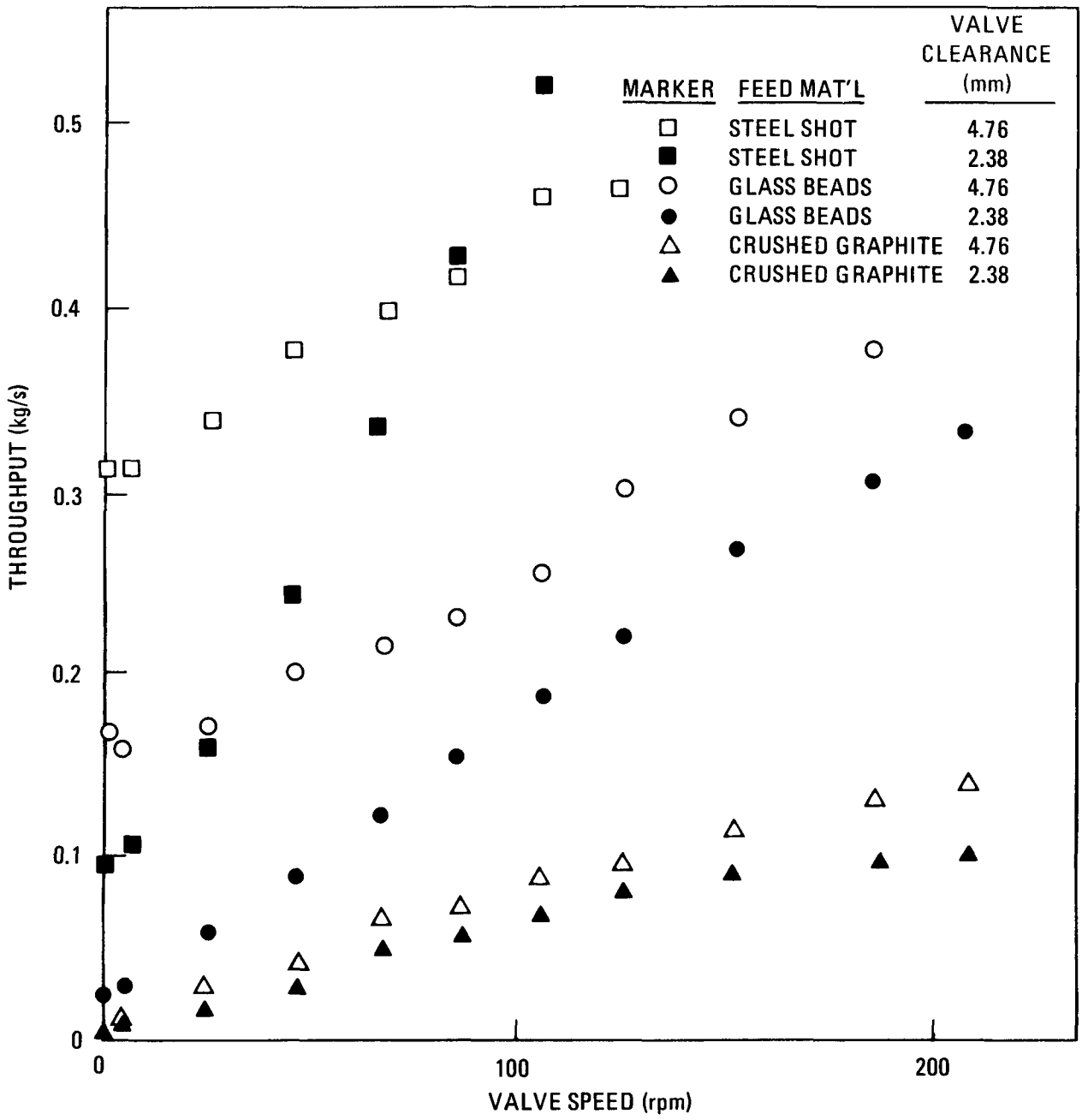

Fig. 7-5. Rotary feeder valve test results [0.005-m (2 in.) inlet]

Inc., concerning discrepancies in the Orbitran documentation and the technical aspects of the system. The discrepancies in the documentation were resolved and corrections made when necessary. The system calibration (Cal min./max.) was discussed. This circuitry checks the system from the junction box at the bunker back through the electronics. Any electrical changes in the external cabling due to moisture or temperature are designed to be electronically compensated for in the preamplifier stage of the system.

Data have been recorded from each channel of all systems with the exception of the unused channels 3 and 4 of System C. Data recorded consisted of Cal min., Cal max., and static zero. These data were recorded once each day. Over a 6-day period, no appreciable change in calibration data was noted. The static zero includes any pertubations the load cells may see because of extraneous stresses applied through either the bunkers or support structure. Of the 10 bunkers, six had a zero change of less than 0.1% of full scale, and the remaining four had a zero change of less than 0.2% of full scale. No heavy work was performed in the pit area or on the evaluated platform during this time and no systems were active. These data will continue to be recorded for some time. In addition, a weight will be placed on one of the bunkers once each day to check that system's repeatability at some known load and to get a check on "return to zero."

The Orbitran system has a resolution of 10 g (0.022 lb). This means that it can detect and display a change in load of 10 g. It is a highly sensitive system, and any load equal to or greater than 10 g transmitted to the load cell through either the bunker or the structure will be seen as a change in output on the display. In other words, not only are the external connections to the bunker very important, the external connections to the support structure are equally important. For example, the particle crusher and the particle crusher feed bunker are supported by a common structure. When the particle crusher is running, vibration from it is transmitted through the common support structure to the load cell pad, causing a ±1-kg fluctuation in the particle crusher feed bunker weight display. The fines

east and west bunkers are also supported by a common structure. Any weight added to either bunker is transmitted, to some degree, to the load cell pad of the other bunker.

Preliminary evaluation of the weigh system indicates that the electronics portion of the system is performing within the specifications as purchased. Some bunkers have zero shifts due to insufficient isolation of forces from bunker connections, primarily from inaccurately installed bellows. All support structures for the bunkers have extraneous items attached to them, causing vibration and false loads to be transmitted to the load cell pads. The support structures are the portions of the weigh system which limit the system accuracy. Further work is planned for the support structure design in conjunction with necessary structural changes required for addition of product samplers.

7.4.1.1.7. Samplers. In a previous quarterly report (Ref. 7-2), the need for sampling in the pilot plant was discussed. A selection of samplers has been acquired, and in the coming months each will be tested for suitability prior to installation in the relevant part of the system. At the same time, other ideas for taking samples will be investigated. Crusher product and primary burner product sampling tests are discussed below.

Crusher Product Sampling. A cross cutting sampler acquired for use under the crusher product bunker was tested during the quarter. This particular sampler extracts samples from gravity flows. A hollow blade moves in a flat arc across the falling stream of feed material. A portion of the material stream falls down the hollow blade to the discharge tube. The speed at which the hollow blade sweeps across the material stream may be varied as well as the frequency of such moves, allowing some flexibility in individual and bulk sample sizes.

This device is gentle with the material, making it suitable from a particle breakage standpoint. Considerable height is required, however, to fit the sampler in a gravity flow line -- approximately 1 m (see Fig. 7-6).

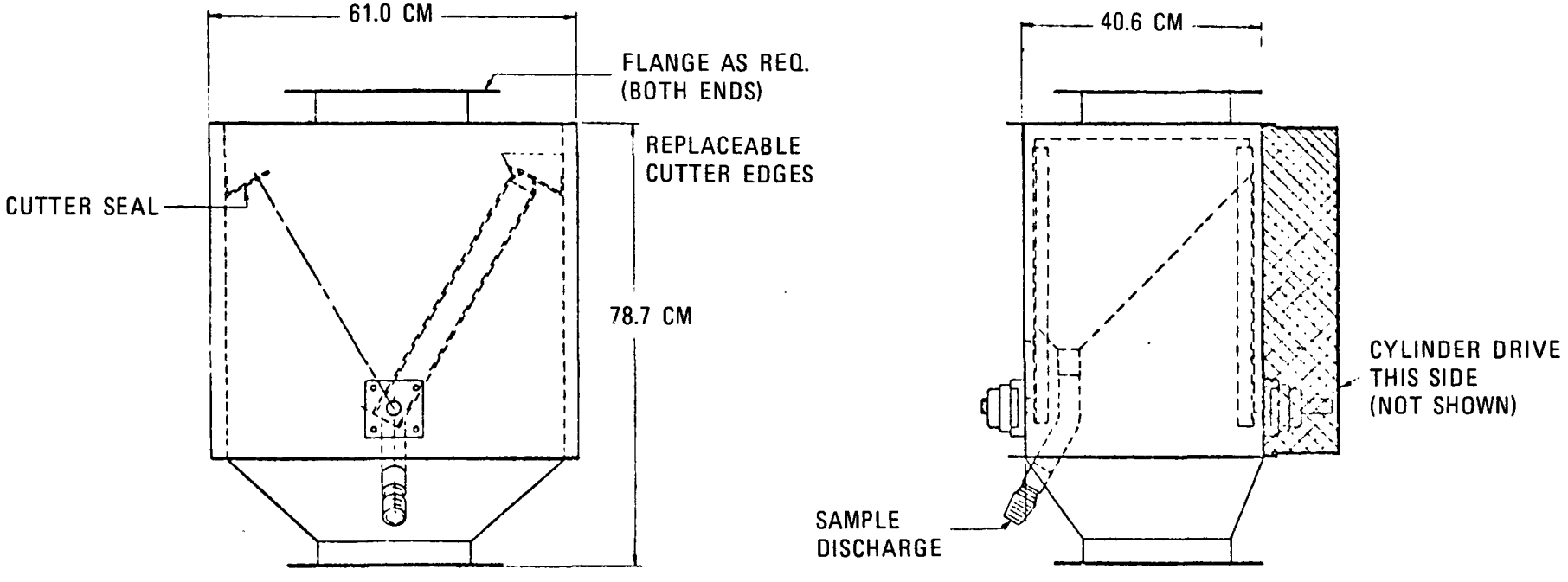

Fig. 7-6. Cross cutting crusher product sampler

The sampler was adjusted to separate approximately 1% of the crushed graphite feed material flowing from a 0.051-m orifice at approximately 0.57 kg/s. A 3-sec interval between sampler sweeps was used. The size distribution of the material separated by the cross cutting sampler was determined by screening and compared with the size distributions of several samples of the feed material taken by a more conventional 12-to-1 splitter. In all cases, the screened size distributions did not differ significantly, providing justification for further tests with the sampler installed beneath the crusher product hopper for future sequential operation of the pilot plant.

Primary Burner Product Sampling. A tube sampler was designed, fabricated, and tested for use beneath the primary burner outlet. The sampler (see Fig. 7-7) consists of a 3.79-mm-I.D. tube extending through the wall of the discharge line into the product flow path. A second tube attached to the sample tube provides a gas purge to clean the sampler and to control flow of material into the sampler. The tube sampler was bench tested using a high-temperature, variable position knifegate valve which is also to be located beneath the primary burner. The knifegate valve is a bonnetless type with an electropneumatic actuator and electronic position transmitter located behind heat shields (see Fig. 7-8). Throughput rates of the knifegate valve were studied in parallel with the tube sampler tests (see Fig. 7-9).

For these tests, glass beads with a particle diameter on the order of 500 μm and a bulk density of 1500 kg/m^3 were used as the feed material. The valve operated under choked feed conditions. Sample size data taken by the tube sampler and throughput rates of the variable width knifegate valve were studied by varying the aperture voltage and the purge conditions (see Fig. 7-10). The sample size increases with aperture size increase. With the aperture size constant, the sample size remains fairly constant regardless of purge gas quantity (see Fig. 7-11).

Once the sampler and valve are installed beneath the primary burner, additional tests will be performed to determine how accurately the tube

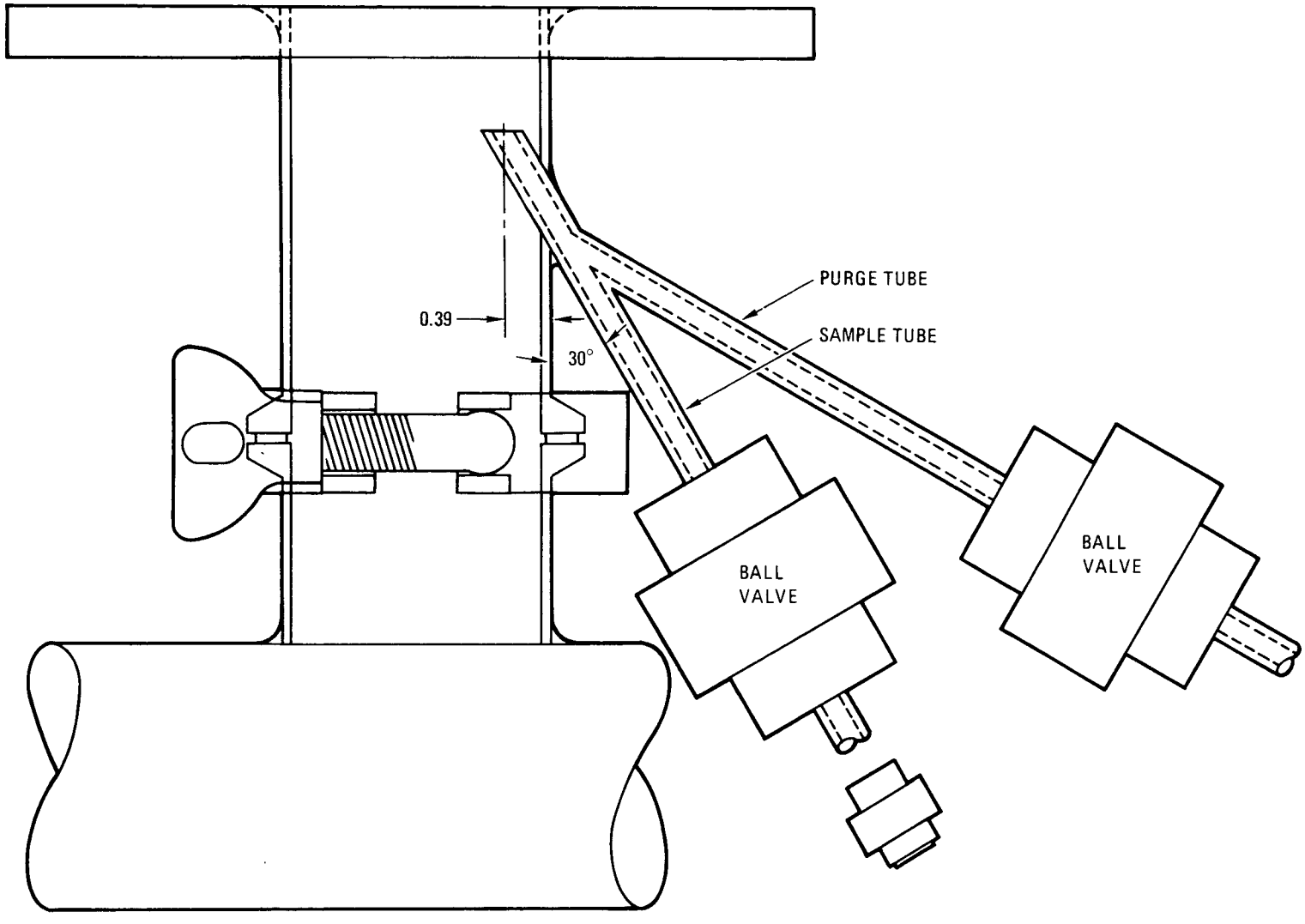

Fig. 7-7. Tube sampler for use below primary burner outlet valve

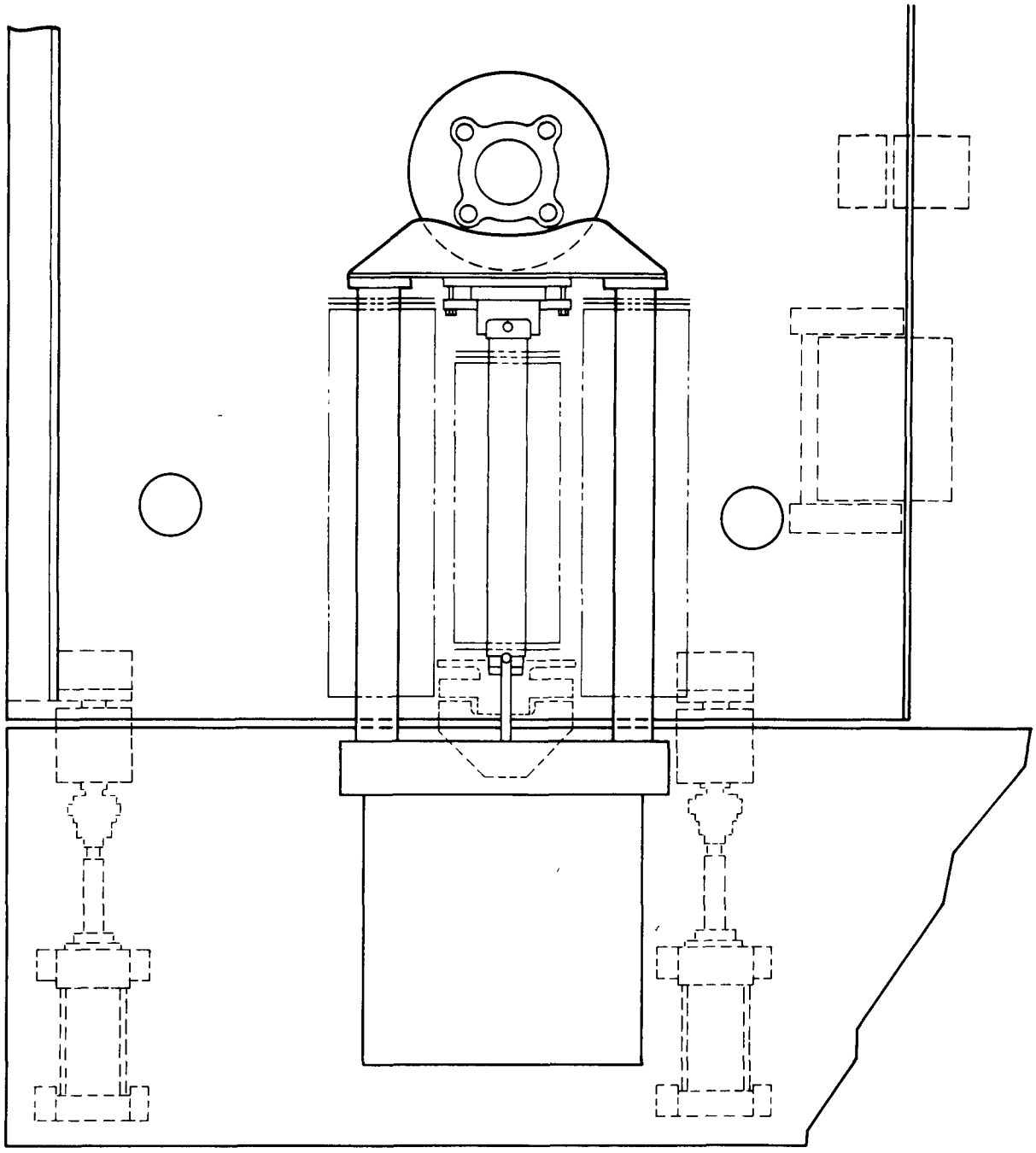

Fig. 7-8. Variable position knifegate valve to be used in primary burner product removal system

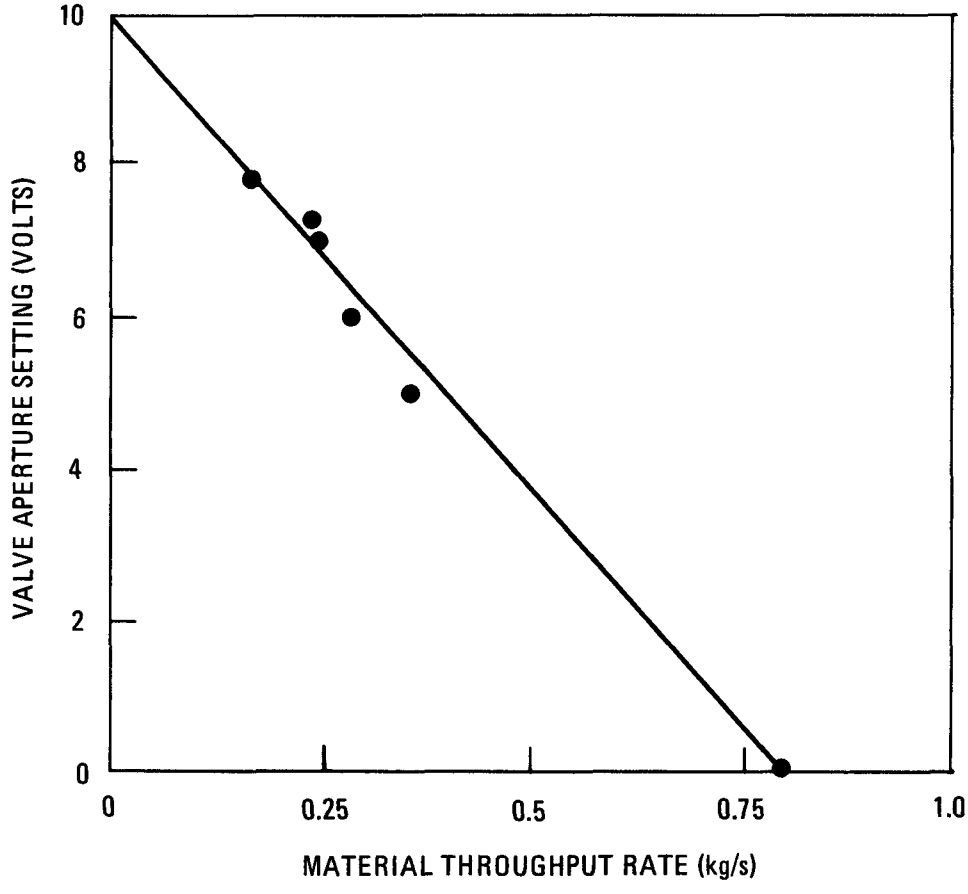

Fig. 7-9. Valve setting versus throughput rate for variable position knifegate valve

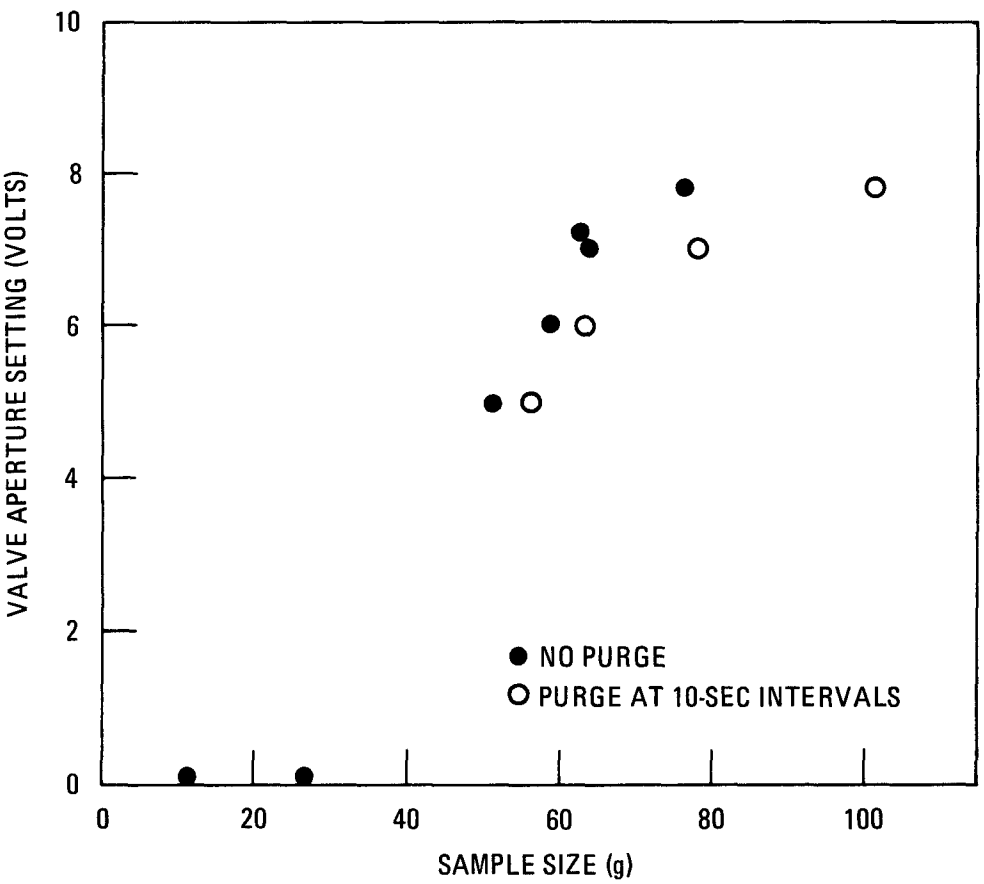

Fig. 7-10. Valve setting versus sample size for primary burner product tube sampler

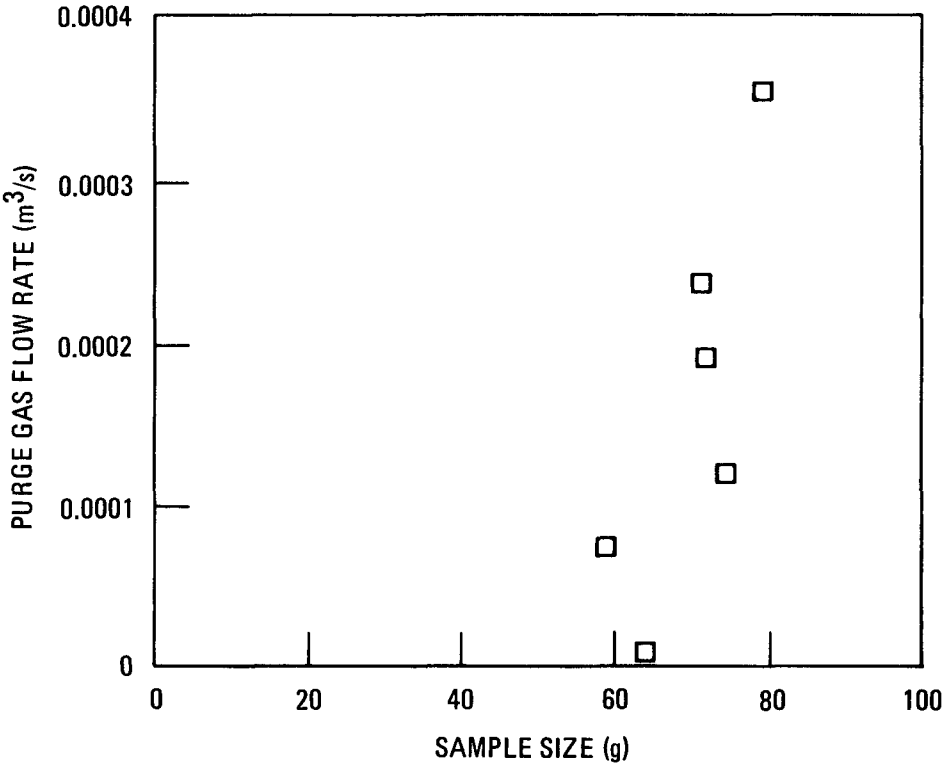

Fig. 7-11. Purge gas flow versus sample size for primary burner product tube sampler

sampler product size distribution matches the particle size distribution of the feed material.

7.4.1.2. System Qualification

7.4.1.2.1. Introduction. The goal of system qualification is to ensure that each subsystem can convey material at a rate compatible with upstream and downstream operations so that particle breakage is minimal. This involves establishing the conveying characteristics of each system by measuring pressure drops at different solids flow rates over a range of gas velocities. The determination of the saltation point, i.e., where the suspension collapses and particles fill up the line, is also required. The ability to restart, after plugging the line, by use of the blower only should also be investigated.

The solids handling test rig, described in previous quarterly reports, is equipped with a variable speed blower, which is being used for system qualification. Once the optimal conditions for a given system have been determined, a fixed speed blower, suitably set, can be used.

The final part of system qualification, which is the measurement of fuel particle breakage during sequential operation, can be performed only during pilot plant operation with loaded fuel elements.

Progress with system testing is described below.

7.4.1.2.2. Primary Burner Feed System (Subsystem No. 2). The primary burner feed system tests consisted of transporting crushed graphite from the crusher product bunker to the primary burner feed bunker. The variable speed blower from the test rig was used so that transport gas velocities could be varied. Pressure drop data across the transport system were collected for various blower settings, with the transport gas velocity being lowered until unsteady flow was approached. These data will be presented in future reports.

7.4.1.2.3. Primary Burner Product Removal System (Subsystem No. 3). In the last quarterly report (Ref. 7-1), the experiments in the system to date were described. Since then, the results obtained from the removal of heated fuel particles have been analyzed. Also, particle breakage data have been scrutinized in more detail.

The system is shown in Fig. 7-12.

Heat Transfer. The full analysis of the heat transfer would be complex. Primary burner product in the form of burned-back fuel particles enters a conveying gas stream which is at ambient temperature. Through a combination of forced convection and radiation, the gas is heated. Forced convection of the gas/solids mixture, together with direct radiation from the fuel particles, heats the conveying pipe. As the discharge of a batch of product proceeds, the conveying pipe becomes hotter and steadily loses more heat to the surroundings through natural convection and radiation. As the mixture of gas and solids enters the bunker, the particles fall down and the gas rises and circulates around the filters, together with any fines, until all the gas passes through the filters, which themselves absorb the heat of the gas. The particles meanwhile heat the surrounding bunker by conduction and the filters by radiation and natural convection of the interstitial gas. The conveying gas reaching the blower increases in temperature as the in-bunker filters are heated.

The forced convective heat transfer from particles to gas in the conveying line depends strongly upon the slip velocity, or the difference in the gas and particle velocities. Since the initially stationary particles must be accelerated, and re-accelerated after each bend in the system, and since the gas temperature and hence velocity are changing, both with time and position in the line, the estimation of the slip velocity is complicated.

Nevertheless, an attempt to correlate measurement with simplified prediction needs to be made for system qualification and improvement. The

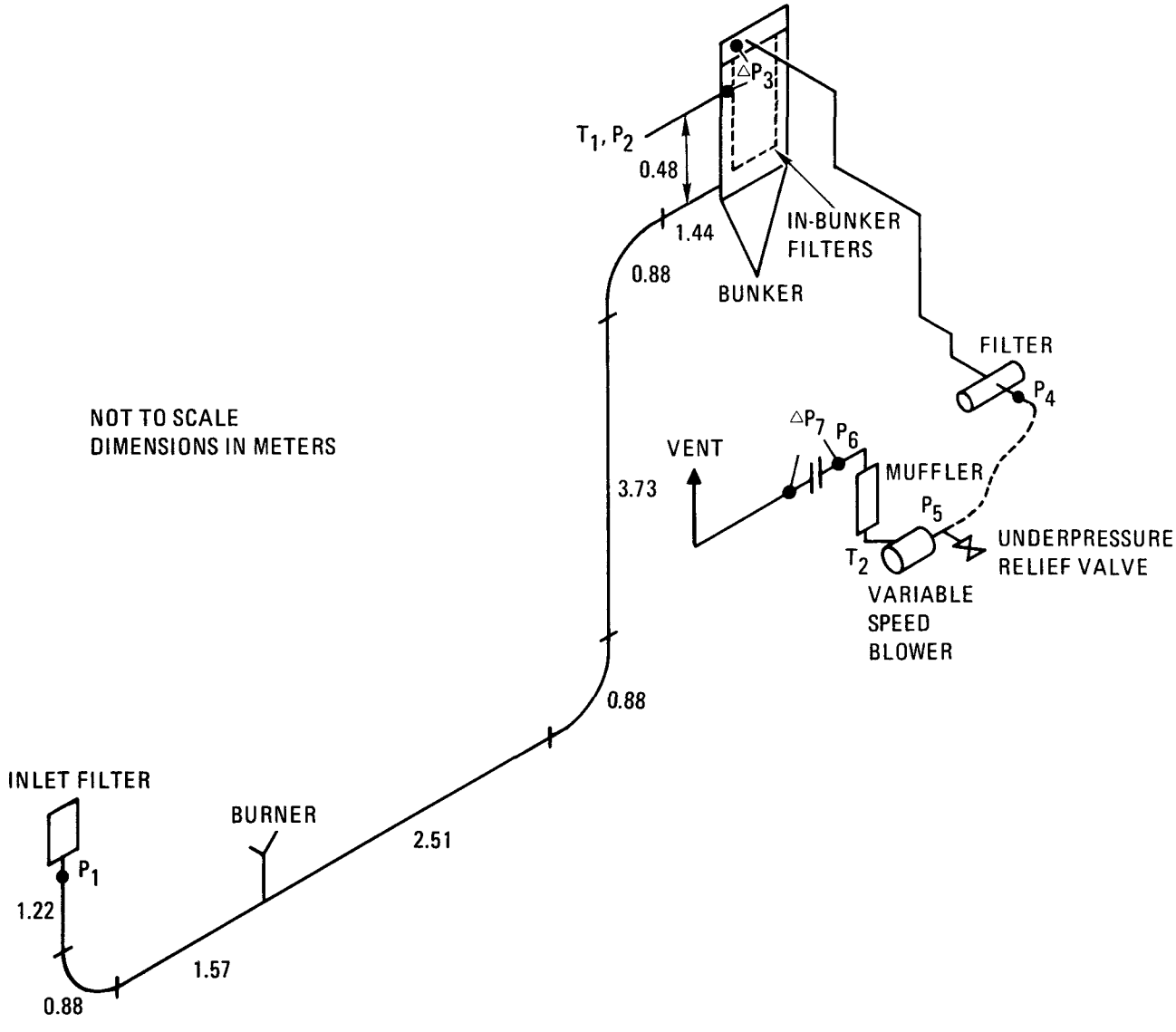

Fig. 7-12. Primary burner product removal system

data comprise solids flow rate, pressure differences, gas flow rate, particle inlet temperature, and gas temperature in the bunker, T_1 (see Fig. 7-12). The thermometer was some 0.48 m above the conveying pipe inlet, so the conveying gas would have cooled off somewhat. The simple analysis has been divided into steady-state and transient transfer, as discussed below.

1. Steady-state heat transfer.

Assumptions:

a. Radiation from particles is negligible.

b. The temperature of the wall is steady along the length of the system. The conveyed solids are accelerated instantaneously and maintain a constant slip velocity of twice the terminal velocity.

c. Conduction through the pipe wall is rapid.

Heat transfer from particles to gas: Kunii and Levenspiel (Ref. 7-3) quote the expression

$$Nu_p = \frac{h_p d_p}{kg} = 2 + 0.6\ Pr^{1/3}\ Re_p^{1/2} \quad ,$$

$$Pr = \frac{\mu C_{p_g}}{kg} \quad , \quad Re_p = \frac{\rho_g\ (V_g - V_p)\ d_p}{\mu} \quad .$$

$$\text{Assume } (V_g - V_p) = 2\ V_T = 2\sqrt{\frac{4 d_p \rho_{p_g}}{3 C_D \rho_g}} \quad ,$$

where $C_D = 18/Re_p^{0.6}$, $Re_p < 550$,

$Re_p = (\rho_g V_T d_p)/\mu$,

h_p = particle heat transfer coefficient (W/m^2-K),

d_p = particle diameter (m),
kg = gas thermal conductivity (W/m-K),
μ = gas viscosity (Ns/m^2),
C_{p_g} = gas specific heat (J/kg-K),
ρ_g = gas density (kg/m^3),
V_g = gas velocity (m/s),
V_p = particle velocity (m/s),
V_T = terminal velocity (m/s),
ρ_p = particle density (kg/m^3),
g = acceleration due to gravity (m/s^2),
Nu_p = particle Nusselt number,
Pr = Prandtl number,
Re_p = particle Reynolds number.

The particle heat transfer coefficient is based on particle external surface area. This can be calculated from

$$A_p = \frac{L}{(V_G - 2V_T)} \cdot \frac{F_p}{m_p} \cdot 4\pi d_p^2 \quad ,$$

where A_p = external surface area of particles (m^2),
L = length of conveying pipe (m),
$(V_G - 2V_T)$ = particle velocity (m/s),
F_p = mass flow rate of particles (kg/s),
m_p = mass of one particle (kg),
d_p = particle diameter (m).

Heat transfer from flowing suspension to wall: Few investigations into forced convective heat transfer from flowing gas-solids suspensions have been published. Hawes et al. (Ref. 7-4) obtained a correlation between the heat transfer coefficient and the loading of graphite in carbon dioxide and nitrogen, i.e.,

$$\frac{Nu_{mixture}}{Nu_{gas}} = f_n \left(1 + \frac{F_p C_{p_p}}{F_g C_{p_g}} = \frac{h_{mixture}}{h_{gas}} \right) \quad ,$$

where C_{p_p} = specific heat of particles (J/kg-K),
F_g = mass flow rate of gas (kg/s).

Heat transfer from outside of conveying pipe: The heat is transferred by a combination of natural convection and radiation. The dependence on temperature is almost linear such that the combined effects may be expressed by

$$h_{ow} = 0.0738\ T_w \quad ,$$

where h_{ow} = heat transfer coefficient from outside wall of conveying pipe (W/m^2-K),
T_w = temperature of wall (°C).

The combination of these three resistances to heat transfer gives

$$h_p A_p\ (T_p - T_g) = h_{mixture}\ A_{iw}\ (T_g - T_w)$$

$$= h_{ow} A_{ow}\ (T_w - T_{ambient}) = Q \quad ,$$

$$Q = F_p C_{p_p}\ \Delta T_p + F_g C_{p_g}\ \Delta T_g \quad ,$$

where A_{iw} = area of inside of pipe wall (m^2),
A_{ow} = area of outside of pipe wall (m^2),
$T_{ambient}$ = temperature of outside surroundings (°C),
Q = heat flux (W).

Other temperatures refer to mean values.

In order to compensate for the initial heating of the gas, assume that the gas and particles are in thermal equilibrium at the beginning, as given by

$$F_p C_{p_p}\ (T_{pb} - T_{pi}) = F_g C_{p_g}\ (T_{pi} - T_{ambient}) \quad ,$$

where T_{pb} = temperature of particles leaving the burner (°C),
T_{pi} = initial particle temperature in the conveying line.

These equations can be solved to give the wall temperature and the drop in temperature of the particles and gas as they pass through the system, as well as the individual heat transfer coefficients. These are needed for the analysis of the transient heat transfer.

2. Transient heat transfer.

Assumptions:

a. The particles heat up the gas instantaneously and then transfer heat to the wall according to

$$\frac{1}{x} = \frac{1}{h_p A_p} + \frac{1}{h_{mixture} A_{iw}} \quad ,$$

where x (W/K) is a combined coefficient.

b. The heat transfer from the wall is constant and equal to the steady-state value (this tends to decrease the rate of heating of the pipe, but the mass of metal of the pipe does not include fittings, valves, etc.).

c. The gas temperature is close to that of the wall.

The heat balance is

$$m_p C_{p_p} \Delta T_p = x\,(T_p - T_w) = m_w C_{p_w} \frac{dT_w}{dt} + h_{ow} A_{ow}\,(T_w - T_{ambient}) \quad ,$$

where m_w = mass of wall (kg),
C_{p_w} = specific heat of wall material (J/kg-K).

ΔT_p, the temperature change of the particles, is related to the mean and initial particle temperatures by

$$T_p = T_{p_i} - \frac{\Delta T_p}{2} \quad .$$

The equation can be solved to give

$$T_w = \frac{\alpha}{\beta} - \left(\frac{\alpha}{\beta} - T_{wi}\right) e^{-\beta t} \quad ,$$

where T_{wi} = initial wall temperature,

$$\alpha = \left[\frac{x F_p C_{p_p} T_{p_i}}{\left(x + F_p C_{p_p}\right) m_w C_{p_w}} + \frac{A_{ow} h_{ow} T_{ambient}}{m_w C_{p_w}} \right] \quad ,$$

$$\beta = \left[\frac{x F_p C_{p_p}}{\left(x + F_p C_{p_p}\right) m_w C_{p_w}} + \frac{A_{ow} h_{ow}}{m_w C_{p_w}} \right] \quad .$$

The gas temperature, assumed to be close to the wall temperature in this analysis, is not measured at the end of the conveying line, however, but higher up in the bunker. In order to get some indication of how much temperature is lost between the end of the conveying line and the thermometer, assume that the gas heats up the shell of the bunker according to

$$\frac{dT_s}{dt} = (T_g - T_s) \frac{F_g C_{p_g}}{m_s C_{p_s}} \quad ,$$

where T_s = temperature of bunker shell (°C),
m_s = mass of relevant part of bunker shell (kg),
C_{p_s} = specific heat of shell material (J/kg-K);

i.e., the gas and bunker shell are assumed to come to thermal equilibrium. No account is taken of heat loss from the outside of the bunker.

Let

$$T_g = \frac{\alpha}{\beta} - \left(\frac{\alpha}{\beta} - T_{wi}\right) e^{-\beta t} \quad . \tag{7-1}$$

Let

$$\frac{F_g C_{p_g}}{m_s C_{p_s}} = \gamma \quad ,$$

$$T_s = \frac{\alpha}{\beta} \frac{(e^{\gamma t} - 1)}{e^{\gamma t}} - \left(\frac{\frac{\alpha}{\beta} - T_{wi}}{\beta - \gamma}\right) \frac{\gamma}{e^{\gamma t}} \left[1 - e^{-(\beta-\gamma)t}\right] + \frac{T_{si}}{e^{\gamma t}} \ (°C) \tag{7-2}$$

These equations have been solved for air at 200°C, 0.225 kg/s of FSV TRISO A particles which were discharged from the 0.40-m primary burner at temperatures of 200°C, 400°C, and 680°C. The predicted gas temperatures at the end of the conveying line (Eq. 7-1) and at the thermometer (Eq. 7-2) are given in Fig. 7-13 together with the measurements. It can be seen that the measurements are bracketed by the two sets of gas temperature predictions. The initial and equilibrium gas temperatures at the end of the conveying line, given in Table 7-6, can be used with a measure of confidence for pressure drop calculations.

Pressure Drop. The pressure drop formula published by the Engineering Equipment Users Association, EEUA (Ref. 7-5), is as follows:

$$\Delta P = \frac{1}{2} \rho_{ns} \bar{V}_G^2 \left(F_1 + F_2 \frac{L}{D} + F_3 N\right) + \rho_{ns} g H \quad ,$$

where ΔP = pressure difference (Pa),

ρ_{ns} = non-slip density = $\bar{\rho}_g + (F_p \cdot 4/\pi D^2 \bar{V}_G)$ (kg/m^3),

F_p = particle flow rate (kg/s),

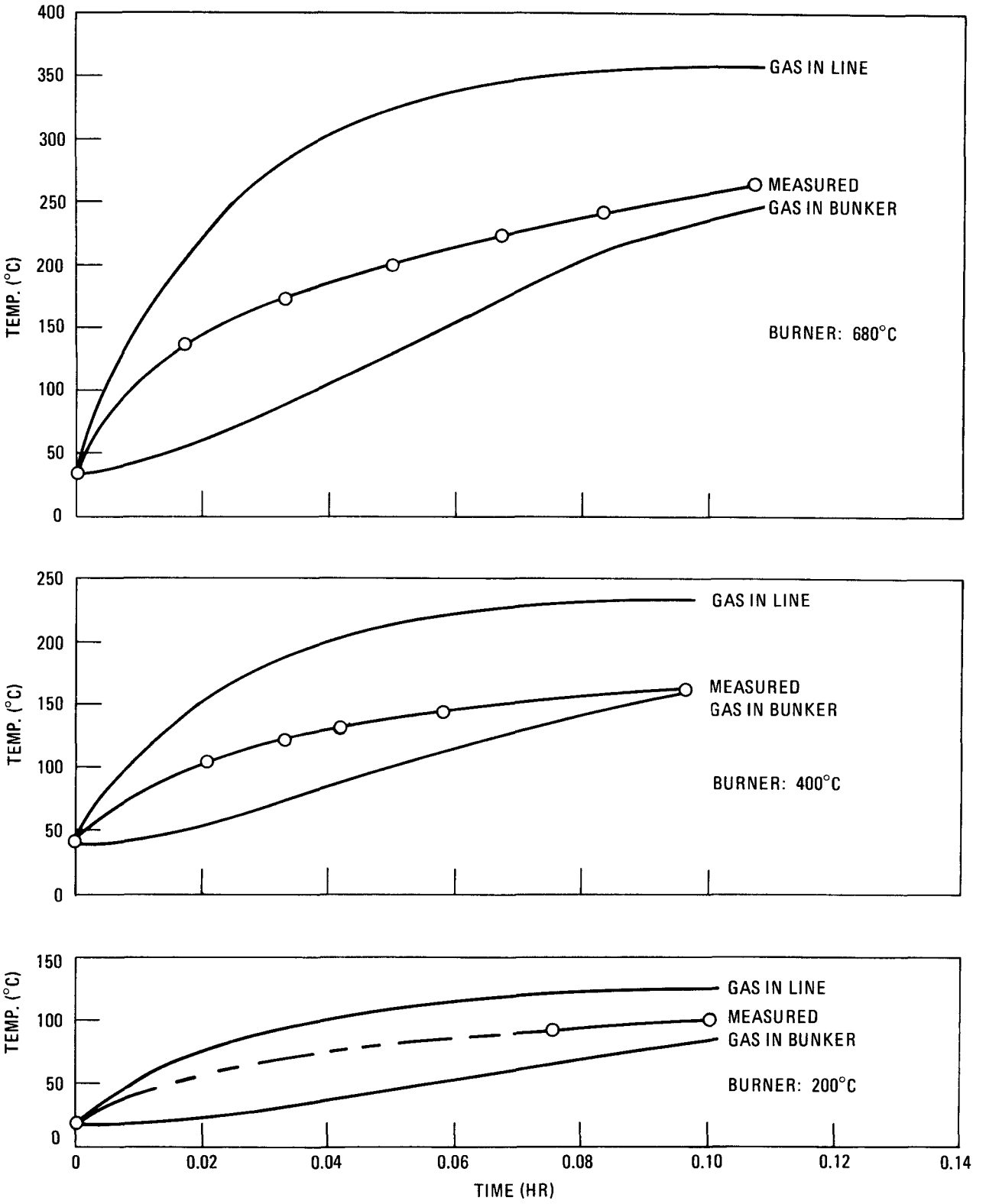

Fig. 7-13. Measured and predicted gas temperatures at end of primary burner product removal system

TABLE 7-6
PRESSURE DROPS AND GAS VELOCITIES OBSERVED
DURING DISCHARGE OF HOT PARTICLES INTO
PRIMARY BURNER PRODUCT REMOVAL SYSTEM

Particle Temperature in Burner (°C)	Mean Gas Velocity at Ambient Temperature (m/s)		Observed Conveying Line Pressure Drop (kPa)	
	Initial	Final	Initial	Final
200	29	20	13.4	11.9
400	24	18	15.0	12.2
680	23	18	16.6	12.9

$\bar{V}_G$ = mean gas velocity (m/s),
$\bar{\rho}_g$ = mean gas density (kg/m^3),
L = length of conveying system (m),
H = change in elevation (m),
D = internal diameter of the conveying line (m),
F_1 = acceleration factor = 2.5,
F_2 = friction factor = $0.0127 + 2.71/\bar{V}_G^2$,
F_3 = bend factor = 0.5 for gradual bends,
N = number of bends.

As discussed in the last quarterly report (Ref. 7-1), half of the value of the pressure drop gives a very acceptable estimate for conveying materials at ambient temperatures. In Fig. 7-14, the pressure drops observed during the conveying of hot particles are compared with predictions based on ambient temperatures and with predictions based on calculated temperatures. The six points refer to the initial and final temperatures and pressure drops (see Table 7-7). The acceleration pressure drop, $F_1 \cdot (1/2)\ \rho_{ns} \bar{V}_G^2$, was calculated using inlet temperatures, and the remainder using mean temperatures.

Even though Fig. 7-14 demonstrates the need to consider the effect of temperature, as expressed in gas velocity and density, it can be seen that the modified EEUA method is not very successful at predicting the pressure drop. The phenomena occurring in the system are complex, and this simple method requires an additional safety margin to take account of an increased pressure drop when conveying material at elevated temperatures. This is of immediate importance for the secondary burner removal system and of future interest for hot reprocessing facilities.

Particle Breakage. Data from the initial experiments in the 0.40-m primary burner have been analyzed in order to ascertain the breakage during fluidization and during transport. The fuel particles used were FSV TRISO A particles, which have the nominal specifications given in Table 7-8.

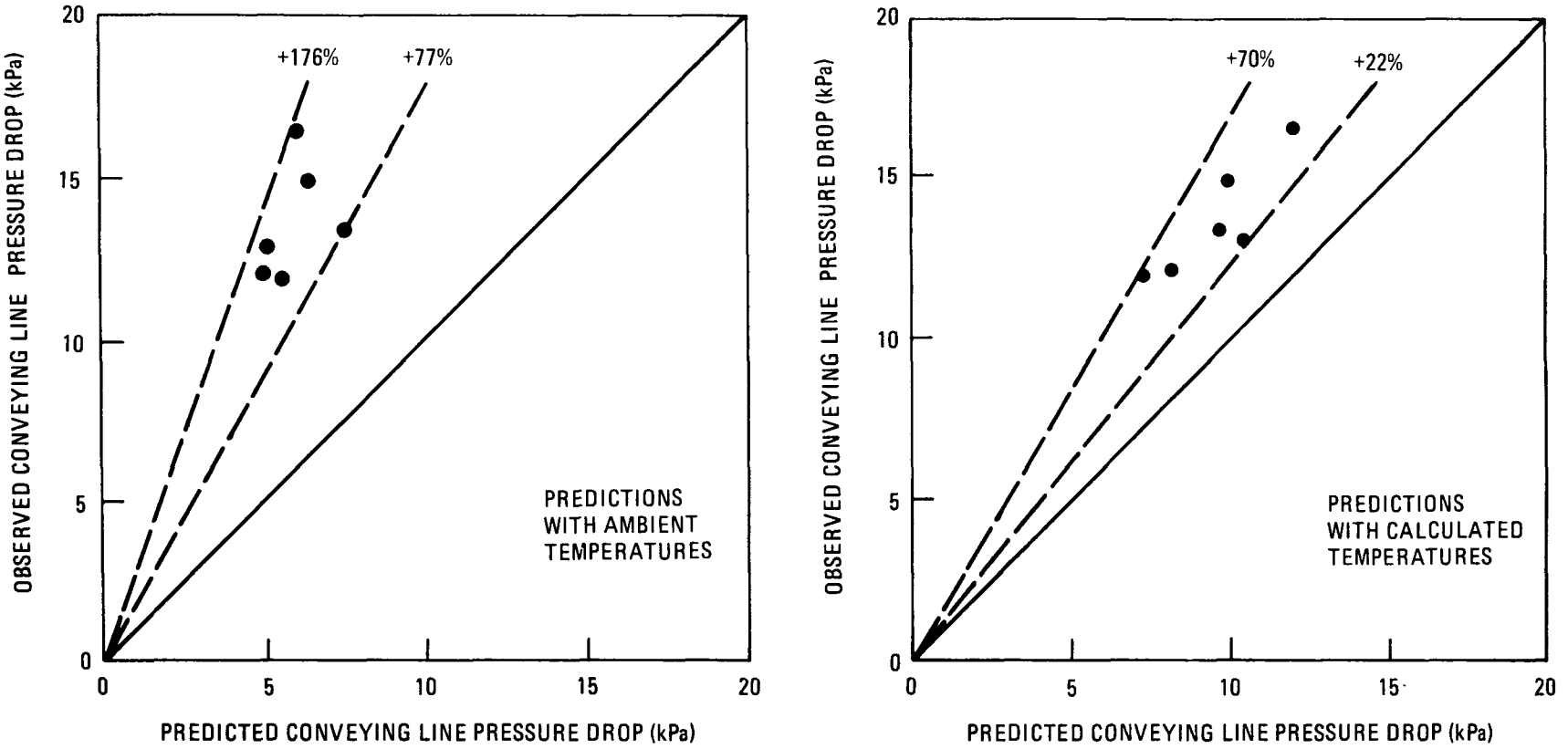

Fig. 7-14. Measured and predicted conveying line pressure drops in primary burner product removal system with heated fuel particles

TABLE 7-7
GAS/PARTICLE MIXTURE TEMPERATURES AT BEGINNING
AND END OF PRIMARY BURNER PRODUCT REMOVAL SYSTEM

Particle Temperature in Burner (°C)	Inlet Mixture Temperature (Calculated) (°C)	Outlet Mixture Temperature (°C)		Mean Mixture Temperature (°C)	
		Initial	Equilibrium (Calculated)	Initial (Calculated)	Equilibrium (Calculated)
200	160	16	126	88	143
400	316	38	234	177	275
680	538	32	358	285	448

TABLE 7-8
NOMINAL SPECIFICATIONS AND RANGE OF VALUES
FOR FSV FERTILE TRISO "A" FUEL PARTICLES

Material	Range of Thickness (μm)	Nominal Thickness (μm)	Range of Densities (kg/m^3)	Nominal Density (kg/m^3)	Nominal Weight of Each Material (g)
Thorium carbide	300-410 (diameter)	355 (diameter)	≥8400	9200	21.6×10^{-5}
Buffer layer	45-65	55	900-1300	1100	3.21×10^{-5}
Inner isotropic carbon	20-40	30	1750-1950	1850	4.29×10^{-5}
Silicon carbide	20-30	25	>3170	3190	7.57×10^{-5}
Outer isotropic carbon	≥30	35	1700-1900	1800	7.38×10^{-5}

The analysis of samples taken from particles after they have been transported is performed as follows:

1. Divide into fractions above and below 450 μm.

2. Burn both in an oven at 900°C for 24 hr.

3. Divide the ash into burned-back particles, hulls (silicon carbide), and oxide (thorium oxide).

Experience to date has shown that the oxide passes through a 125-μm screen. Hulls and particles are separated by brushing small samples and collecting hulls. This procedure is tedious, and the use of small samples reduces the time required. The smaller the quantities involved, however, the larger the relative weighing error.

The particle breakage as a result of fluidization is assessed by analyzing the contents of the fines hoppers. This is done by taking a number of samples, measuring the particle size distribution, and then analyzing each size fraction after burning.

The interpretation of the results is complicated by four factors:

1. Number of fragments in the initial feed. The particles used in the experiments had, in large part, not been through the final washing stage of the manufacturing process. Consequently, some thorium oxide fines were probably adhering to the outside of the particles. Prior to being put into the burner, the particles were sieved and the oversize (+864 μm) and undersize (-412 μm) material was discarded. Since the nominal diameter of a complete particle is 645 μm, it is quite possible that a half-particle fragment is retained on a 412-μm screen. The thorium carbide kernel is pyrophoric and given time will oxidize to thorium oxide, which is a fine powder, much of which will fall out of a

fragment. In other words, an initial excess of hulls was probably present in the feed.

2. Breakage during storage and analysis. A number of particles will "pop" during storage, sieving, and, above all, burning. Once this has been recognized, however, some allowance can be made, for instance:

   a. Assume all +425-μm material comprises whole particles and fragments from which thorium oxide has been detached.

   b. Any thorium oxide found in the burned-back +425-μm fraction is therefore assumed to have come from "popped" particles.

3. Re-use of particles. The inventory of fuel particles is limited, and so the same ones need to be re-used. The general trend of the material found in the fines hoppers is for there to be excess thorium oxide. This indicates an excess of hulls in the particle bed. This effect will be cumulative.

4. Deviations from the specification. Table 7-8 shows the range of coating thicknesses and densities. If a high density were to occur with a thick coat, the relative proportion of a given component could change significantly. Furthermore, the particles available were rejected for one reason or another. The measure of confidence with which the relative quantities of ThO_2, silicon carbide, and carbon can be used is therefore small.

Despite such difficulties, it is important to glean as much information as possible from breakage data because the primary burner product removal system must be developed to a point where there is minimal particle breakage. This development must take place in conjunction with experiments in the burner, which are few in number. Hence, the maximum information must be obtained from each experiment.

The primary burner runs to date are as follows:

Run	Description
A-1	Crushed graphite heatup. Transported cold.
A-2.1	Heatup of fuel particles (180 kg). Transported cold.
A-2.2	Heatup of fuel particles (470 kg). Transported hot.
A-3.1	Heatup of simulated feed (130 kg). Material left in burner.
A-3.2	Heatup of simulated feed (270 kg). Additional feed was added.
	Excess of 140 kg added after the tests. Transported cold.

The breakage data have been calculated based on the following assumptions:

1. Thorium oxide indicates broken particles. The presence of an unknown but possibly significant amount of silicon carbide fragments is not thought to be indicative of breakage. Another interpretation of the results, which show excess silicon carbide, is that significant quantities of ThO_2 have not been located. The filters in the primary burner are the same as those in the solids handling system. Results obtained as part of the solids handling equipment qualification testing (see Section 7.4.1.1.3) have shown them to be very efficient. Careful examination of the burner filter chamber and fines hoppers has failed to reveal quantities of ThO_2.

2. Only that thorium oxide found in -425-μm fractions is relevant. Thorium oxide in +425-μm fractions is attributed to particles which "popped" during burning of the sample. The effect of "popping" was measured with a sample which was carefully inspected and found to contain no fragments. The resulting ash was analyzed by brushing and weighing and also by dissolution of the fragments. The results are shown in Table 7-9. Approximately 2% of those examined as whole particles broke as the

TABLE 7-9
RESULTS OF BURNING BACK WHOLE PARTICLES TO MEASURE
THE NUMBER WHICH BREAK DURING BURNING

Wt % particles in = 100.00 g
Wt % particles out = 82.92 g
Wt % fragments = 1.27 g

	Analyzed by Brushing and Weighing	Analyzed by Dissolution
Wt % SiC, (g)	0.40	0.31
Wt % ThO_2 (g)	0.87	0.96
Wt % ThC_2 ($ThO_2 \div 1.03$) (g)	0.84	0.93
Ratio $\frac{ThC_2}{SiC}$ (nominally 2.84)	2.10	3.00
Percent particles broken		
Based on SiC (x 5.83)	2.33	1.81
Based on ThC_2 (x 2.04)	1.71	2.23
Average	2.02	2.02

Combined average = 2.02%

result of being burned back. The dual methods of analysis of the fragments gave some difference in the ratio of ThC_2/SiC, but they bracketed the nominal value, which is used for the rest of the analysis.

The figure of 2% is of interest for the analysis of breakage during combustion in the burner. Since those particles which broke are presumably defective, the number which break during successive burning experiments will decrease significantly.

Table 7-10 gives the percentage of particles broken during fluidization and transport for each burner run. The figures are based on thorium oxide found in -425-μm fractions in fines hoppers and the primary burner product bunker. The percentages of excess of silicon carbide hulls are also given for the transported product. These are based on subtracting from the weighed amount of silicon carbide the silicon carbide associated with the weighed amount of ThO_2 found in the +425-μm fractions. To this is added the excess silicon carbide found in the -425-μm fractions. In all cases, the total excess silicon carbide in the transported material was larger than the silicon carbide deficiency found in the material in the fines hoppers.

The breakage during conveying, particularly in run A-2.2, when particles were transported at elevated temperatures, is pleasingly small.

7.4.1.2.4. Secondary Burner Product Removal System (Subsystem No. 6). Experimental data and analytical results for this system are discussed below.

Experimental Data. A summary of the operational experience with this system is given below.

Heatup, 8/17/76: BISO particle heatup test. At ambient temperature, 50 kg of fully coated BISO particles were successfully conveyed with the fixed speed blower at 2100 rpm.

TABLE 7-10
PARTICLE BREAKAGE DURING FLUIDIZATION AND TRANSPORT OF FSV TRISO "A" FERTILE PARTICLES DURING 0.40-m PRIMARY BURNER HEATUP TESTS

Run Number (weight of material, kg)	Percent Broken in Fluidization	Percent Broken in Conveying	Percent Excess SiC in Transported Material (after adjusting for SiC deficiency in fines hoppers)
A-2.1 (180 kg fuel particles)	0.31	0.68	0.96
A-2.2 (470 kg fuel particles)	0.78	0.56 0.70	1.60[a]
A-3.1 (26 kg fuel particles, 104 kg graphite)[b]	1.50	0.54	0.52
A-3.2 (42 kg fuel particles, 178 kg graphite)[b]	1.00[c]	0.54	
Excess feed (15 kg fuel particles, 125 kg graphite)[b]	--	0.38 0.34	0.37 0.50

[a] Contains 0.37% from particles from A-2.1 which were reused.

[b] The weight of fuel particles is based on an analysis of material removed from the burner after testing and excess feed removed after the burner tests. The proportion of particles was probably higher in A-3.1 and lower in A-3.2, and so the percent breakage is probably lower for A-3.1 and higher for A-3.2.

[c] The breakage figure is based on the additional 16 kg of fuel particles added after run A-3.1.

Run 1, 9/15/76: FSV TRISO fertile ash. Approximately 45 kg were discharged at ambient temperatures. The variable speed blower was set at 65% power. The underpressure at the blower exceeded 40 kPa, the relief valve opened, and the line plugged. The small amount left in the burner was removed at 100% power.

Run 2, 10/5/76: As for run 1, but 100% power was used. The line plugged. The remaining material (23 kg) was removed with the fixed speed blower (0.5 kg/s, ΔP = 37 kPa).

Run 3, 12/8/76: As for run 1, but the fixed speed blower was resheaved from 2100 to 2550 rpm, the underpressure relief valve was reset to 50 kPa, and the bunker top was stiffened. The 46-kg batch was successfully conveyed at 0.69 kg/s at a ΔP of 47 kPa, which remained steady.

Run 4, 1/18/77: The burner product was at a temperature of 140°C. Transport was interrupted when a bursting disc, intended as a backup, ruptured. The line plugged and transport could not be restarted. After cleaning, and blinding off the bursting disc, the remainder was transported.

Run 5, 2/3/77: The burner product was at 100°C. Shortly after discharge began, the ΔP exceeded 48-1/2 kPa and the relief valve opened. The secondary burner outlet valve was closed promptly. The line cleared itself, presumably due to the presence of only modest quantities of product, and transport was resumed. The ΔP never became higher than 47 kPa and died away quite quickly.

This rather scant amount of experimental data will be the basis of the redesign of the system. Until a new system is installed, the burner can best be discharged in bursts, whereby the burner outlet valve is closed before the pressure drop becomes excessive. The ultimate goal of the secondary burner product removal system is to convey product leaving the burner at 800°C, so that the burner does not need to be cooled and reheated

between successive batches. In order to make design calculations, design methods must be verified using the available experimental data.

Analysis of Gas Only Flow. The secondary burner product removal system is shown in Fig. 7-15. The pressure in the bunker, P_2, was observed prior to each attempt to convey product using the fixed speed blower. In Section 7.4.1.1.4, a formula connecting blower speed, pressure drop, and capacity is given. Verification of this expression was obtained by calculating the gas flow through the conveying line from the pressure drop.

Case 1: Speed of blower = 2100 rpm, P_1 = 1.5 kPa, $P_2 - P_1$ = 10.3 kPa, P_4 = 14.3 kPa. Assume the conveying line is hydrodynamically smooth. The Blasius expression for the friction factor can be used ($C_f = 0.08\ Re^{-1/4}$):

$$P_2 - P_1 = 4C_f \cdot \frac{L}{D} \cdot \frac{1}{2} \bar{\rho}\bar{V}^2 \quad , \qquad Re = \rho \frac{\bar{V}D}{\mu} \quad ,$$

where $\bar{\rho}$ = mean gas density = 1.12 kg/m^3,
D = conveying line diameter = 0.0475 m,
μ = gas viscosity = 2 x 10^{-5} Ns/m^2,
L/D = 294.

Using these data, $\bar{V}$ = mean gas velocity = 66 m/s.

The system inlet flow rate is therefore 0.104 m^3/s. Based on the blower formula, the inlet flow rate is 0.108 m^3/s.

Case 2: Blower speed = 2550 rpm, P_1 = 1.6 kPa, $P_2 - P_1$ = 13.8 kPa, P_4 = 18.4 kPa.

The conveying line pressure drop yields a flow of 0.123 m^3/s. The blower formula gives 0.126 m^3/s.

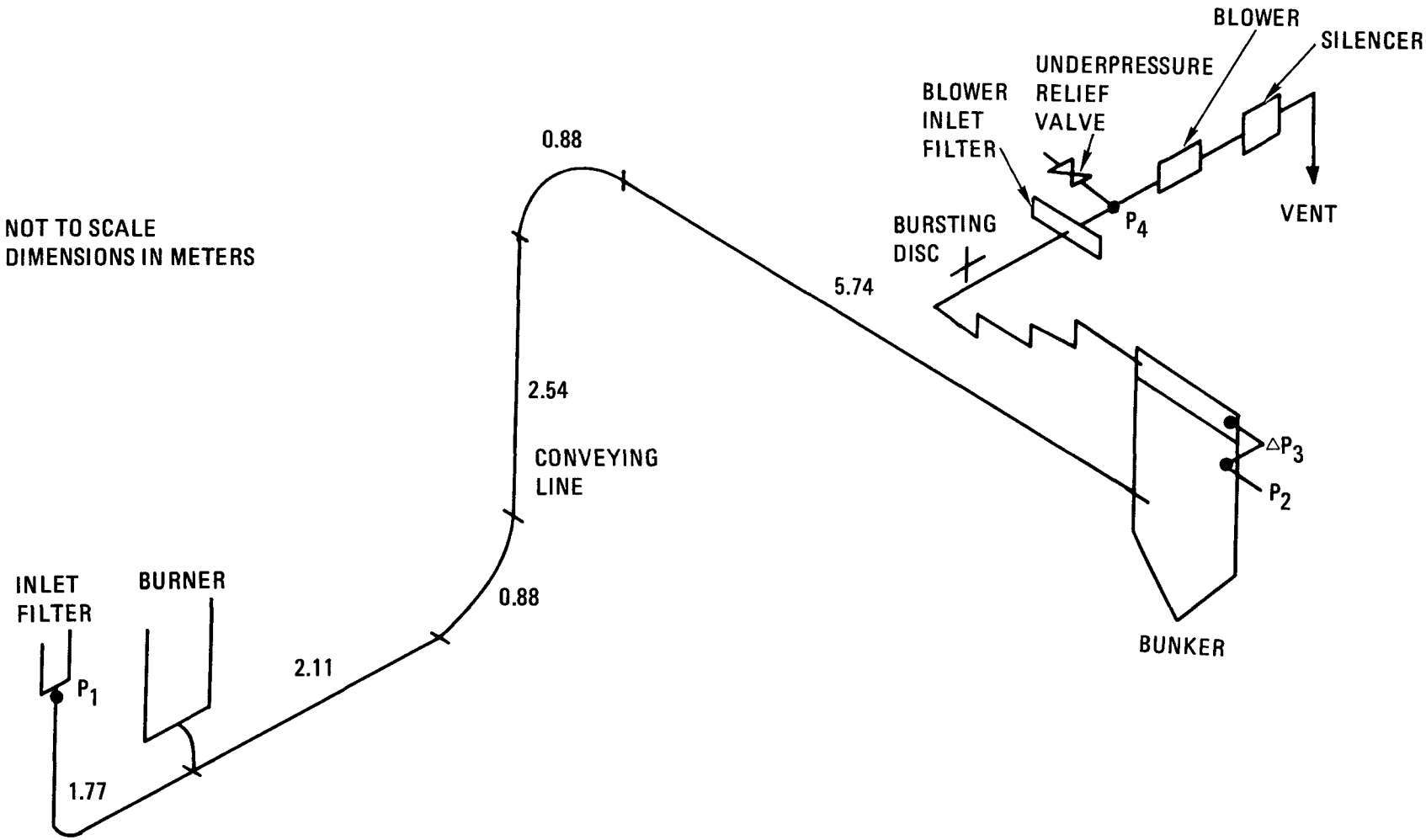

Fig. 7-15. Secondary burner product removal system

These two cases give ample verification of the performance of a fixed speed blower. Henceforth, the blower formula can be used for analyzing experimental data and for design calculations.

Analysis of Gas and Solid Flow. As described above in the discussion of experimental data, there are only two useful readings, from runs 2 and 3. The duration of the runs is small, and some doubt exists with respect to the ability of the pressure gauges to respond to any rapid changes. Similarly, changes in pressure drop will cause the load cells to fluctuate, making the assessment of any initial surge in the solids flow rate difficult. For the purposes of these calculations, the solids flow rate is assumed to be constant. The pressure drop in the conveying line can be obtained from P_4 by deducting the contributions from the off-gas system, the filters, and the initial part of the conveying system. The blower formula can be used to calculate the gas flow. The pressure drop in the conveying line can be predicted using the method published by the EEUA (Ref. 7-5), which is described in Section 7.4.1.2.3. The comparison between observation and prediction is given in Table 7-11. While the agreement is fair, it is not as good as that obtained with cold fuel particles and crushed graphite as reported in the last quarterly report (Ref. 7-1). The failure of the system to convey secondary burner product at an elevated temperature amplifies the experience so far with the primary burner product removal system in that the increase in pressure drop is more severe than would be predicted by the EEUA model.

System Design Improvement. Let the improved system have a total pressure drop of 20 kPa, of which 16.7 kPa is in the conveying line. Let the inlet velocity be 34 m/s. The mean velocity is therefore 40.4 m/s. The solids flow rate is assumed to be 0.692 kg/s. The EEUA formula then becomes

$$\frac{0.173}{D} + \frac{0.0770}{D^2} + \frac{0.00385}{D^3} = 17.29 \quad .$$

TABLE 7-11
COMPARISON BETWEEN OBSERVED AND PREDICTED VALUES OF PRESSURE DROPS IN SECONDARY BURNER PRODUCT REMOVAL SYSTEM

Run No.	P_4 (kPa)	Solids Flow (kg/s)	Mean Gas Velocity (m/s)	Conveying Line ΔP		$\frac{\Delta P_{obs} - \Delta P_{pred}}{\Delta P_{pred}}$ (%)
				Observed (kPa)	Predicted (kPa)	
2	37.0	0.500	42.8	34.1	24.9	37
3	47.0	0.692	43.7	44.6	33.6	33

The solution is D = 0.089 m. There are two standard pipe sizes in the range: 0.0856 m (3-1/2-in. O.D., 3.37-in. I.D.) and 0.0983 m (4-in. O.D., 3.87-in. I.D.). The range of pressures that can be expected, together with the speeds of the two blowers, is given in Table 7-12. The pressure range is the EEUA prediction plus 35%. The blower speeds are based on leaving the present blower at 2550 rpm and setting the speed of the second blower. The range of gas velocities comes from the effect of the range of pressure drops on blower performance.

The basis for selecting a low system pressure drop is the need to allow a generous margin for increased pressure losses when conveying product at elevated temperatures.

REFERENCES

7-1. "Thorium Utilization Program Quarterly Progress Report for the Period Ending November 30, 1976," ERDA Report GA-A14214, General Atomic Company, December 30, 1976.

7-2. "Thorium Utilization Program Quarterly Progress Report for the Period Ending August 31, 1976," ERDA Report GA-A14085, General Atomic Company, September 30, 1976.

7-3. Kunii, D., and O. Levenspiel, Fluidization Engineering, John Wiley & Sons, Inc., New York, 1969, pp. 210-211.

7-4. Hawes, R. I., et al., "An Experimental Investigation into Heat Transfer and Pressure Drop Properties of Gaseous Suspensions of Solids," Atomic Energy Research Establishment Report AEEW-R-244, Atomic Energy Establishment, Winfrith, June 1964.

7-5. Pneumatic Handling of Powdered Materials, Engineering Equipment Users Association (EEUA), Constable and Company, LTD., London, 1963.

TABLE 7-12
PREDICTED PERFORMANCE OF CANDIDATE PIPE SIZE FOR AN IMPROVED SECONDARY BURNER PRODUCT REMOVAL SYSTEM

Pipe Diameter (m)	Pressure Drop in Conveying Line (kPa)	System Pressure Drop (kPa)	Blower Speeds (rpm)	Inlet Gas Velocity (m/s)	Mean Gas Velocity (m/s)
Current 0.0475	44.6	47	2550	34	44
0.0856 (3-1/2 in.)	18.1 to 24.4	21.4 to 27.7	2550 to 1780	31 to 34	36 to 40
0.0983 (4 in.)	14.0 to 18.9	17.3 to 22.2	2550 to 2600	31 to 34	35 to 40

8. GASEOUS EFFLUENT TREATMENT (U. Park)

Support work on HRDF and HET off-gas treatment was provided during the quarter. However, the overall activity was at a low level owing to the diversion of the cognizant engineer to a previously committed project (the prototype secondary burner design report).

9. PLANT MANAGEMENT

9.1. SUMMARY

The Work Plan for the Maintainability and Reliability Phase I study was prepared, and methodology development was initiated. The HET conceptual design has been completed to the 90% level and the Conceptual Design Report is in progress. HET Technical Review meetings were held during the quarter to discuss the facility and equipment arrangement, cost estimating ground rules, sampling plan, waste handling, off-gas treatment, and spent fuel shipping. System description and design criteria activities were initiated for an integrated HRDF Reprocessing Head-End and Solvent Extraction remote maintenance system.

9.2. MAINTAINABILITY AND RELIABILITY (L. Abraham)

9.2.1. Introduction

Work on Phase I of this study was initiated in January 1977. The objective of the Phase I study is to establish preliminary availability allocation requirements for the HRDF reprocessing facility and its major process systems, based on the HRDF Recycle Plant overall availability requirement. A specific near-term objective is to develop a methodology for establishing availability requirements of major systems.

9.2.2. Activity

A work plan for the Phase I study, which extends to October 1977, was prepared, and methodology development was initiated.

For the purpose of developing appropriate methodology, the availability requirements of the major systems in a limited portion of the HRDF reprocessing facility are being investigated. The dry head-end was chosen for this purpose, and 100% major system reliability is being assumed. In a subsequent parametric analysis, several assumed levels of reliability and maintenance downtimes will be factored into the availability allocation study.

Three assumed cases of HRDF dry head-end equipment system capacity and the associated numbers of required parallel systems were defined, and functional diagrams depicting the three cases were completed. Figure 9-1 is the functional diagram for Case III. Corresponding operating profiles for each assumed major equipment system were then prepared. An example of system operating profiles is shown in Fig. 9-2. The next step will be to determine the major system availability requirements for the three cases at an assumed level of 100% system reliability.

9.3. HOT ENGINEERING TEST REPROCESSING PRELIMINARY DESIGN

9.3.1. HET Project (HCC, VHP, RMB, NWJ, NDH, GEB)

The conceptual design work on the HETE-Reprocessing systems initiated during the previous reporting period has been completed essentially to the 90% level. The piping and instrumentation diagrams were finalized for each process system and are being final-drafted for the HET Conceptual Design Report. Conceptual design and arrangement drawings have been completed for the process system mechanical equipment and the equipment for remote maintenance. For all equipment of each process system, the material take-off data have been completed and transmitted to the architect-engineer preparatory to the cost estimating effort to be done by the architect-engineer. The drafts for the HET Conceptual Design Report are being prepared by the prime engineers for each HET-Reprocessing system. The completed report is scheduled for submittal to the architect-engineer for final report editing on March 4, 1977.

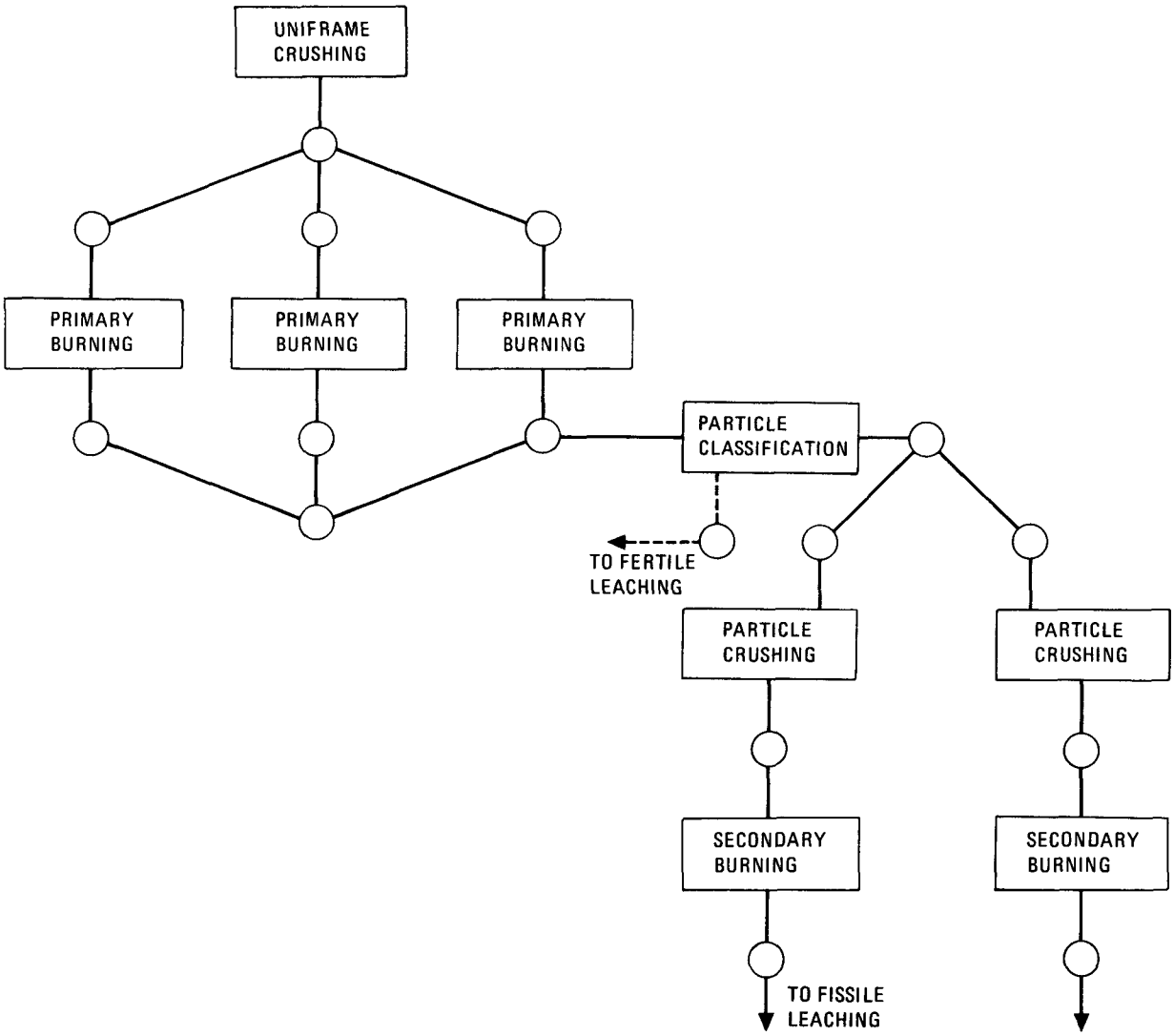

Fig. 9-1. Functional diagram for dry head-end, Case III

1. UNIFRAME CRUSHING, REF. DESIGN, 4 FE/hr CAPACITY AT 119 kg/FE

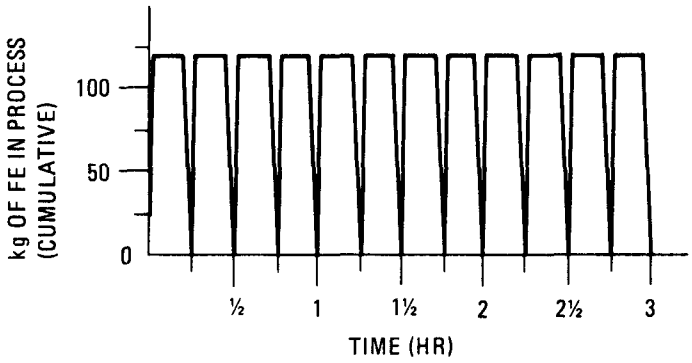

DIAGRAM REPRESENTS FEED THROUGHPUT AS WELL AS PRODUCT OUTPUT RATE

2. PARTICLE CLASSIFICATION, REF. DESIGN (1½ in. x 3 in.), 120 kg/hr CAPACITY (LHTGR TRISO/BISO)

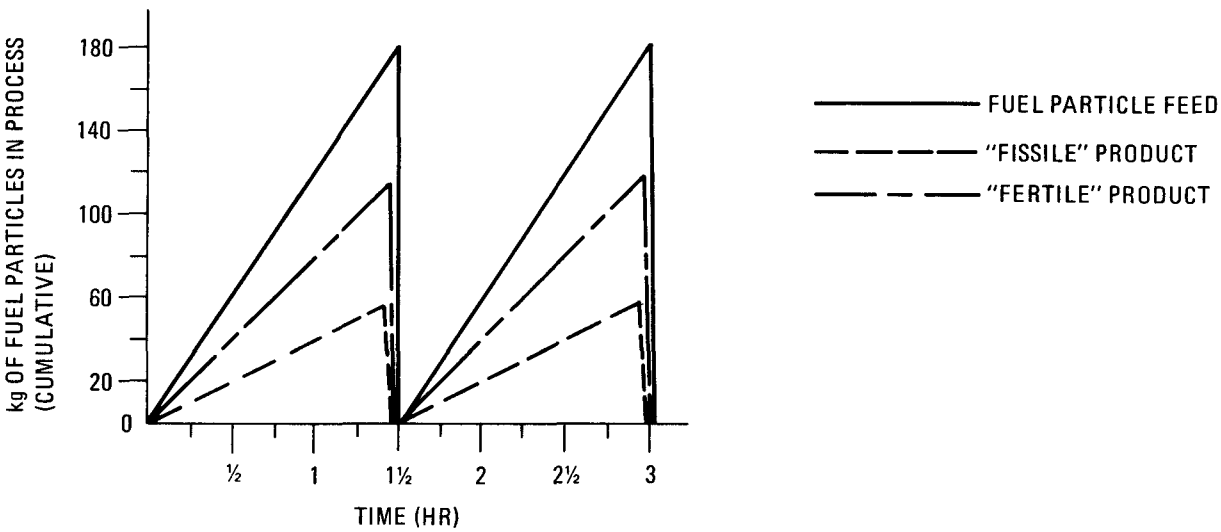

Fig. 9-2. Operating profiles for two head-end systems

During the present quarter, a number of HETP technical review meetings and working sessions were attended by the project engineers. Following the review of the initial mechanical equipment and facility arrangement drawings submitted early in December, equipment and facility interface details were identified and design problems were resolved at a working session on December 9, 1976.

A formal review by representatives from ORO, UCC-ND, ORNL, GA, and RMPCo covering the progress up to the 30% level was made at the 30% Technical Review Meeting held on January 15-16, 1977. A major action item from this meeting was to resolve the need for individual off-gas treatment systems for the primary and secondary burners.

On January 18-20, 1977, a Cost Estimating and Technical Review Meeting was held at ORNL with attendees from each of the HETP participants for the purpose of setting up the project cost estimating ground rules in accordance with ERDA requirements. In working sessions, an initial HET-Reprocessing sampling plan was developed, the HETF waste handling plans were reviewed, the dual train off-gas question was resolved in favor of a partial dual system, the GA plan for a HET-Reprocessing spent fuel feed material shipping and handling system was presented, and the spent fuel element segmenting and material concept utilizing ORNL facilities was reviewed.

The GA spent fuel handling concept for packaging and shipping FSV fuel elements from the INEL Irradiated Fuel Storage Facility was discussed with ACC staff at an INEL meeting on February 1-2, 1977. The handling method incorporating the use of a Peach Bottom spent fuel shipping cask and seal-welded single-use fuel element canister was reviewed and tentatively accepted by ACC personnel. A work scope has been prepared to initiate the ACC conceptual work and cost estimate.

9.3.2. HETE-Reprocessing Systems

The HET-Reprocessing systems and equipment have been developed from the HET Criteria Document into the conceptual design described briefly in the following sections.

9.3.2.1. Primary Burning System - 1200 (DTY, NWJ, RMB, LAO)

The primary burning system burns away graphite and exposed outer carbon coating from irradiated HTGR type fuel particles to produce uniform batches of ash and burned-back fissile-fertile particles with a minimum of particle breakage. All operations are performed in Cell E of the TURF. The primary functions are:

1. Receiving batches of crushed spent fuel elements from the fuel size reduction system (1100).

2. Feeding batches of crushed spent fuel to the primary fluidized bed burner.

3. Burning away graphite and exposed carbon from the fissile and fertile particles in a fluidized bed.

4. Removing and collecting fines and particulates from the burner off-gas.

5. Returning the material from fines collection to the fluidized bed burner for further oxidation of carbon.

6. Discharging burner ash for transfer to System 1300 for classification of the burned-back particles.

Figure 9-3 shows the major items of equipment contained in this system, including the feed hopper and feeder, the primary fluidized bed burner, and the separation and recycle units including a fines sampler.

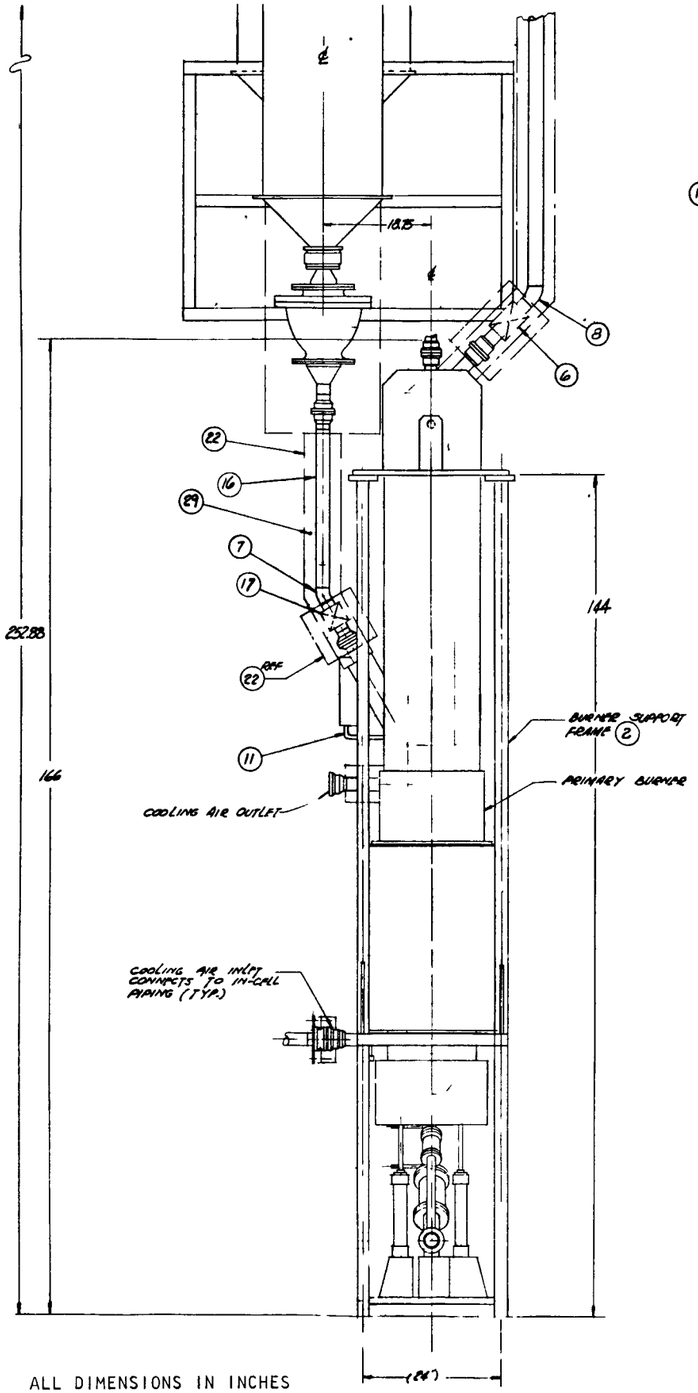

ITEM	DESCRIPTION LIST OF MATERIAL	MATL
32		
31		
30		
29	INSULATION	
28	ELECT POWER CONNECTOR	
27	TUBE JUMPER, 3/4 DIA	COPPER
26	TUBE, 3/8 DIA X 29 1/4"	COPPER
25	TUBING, 3/4 I.D	VARGLAS 30
24	TUBING 1/2 O.D. x .035 W6	COPPER
23	TUBING 1" O.D. x .028 x 24"	COPPER
22	S-SEE" .135 X 67 1/4"	304 SS
21	LEAD SHIELDING 9335#	
20	CAPACITOR	
19	WIRE #1-0	
18	TUBE, 3/4 DIA X 36"	TYGON
17	BELLOWS, 2 DIA (3 STROKE 1.5 PSIG, 1200°F)	
16	PIPE, 2" SCH 40, 6 LONG	304 SS
15	PRIMARY FEEDER HOPPER	
14	FINES RECYCLE ASSY	
13	FEED HOPPER & SUPPORT FRAME	
12	DISCONNECT PANEL PANEL	
11	TUBE 1/8 DIA	304 SS
10	ROD 1/2 DIA X 6	304 SS
9	PLATE 1/2 X 3 X 7	304 SS
8	ELBOW 2" 45°	304 SS
7	ELBOW, 2", 3)"	304 SS
6	BELLOWS (2") STROKE 1200°F	
5	PRIMARY VESSEL ASSY	(BDA-121)
4	REBUTT WELD	
3	PLATE, 1" X 11 X 29"	304 SS
2	TUBING, 4 DIA X 13	304 SS
1	ASSY	

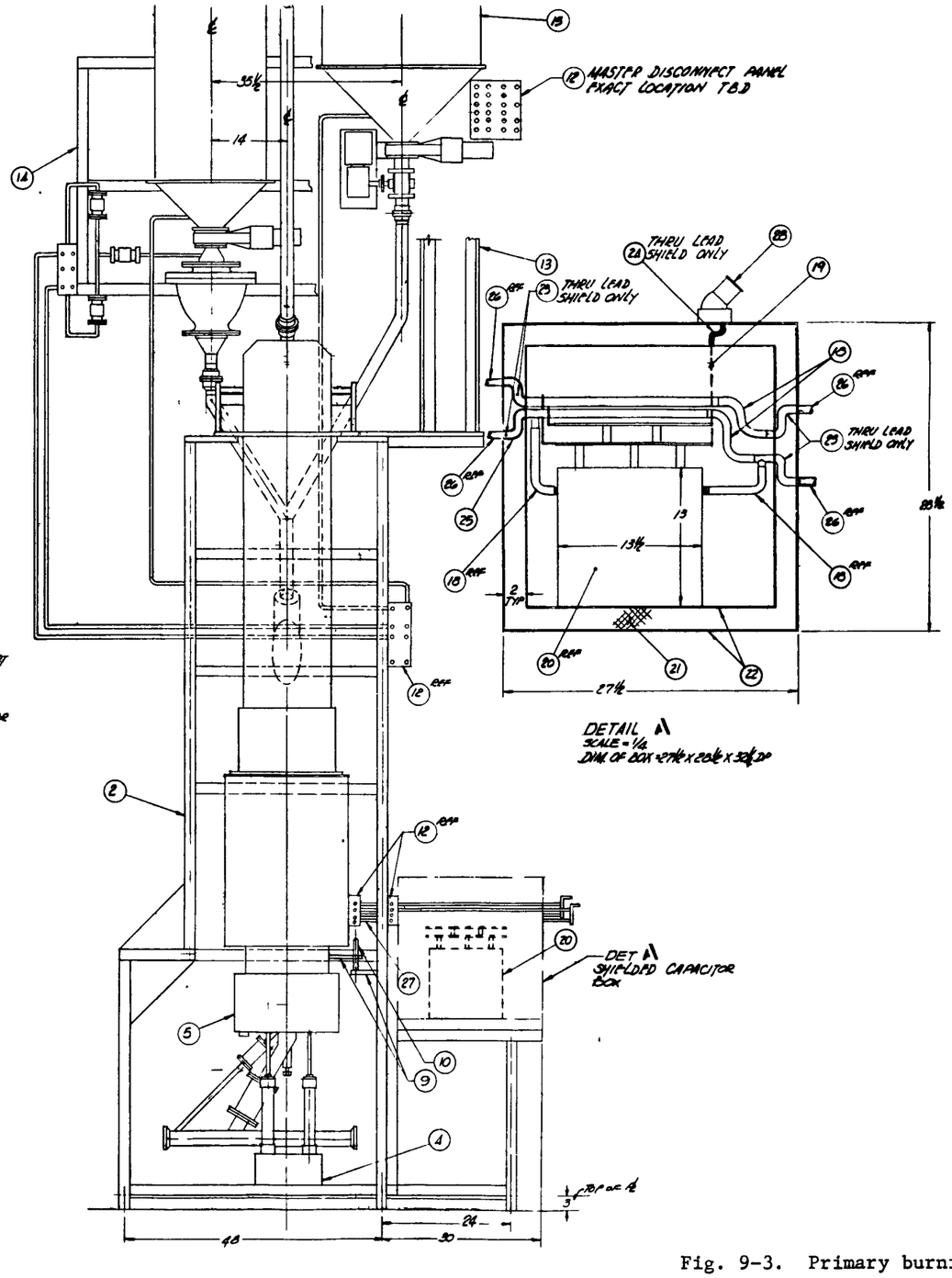

Fig. 9-3. Primary burning system general arrangement

9.3.2.2. Particle Classification and Material Handling System - 1300 (DDL, PCR, NWJ, RMB, LAO)

The Particle Classification and Material Handling System separates the burned-back batches of mixed fissile-fertile particles from primary burning into two separate fractions with minimum crossover. The material handling functions provide inter-system handling by pneumatic transport, including the receipt, weighing, and sampling of solid material for the head-end processes. All operations are performed in Cell D of the TURF. The primary functions are:

1. Receiving (from System 1100), weighing, and storing batches of crushed fuel elements in storage hoppers.

2. Transferring crushed fuel to the primary burner feed hopper.

3. Receiving batches of mixed fissile and fertile particles from the Primary Burning System (1200).

4. Feeding batches of granular fissile and fertile particles, containing some graphite and fine ash, to the classifier at a controlled rate.

5. Classifying fissile and fertile particles into two separate streams.

6. Collecting the classified fissile and fertile particle streams in receiving hoppers.

7. Transferring fertile and fissile product back to the classifier for reclassification, to the particle crushers in System 1400, or to System 1900 for canning.

8. Receiving batches of secondary burning product oxide, sampling the material, and transferring the material into product transfer cans.

9. Providing sampling capability for all solids streams.

The major items of equipment contained in this system are shown in Fig. 9-4, including the pneumatic transport systems, the central receiving weigh hopper, the crushed fuel element storage hoppers, the pneumatic zig-zag type classifier with the vibratory feeder and collection hoppers, and the in-line solids samplers.

9.3.2.3. Particle Crushing and Secondary Burning System - 1400 (JBS, WSR, NWJ, RMB, LAO)

The Particle Crushing and Secondary Burning System receives and crushes classified batches of silicon carbide coated particles, burns away the exposed carbon coating, and oxidizes the thorium and/or uranium carbide kernels. All operations are performed in Cell E of the TURF. The primary functions of this system are:

1. Receiving batches of classified (fissile or fertile) burned-back fuel particles from System 1900.

2. Feeding batches of granular spent fuel particles to the crusher.

3. Crushing the silicon carbide coated fuel particles.

4. Feeding the product from the crusher to the secondary fluidized bed burner.

5. Burning away all carbonaceous material from the broken fuel kernels in a fluidized bed and simultaneously converting the heavy metal carbides to oxides.

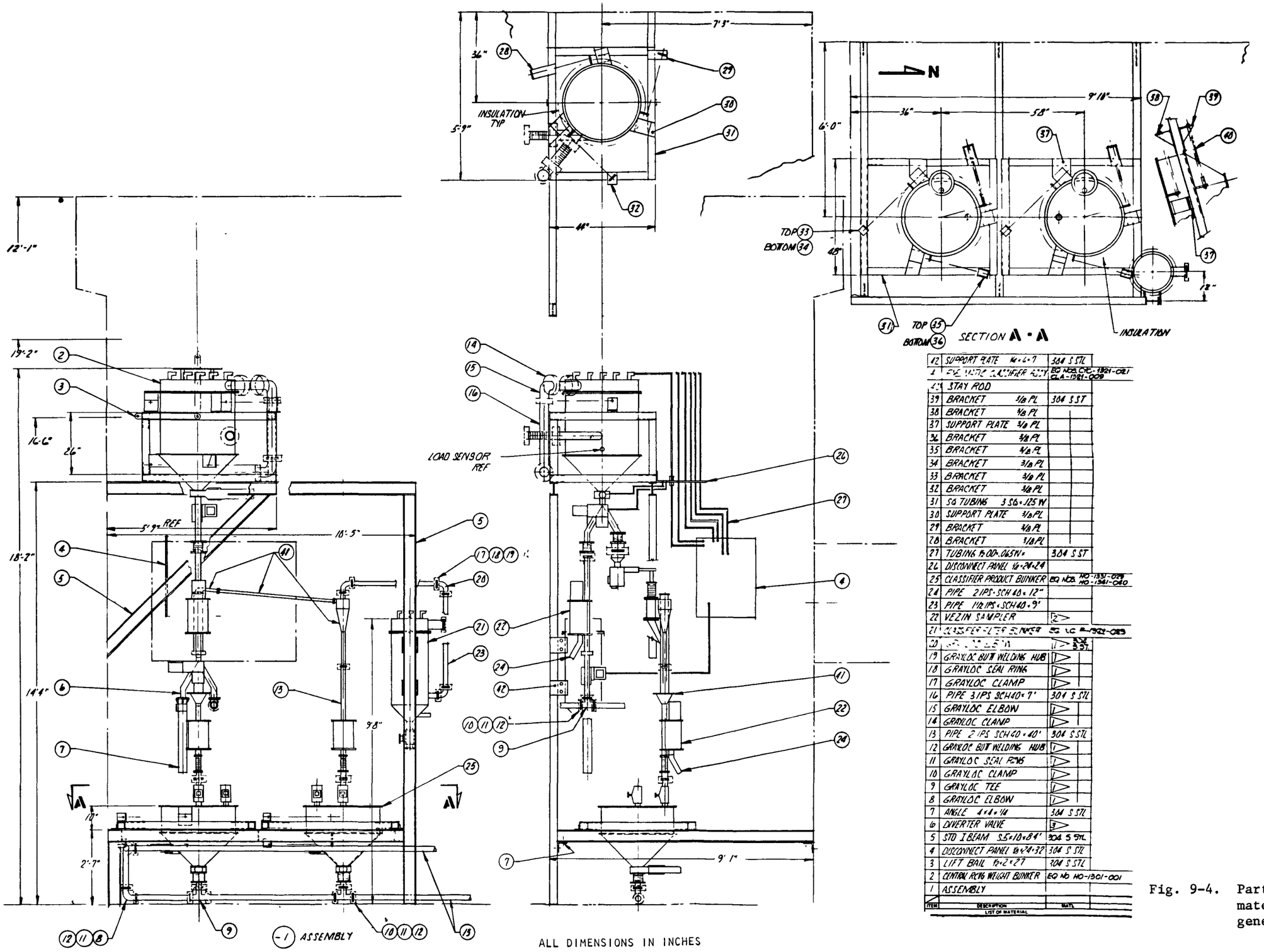

ITEM	DESCRIPTION LIST OF MATERIAL	MATL
42	SUPPORT PLATE 14×2.7	304 S STL
1	FVE HOT GAS CLASSIFIER ASSY	EQ NOS. CHE-1321-021 CLA-1321-009
41	STAY ROD	
39	BRACKET 1/8 PL	304 S ST
38	BRACKET 1/8 PL	
37	SUPPORT PLATE 1/8 PL	
36	BRACKET 1/8 PL	
35	BRACKET 1/8 PL	
34	BRACKET 1/8 PL	
33	BRACKET 1/8 PL	
32	BRACKET 1/8 PL	
31	SG TUBING 3 SG×.125 W	
30	SUPPORT PLATE 1/8 PL	
29	BRACKET 1/8 PL	
28	BRACKET 1/8 PL	
27	TUBING 1½ OD×.065 W	304 S ST
26	DISCONNECT PANEL 16×24×24	
25	CLASSIFIER PRODUCT BUNKER	EQ NOS. HO-1331-029 HO-1341-040
24	PIPE 2 IPS×SCH 40×12"	
23	PIPE 1½ IPS×SCH 40×9'	
22	VEZIN SAMPLER	2
21	CLASSIFIER FINES BUNKER	EQ NO. HO-1321-013
20		1 304 S ST
19	GRAYLOC BUTT WELDING HUB	3
18	GRAYLOC SEAL RING	3
17	GRAYLOC CLAMP	3
16	PIPE 3 IPS SCH40×7'	304 S STL
15	GRAYLOC ELBOW	3
14	GRAYLOC CLAMP	3
13	PIPE 2 IPS SCH40×40'	304 S STL
12	GRAYLOC BUTT WELDING HUB	1
11	GRAYLOC SEAL RING	3
10	GRAYLAC CLAMP	3
9	GRAYLOC TEE	1
8	GRAYLOC ELBOW	1
7	ANGLE 4×4×1/4	304 S STL
6	DIVERTER VALVE	1
5	STD I BEAM S5×10×84'	304 S STL
4	DISCONNECT PANEL 16×24×32	304 S STL
3	LIFT BAIL 12×2×27	304 S STL
2	CENTRAL RCYG WEIGHT BUNKER	EQ NO. HO-1301-001
1	ASSEMBLY	

Fig. 9-4. Particle classification and material handling system general arrangement

6. Removing particulates from the off-gas stream with in-vessel sintered metal filters.

7. Discharging burner ash for transport to System 1300.

8. Providing sampling of crushed fuel particles.

Figure 9-5 shows the major items of equipment in this system, which includes the particle roll crusher, secondary fluidized bed burner, and feed sampler.

9.3.2.4. Dissolution and Feed Adjustment System - 1500 (GEB, NWJ, LAO)

The Dissolution and Feed Adjustment System receives the oxide product from the secondary burner, dissolves the heavy-metal-bearing solids into an aqueous solution, separates and dries the insols, and adjusts the solution to conditions required for the solvent extraction feed. All operations are performed in Cell G of the TURF. The primary functions are:

1. Receiving solids from System 1400 via System 1900, Solid Product Handling.

2. Dissolving the contained heavy metals.

3. Separating the solutions from the insols.

4. Washing and rinsing the insols, with the solution joining the solution from dissolution.

5. Adjusting the combined solutions to the required solvent extraction feed conditions.

6. Drying the separated insols.

7. Placing the dried insols into transfer cans for handling by System 1900, Solid Waste and Scrap Disposal.

The major items of equipment contained in this system include the dissolver, the centrifuge, the insols dryer, the dissolver solution sample tank, the feed adjustment hold tank, the feed concentrator and feed concentrator product tank, and the 1AF feed storage tank. The design concepts for the dissolver and the insols dryer are shown in Figs. 9-6 and 9-7. Figure 9-8 shows the conceptual design for the solution sample tank, the feed adjustment hold tank, and the feed adjustment product tank. The feed concentrator and the storage tanks for the 1A solvent extraction column are shown in Figs. 9-9 and 9-10.

9.3.2.5. Solvent Extraction System - 1600 (GEB, NWJ, LAO)

The Solvent Extraction System receives the adjusted aqueous feed from System 1500 and, using the Acid-Thorex process, recovers, partially purifies, and separates the thorium, uranium, contained fission products, and chemical impurities. All operations are performed in Cell G of the TURF. The primary functions are:

1. Co-extracting uranium and thorium from the fission products and contaminants in the feed solution.

2. Partitioning uranium and thorium by selectively returning the thorium to the aqueous phase.

3. Stripping the uranium into the aqueous phase for storage or further processing.

4. Providing for solvent cleanup for recycle.

5. Providing for flowing stream samples of process streams.

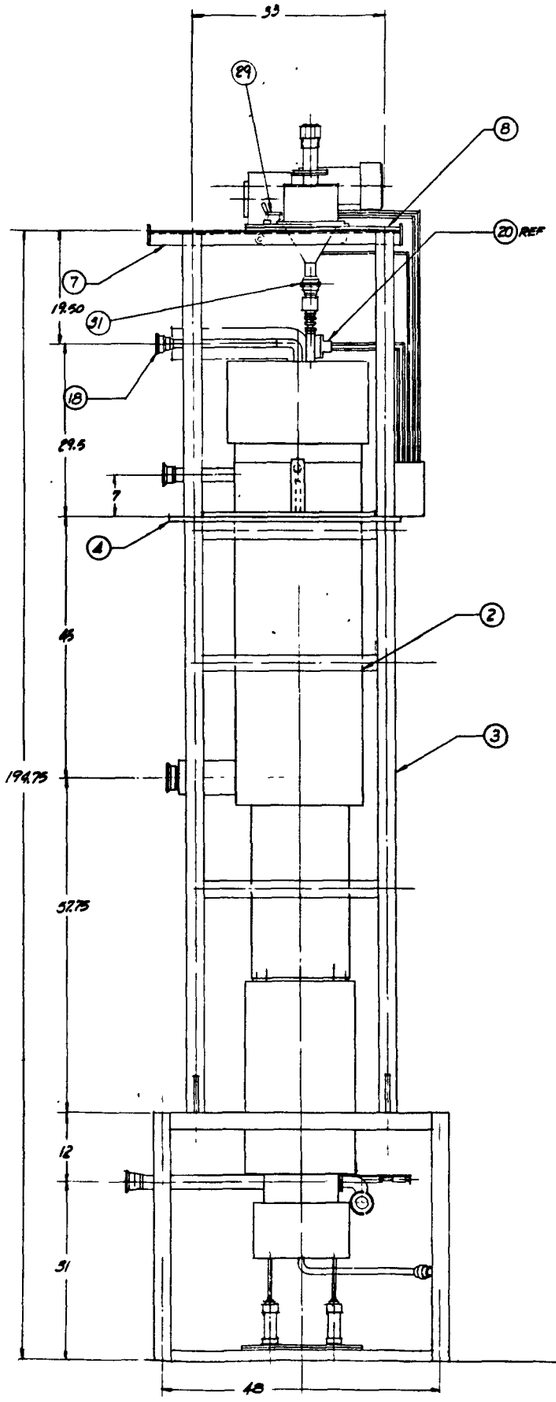

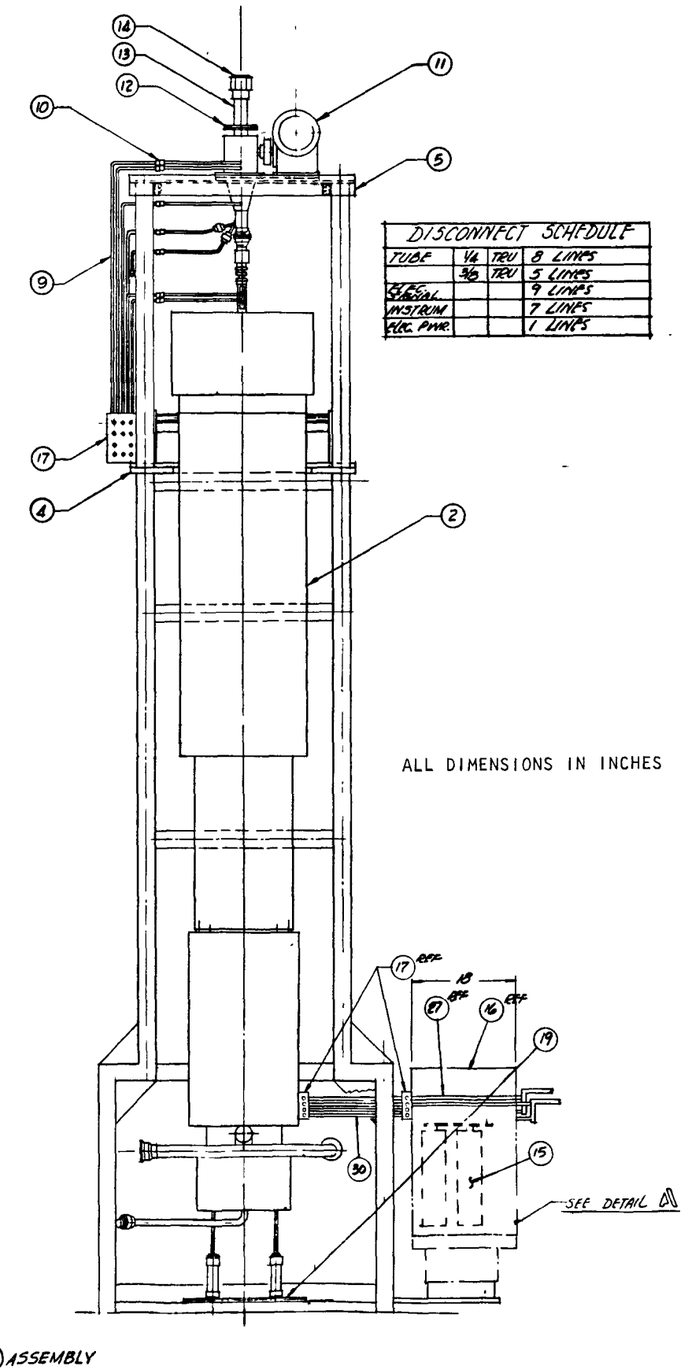

DISCONNECT SCHEDULE			
TUBE	1/4	TRU	8 LINES
	3/8	TRU	5 LINES
SPECIAL			9 LINES
INSTRUM			7 LINES
ELEC. PWR.			1 LINES

ALL DIMENSIONS IN INCHES

(-1) ASSEMBLY

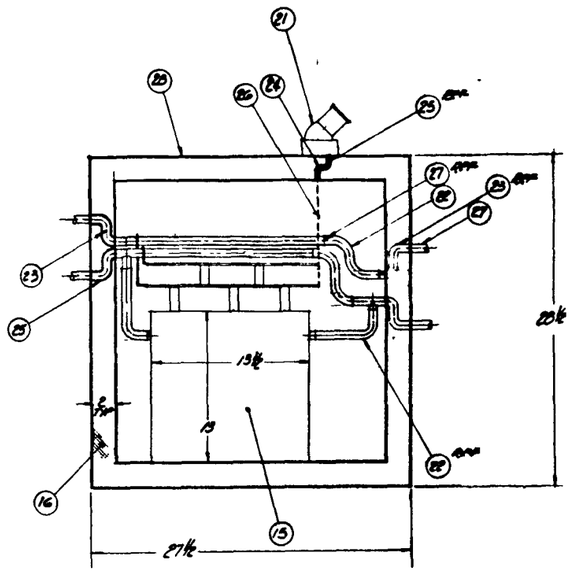

DETAIL A
SCALE 1/4

ITEM	DESCRIPTION	MATL
31	HUB	304 SS
30	TUBE, JUMPER 3/8 DIA.	COPPER
29	TOGGLE HOLD DOWN	304 SS
28	SHAFT, .135 X 52 LG	304 SS
27	TUBE, COPPER, 3/8 X 12 1/2	COPPER
26	WIRE, #1-0	
25	TUBING, 3/4 I.D	VARGLAS
24	TUBING, 1/4 OD X .035 X 6"	304 SS
23	TUBING, 1 OD X .028 X 8"	304 SS
22	TUBING, 3/4 X 36" LG	TYGON
21	[illegible]	
20	VIBROLATOR	
19	REMOTE CART ASSY	
18	DISCONNECT	304 SS
17	DISCONNECT BACK PANEL	
16	LEAD SHIELDING (6762)	
15	CAPACITOR BANK	
14	DISCONNECT	
13	PIPE, 2 SCH 40 X 3	304 SS
12	FLANGE, 6 DIA X 3/4	304 SS
11	PARTICLE CRUSHER (280-1811-001 280-1812-001)	
10	DISCONNECT (SEE SCHEDULE)	
9	TUBE 1/4 O.D. 30 LN FT	304 SS
8	PLATE 18 X 26 3/4 X 1/2	304 SS
7	ANGLE 13 1/2 X 13 - 3/4 X 43"	304 SS
6	PLATE 39 X 43 X 1/2	304 SS
5	PLATE 13 3/4 X 19 1/2 X 1/2"	304 SS
4	PLATE 3 3/4 X 23 X 3/4"	304 SS
3	TUBING 4 X 4 X .125 [illegible]	304 SS
2	VESSEL ASSY SEE B-21	[illegible]
1	ASSEMBLY	

LIST OF MATERIAL

Fig. 9-5. Particle crushing and secondary burning system general arrangement

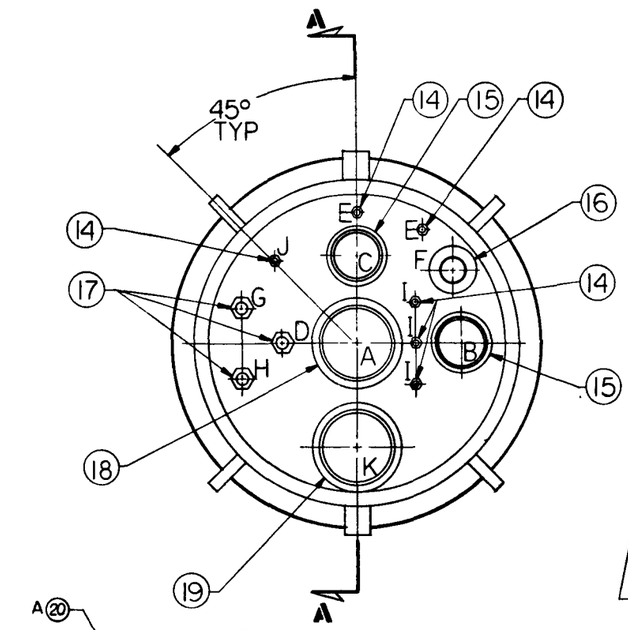

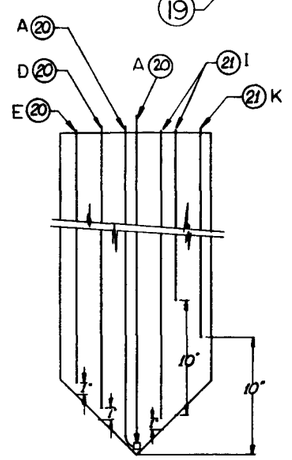

VESSEL INTERNAL TUBING AS SHOWN

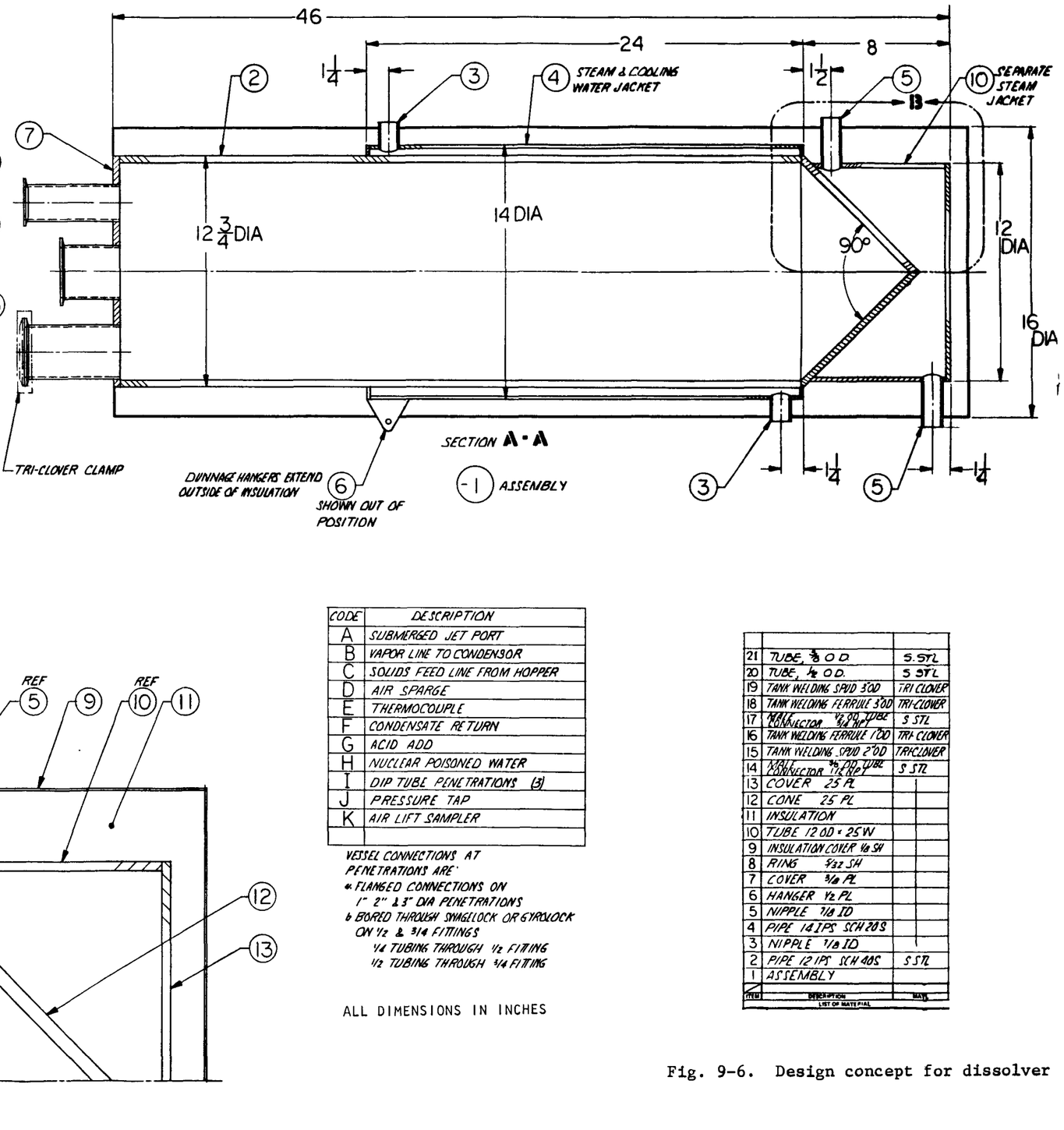

CODE	DESCRIPTION
A	SUBMERGED JET PORT
B	VAPOR LINE TO CONDENSOR
C	SOLIDS FEED LINE FROM HOPPER
D	AIR SPARGE
E	THERMOCOUPLE
F	CONDENSATE RETURN
G	ACID ADD
H	NUCLEAR POISONED WATER
I	DIP TUBE PENETRATIONS (3)
J	PRESSURE TAP
K	AIR LIFT SAMPLER

VESSEL CONNECTIONS AT PENETRATIONS ARE:
a. FLANGED CONNECTIONS ON 1" 2" & 3" DIA PENETRATIONS
b. BORED THROUGH SWAGELOCK OR GYROLOCK ON 1/2 & 3/4 FITTINGS
1/4 TUBING THROUGH 1/2 FITTING
1/2 TUBING THROUGH 3/4 FITTING

ALL DIMENSIONS IN INCHES

ITEM	DESCRIPTION LIST OF MATERIAL	MATL
21	TUBE, 3/8 O.D.	S.STL
20	TUBE, 1/2 O.D.	S STL
19	TANK WELDING SPUD 3"OD	TRI CLOVER
18	TANK WELDING FERRULE 3"OD	TRI-CLOVER
17	MALE CONNECTOR 1/2 OD TUBE 3/4 NPT	S STL
16	TANK WELDING FERRULE 1"OD	TRI-CLOVER
15	TANK WELDING SPUD 2"OD	TRI-CLOVER
14	MALE CONNECTOR 3/8 OD TUBE 1/4 NPT	S STL
13	COVER 25 PL	
12	CONE 25 PL	
11	INSULATION	
10	TUBE 12 OD x 25 W	
9	INSULATION COVER 1/8 SH	
8	RING 3/32 SH	
7	COVER 3/16 PL	
6	HANGER 1/2 PL	
5	NIPPLE 1/8 ID	
4	PIPE 14 IPS SCH 20S	
3	NIPPLE 1/8 ID	
2	PIPE 12 IPS SCH 40S	S STL
1	ASSEMBLY	

Fig. 9-6. Design concept for dissolver

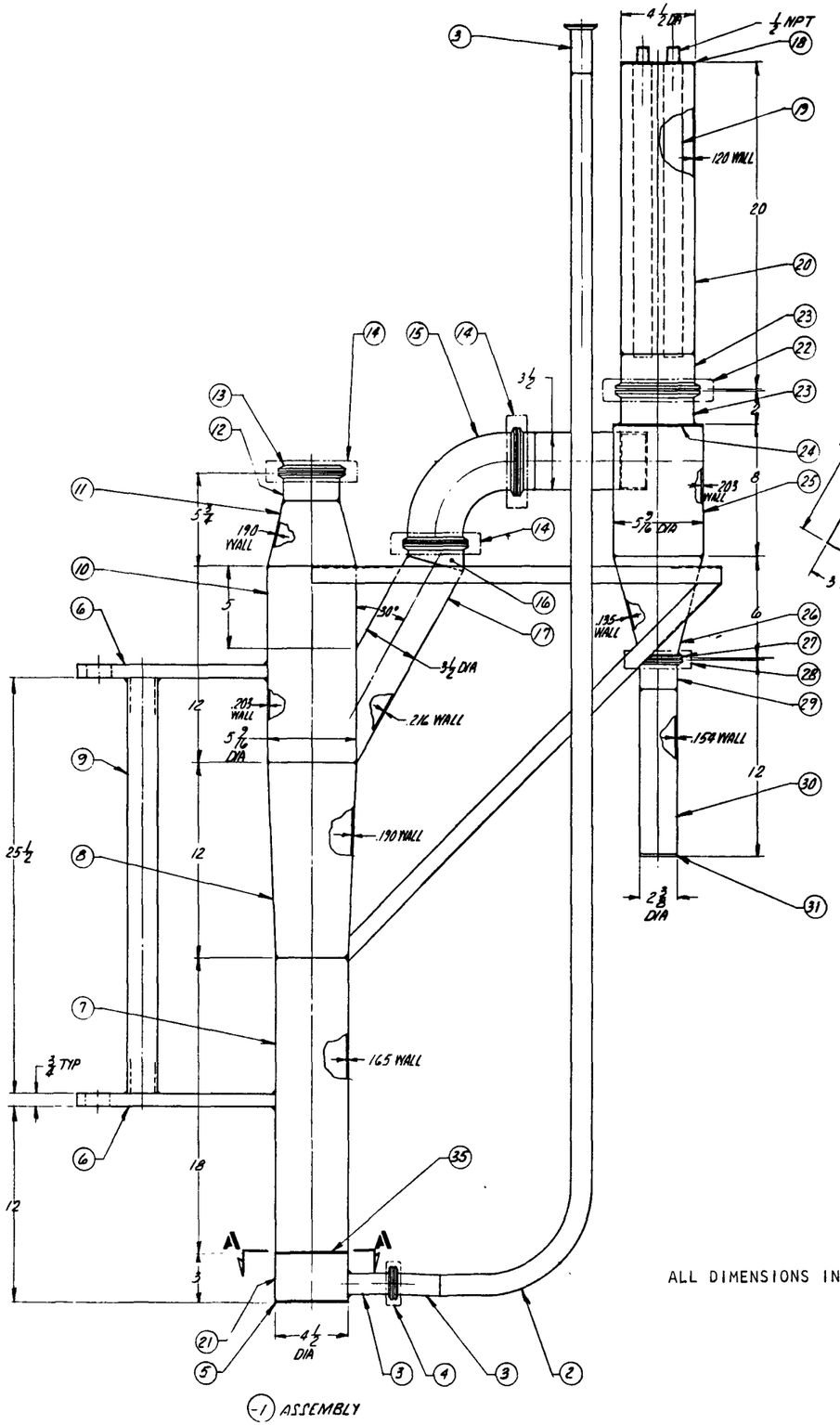

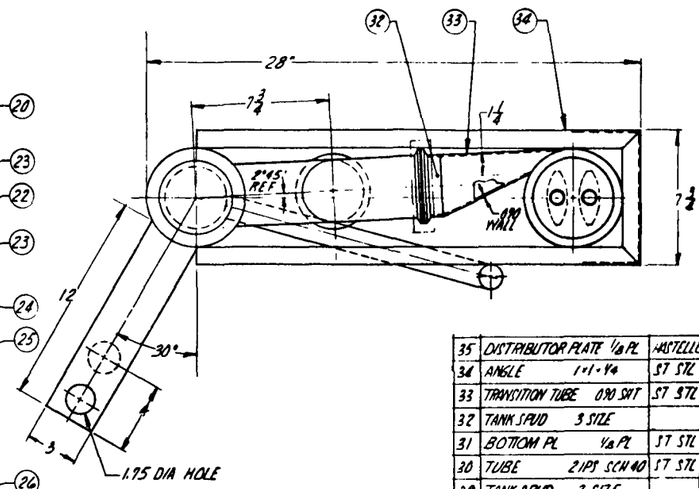

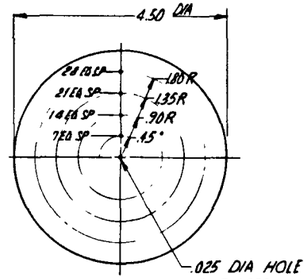

SECTION A-A

35 DISTRIBUTOR PLATE
SCALE: 1

ALL DIMENSIONS IN INCHES

ITEM	DESCRIPTION LIST OF MATERIAL	MATL
35	DISTRIBUTOR PLATE 1/8 PL	HASTELLOY X
34	ANGLE 1×1×¼	ST STL
33	TRANSITION TUBE .090 SHT	ST STL
32	TANK SPUD 3 SIZE	
31	BOTTOM PL ½ PL	ST STL
30	TUBE 2 IPS SCH 40	ST STL
29	TANK SPUD 2 SIZE	
28	CLAMP 2 SIZE	
27	CAP 2 SIZE	
26	CONE .135 SHT	
25	PIPE 5 IPS SCH 10	
24	PLATE ⅛ PL	
23	TANK SPUD 4 SIZE	
22	CLAMP 4 SIZE	
21	PIPE 4 IPS SCH 20	ST STL
20	PIPE 4 IPS SCH 10	
19	FILTER 5 MICRON	
18	COVER ⅛ PL	
17	PIPE 3 IPS SCH 40	
16	TANK SPUD	
15	ELBOW 3 SIZE	
14	CLAMP 3 SIZE	
13	CAP 3 SIZE	
12	TANK SPUD 3 SIZE	
11	CONE .190 SH	
10	PIPE 5 IPS SCH 20	
9	PIPE 14½ IPS SCH 40	
8	CONE SHT	
7	PIPE 4 IPS SCH 20	
6	BRACKET ¾ BAR	
5	BOTTOM COVER ⅛ PL	
4	CLAMP 1 SIZE	
3	FERRULE 1 SIZE	
2	PIPE 1 IPS SCH 40	ST STL
1	ASSEMBLY	

Fig. 9-7. Design concept for insols dryer

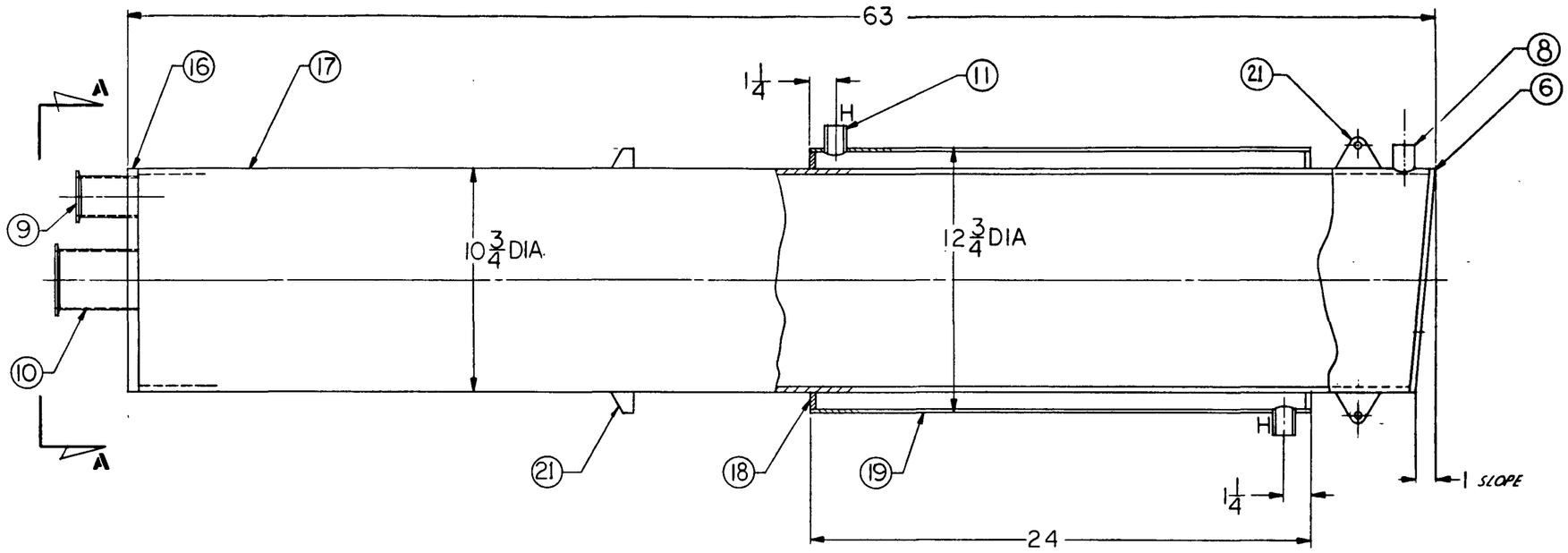

(-1) TK-1531-006 DISSOLVER SOLUTION SAMPLE TANK (-4) TK-1621-074 10 W TANK

(-2) TK-1531-008 FEED ADJUSTMENT HOLD TANK (-5) TK-1621-003 TAX TANK

(-3) TK-1531-031 FEED ADJUSTMENT PRODUCT TANK

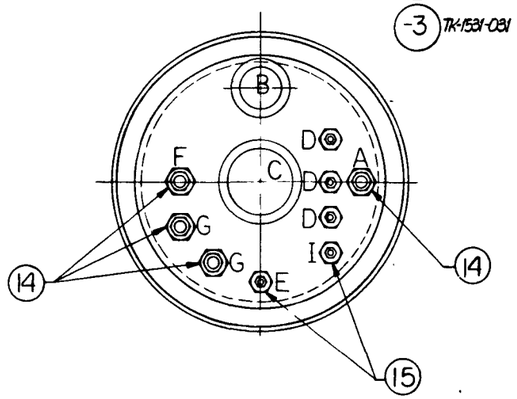

VIEW A-A

CODE	ITEM NO.	LINE DESCRIPTION
A	14	JET OUT SUCTION LEG
B	9	VESSEL VENT
C	10	AIR LIFT SAMPLER
D	15	DIP TUBE PENETRATIONS (5)
E	15	THERMO WELL
F	14	FILL LINE
G	14	CHEM ADD
H	11	COOLING WATER
I	15	AIR SPARGE

VESSEL CONNECTIONS AT PENETRATION ARE:
a) FLANGED CONNECTIONS ON 2 & 3 DIA PENETRATIONS
b BORED THROUGH SWAGELOCK OR GYROLOCK
ON 1/2 & 3/4 NPT FITTINGS
1/4 DIA TUBING THROUGH 1/2 NPT
1/2 DIA TUBING THROUGH 3/4 NPT

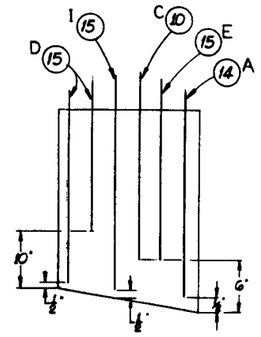

ALL DIMENSIONS IN INCHES

ITEM	DESCRIPTION	MATL
	LIST OF MATERIAL	
21	HANGER 1/2 PL	SST
20	MALE CONNECTOR 3/4"	
19	PIPE 12 IPS SCH 20S	
18	END PLATE 1/2 PL	
17	PIPE IPS SCH 20S	
16	TOP PLATE 1/2 PL	
15	MALE CONNECTOR 1/4 OD TUBE - 1/2 NPT	
14	MALE CONNECTOR 1/2 OD TUBE - 3/4 NPT	
13		
12		
11	NIPPLE 1/8 ID	
10	TANK WELDING SPUD 3 DIA	
9	TANK WELDING SPUD 2 DIA	
8		
7		
6	BOTTOM PLATE 1/2 PL	SST
5	ASSEMBLY	
4	ASSEMBLY	
3	ASSEMBLY	
2	ASSEMBLY	
1	ASSEMBLY	

Fig. 9-8. Design concept for solution sample tank, feed adjustment hold tank, and feed adjustment product tank

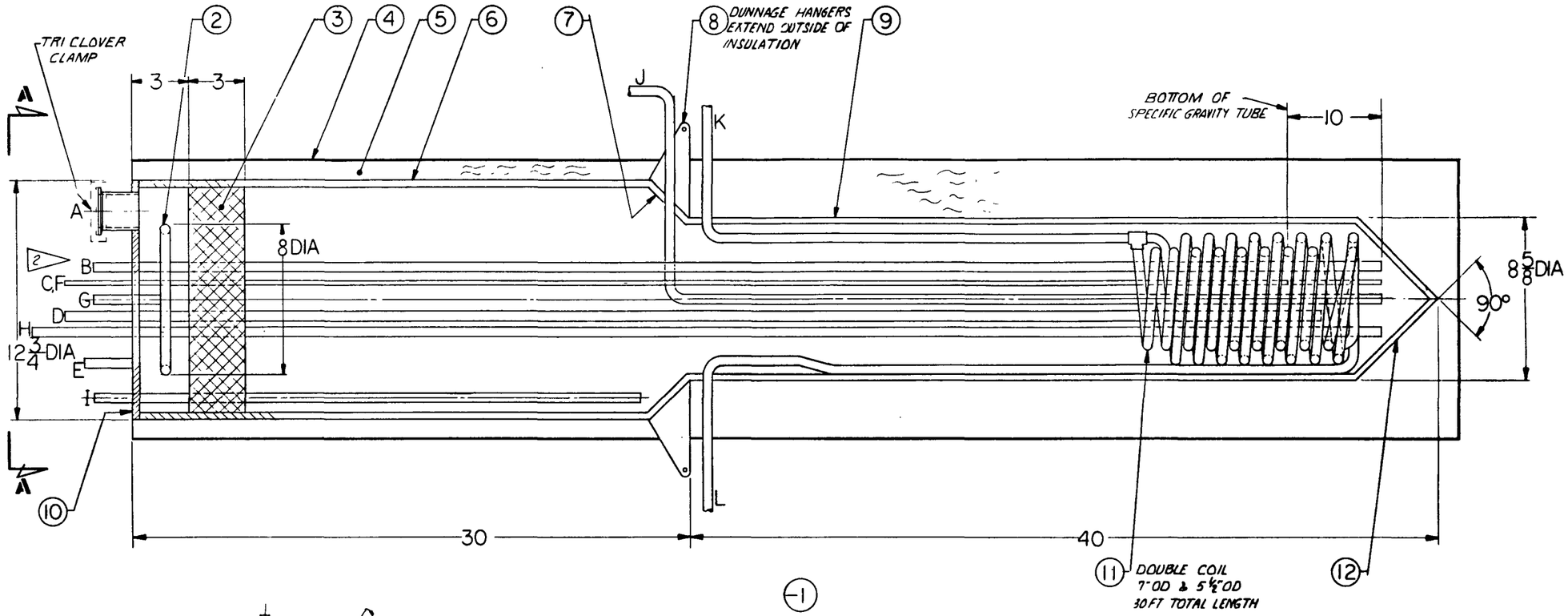

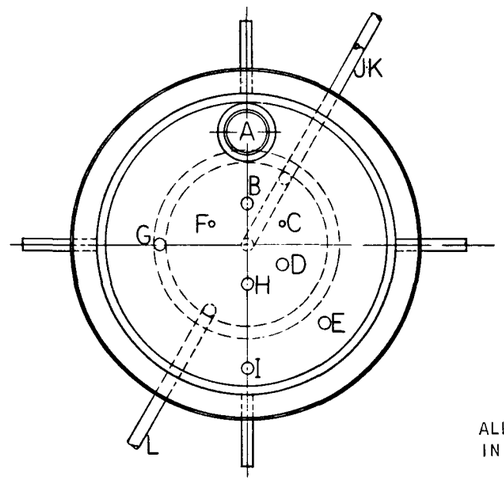

VIEW A-A

ALL DIMENSIONS IN INCHES

CODE	ITEM NO	DESCRIPTION
A	13	VAPOR LINE
B	14	STEAM SPARGE
C	15	SPECIFIC GRAVITY
D	14	THERMOCOUPLE WELL
E	14	THERMOCOUPLE WELL
F	15	WEIGHT FACTOR
G	14	SPRAY RING INLET
H		AIR SPARGE
I		SOLUTION ADD
J		JET SUCTION LEG
K		STEAM & COOLING OUT
L	14	STEAM & COOLING IN

ITEM	DESCRIPTION	MATL
15	TUBE 1/4 OD x .035 W	ST STL
14	TUBE 1/2 OD x .065 W	ST STL
13	TANK WELDING FERRULE 2"	
12	CONE 3/16 PL	
11	TUBE 1/2 OD x .065 W	
10	COVER 3/16 PL	
9	PIPE 8 IPS SCH 40S	
8	HANGER 1/2 PL	
7	CONE 3/16 PL	
6	PIPE 12 IPS SCH 40S	
5	INSULATION	
4	INSULATION COVER 16 GA SH	ST STL
3	DEMISTER PAD	
2	SPRAY RING TUBE 1/2 @ .065 W	ST STL
1	ASSEMBLY	

LIST OF MATERIAL

Fig. 9-9. Design concept for feed concentrator

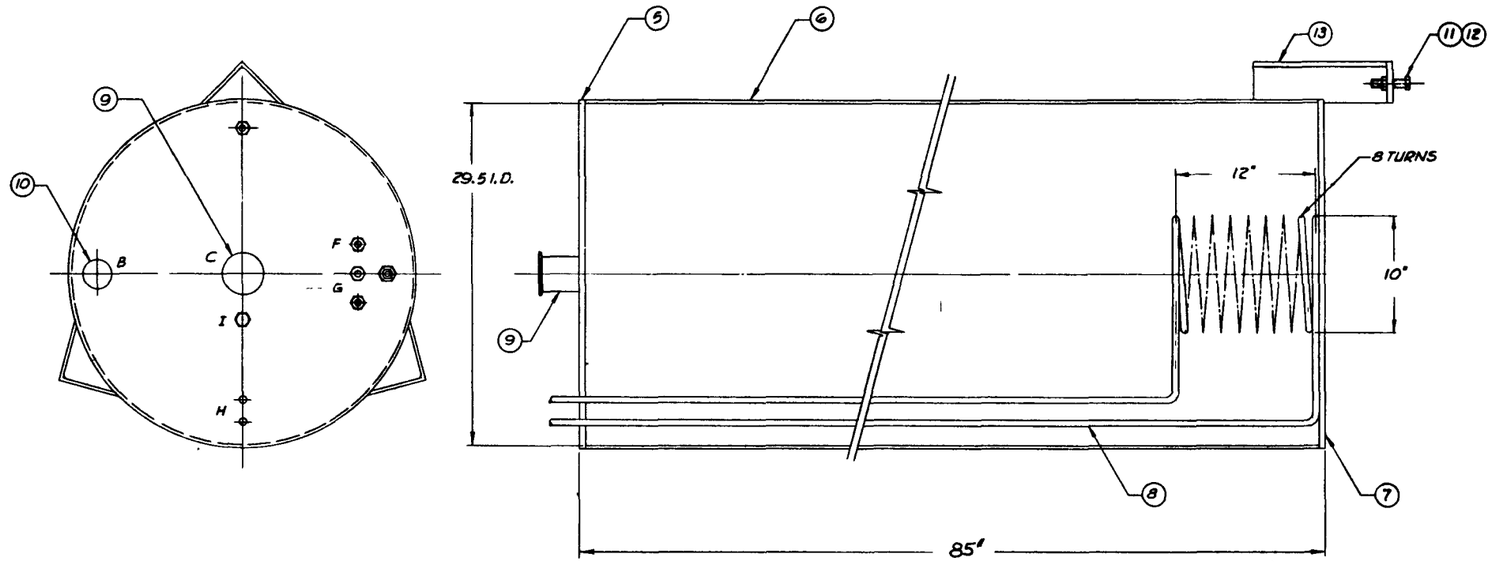

CODE	ITEM NO.	LINE DESCRIPTION
A		EMPTY SUCTION LEG
B	10	VESSEL VENT
C	9	AIR LIFT SAMPLER
D		DIP TUBE PENETRATIONS
E		THERMO WELL
F		FILL LINE
G		CHEM ADD
H	8	COOLING COIL
I		AIR SPARGE

(-1) TH-1601-4
(-2) TH-1611-2
(-3) TH-1601-3
(-4) TH-1531-4

ALL DIMENSIONS IN INCHES

ITEM	DESCRIPTION	MATL
	LIST OF MATERIAL	
15	MALE CONNECTOR 1/4 O.D. TUBE 1/2 NPT	SST
14	MALE CONNECTOR 1/2 O.D. TUBE 3/4 NPT	
13	ANGLE	
12	HEX. NUT	
11	HEX. HD. BOLT	
10	TANK WELDING SPUD	
9	TANK WELDING SPUD	
8	COOLING COIL	
7	BOTTOM PLATE	
6	PIPE 30" SCH 5S	
5	TOP PLATE	
4	ASSEMBLY	
3	ASSEMBLY	
2	ASSEMBLY	
1	ASSEMBLY	

Fig. 9-10. Design concept for feed adjustment product storage tank

The major items of equipment in System 1600 include:

1. The 1A extraction column shown in Fig. 9-11.

2. The 1BX and 1C partition columns shown in Fig. 9-12.

3. The 1BS partition scrub column shown in Fig. 9-13.

4. The 10 solvent wash column shown in Fig. 9-14.

5. The 1A feed storage tank and the 1B solvent tank shown in Fig. 9-15.

6. The storage tanks for the 1A column feed, 1A waste stream, and 1B thorium stream shown in Fig. 9-16.

7. The column drain tank and 10 organic storage tank shown in Fig. 9-17.

9.4. HRDF REMOTE MAINTENANCE

9.4.1. Introduction

During the quarter a study was initiated with the objective of establishing overall systems descriptions and design criteria for an integrated remote maintenance system for the HRDF-Reprocessing Head-End and Solvent Extraction Systems.

Activities were directed toward specific definition of the task work scope. This effort encompassed preparation of a work plan which identified the task objectives, outlined the technical approach to be followed, and established reporting milestones.

Additional activities included preparation of a report outline covering the reprocessing head-end systems and performance of a literature search covering previous maintenance experience.

9.4.2. Activity

The work plan developed for this task has established the following objectives:

1. In conjunction with separate maintainability, reliability, and availability studies, establish overall plant remote maintenance requirements and philosophies.

2. Identify interface parameters required to establish prototypical equipment configurations and facility arrangements compatible with process equipment remote maintenance techniques.

3. Establish requirements for integrated remote maintenance plant support equipment and facilities, including in-plant handling of failed equipment and preparation for disposal.

In order to accomplish these objectives, the technical approach to be taken will include a comprehensive study of previous maintenance work with particular attention given to techniques which have proven successful. These will be studied to determine their suitability for the various HRDF maintenance programs. In addition, studies will be made to determine the current state of development for maintenance equipment and techniques to determine if advanced technology in this area has application to HRDF maintenance programs. In addition, process equipment design concepts and facility arrangements will be studied in conjunction with availability, maintainability, and reliability data to establish optimum equipment and facility maintenance interface criteria. These studies will include identification of recommended maintenance development programs which will be required to establish final design criteria.

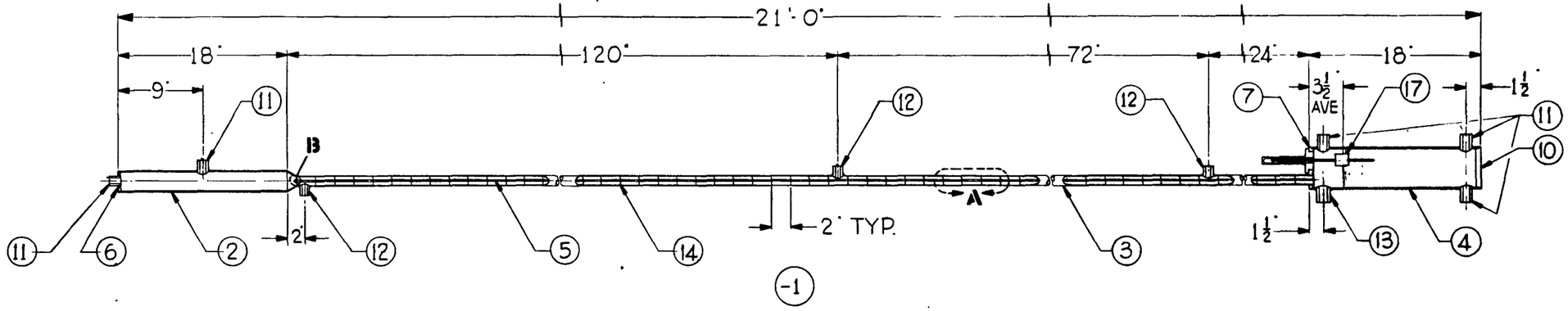

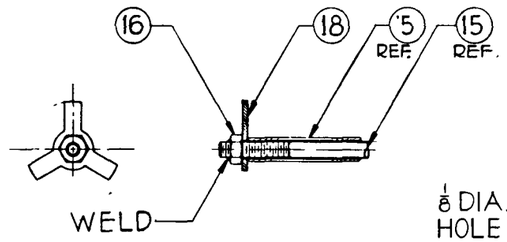

VIEW - B
SCALE 2×1

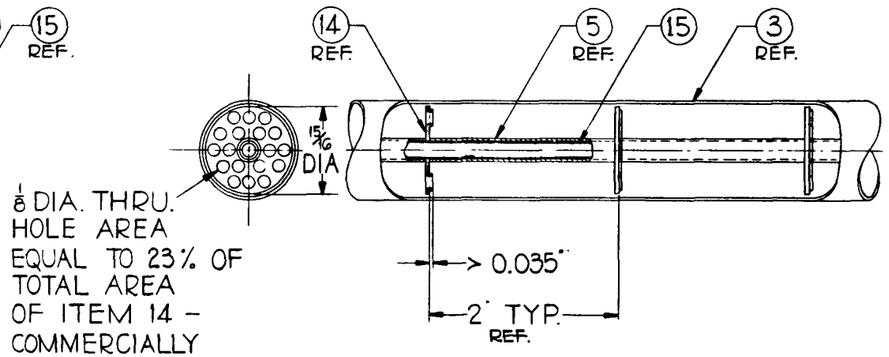

VIEW - A
SCALE 2×1

ALL DIMENSIONS IN INCHES

ITEM	DESCRIPTION	MATL
	LIST OF MATERIAL	
18	STAR PL $\frac{3}{16}$ DIA × $\frac{1}{16}$ THK	ST. ST.
17	FLOAT	
16	*8-32 HEX NUT	ST ST.
15	TIE ROD - $\frac{3}{16}$ DIA × 18" Lg	ST ST.
14	PLATE - $\frac{15}{16}$ DIA × $\frac{1}{16}$ TK.	
13	NIPPLE - $1\frac{1}{16}$" I.D.	
12	NIPPLE - $\frac{7}{8}$" I.D.	
11	NIPPLE - $\frac{3}{8}$" I.D.	
10	PLUG - $4\frac{1}{2}$ DIA × $\frac{1}{2}$ TK.	
9		
8		
7	PLUG - $4\frac{1}{2}$ DIA × $\frac{1}{2}$ TK	
6	PLUG - $2\frac{1}{8}$ DIA × $\frac{1}{4}$ TK.	
5	TUBE - $\frac{1}{4}^{OD}$ × .028 W × 2' LG	
4	TUBE - $4\frac{1}{4}^{OD}$ × .120 W × 18' LG	
3	TUBE - $1\frac{1}{4}^{OD}$ × .125 W × 18' LG ST. ST.	
2	TUBE - $2\frac{1}{4}^{OD}$ × .125 W × 18' LG ST. ST.	
1	ASSEMBLY	

Fig. 9-11. Design concept for 1A extraction scrub column

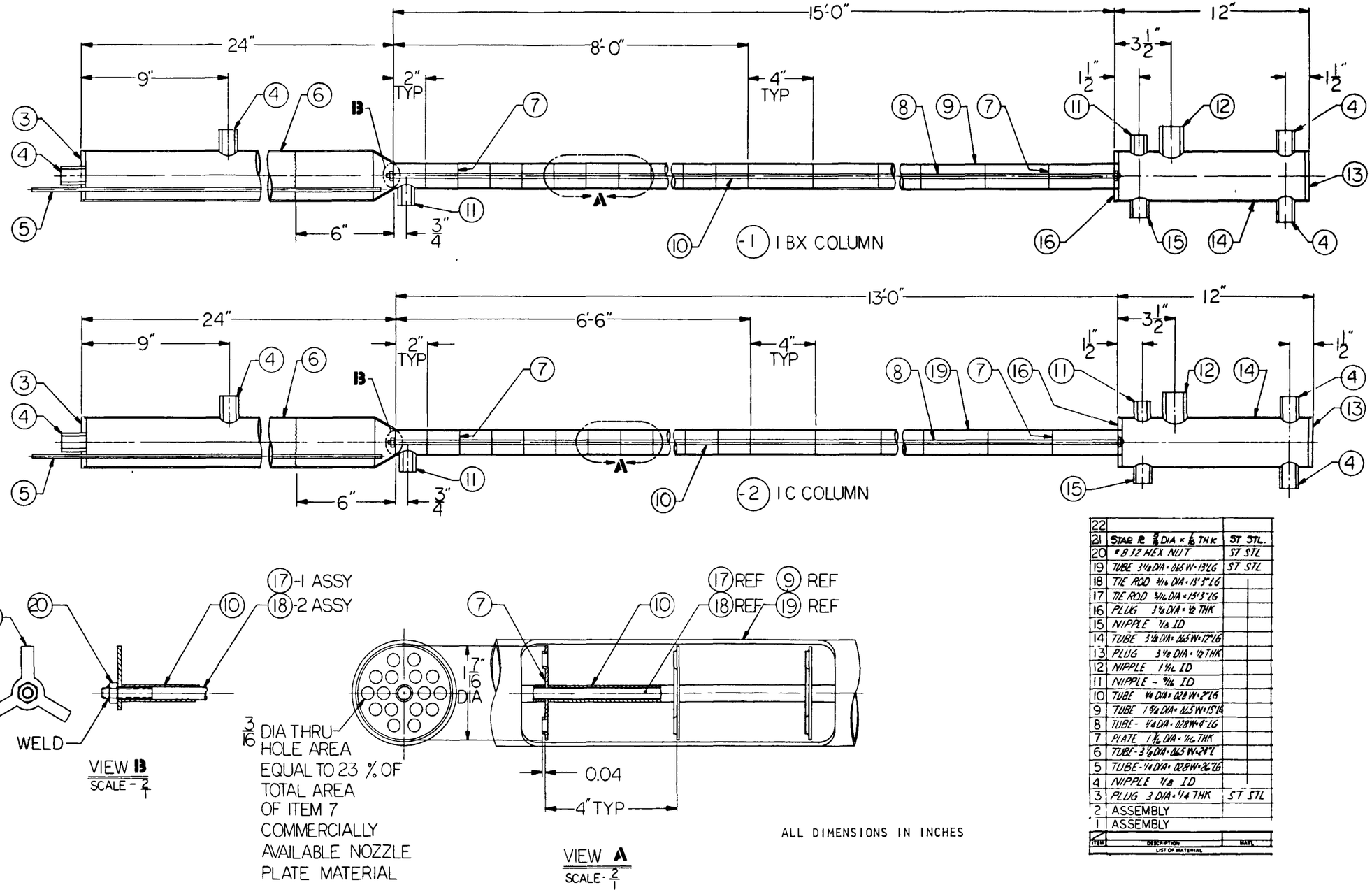

ITEM	DESCRIPTION	MATL
	LIST OF MATERIAL	
22		
21	STAR R ⅜ DIA × 1/16 THK	ST STL.
20	#8 32 HEX NUT	ST STL
19	TUBE 3½ DIA · 065 W · 13"LG	ST STL
18	TIE ROD ⅜ DIA · 13'3"LG	
17	TIE ROD ⅜ DIA · 15'3"LG	
16	PLUG 3½ DIA · ½ THK	
15	NIPPLE 1½ ID	
14	TUBE 3½ DIA · 065 W · 12"LG	
13	PLUG 3½ DIA · ½ THK	
12	NIPPLE 1½ ID	
11	NIPPLE - ¾ ID	
10	TUBE ¼ DIA · 028 W · 2"LG	
9	TUBE 1⅝ DIA · 065 W · 15"LG	
8	TUBE - ¼ DIA · 028 W · 6"LG	
7	PLATE 1⅜ DIA · 1½ THK	
6	TUBE - 3⅛ DIA · 065 W · 24"L	
5	TUBE - ¼ DIA · 028 W · 26"LG	
4	NIPPLE ½ ID	
3	PLUG 3 DIA · ¼ THK	ST STL
2	ASSEMBLY	
1	ASSEMBLY	

Fig. 9-12. Design concept for 1BX and 1C partition strip columns

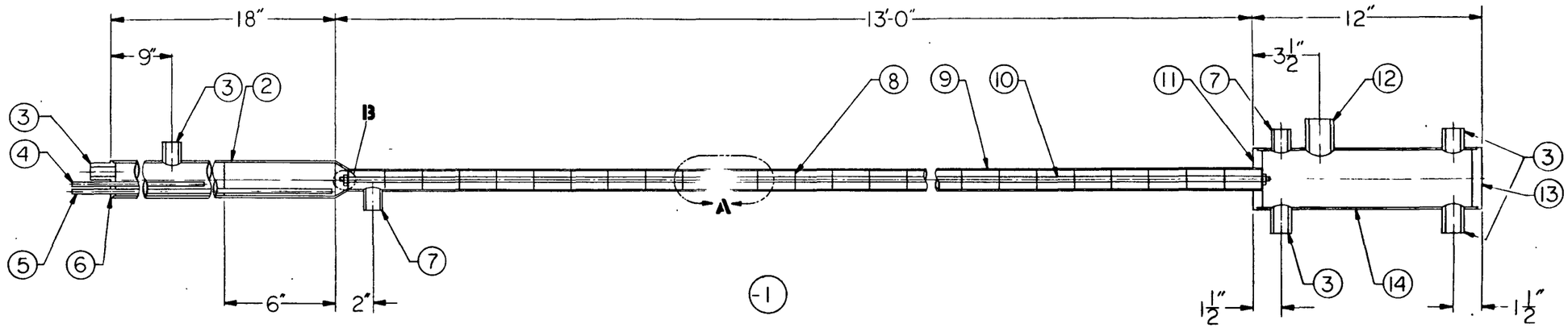

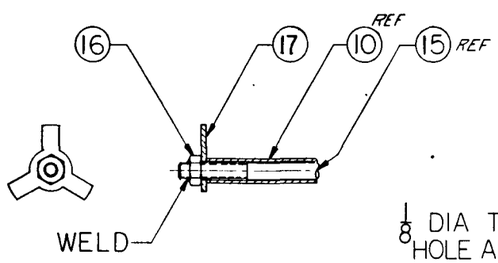

VIEW B
SCALE 2×1

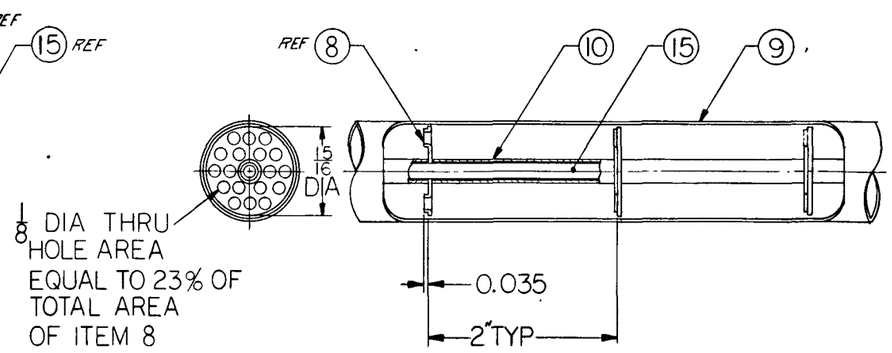

VIEW A
SCALE 2×1

ITEM	DESCRIPTION LIST OF MATERIAL	MATL
17	STAR PL 15/16 DIA × 1/16 THK	ST STL.
16	#8 32 HEX NUT	ST STL
15	TIE ROD 3/16 DIA × 13"	
14	TUBE 3/16 OD × 1/8 WALL × 12	
13	PLUG 3/16 DIA × 1/2 THK	
12	NIPPLE 1/16 ID	
11	PLUG 3/16 DIA × 1/2 THK	
10	TUBE 1/4 OD × .028 WALL × 2	
9	TUBE 1/4 OD × 1/16 WALL × 13"	
8	PLATE 15/16 DIA × 1/16	
7	NIPPLE 3/16 ID	
6	PLUG 2/16 DIA × 1/4 THK	
5	TUBE 1/8 OD × .028 WALL × 20"	
4	TUBE 1/8 OD × .028 WALL × 10"	
3	NIPPLE 1/8 ID	
2	TUBE 2 1/4 OD × .125 WALL × 18"	ST STL
1	ASSEMBLY	

ALL DIMENSIONS IN INCHES

Fig. 9-13. Design concept for 1BS partition scrub column

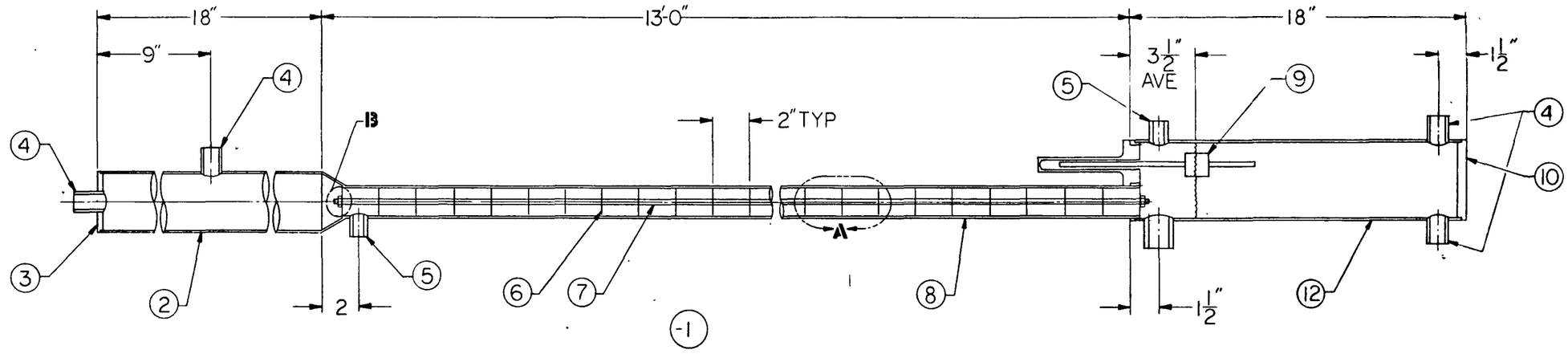

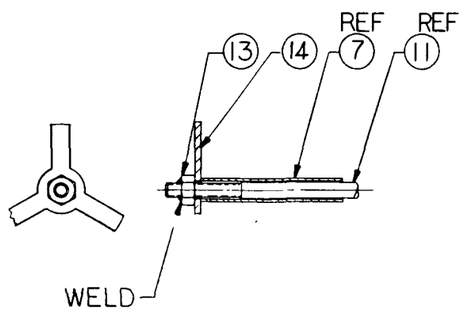

VIEW B
SCALE 2×1

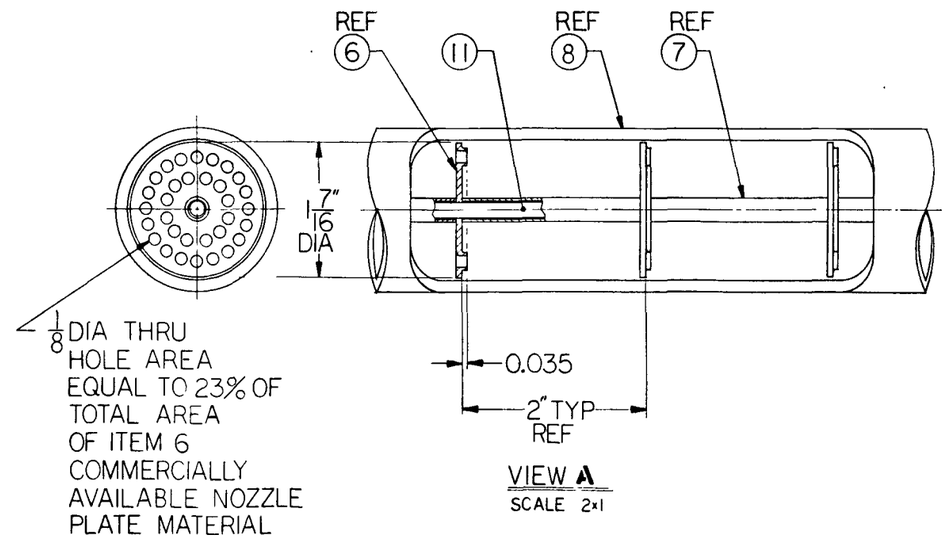

VIEW A
SCALE 2×1

ITEM	DESCRIPTION LIST OF MATERIAL	MAT'L
14	STAR Ø 1⅛ DIA × 1/16 THK.	ST. STL
13	#8 32 HEX NUT	ST STL
12	TUBE 4¼OD × ⅛W × 18LG	
11	TIE ROD 3/16 DIA × 13'LG	
10	PLUG 4¼OD × ½ THK	
9	FLOAT	
8	TUBE 1¾OD × .125W × 13'LG	
7	TUBE · ¼OD × .028W × 2LG	
6	PLATE · 1 7/16 DIA · 1/16	
5	NIPPLE 9/16 ID	
4	NIPPLE · ⅛ ID	
3	PLUG 3/4 OD · ¼ THK	
2	TUBE 3¼OD · .125 W × 18 LG	ST STL
1	ASSEMBLY	

ALL DIMENSIONS IN INCHES

Fig. 9-14. Design concept for 10 solvent wash column

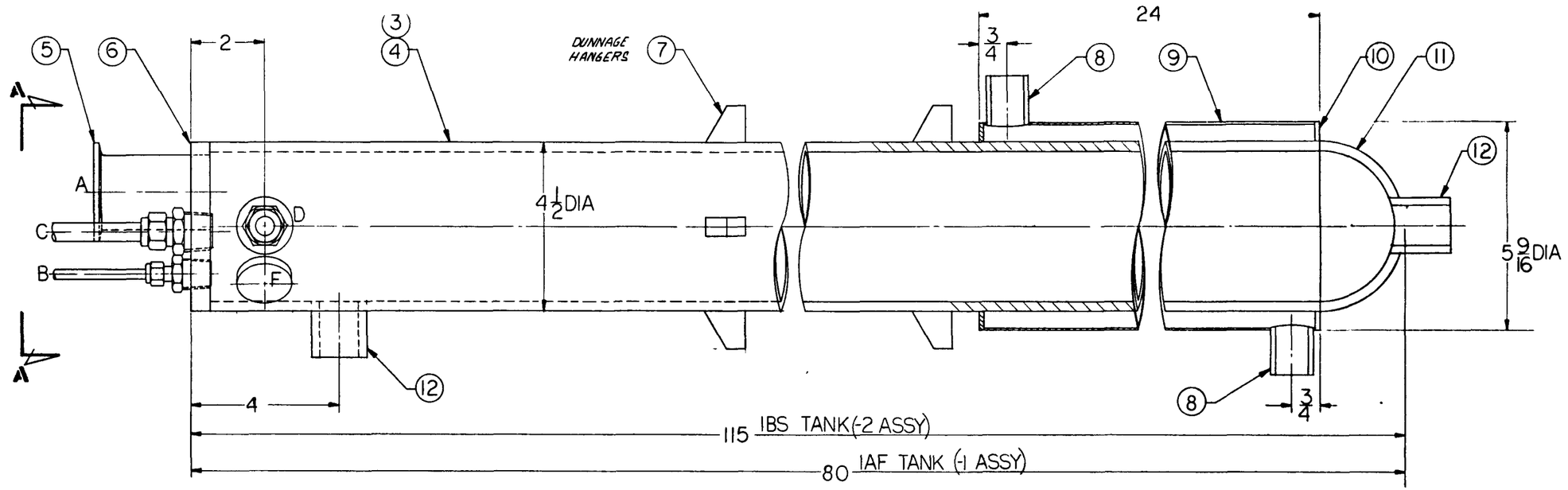

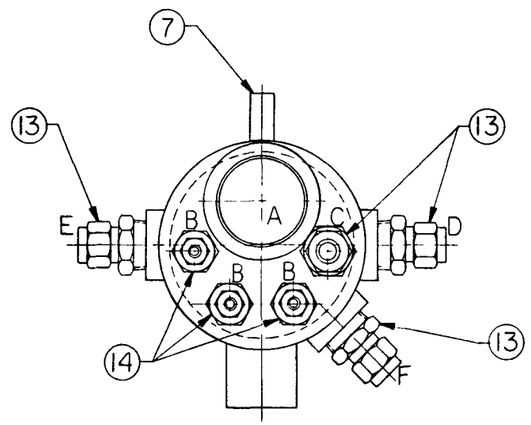

VIEW A-A

(-1) ASSY IAF TANK
TK1601-001
TK1601-002

(-2) ASSY IBS TANK
TK1611-035

CODE	ITEM NO.	LINE DESCRIPTION
A	5	VESSEL VENT
B	14	DIP TUBES (3)
C	13	AIR SPARGE
D	13	FILL LINE
E	13	CHEM ADD
F	13	PUMP RECIRCULATE NOT USED ON -2 ASSY

VESSEL CONNECTIONS AT PENETRATIONS ARE
a. FLANGED CONNECTION ON 2" DIA PENETRATION
b. BORED THROUGH SWAGELOCK OR GYROLOCK ON 1/2 & 3/4 FITTINGS
1/4 TUBING THROUGH 1/2 NPT FITTING
1/2 TUBING THROUGH 3/4 NPT FITTING

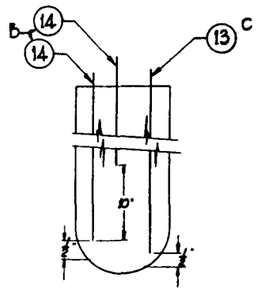

VESSEL INTERNAL TUBES AS SHOWN

ITEM	DESCRIPTION LIST OF MATERIAL	MATL
16	TUBE, 1/2 OD	ST STL
15	TUBE, 1/2 OD	ST STL.
14	NALE 1/4 OD TUBE CONNECTOR 1/2 NPT	S STL
13	NALE 1/2 OD TUBE CONNECTOR 3/4 NPT	
12	NIPPLE 1 1/16 ID	
11	TANK HEAD	
10	END PLATE 1/8 SH	
9	PIPE 5 IPS SCH 10S	
8	NIPPLE 1/8 ID	
7	HANGER 1/2 PL	
6	COVER 1/2 PL	
5	TANK WELDING SPUD 2"OD	
4	PIPE 4 IPS SCH 40S	ST STL
3	PIPE 4 IPS SCH 40S	ST STL
2	ASSEMBLY	
1	ASSEMBLY	

ALL DIMENSIONS IN INCHES

Fig. 9-15. Design concept for 1A feed storage tank and 1B solvent tank

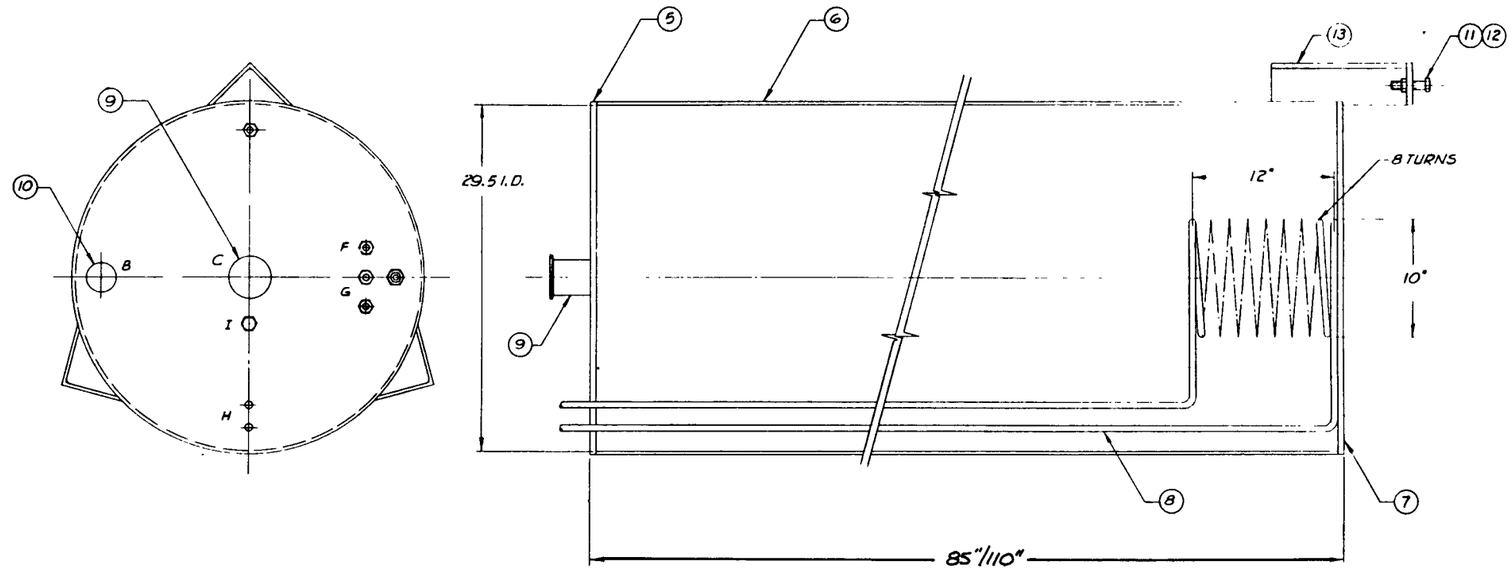

CODE	ITEM NO.	LINE DESCRIPTION
A		EMPTY SUCTION LEG
B	10	VESSEL VENT
C	9	AIR LIFT SAMPLER
D		DIP TUBE PENETRATIONS
E		THERMO WELL
F		FILL LINE
G		CHEM ADD
H	8	COOLING COIL
I		AIR SPARGE

ITEM	DESCRIPTION	MATL
	LIST OF MATERIAL	
15	MALE CONNECTOR 1/4 O.D. TUBE 1/8 NPT	SST
14	MALE CONNECTOR 1/2 O.D. TUBE 3/4 NPT	
13	ANGLE	
12	HEX. NUT	
11	HEX. HD. BOLT	
10	TANK WELDING SPUD	
9	TANK WELDING SPUD	
8	COOLING COIL	
7	BOTTOM PLATE	
6	PIPE 30" SCH 55	
5	TOP PLATE	
4	ASSEMBLY	
3	ASSEMBLY	
2	ASSEMBLY	
1	ASSEMBLY	

(-1) TH-1601-4
(-2) TH-1611-2
(-3) TH-1601-3
(-4) TH-1531-4

ALL DIMENSIONS IN INCHES

Fig. 9-16. Design concept for 1A waste storage tank and 1B thorium storage tank

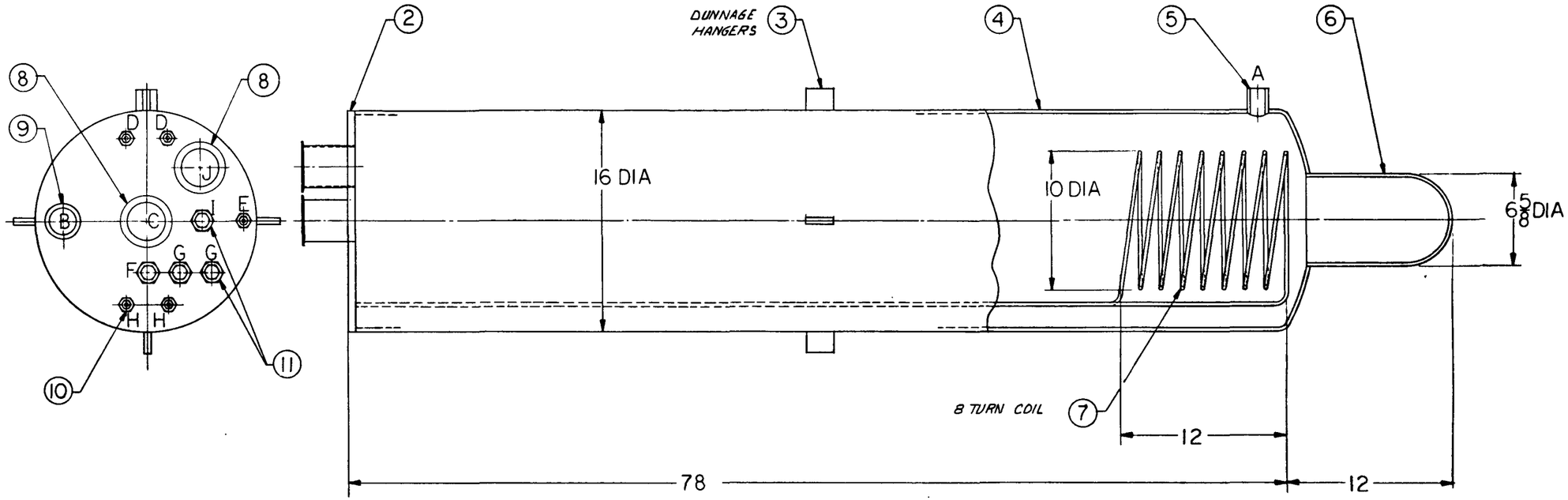

CODE	1"/8" NO.	LINE DESCRIPTION
A	5	PUMP SUCTION LINE
B	9	VESSEL VENT
C	8	AIR LIFT AQUEOUS REMOVAL
D	10	DIP TUBE PENETRATIONS (3)
E	10	THERMOWELL
F	11	FILL LINE
G	11	CHEM ADD (2)
H	10	COOLING COIL
I	11	AIR SPARGE
J	8	AIR LIFT SAMPLER

(-1) ASSEMBLY

COL DRAIN TANK TK 1625-085
100 TANK TK 1621-097

VESSEL CONNECTIONS AT PENETRATIONS ARE

a. FLANGED CONNECTIONS ON 2 2 3 DIA PENETRATIONS
b BORED THROUGH SWAGELOCK OR GYROLOCK
ON 1/2 & 3/4 FITTINGS
1/4 DIA TUBING THROUGH 1/2 NPT
1/2 DIA TUBING THROUGH 3/4 NPT

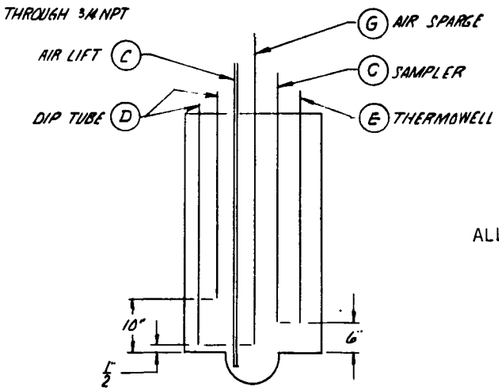

ALL DIMENSIONS IN INCHES

ITEM	DESCRIPTION	MATL
	LIST OF MATERIAL	
11	MALE CONNECTOR 1/2 OD TUBE 3/4 NPT	ST STL
10	MALE CONNECTOR 1/4 OD TUBE 1/2 NPT	
9	TANK WELDING SPUD 2 OD	
8	TANK WELDING SPUD 3 OD	
7	TUBE 1/4 OD x .035 W	
6	PIPE 6 IPS SCH 40 S	
5	NIPPLE 1 1/16 ID	
4	PIPE 16 IPS SCH 20 S	
3	HANGERS 1/2 PL	
2	COVER 1/2 PL	ST STL
1	ASSEMBLY	

Fig. 9-17. Design concept for column drain tank and 10 organic storage tank

As part of this effort, three milestone reports were identified. The first report will deal with the head-end maintenance, while the second report will cover the solvent extraction systems. The third report will address an integrated remote maintenance system and will include complete systems descriptions and design criteria.

An outline for the first of these reports was prepared and reviewed internally with cognizant design and operating personnel. Based on the agreed upon format, a preliminary draft report for the head-end system reviewing current maintenance strategies in the industry has been prepared and is being circulated for preliminary policy review. The draft report draws conclusions based on previous industry maintenance experience and provides recommended maintenance philosophies, many of which are applicable to both the head-end and aqueous process systems. Policy decisions are involved regarding the acceptability of the recommendations and the extent to which they will be implemented in the current development program.

10. HET FUEL SHIPPING

10.1. SUMMARY

The objective of the HET Fuel Shipping Subtask is to coordinate the design and development of all equipment required to ensure economic and timely shipment of the spent FSV fuel selected as feed material for the HETP. Shipment will be required from the Irradiated Fuel Storage Facility (IFSF) in Idaho to the ORNL-TURF facility.

Current program activities are being directed toward definition of the shipping system conceptual design and identification of equipment and transportation costs.

During the quarter efforts have been focused on completion of the conceptual design report, development of detailed costs, and identification of all system interfaces. This activity has included final selection of the PB-2 cask as the reference design and confirmation of the design and suitability of the welded canister concept. The decision to use the PB-2 cask as the reference design in lieu of the FSV cask was based on:

1. Marginal availability of the FSV cask.
2. Better operational suitability of the PB-2 cask.
3. Lower risk in licensing the PB-2 cask.

The reference shipping system design has been reviewed with both ORNL and Allied Chemical from an operational and interface standpoint and has been accepted for use on the HETP.

10.2. WELDED SHIPPING CANISTER DESIGN (FIG. 10-1).

The selection of a welded shipping canister design as the primary containment for the PB-2 shipping system provides handling and licensing advantages over alternate concepts. The metallurgical seal is more reliable and not subject to radiation degradation as a bolted and gasketed closure would be. This contributes to improved system licensability and reduces concerns about canisters leaking into the fuel storage basin (FSB) when removed from the cask at the TURF facility.

Additional design and analysis were performed during the quarter to finalize the canister configuration. This was done in conjunction with Allied Chemical and ORNL/RMPCo to assure compatibility of all interfaces. Further design analysis of the cask internal support assemblies has confirmed the suitability of the canister design from the standpoint of the shipping environment.

10.3. PB-2 CASK DESIGN EVALUATION

Design evaluation of the cask system continued through the quarter in conjunction with finalization of the canister design. A detailed review of the cask safety analysis report (SAR) was performed to establish the licensability of the system. This included investigation of the thermal, shielding, criticality, and structural characteristics associated with shipping the FSV fuel in the PB-2 cask. An estimate of the impact of the different fuel characteristics and structural responses for the new internal configuration on the existing license was made. These investigations will be documented in a separate conceptual design report which is scheduled for release March 31, 1977.

The final shipping arrangement adopted is shown in Fig. 10-2.

Details of the cask internal adapters required to support the shipping canister within the cask during transport are shown in Fig. 10-3.

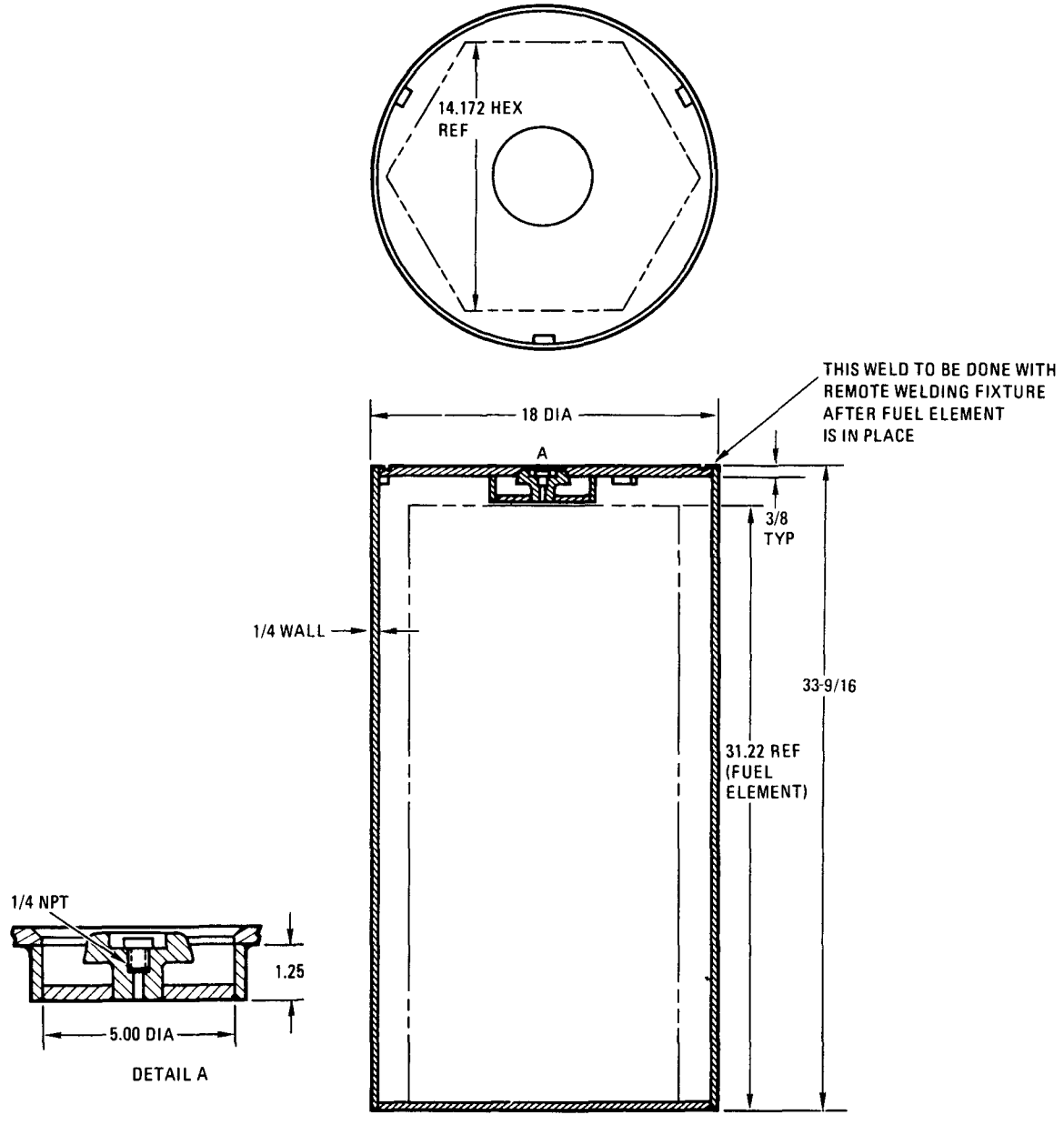

Fig. 10-1. Welded fuel shipping canister

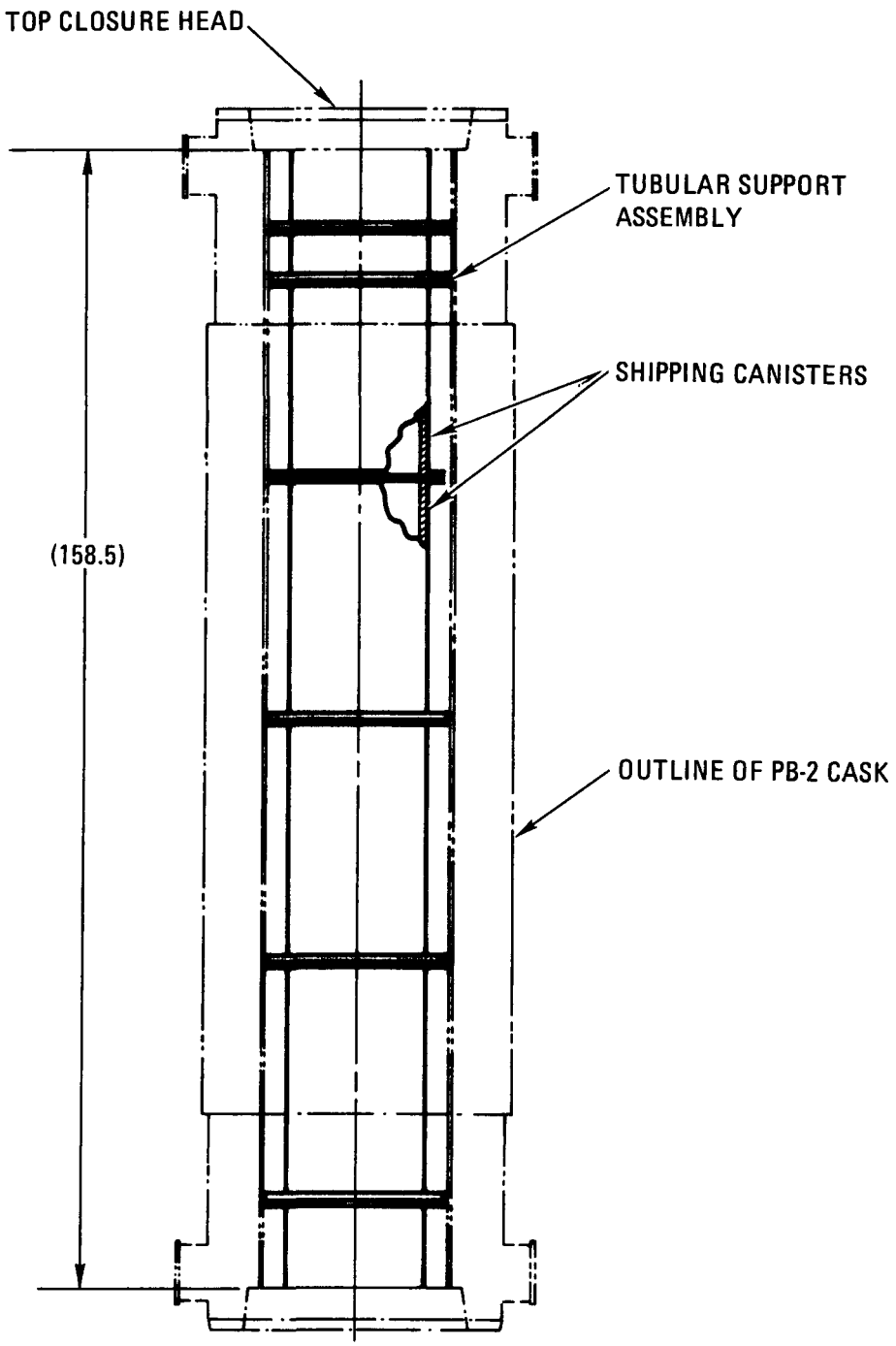

Fig. 10-2. PB-2 cask shipping arrangement

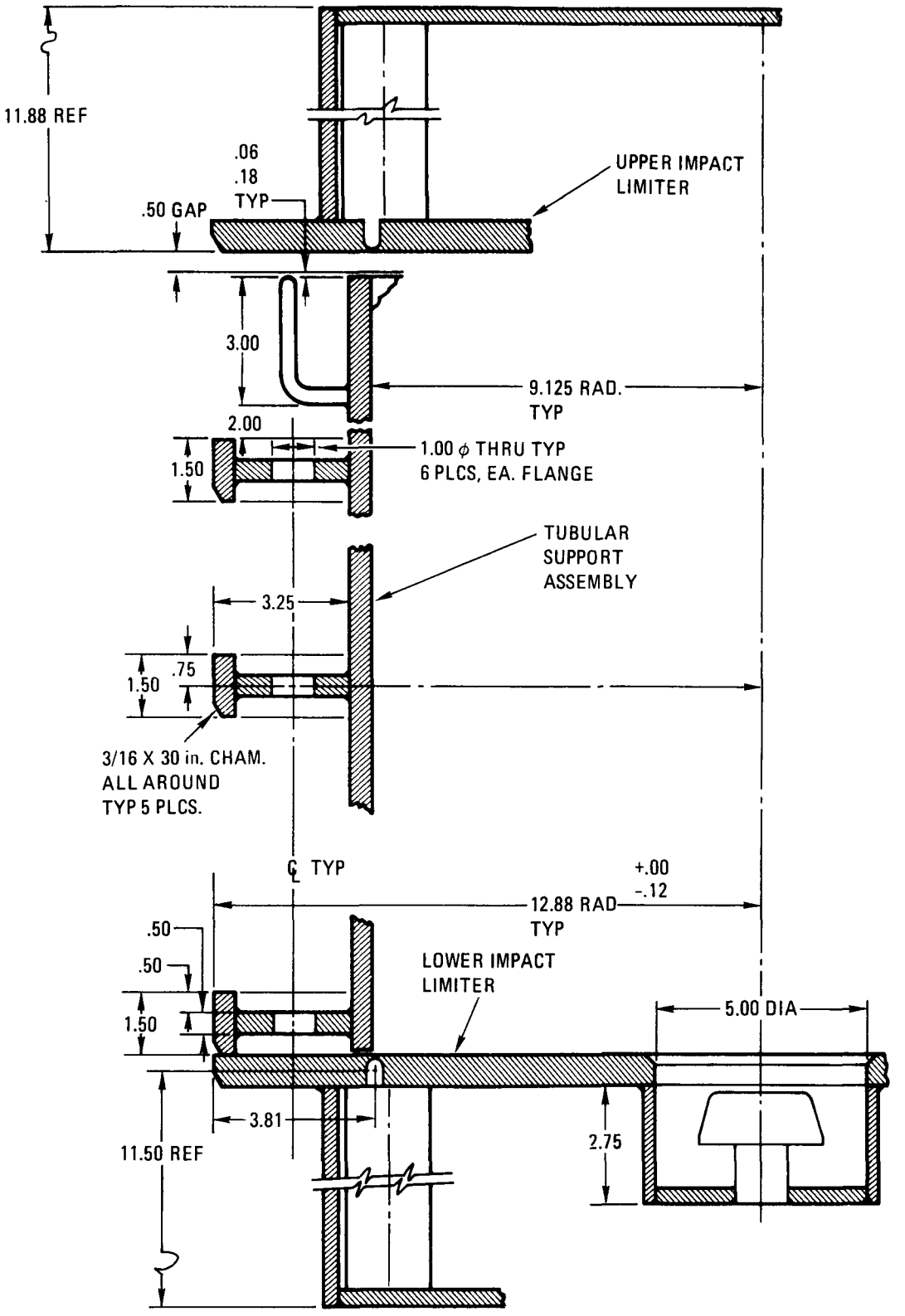

Fig. 10-3. PB-2 cask internal adapter assembly

11. HTGR RECYCLE DEMONSTRATION FACILITY

11.1. SUMMARY

The Reprocessing Flowsheet Review and Material Balance Study of reprocessing head-end processes and the off-gas treatment system is in technical review. Material balances and summary assumption statements for each process stream were prepared for the Reprocessing Yields and Material Throughput Study. The Spent Fuel Element Decay Heat and Source Term Analysis report was completed and is available for distribution. The SIMSCRIPT program language has been chosen for the reprocessing model to be used in the simulation of the Reprocessing Plant Operating Modes Study.

11.2. REPROCESSING FLOWSHEET REVIEW AND MATERIAL BALANCE (L. Abraham)

11.2.1. Introduction

This study is part of the continuing technology assessment to ensure that (1) the proposed HRDF flowsheet incorporates recent technology development improvements and new design data, and (2) supporting technical programs are apprised of flowsheet design issues requiring resolution. The updated reprocessing flowsheet is intended to become an approved baseline document for HRDF design definition and to provide guidance for technical development activities.

During the preceding quarter, HRDF flowsheets for the reprocessing head-end and off-gas treatment systems were updated to incorporate process and design improvements developed at GA and other sites during the past year. The flowsheet revisions included a number of changes which address specific design issues and are summarized in Ref. 11-1.

11.2.2. Activity

During this reporting period, topical report drafts covering the flowsheet review and material balances for the head-end process and off-gas treatment systems were completed and circulated for technical review within the Recycle Development Department. The review comments are currently being resolved and incorporated into the report drafts as appropriate.

Topics addressed in the flowsheet review and material balance report include:

1. Design basis for flowsheet review.
2. Assumed operating mode.
3. Technical issues and resultant flowsheet changes.
4. Process system description.
5. Process development requirements.
6. Material balance assumptions and detailed material balances.
7. Updated process flowsheets.

11.3. REPROCESSING YIELDS AND MATERIAL THROUGHPUT (N. Holder)

11.3.1. Introduction

This study defines the basis for material balances to accompany the HRDF reprocessing flowsheets described in the previous quarterly report (Ref. 11-1). As previously reported, HRDF feed material characteristics have been defined based on average fuel element specifications (Ref. 11-2) and equilibrium spent fuel element content (Refs. 11-3,11-4) for large HTGR TRISO/BISO fuel. A daily throughput basis for reprocessing operations was defined based on the large HTGR standard makeup fuel element discharged at reactor reload 13 and cooled for 180 days (Refs. 11-3,11-4). Particle breakage limit and particle classification efficiency goals were established for use in detailed material balances for HRDF reprocessing.

11.3.2. Activity

Detailed material balances for head-end and off-gas treatment systems were prepared to accompany the Reprocessing Flowsheet Review report. Summary assumption statements for each process stream included in the material balances were also prepared. The material balances are currently being internally reviewed with the flowsheet review report and are scheduled for publication in May 1977.

A draft report entitled "Reprocessing Yields and Material Throughput HTGR Recycle Demonstration Facility" has been prepared and is being internally reviewed. Publication is scheduled for May 1977. This report addresses feed and product specifications, waste stream composition, special nuclear material inventory effects, contaminant paths, and throughput rates for each head-end process step. The resulting head-end product streams to solvent extraction are shown in Table 11-1. The products result from an average daily feed throughput as shown in Table 11-2.

11.3.3. Conclusions

Definitive process yields cannot be predicted with confidence for HRDF at the present time due to insufficient experimental data and to pending fuel design changes (Lead Unit Plant). The current study has, however, resulted in uranium loss projections (Table 11-3) that can be used as guidance for the development program. Those operations where losses can be reasonably predicted generally indicate negligible losses, except in the areas affected by particle crossover due to particle breakage and/or separation efficiencies. The relatively high potential losses attributable to crossover have resulted in the addition to the flowsheet of means for recovery of fuel particles remaining in the leaching insols. Losses due to material holdup in equipment removed for repair or replacement, holdup in filters, and special nuclear material in agglomerates formed in burning can all be identified and the need for recovery established from cold pilot plant and hot engineering test data obtained over the next few years.

TABLE 11-1
HRDF PHASE I - LEACHER PRODUCT TO SOLVENT EXTRACTION

	Fertile Leacher Product	Fissile Leacher Product
Avg. liquid flow (l/DY)[a]	1479.6	1132.2
Heat load (W/liter)[b]	5.1	5.0
Activity (Ci/liter)	1351.9	1145.6
Carbon (g/liter)	0.3	0.2
Uranium (g/liter)	7.3	8.0
Thorium (g/liter)	224.2	Negl.
Plutonium (g/liter)	Negl.	0.4
Fission products (g/liter)	7.3	15.5
Boron (g/liter)	--	0.4
HNO_3 (M)	8.4	2.0
F^- (M)	0.05	--
Al^{+++} (M)	0.1	--
Cd^{++} (M)	0.075	0.075
Total NO_3^- (M)	13.0	2.5

[a] Exclusive of rework material. Based on 233 equivalent operating days/year, 43 standard large HTGR makeup elements/day (Refs. 11-3, 11-4).

[b] Decay heat only.

TABLE 11-2
ASSUMED HRDF - PHASE I AVERAGE DAILY THROUGHPUT[a]
(kg of feed)

	Fuel Elements	Fissile Particles	Fertile Particles	SiC Hulls	Uranium	Thorium
Crushing	5098					
Primary burning	5098					
Classifying		185	419	9		
Fertile leaching		4	407			
Particle crushing		181	12	9		
Particle burning		181	12	9		
Fissile leaching		44	12	90		
Thorex solvent extraction					11	332
Purex solvent extraction					9	Negl.

[a]Based on 43 standard large HTGR makeup fuel elements per day.

TABLE 11-3
URANIUM LOSS PROJECTIONS - HRDF REPROCESSING

Unit Operation	Percent Combined U-235/U-233 Loss	Basis
FE crushing	0.001	0.5% material holdup for first fuel element of a customer batch (arbitrarily assumes holdup equally distributed between particles and graphite).
Material transport (solids)	To be determined	Holdup in transport lines for a minimum of 27 transfers.
		Holdup in filters and hoppers for a minimum of 16 storage locations.
Primary burning	To be determined	<1 μ material loss to off-gas.
		Holdup in filters and equipment.
		Agglomerate content.
Particle separation	0.3	Fissile particles retired from 320 25RS elements at equilibrium - Phase II.
	0.04	Fissile kernel crossover to retired stream at equilibrium - Phase II (1.5% of whole kernels, 75% of broken kernels).
	To be determined	Holdup in equipment and filters.
Fertile leaching	0.004	Insoluble compounds based on LWR UO_2 fuel dissolution results.
	<0.4	Fissile particle crossover to fertile particle stream - recovery efficiency to be determined.
Secondary crushing and burning	To be determined	Agglomerate content.
		Equipment and filter holdup.
		Material loss to off-gas.

TABLE 11-3 (CONTINUED)

Unit Operation	Percent Combined U-235/U-233 Loss	Basis
Fissile leaching	0.02	0.1% of fissile fraction uranium in hulls.
	0.001	Insoluble compounds based on LWR UO_2 dissolution results.
	<0.2	Whole fissile particle content in insols - recovery efficiency to be determined.
	<2.1	Fertile kernel content in insols from crossover - recovery efficiency to be determined.
All	To be determined	Sampling losses due to archive samples and destructive testing.
All	To be determined	Decontamination waste streams for equipment removed for repair or replacement.

Losses due to sampling can be reduced by specifying analytical techniques that will allow maximum return of sample material to processes.

11.3.4. Recommendations

Development recommendations resulting from the study are summarized in Table 11-4. Many of these recommendations are already included in appropriate activity and experimental plans, and the dates that data will be available are shown in Table 11-4. Crossover material recovery can be assessed with equipment already included in development plans. A sampling plan for HRDF will no doubt be included in future Task 600 work.

11.4. SPENT FUEL ELEMENT DECAY HEAT AND SOURCE TERM ANALYSIS (V. Pierce)

The topical report covering this task (Ref. 11-4) has been completed and approved and is available for distribution.

11.5. SIMULATION OF REPROCESSING PLANT OPERATING MODES (N. Holder)

11.5.1. Introduction

The objective of this subtask is to develop a computerized simulation model of the HRDF reprocessing plant. Specific problems to be studied and reported are:

1. The effects of system reliability on plant performance.

2. The dependence of system performance on the level of surge capacities available.

3. The effects of batch versus continuous operation on system performance.

TABLE 11-4
DEVELOPMENT PLAN INFORMATION AVAILABILITY FOR HRDF
(APPLICABLE TO YIELDS AND THROUGHPUT)

Information Required	Development Recommendations	Data Available
Particle breakage	(1) Characterize cold pilot system particle breakage for typically sized and coated BISO and TRISO particles in ratios expected for various HRDF process operations (including crossover material ratios).	1977 - 1978
	(2) Compare radioactive vs. non-radioactive particle breakage for non-typical fuel in hot engineering test systems.	1985 - 1986[a]
	(3) Obtain strength calculations for irradiated and non-irradiated LHTGR and FSV particles.	TBD
	(4) Extrapolate data from (2) and (3) to (1) to predict breakage for HRDF.	∿1986
Special nuclear material holdup and losses	Filter holdup	
	(1) Characterize material holdup in filters for LHTGR fuel (heavy metal vs. other) in cold pilot systems.	1977 - 1978
	(2) Compare filter material held up for irradiated and non-irradiated non-typical fuel in HET-Repro. systems.	1985 - 1986[a]
	(3) Extrapolate (2) to (1) to project HRDF holdup and need to recover SNM for holdup.	∿1986
	Equipment holdup	
	(1) Determine degree of equipment cleanout achievable in cold pilot systems for LHTGR fuel.	1977 - 1978
	(2) Characterize material remaining in failed equipment (heavy metal vs. other) in cold pilot systems for LHTGR fuel.	1977 - 1978
	(3) Compare degree of cleanout and characterize material holdup for irradiated and non-irradiated non-typical fuel in HET-Repro. systems.	1985 - 1986
	(4) Extrapolate (3) to (1) and (2) to project SNM losses to HRDF and determine need for recovery of decontamination materials.	∿1986

[a] Refers to data summary period at end of hot engineering tests.

TABLE 11-4 (CONTINUED)

Information Required	Development Recommendations	Data Available
Special nuclear, etc. (continued)	Crossover material recovery	
	(1) Characterize classification efficiency for insols.	TBD
	(2) Characterize particle breakage in various ratios of crossover streams in transport..	TBD
	(3) Establish fertile particle dissolution rate in fissile dissolver.	TBD
	(4) Characterize uranium in hulls and agglomerates for LHTGR fuel to determine need for recovery.	TBD
Product contamination	(1) Characterize any contamination added to product by equipment wear and failures	
	Cold pilot systems	1977 on
	Hot engineering systems	1986
	(2) Determine paths of cold contaminants to product vs. waste streams, e.g.,	1978 on
	Sulfur	
	Boron and other poisons	
	Metallic impurities	
	(3) Determine paths of radioactive contaminants to product vs. waste streams (e.g., semi-volatiles).	1985 - 1986
	(4) Extrapolate to HRDF to determine product cleanup and waste stream treatment requirements.	
Throughput rates and surge storage requirements	(1) Perform computer simulation of process operations to project required throughput rates and surge requirements.	1978
	(2) Verify selected throughput rates in cold pilot process and identify required scale factors.	1978 on
	(3) Identify irradiated fuel effects on throughput rates in hot engineering test systems.	1986
	(4) Identify sampling and analytical requirements and evaluate techniques for achieving required data turnaround.	TBD
	(5) Evaluate fuel surge storage requirements and capacities, and reactor discharge and fuel shipping schedule effects on throughput.	TBD

This subtask interfaces with the maintainability and reliability subtask described in Section 9.1 for the development of system operating profiles and availability data.

11.5.2. Activity

A review of previous GPSS (General Purpose Systems Simulator) and SIMSCRIPT programming language modeling work at GA has been completed. SIMSCRIPT was tentatively chosen as the preferred language for the reprocessing model, since it appears to be a better tool for modeling systems that are more complex than a normal manufacturing operation. SIMSCRIPT will require more programming time but should be less expensive to run. In addition, a spent fuel shipping model in SIMSCRIPT language was previously prepared (Ref. 11-5). A reprocessing model in SIMSCRIPT can be interfaced with the transportation model in the future to assess the effect of shipping and storage on reprocessing throughput.

The SIMSCRIPT programming language package has been obtained and entered on the GA UNIVAC 1110 catalog file system. A simple model of the fuel element crushing system (Fig. 11-1) is being programmed as a trial case for familiarization with SIMSCRIPT capabilities.

Information on the GASP IV simulation language has been ordered for comparison with SIMSCRIPT. The GASP IV language may be advantageous as it can be compiled in a FORTRAN compiler and could eventually interface with ORNL refabrication modeling work.

REFERENCES

11-1. "Thorium Utilization Program Quarterly Progress Report for the Period Ending November 30, 1976," ERDA Report GA-A14214, General Atomic Company, December 1976.

11-2. "HTGR Fuel Product Specification," ERDA Report GA-A13464, Issue B, General Atomic Company, January 1976.

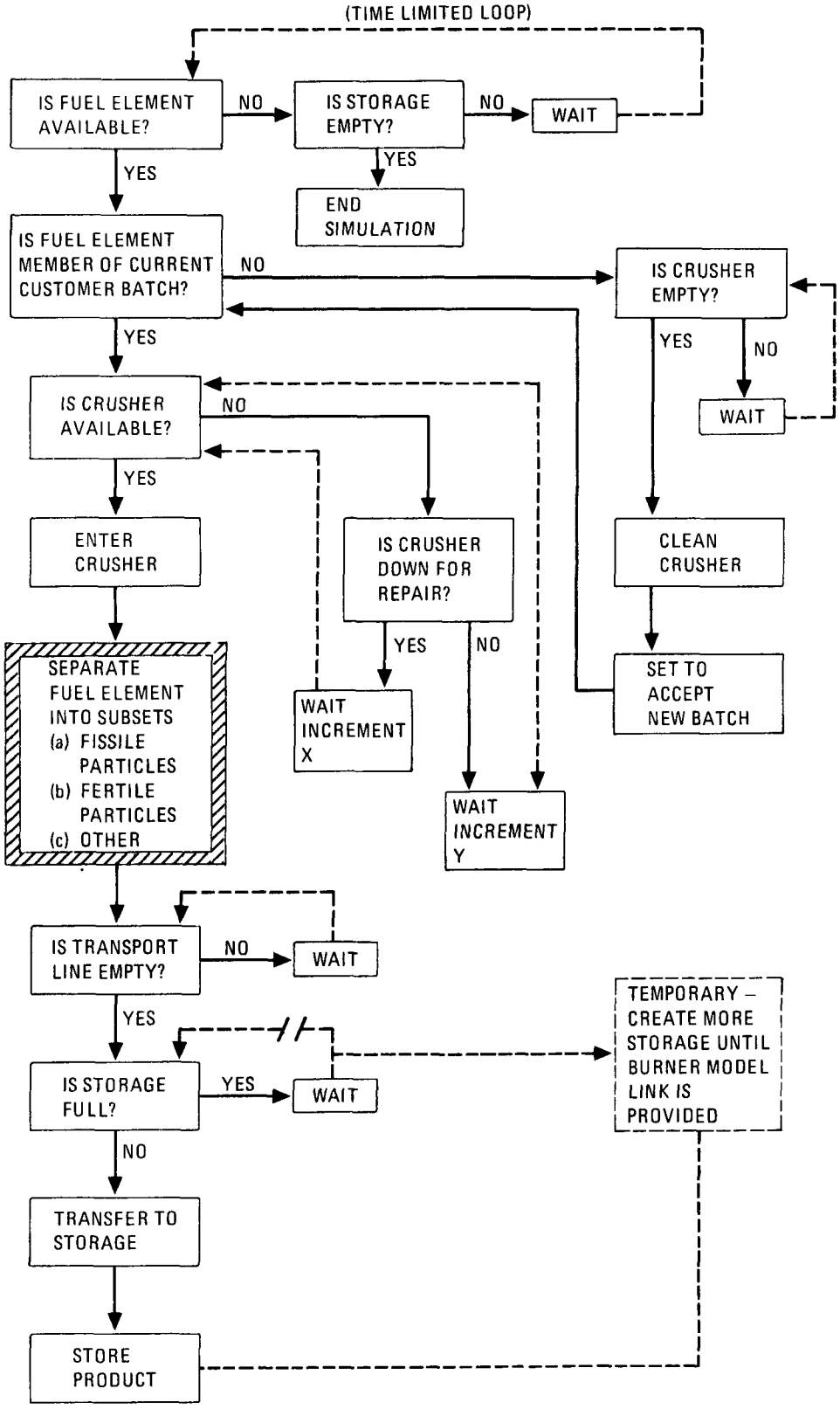

Fig. 11-1. SIMSCRIPT fuel element crushing model

11-3. Hamilton, C. J., et al., "HTGR Spent Fuel Composition and Fuel Element Block Flow," ERDA Report GA-A13886, General Atomic Company, July 1, 1976.

11-4. Sund, R. E., et al., "HTGR Spent Fuel Element Decay Heat and Source Term Analysis," ERDA Report GA-A14140, General Atomic Company, to be published.

11-5. Borgonovi, G. M., "Computer Simulation of HTGR Fuel Transportation and Recycling," General Atomic Report GA-A13757, November 1975.

APPENDIX A
PROJECT REPORTS PUBLISHED DURING THE QUARTER

Burgoyne, R. M., "Interim Design Status and Operational Report for Remote Handling Fixtures: Primary and Secondary Burners," ERDA Report GA-A14125, December 1976.

Robertson, M. W., "EXTENDCHAIN: A Package of Computer Programs for Calculating the Buildup of Heavy Metals, Fission Products, and Activation Products in Reactor Fuel Elements," ERDA Report GA-A14080, January 1977.

APPENDIX B

DISTRIBUTION LIST

L. BROOKS	SV-101	J. F. WATSON	L-640
R. C. DAHLBERG	L-503	B. BAXTER	ORNL*
G. B. ENGLE	L-364	R. D. ZIMMERMAN	E-179
W. V. GOEDDEL	SV-101	M. H. MERRILL	L-510
A. J. GOODJOHN	E-217	H. C. CARNEY	E-086
T. D. GULDEN	L-444	A. H. SCHWARTZ	EA2-211
S. LANGER	TO-559	G. E. BENEDICT	E-249
G. B. MELESE d'HOSPITAL	TO-365	J. W. ALLEN	E-166
C. L. RICKARD	L-205	R. M. BURGOYNE	E-165
O. STANSFIELD	L-440	P. L. WARNER	E-167
H. B. STEWART	L-602	G. CHANDLER	E-161
J. J. SHEFCIK	E-244	N. W. JOHANSON	E-165
R. F. TURNER	L-507	J. S. RODE	E-174
R. C. NOREN	SVB-131	U-S PARK	E-243
B. YALOF	S-117		

LEGAL

WASHINGTON

15 DOCUMENT CENTER

177 TIC

---

*Room 215, Bldg. 4508
ORNL, P. O. Box X
Oak Ridge, Tenn. 37830

1 R. D. Thorne, Manager, SAN
U.S. ERDA
San Francisco Operations Office
1333 Broadway
Oakland, Ca. 94612

1 J. B. Radcliffe
PMRS-SD

1 Assistant Director, Commercial
Fuel Cycle Division of Nuclear
Fuel Cycle and Productions
U.S. ERDA
Washington, D. C. 20545

5 Chief, HTGR Fuel Recycle Branch
Division of Nuclear Fuel Cycle
and Productions
U.S. ERDA
Washington, D. C. 20545

2 Project Manager, HTGR Fuel
Reprocessing Development
Allied Chemical Corp.
P. O. Box 2204
Idaho Falls, Idaho 83401

1 Director, Reactor Division,
Attn: Fred E. Dearing
Oak Ridge Operations Office
U.S. ERDA
P. O. Box E
Oak Ridge, Tennessee 37830

1 Director, Advanced Gas-Cooled
Reactor Programs
Attn: P. R. Kasten
Oak Ridge National Laboratory
P. O. Box X
Oak Ridge, Tennessee 37830

1 C. E. Williams
Office of the Manager
Idaho Operations Office
U.S. ERDA
Idaho Falls, Idaho 83401

1 Barry Smith
Idaho Operations Office
U.S. ERDA
Idaho Falls, Idaho 83401

1 V.C.A. Vaughen
Chemical Technology Division
Union Carbide Co.
P. O. Box X
Oak Ridge, Tennessee 37830

1 W. D. Woods
1 E. E. Fisher
R. M. Parsons Co.
Pasadena, Ca 91124

1 Chong Lewe
Nuclear Utility Services
4 Research Place
Rockville, Maryland 20850

1 W. G. Price
Vice President - Generation
Delmarva Power and Light
800 King St.
Wilmington, Delaware 19899

1 J. D. Hornbuckle
So. Calif. Edison
P. O. Box 351
Los Angeles, Ca. 90053

1 G. F. Daebeler
Branch Head, Safety and
Licensing
1 R. F. Manty
Branch Head, Fuel Management
1 H. D. Honan
Philadelphia Electric
2301 Market St.
Philadelphia, Penn. 19101

1 P. U. Fischer
1 R. Finkbeiner
General Atomic Europe
Weinbergstrasse 109
8006 Zurich
Switzerland

1 Director, Office of Public Affairs,
U.S. ERDA
San Francisco Operations Office
1333 Broadway
Oakland, Ca. 94612

1 California Patent Group
U.S. ERDA
San Francisco Operations Office
1333 Broadway
Oakland, Ca. 94612

1 John Ganley
GAC Fuels Group
France
(via M. H. Merrill)

1 Mr. Claude Moreau
Commissariat a l'Energie Atomique
Centre d'Etudes Nucleaires de Saclay
BP No. 2
91190 Gif-sur-Yvette
France

1 J. L. McElroy
Battelle Northwest Laboratories
P.O. Box 999
Richland, Washington 99352

1 Dr. K. Hackstein
HOBEG
6450 Hanau/Main
Postfach 787
Germany

1 Dr. D. Stoelzl
Hochtemperatur Reaktorbau Gmbh
Gottlieb-Daimler-Strasse 8
D-68 Mannheim - 1
Postfach 5360
Germany

1 K. Notz
Oak Ridge National Laboratory
Oak Ridge, Tennessee 37830

1 A. L. Lotts, Program Manager
Thorium Utilization Program
Oak Ridge National Laboratory
P.O. Box X
Oak Ridge, Tennessee 37830